UNIVERSITY OF COPENHAGEN
FACULTY OF HEALTH AND MEDICAL SCIENCES

Optimizing ^{18}F-FDG-PET in the diagnosis of dementia disorders

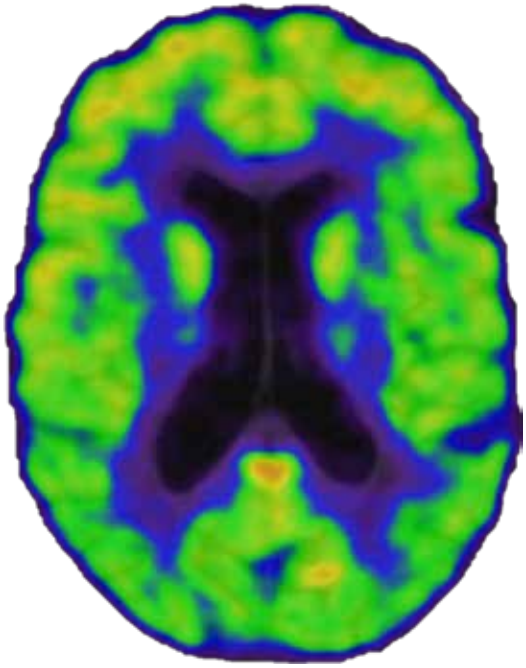

PhD thesis
Le Gjerum

This thesis has been submitted to the Graduate School of Health and Medical Sciences, University of Copenhagen, March 31, 2020

Optimizing ^{18}F-FDG-PET in the diagnosis of dementia disorders

Le Gjerum

MD

Danish Dementia Research Centre

Department of Neurology

Rigshospitalet

Department of Clinical Medicine

Faculty of Health and Medical Sciences

University of Copenhagen

Supervisors:
Steen Gregers Hasselbalch, professor, MD, DMSc (principal supervisor)
Danish Dementia Research Centre, Department of Neurology, Rigshospitalet, University of Copenhagen, Denmark

Ian Law, professor, MD, PhD, DMSc (primary co-supervisor)
Department of Clinical Physiology, Nuclear Medicine and PET, Rigshospitalet, University of Copenhagen, Denmark

Kristian Steen Frederiksen, MD, PhD (co-supervisor)
Danish Dementia Research Centre, Department of Neurology, Rigshospitalet, University of Copenhagen, Denmark

Otto Mølby Henriksen, MD, PhD (co-supervisor)
Department of Clinical Physiology, Nuclear Medicine and PET, Rigshospitalet, University of Copenhagen, Denmark

External assessor:
Peter Høgh, associate professor, MD, PhD
Regional Dementia Research Centre, Department of Neurology, Zealand University Hospital, Denmark

Frontpage illustration: 2-[^{18}F]FDG-PET image with cingulate island sign. Image courtesy of professor Ian Law and Otto Mølby Henriksen, Department of Clinical Physiology, Nuclear Medicine and PET, Rigshospitalet.

Assessment committee:

Rigmor Højland Jensen, professor, MD, DMSc (chairperson)
Department of Clinical Medicine, University of Copenhagen, Denmark

Per Borghammer, professor, MD, PhD, DMSc
Department of Clinical Medicine - Nuclear Medicine and PET, Aarhus University, Denmark

Ruben Smith, associated professor, MD, PhD
Lund University Research Groups, Department of Clinical Sciences, Malmö, Sweden

Table of contents

Preface and Acknowledgements

This PhD project was carried out at the Danish Dementia Research Centre, Department of Neurology, Rigshospitalet from January 2017 to February 2020.
The work was funded by the Research Fund of Rigshospitalet, the Danish Alzheimer's Association Research Fund, the Family Hede Nielsen foundation, and the Absalon Foundation of 1st May 1978.

I would like to express my sincere gratitude to all the great people who have been involved in this Ph.D. project. First and foremost, I wish to thank the patients and research volunteers who have participated in the PredictND project. Moreover, I wish to express my gratefulness to the many supportive and competent people who have contributed to the study projects.

I am very grateful for my four fantastic supervisors who have been very encouraging throughout the PhD project. Steen Gregers Hasselbalch, I am very honored that you gave me this unique opportunity. I am very inspired by your great scientific knowledge and your friendly and respectful approach towards patients, colleagues and me. Thank you for always being so optimistic. A great thanks to Kristian Steen Frederiksen, for your supportive and caring supervision through the whole process and for seeing possibilities rather than limitations. To Ian Law and Otto Mølby Henriksen, thank you for your help and guidance into neuroimaging, which has been indispensable for a novice like me. Thank you for sharing many great ideas and scientific knowledge. Lastly, thank you, Peter Høgh, for being the external assessor and for your contribution to study II.

I also wish to thank the many collaborators at the PredictND project, it has been very enlightening and a great pleasure to work with all of you. I would especially like to thank Jyrki Lötjönen and Juha Koikkalainen for providing me the opportunity to visit Combinostics, and for their great assistance with analyses and scientific discussions.
A special thanks to Marie Bruun for entrusting me with the PredictND project while you were on maternity leave. It has been a great pleasure to work with you.

I would also like to thank all co-authors for their contribution to the study projects and manuscripts, in particular Birgitte Bo Andersen for your great involvement in the consensus evaluation. I would also like to thank the staff at the Department of Clinical Physiology, Nuclear Medicine and PET at Rigshospitalet for assisting with the 2-[^{18}F]FDG-PET images of the research volunteers.

I have been very proud of being part of the Danish Dementia Research Centre for more than four years. Thank you to Gunhild Waldemar for giving me the opportunity. I feel very fortunate to have worked with so many competent and inspiring colleagues at the Copenhagen memory clinic and the Danish Dementia Research Centre at Rigshospitalet. A very special thanks to all the fantastic colleagues in the "research basement". It has been a great pleasure to work with all of you.

Finally, I wish to express my gratitude for the great support and understanding from friends, family and backup-families, thank you for being part of my life for many years.
To my sister Pil Gjerum, I feel incredibly thankful for your persistent support - you and your family bring so much joy to my life!
Lastly, a very special thanks to my loving soon-to-be-husband and very long-bearded partner, Torbjørn C. Pedersen. Thank you for your amazing support and for your inspiring strong-will and hard-working mind. I am so grateful that you are in my life!

Le Gjerum
Copenhagen, March 2020

List of Manuscripts

I. Gjerum L, Andersen BB, Bruun M, Simonsen AH, Henriksen OM, Law I, Hasselbalch SG, Frederiksen KS. Comparison of the added clinical value of 2-[^{18}F]FDG-PET and cerebrospinal fluid biomarkers in patients suspected of Alzheimer's disease.
Submitted.

II. Gjerum L, Frederiksen KS, Henriksen OM, Law I, Anderberg L, Andersen BB, Bjerregaard E, Hejl A-M, Høgh P, Hasselbalch SG. A visual rating scale for cingulate island sign on ^{18}F-FDG-PET to differentiate dementia with Lewy bodies and Alzheimer's disease.
Journal of Neurological Sciences, 2020: 410; 116645.

III. Gjerum L, Frederiksen KS, Henriksen OM, Law I, Bruun M, Simonsen AH, Mecocci P, Baroni M, Dottorini ME, Koikkalainen J, Lötjönen J, Hasselbalch SG. Evaluating 2-[^{18}F]FDG-PET in differential diagnosis of dementia using a data-driven decision model.
NeuroImage: Clinical, 2020: 27; 10226.

Relevant publications, which are not included in this thesis:

Bruun M, Rhodius-Meester HFM, Koikkalainen J, Baroni M, **Gjerum L**, Lemstra AW, Barkhof F, Remes AM, Urhemaa T, Tolonen A, Rueckert D, van Gils M, Frederiksen KS, Waldemar G, Scheltens P, Mecocci P, Soininen H, Lötjönen J, Hasselbalch SG, van der Flier, WM. Evaluating combinations of diagnostic tests to discriminate different dementia types.
Alzheimer's & Dementia: Diagnosis, Assessment & Disease Monitoring, 2018: 10; 509-518.

Bruun M, Frederiksen KS, Rhodius-Meester HFM, Baroni M, **Gjerum L**, Koikkalainen J, Urhemaa T, Tolonen A, van Gils M, Tong T, Guerrero R, Rueckert D, Dyremose N, Andersen BB, Simonsen AH, Lemstra A, Hallikainen M, Kurl S, Herukka S-K, Remes AM, Waldemar G, Soininen H, Mecocci P, van der Flier WM, Lötjönen J, Hasselbalch SG. Impact of a clinical decision support tool on dementia diagnostics in memory clinics: The PredictND validation study.
Current Alzheimer Research, 2019: 16; 91-101.

Bruun M, Koikkalainen J, Rhodius-Meester HFM, Baroni M, **Gjerum L**, van Gils M, Soininen H, Remes AM, Hartikainen P, Waldemar G, Mecocci P, Barkhof F, Pijnenburg Y, van der Flier WM, Hasselbalch SG, Lötjönen J, Frederiksen KS. Detecting frontotemporal dementia syndromes using MRI biomarkers.
Neuroimage: Clinical, 2019: 22; 1-9.

Bruun M, Frederiksen KS, Rhodius-Meester HFM, Baroni M, **Gjerum L**, Koikkalainen J, Urhemaa T, Tolonen A, van Gils M, Rueckert D, Dyremose N, Andersen BB, Lemstra AW, Hallikainen M, Kurl S, Herukka S-K, Remes AM, Waldemar G, Soininen H, Mecocci P, van der Flier WM, Lötjönen J, Hasselbalch SG. Impact of a clinical decision support tool on prediction of progression in early-stage dementia: A prospective validation study.
Alzheimer's Research & Therapy, 2019: 11; 1-11.

English Summary

Early and accurate diagnosis of dementia is essential to establish proper treatment, support, and care. However, the clinical diagnosis may be complicated by a clinicopathological heterogeneity in Alzheimer's disease and other dementias together with a considerable overlap between the dementia diseases.

2-[^{18}F]fluoro-2-deoxy-D-glucose positron emission tomography (2-[^{18}F]FDG-PET) has achieved an emerging supportive role in dementia diagnostic as distinctive metabolic patterns are specific for both Alzheimer's disease, dementia with Lewy bodies and frontotemporal dementia.

The addition of biomarkers such as 2-[^{18}F]FDG-PET and cerebrospinal fluid biomarkers are recommended, if clinical diagnosis is uncertain after standard diagnostic assessment. However, there is limited knowledge on how to weigh, combine and interpret the biomarkers across the spectrum of dementia diseases. Another challenge is the growing amount of extensive and complex patient data, which potentially result in underutilization of important diagnostic information.

The studies in this PhD project aimed at optimizing the clinical value of 2-[^{18}F]FDG-PET in the diagnosis of dementia disorders by proposing three disease-specific 2-[^{18}F]FDG-PET biomarkers and evaluating the clinical value of 2-[^{18}F]FDG-PET against commonly used biomarkers.

In study I, the objective was to compare the added clinical value of cerebrospinal fluid biomarkers and 2-[^{18}F]FDG-PET to a standard diagnostic program in a routine clinical setting. The study population consisted of 81 subjects suspected of having Alzheimer's disease, who were examined with a standard diagnostic program, 2-[^{18}F]FDG-PET and cerebrospinal fluid biomarkers as part of the clinical work-up. The clinical value on diagnosis, prognosis and patient management was comparable for the two biomarkers across all diagnoses when added individually to the standard diagnostic program. However, the clinical value for correctly classified Alzheimer's disease patients was higher for cerebrospinal fluid biomarkers than for 2-[^{18}F]FDG-PET.

In study II, the objective was to develop and evaluate a visual rating scale for cingulate island sign on 2-[^{18}F]FDG-PET to support the diagnosis of dementia with Lewy bodies and

differentiating from Alzheimer's disease. The study population consisted of 35 patients with dementia with Lewy bodies, 36 patients with Alzheimer's disease and 23 controls. The visual rating scale for cingulate island sign was able to significantly differentiate patients with dementia with Lewy bodies from patients with Alzheimer's disease and controls.

In study III, the objective was to evaluate the value of 2-[^{18}F]FDG-PET biomarkers to commonly used diagnostic tests in the differential diagnosis of dementia using a data-driven decision model. In addition, two automated disease-specific 2-[^{18}F]FDG-PET biomarkers were proposed, i.e. API-PET and occipital vs. temporal index, to improve the diagnostic accuracy for frontotemporal dementia and dementia with Lewy bodies, respectively.
The study population consisted of 259 subjects diagnosed with either Alzheimer's disease, dementia with Lewy bodies, frontotemporal dementia, vascular dementia, or subjective cognitive decline. The addition of 2-[^{18}F]FDG-PET biomarkers to the other diagnostic tests improved the classification accuracy for both frontotemporal dementia and dementia with Lewy bodies. Moreover, API-PET and occipital vs. temporal index improved the accuracy for frontotemporal dementia and dementia with Lewy bodies.

In conclusion, the addition of 2-[^{18}F]FDG-PET was valuable in the clinical decision-making. Particularly, the proposed visual rating scale for cingulate island sign showed promising results for distinguishing dementia with Lewy bodies from Alzheimer's disease. In addition, the two automated disease-specific 2-[^{18}F]FDG-PET biomarkers for identifying dementia with Lewy bodies and frontotemporal dementia had potential for improving the differentiation from Alzheimer's disease. Future prospective studies are needed to validate the proposed visual rating scale for cingulate island sign and the automated disease-specific 2-[^{18}F]FDG-PET biomarkers.

Danish Summary

En rettidig, korrekt udredning og demensdiagnose er en vigtig forudsætning for, at patienten kan få adgang til relevant behandling, støtte og pleje. Imidlertid kompliceres den diagnostiske udredning dels af en betydelige heterogenitet i både de kliniske symptomer og neuropatologi ved Alzheimers demens og andre demenssygdomme samt et betydelige overlap i de kliniske symptomer mellem demenssygdomme.
Den funktionelle positron emission tomografi-skanning med glukoseanalogen fluordeoxyglukose som sporstof (FDG-PET) har opnået en fremtrædende rolle i demensdiagnostikken, idet reduktion af glukoseoptagelsen kan påvises i karakteristiske områder i cortex ved både Alzheimers demens, Lewy body demens og frontotemporal demens.
Det anbefales, at foretage supplerende undersøgelser for at øge den diagnostiske sikkerhed, hvis der er usikkerhed om diagnosen efter det basale udredningsprogram. Disse supplerende undersøgelser omfatter blandt andet FDG-PET og biomarkører i cerebrospinalvæsken. Der er dog fortsat begrænset viden om hvordan de enkelte biomarkører skal vægtes og kombineres for at øge den diagnostiske sikkerhed. Den diagnostiske udredningsproces kompliceres tillige i takt med at flere biomarkører bliver tilgængelige, idet den voksende mængde af komplekse patientdata kan medføre at diagnostisk information ikke udnyttes optimalt.

Det overordnede formål med dette ph.d.-projekt var at optimere den kliniske anvendelse af FDG-PET i demensdiagnostikken ved dels at udvikle sygdomsspecifikke FDG-PET biomarkører samt at evaluere den kliniske værdi af FDG-PET i forhold til andre hyppigt anvendte biomarkører i demensdiagnostikken.

I studie I var formålet at sammenligne den kliniske værdi af biomarkører i cerebrospinalvæsken og FDG-PET i et klinisk relevant diagnostisk udredningsscenarie. Kohorten bestod af 81 patienter der var under klinisk udredning for Alzheimers demens. Alle patienterne blev undersøgt med et basalt udredningsprogram samt FDG-PET og biomarkører i cerebrospinalvæsken som led i den diagnostiske udredning. Overordnet havde de to biomarkører samme diagnostiske værdi for hele kohorten. Men når de to biomarkører blev sammenholdt i den patientkohorte som fik en Alzheimers demens diagnose, havde biomarkøerne i cerebrospinalvæsken en større diagnostisk værdi i forhold til FDG-PET.

I studie II var formålet at udvikle og validere en visuel skala til påvisning af cingulate island sign på FDG-PET-skanninger for dels at forbedre identifikationen af Lewy body demens samt at forbedre differentieringen af Lewy body demens fra Alzheimers demens. Kohorten bestod af 35 patienter med Lewy body demens, 36 patienter med Alzheimers demens og 23 raske kontroller. Den visuelle skala til påvisning af cingulate island sign var en sensitiv metode til at skelne patienter med Lewy body demens fra patienter med Alzheimers demens og raske kontroller.

I studie III var formålet at evaluere den diagnostiske værdi af FDG-PET-biomarkører i forhold til hyppigt anvendte diagnostiske tests i en computerassisteret beslutningsmodel. Tillige blev de to sygdomsspecifikke FDG-PET-biomarkører, API-PET og occipital vs. temporal indeks, udviklet for at forbedre differentieldiagnostikken af henholdsvis frontotemporal demens og Lewy body demens. Kohorten bestod af 259 patienter diagnosticeret med Alzheimers demens, Lewy body demens, frontotemporal demens, vaskulær demens eller subjektiv kognitiv svækkelse. Differentieldiagnostikken af såvel frontotemporal demens og Lewy body demens blev forbedret, når FDG-PET-biomarkørerne blev tilføjet til de andre diagnostiske test. Derudover forbedrede de to FDG-PET biomarkører, API-PET og occipital vs. temporal indeks, differentieringen af henholdsvis frontotemporal demens og Lewy body demens fra med Alzheimers demens.

Sammenfattende viste de tre studier, at FDG-PET biomarkørerne har en vigtig rolle i demensdiagnostikken. Særligt den visuelle skala til påvisning af cingulate island sign viste lovende resultater til at skelne Lewy body demens fra Alzheimers demens. Derudover forbedrede de to sygdomsspecifikke FDG-PET-biomarkører, API-PET og occipital vs. temporal indeks, identifikation af henholdsvis frontotemporal demens og Lewy body demens samt differentieringen fra Alzheimers demens. Disse resultater skal efterprøves i større, prospektive studier, herunder validering af den visuelle skala til påvisning af cingulate island sign samt API-PET og occipital vs. temporal indeks.

List of Abbreviations

Aβ	amyloid beta
Aβ42	amyloid beta 1-42
ACE	Addenbrooke's cognitive examination
AD	Alzheimer's disease
AUC	area under the curve
bal. acc.	balanced accuracy
BBH	memory clinic, Copenhagen University Hospital, Bispebjerg Hospital, Copenhagen, Denmark
bvFTD	behavioral variant of frontotemporal dementia
CBD	corticobasal degeneration
CDR	clinical dementia rating
CERAD	consortium to establish a registry for Alzheimer's disease
CI	confidence interval
CIS	cingulate island sign
CSF	cerebrospinal fluid
CT	computed tomography
CVD	cerebrovascular disease
DAT	dopamine transporter
DLB	dementia with Lewy bodies
DSF	disease state fingerprint
DSI	disease state index
EEG	electroencephalogram
FLAIR	fast fluid-attenuated inversion recovery
FTD	frontotemporal dementia
GLO	memory clinic, Glostrup Hospital, Copenhagen, Denmark
IQR	interquartile range
LB	Lewy bodies
MCI	mild cognitive impairment
MIBG	metaiodobenzylguanidine
MMSE	mini-mental state examination

MRI	magnetic resonance imaging
MSA	multiple system atrophy
n	number
ND	neurodegenerative disease
NIA-AA	national institute on aging-Alzheimer's association
NPH	normal pressure hydrocephalus
NRS	numeric rating scale
p-tau	phosphorylated tau at threonine 181
PCC	posterior cingulate cortex
PD	Parkinson's disease
PDD	Parkinson's disease dementia
PER	Section of Gerontology and Geriatrics, University of Perugia and "S. Maria della Misericordia" Hospital of Perugia, Perugia, Italy
PET	positron emission tomography
PNFA	progressive non-fluent aphasia
PSP	progressive supranuclear palsy
RAVLT	Rey auditory verbal learning task
REM	rapid eye movement
RH	memory clinic, Copenhagen University Hospital, Rigshospitalet, Copenhagen, Denmark
ROI	region of interest
ROS	memory clinic, Department of Neurology, Zealand University Hospital, Roskilde, Denmark
SCD	subjective cognitive decline
SD	standard deviation
SPECT	single photon emission computed tomography
SUV	standardized uptake value
VaD	vascular dementia
VBM	voxel-based morphometry
t-tau	total tau
TBM	tensor-based morphometry
TMT	trail making test
2-[^{18}F]FDG-PET	2-[^{18}F]fluoro-2-deoxy-D-glucose positron emission tomography

List of Figures

List of Tables

1. Introduction

Currently, more than 47 million people are living with dementia worldwide, and the number is expected to increase to over 130 million in 2050, largely due to increasing life expectancy [1,2]. Dementia is a syndrome in which there is an acquired loss of cognitive functioning, such as thinking, remembering, and reasoning, that interfere with activities of daily living [3,4]. Dementia results from a broad category of brain diseases with the most common causes being Alzheimer's disease (AD), followed by vascular dementia (VaD), dementia with Lewy bodies (DLB), and frontotemporal dementia (FTD). However, mixed dementia caused by coexisting pathologies, most often AD and VaD or AD and DLB, is very common, especially in older people [5,6].

Early and accurate diagnosis of dementia is essential to establish proper treatment, support, and care [7]. However, the clinical diagnosis may be complicated by a clinical heterogeneity in AD and other dementia disorders together with a considerable clinical overlap between the dementia disorders [8,9]. Biomarkers can improve the diagnosis of dementia by identifying disease-related pathology, which can be measured before clinical symptoms are recognized [10].

Positron emission tomography using 2-[^{18}F]fluoro-2-deoxy-D-glucose as tracer (2-[^{18}F]FDG-PET) has become a widely available and established biomarker in differential diagnosis of dementia by identifying disease-specific patterns of regional hypometabolism [11,12]. Nevertheless, the clinical value of 2-[^{18}F]FDG-PET in the diagnosis of dementia disorders is not completely determined.

The studies in this PhD project aimed at optimizing the clinical value of 2-[^{18}F]FDG-PET in the diagnosis of dementia, particularly in the differential diagnosis of AD, DLB, and FTD, by proposing three disease-specific 2-[^{18}F]FDG-PET biomarkers and evaluating the clinical value of 2-[^{18}F]FDG-PET against commonly used biomarkers.

1.1 Clinical diagnosis of dementia

1.1.1 Diagnostic evaluation in a clinical setting

The current guidelines for diagnosis and assessment of dementia in a clinical setting recommend the use of a standard diagnostic program including clinical history, neurological and physical examination, screening tests for assessment of cognitive functions, blood tests, and a structural neuroimaging, i.e. either computed tomography (CT) or magnetic resonance imaging (MRI). If the

diagnosis is uncertain after the initial assessment, additional investigations can supplement the diagnostic assessment [7,13–15].
The purpose of the clinical work-up is to determine the degree of cognitive impairment and functional disability (syndrome diagnosis) and to identify the specific subtype disease that causes the syndrome (etiological diagnosis) [16].

The syndrome diagnosis is classified according to the severity of cognitive and functional impairment. Subjective cognitive decline (SCD) refers to the self-perception of cognitive decline without impairment in cognition on standard assessment [17]. Mild cognitive impairment (MCI) is regarded as an intermediate state between the cognitive changes of normal aging and dementia, and is defined as an acquired cognitive decline greater than expected based on age and education level without notable interference in activities of daily life [18,19]. Dementia is the most severe stage, and is defined as an acquired cognitive decline with significant interference in activities of daily living [3].

The etiological subtype diagnosis is established by using diagnostic criteria for specific subtypes of dementia. The two major subtypes of dementia are: the neurodegenerative dementias characterized by a progressive loss of nerve cells and synapses; and the dementias caused by cerebrovascular disease (CVD) [20].
The characteristics for the most common subtypes of dementia are presented in the following sections.

1.1.2 Alzheimer's disease

AD accounts for 60-80% of all dementias [21]. The pathologic hallmarks of AD are accumulation of amyloid beta (Aβ) plaques and tau tangles along with cortical atrophy and a prominent cholinergic deficit [22].

The most common clinical presentation of AD is the amnestic presentation characterized by an insidious onset of a progressive impairment in learning and recall and at least one other cognitive domain, such as executive functions, visuospatial abilities, language functions, or behavioral changes. In the non-amnestic presentation, the most prominent early deficits are either language presentation, visuospatial presentation, or executive dysfunction [3]. The diagnostic criteria for AD are summarized in Table 1.

Table 1. Diagnostic criteria for clinical diagnosis of probable and possible AD [3].

	Core clinical criteria for probably AD
1	Meets criteria for dementia [3], and the following characteristics:
2	Insidious onset.
3	Clear-cut history of worsening of cognition.

4	The initial and prominent cognitive deficits are one of the following categories:
	• Amnestic presentation
	• Non-amnestic presentations:
	  o language presentation; or
	  o visuospatial presentation; or
	  o executive dysfunction.

	Exclusion criteria
5	The diagnosis of probably AD should not be applied when there is evidence of: • substantial concomitant CVD; or • core features of DLB; or • prominent features of FTD; or • evidence for another concurrent, active neurological disease, or a non-neurological medical comorbidity or use of medication that could have a substantial effect on cognition.
	Core clinical criteria for possible AD
1	Meets core clinical criteria for probably AD, and has either of the following circumstances:
2	atypical course; or etiologically mixed presentation.

Abbreviations: AD = Alzheimer's disease; CVD = cerebrovascular disease; DLB = dementia with Lewy bodies; FTD = frontotemporal dementia;

Clinicopathological studies have shown good diagnostic accuracy for clinical diagnosis of AD with approximately sensitivity of 80% and specificity of 70% [3,23,24]. The lower specificity is predominantly due to the clinical heterogeneity of AD and a considerable clinical and pathological overlap with other subtypes of dementia, such as DLB and FTD.

The identification and understanding of disease-specific biomarkers for AD have advanced greatly. The growing body of evidence for the utility of biomarkers across the spectrum of AD has led to the incorporation of five AD biomarkers (two CSF proteins and three brain imaging measures) in the research diagnostic criteria for AD [3,24–26]. The recommendations of MCI and dementia due to AD are intended for clinical setting, whereas the recommendations of preclinical AD are intended for research purposes [27].

Figure 1A shows a hypothetical model of the dynamic changes in biomarkers associated with progression of AD. The A/T/N classification scheme has recently been proposed as a biomarker-based research framework due to a new paradigm that focuses on the diagnosis of AD with biomarkers [28]. The classification is not based on the clinical consequences of the disease and

Figure 1. Hypothetical model of prodromal AD (A) and DLB (B).

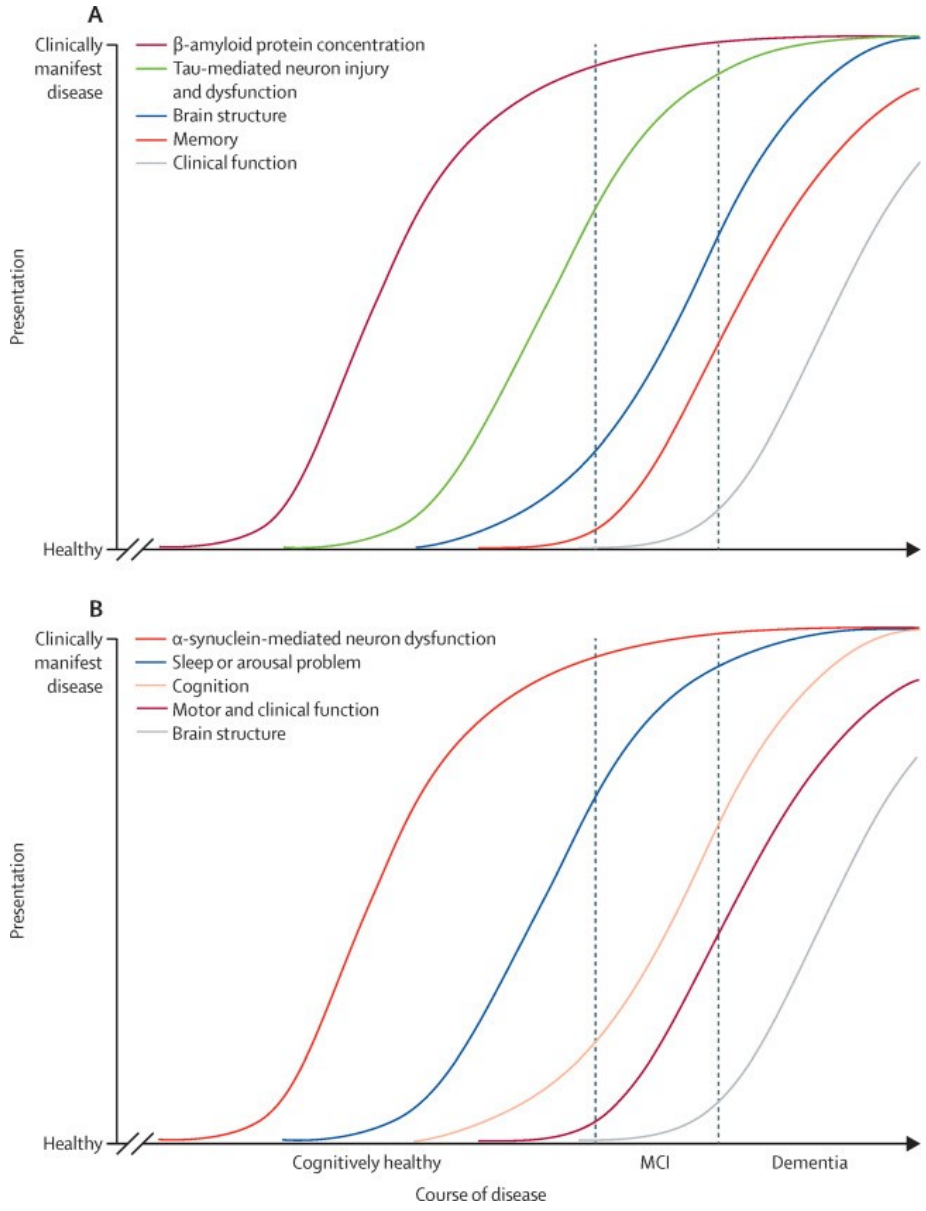

The hypothetical model of temporal ordering of biomarker abnormalities and detectable clinical features in association with progression of AD and DLB is a reprint of the hypothetical model of prodromal dementia with AD and DLB by [30], based on the original model by [10].
(A) In patients with AD, amyloid biomarkers (amyloid PET or CSF Aβ42) become abnormal first, followed by tau biomarkers (tau PET or CSF p-tau) and biomarkers of neurodegeneration (MRI, 2-[^{18}F]FDG-PET, or CSF t-tau), respectively. Subsequently evidence of cognitive impairment becomes evident, and finally clinical symptoms are detectable.
(B) In patients with DLB, progression of α-synuclein-mediated neuron dysfunction precedes detectable alterations of sleep and arousal behavior, followed by alterations in cognition, then alterations in motor and clinical functions, and finally detectable abnormalities on brain neuroimaging.
Abbreviations: Aβ = amyloid beta; AD = Alzheimer's disease; CSF = cerebrospinal fluid; DLB = dementia with Lewy bodies; MCI = mild cognitive impairment; MRI = magnetic resonance imaging; p-tau = phosphorylated tau at threonine 181; PET = positron emission tomography; t-tau = total tau; 2-[^{18}F]FDG-PET = 2-[^{18}F]fluoro-2-deoxy-D-glucose positron emission tomography;
Reprinted from The Lancet, 386; Walker Z, Possin KL, Boeve BF, Aarsland D; Lewy body dementias; 1683-1697, 2015, with permission from Elsevier.

should not be considered as diagnostic criteria for AD. The AD biomarkers were divided into three binary categories based on the specific underlying pathophysiology that the biomarkers measure: “A” refers to measure of brain Aβ deposition with CSF amyloid beta 1-42 (Aβ42) and amyloid PET; “T” refers to measure of tau pathology with CSF phosphorylated tau at threonine 181 (p-tau); and “N” refers to measures of AD-like neurodegeneration with CSF total tau (t-tau), atrophy on structural MRI, and hypometabolism on 2-[^{18}F]FDG-PET [29].

1.1.3 Dementia with Lewy bodies

DLB is the third most common cause of dementia after AD and VaD, accounting for probably 10-15% of all dementias [30].

The pathologic hallmarks of DLB are accumulations of aggregated alpha-synuclein neuronal inclusions of Lewy bodies (LB) and Lewy neurites along with a cortical cholinergic deficit and a nigrostriatal dopamine loss, which are also found in Parkinson's disease (PD) [31,32]. However, more than half of the patients with DLB have coexisting AD pathology, that is Aβ plaques and tau tangles [33–36].

The central feature of DLB is a progressive, disabling cognitive decline, prominently in the domains of attention, visuospatial and executive functioning, whereas memory is relatively spared in the early stage. The core clinical features include fluctuating cognition, recurrent visual hallucinations, parkinsonism, and rapid eye movement (REM) sleep behavior disorder, of which the first three typically occur early. The supportive clinical features are commonly present, but not specific features of DLB [34]. The diagnostic criteria for DLB are summarized in Table 2.

The prodromal phase may be heterogenous, given the diverse clinical presentations of DLB. Figure 1B shows a hypothetical model for the changes in biomarkers and detectable clinical features associated with progression of DLB.

DLB and Parkinson's disease dementia (PDD, when dementia occurs in PD) are clinically similar, however, differ in the temporal sequence with regards to onset of cognitive impairment and parkinsonism. In DLB, the cognitive impairment occurs prior to or simultaneous with onset of parkinsonism, whereas in PDD, the cognitive impairment is arbitrarily set at occurring 12 months or longer after onset of PD. Nearly 80% of patients with PD will progress to dementia [37].

Patients with DLB have a poorer prognosis than patients with AD based on increased healthcare costs, accelerated admission to a nursing-home, and higher mortality. Various clinical and pathological features contribute to the poorer prognosis, and hence emphasize the need for

identification and intervention of these features to optimize treatment and clinical management of DLB [38–40].

Table 2. Diagnostic criteria for clinical diagnosis of probable and possible DLB [34].

I	**Essential criteria for**
	Meets criteria for dementia [3]
II	**Core clinical features**
	• Fluctuating cognition. • Visual hallucinations. • REM sleep behavior disorder. • Parkinsonism.
III	**Supportive clinical features**
	• severe neuroleptic sensibility; • postural instability; • repeated falls; • syncope; • severe autonomic dysfunction; • sleep disorders; • hallucinations in other modalities; • mood disturbances including apathy, anxiety, and depression.
IV	**Indicative biomarkers**
	• Reduced DAT uptake in basal ganglia demonstrated by SPECT or PET. • Abnormal ^{123}iodine-MIBG myocardial scintigraphy. • Polysomnographic confirmation of REM sleep without atonia.
V	**Supportive biomarkers**
	• Relative preservation of medial temporal lobe structures on CT/MRI. • Generalized low uptake on SPECT/PET perfusion/metabolism scan with reduced occipital activity ± CIS on 2-[^{18}F]FDG-PET. • Prominent posterior slow-wave activity on EEG with periodic fluctuations in the pre-alpha/theta range.
VI	**Probable DLB**
	Can be diagnosed if: • Two or more core clinical features of DLB are present, with or without the presence of indicative biomarkers; or • Only one core clinical feature is present, but with one or more indicative biomarkers. Probable DLB should not be diagnosed on basis of biomarkers alone.
VII	**Possible DLB**
	Can be diagnosed if: • Only one core clinical feature of DLB is present, with no indicative biomarker evidence; or • One or more indicative biomarkers is present but there are no core clinical features.

Abbreviations: CIS = cingulate island sign; CT = computed tomography; DAT = dopamine transporter; DLB = dementia with Lewy bodies; EEG = electroencephalogram; MIBG = metaiodobenzylguanidine; MRI = magnetic resonance imaging; PET = positron emission tomography; REM = rapid eye movement; SPECT = single photon emission computed tomography; 2-[^{18}F]FDG-PET = 2-[^{18}F]fluoro-2-deoxy-D-glucose positron emission tomography;

Previous clinicopathological studies have found a poor sensitivity, but a moderate-to-high specificity of the clinical DLB diagnoses and neuropathological diagnoses [23,41], i.e. the clinical diagnosis of DLB was usually correct, but many cases were missed.

Currently, there is no valid biological marker to confirm the diagnosis of DLB, but several indirect biomarkers are available. In the DLB consensus criteria, the indicative and supportive biomarkers are classified according to diagnostic specificity and existing evidence of good quality.

The indicative biomarkers corroborate the detection of clinical features of DLB, i.e. PET or single photon emission computed tomography (SPECT) imaging can detect reduction of dopamine transporter (DAT) in caudate nucleus and putamen to distinguish DLB from AD [42]; metaiodobenzylguanidine (MIBG) myocardial scintigraphy can identify cardiovascular autonomic dysfunction in DLB as opposed to AD [43]; and polysomnographic analysis can demonstrate the presence of REM sleep, which is highly specific for LB pathology [44].

The supportive biomarkers are commonly present in DLB but lack clear diagnostic specificity. The three supportive biomarkers are relative preservation of medial temporal lobe on CT or MRI; generalized low uptake on SPECT and 2-[^{18}F]FDG-PET with reduced occipital activity and presence of cingulate island sign (CIS); and prominent posterior slow-wave activity on electroencephalogram (EEG) [34]. Currently, neither plasma nor CSF α-synuclein are valid biomarkers for DLB [30,34].

Despite the revised DLB consensus criteria, detection and recognition of DLB is still very complex, especially in the early and late stages of the disease, partly because DLB shares clinical, cognitive and neuropathological features with AD and PD [32–34,45]. However, it is essential to make a correct diagnosis of DLB to optimize treatment and clinical management including identifying and managing additional DLB-specific symptoms; to properly inform patients and relatives about the disease and the diverse range of symptoms; and to enroll patients into clinical trials. Therefore, more specific biomarkers for DLB are urgently needed.

1.1.4 Frontotemporal dementia

FTD is the second most common cause of early-onset dementia after AD, i.e. onset of dementia before 65 years of age. Up to 40% of patients with FTD have a history of a similar disorder within the family, however, disease-causing mutations are only identified in about 10% [46,47].

FTD is characterized by prominent frontotemporal lobar degeneration, and associated with characteristic patterns of abnormal protein depositions, predominantly TDP-43 and tau [48,49].

The core clinical feature of FTD is a progressive, insidious change in behavior or language [50]. The diagnostic criteria for FTD are summarized in Table 3. FTD encompasses three main clinical variants with distinct clinical features and patterns of atrophy: behavioral variant of FTD (bvFTD) is the most common FTD syndrome and characterized by behavioral changes with executive dysfunction [51]; progressive non-fluent aphasia (PNFA) is characterized by progressive deficit in expressive language; and semantic dementia is characterized by impaired understanding of semantic knowledge and naming [52].

The prognosis of FTD is variable most likely due to the fact that it is a heterogenous disorder with multiple neuropathological causes, but eventually the patients with FTD will progress toward global cognitive impairment and associated motor deficits [46].

Table 3. Diagnostic criteria for clinical diagnosis of FTD [50].

	Core clinical criteria for FTD
1.	Development of behavior or cognitive deficits manifested by either: early and progressive changes in personality, characterized by difficulty in modulating behavior, often resulting in inappropriate responses or activities; or early and progressive change in language, characterized by problems with expression of language or severe naming difficulty and problems with word meaning.
2.	The deficits outlined in 1a or 1b cause significant impairment in social or occupational functioning and represent a significant decline from a previous level of functioning.
3.	The course is characterized by a gradual onset and continuing decline in function.
	Exclusion criteria for FTD
4.	The deficits outlined in 1a or 1b are due to other nervous system conditions, systemic condition, or substance-induced conditions.
5.	The deficits occur exclusively during a delirium.
6.	The disturbance is better accounted for by a psychiatric diagnosis.

Abbreviations: FTD = frontotemporal dementia;

The clinical variants of FTD are associated with various neuropathological abnormalities, and specific pathological findings have not been associated with specific clinical manifestations [50].

The current validated biomarkers for FTD include specific frontotemporal patterns of atrophy on MRI and hypometabolism on 2-[^{18}F]FDG-PET. In addition, the CSF concentrations of Aβ42, p-tau, and t-tau can be supportive to distinguish underlying AD pathology from other FTD pathologies in patients suspected of FTD [53] since normal Aβ42 rules out AD.

Even though no disease-modifying drugs are available for treatment of FTD, correct diagnosis is central to establish proper management of the behavioral symptoms. However, it is often difficult to distinguish FTD from AD and other neurologic or psychiatric disorders, which emphasizes the need for sensitive biomarkers for FTD [46].

1.1.5 Vascular dementia

VaD is the second most common cause of dementia after AD, accounting for about 20% of all cases of dementia, which also includes the frequently present mixed dementia with predominant AD pathology and coexisting vascular lesions. VaD is common among the older population [54].
VaD is a clinical syndrome that imply the presence of an acquired cognitive deficit secondary to proven evidence of a wide range of vascular pathologies. The diagnostic criteria for VaD are summarized in Table 4. Recently, vascular cognitive disorder has been proposed as a broader term for the clinical syndrome to encompass the entire spectrum of cognitive decline, i.e. MCI and dementia, associated with CVD regardless of underlying mechanism and occurrence of stroke symptoms [55,56].

Several vascular pathologies are associated with cognitive decline and dementia. Small vessel arteriosclerosis and large vessel atherosclerosis can result in cortical and subcortical infarcts, subcortical ischaemic lesions (white matter lesions and lacunar infarcts), and large and small cerebral hemorrhages [54,58].
The clinical features are very variable given the great heterogeneity of vascular pathologies (e.g. location, size, number and type of lesions). However, the clinical characteristics of cerebral small vessel disease commonly involve domains of complex attention and executive functions, together with frequent occurrence of gait disturbance, urinary symptoms, and changes in behavior and mood such as depression and apathy [59]; whereas the clinical characteristics of large vessel disease involve cognitive domains and focal neurological deficits consistent with the location of the infarct [54,57].

The progression of the vascular cognitive impairment is less predictable including both acute and stepwise, gradually and fluctuating courses according to etiology, lesion, and location. However, whereas the cognitive decline may be similar in VaD and AD, mortality is higher for VaD with a mean survival of less than five years, particularly due to cardiovascular and cerebrovascular causes [54].

Structural neuroimaging of CT or MRI is the only validated biomarker for VaD, with the latter being more sensitive to identify location, lesion, and extent of the CVD [57,58]. Additionally, biomarkers of AD pathology, i.e. CSF AD biomarkers and amyloid PET, may be useful to indicate if the vascular cognitive impairment is caused by a mixed dementia etiology [3,24,58].

Table 4. Diagnostic criteria for clinical diagnosis of probable and possible VaD [57].

I	**Core clinical criteria for probable VaD**
1.	Meets criteria for dementia [3]. Exclusion criteria*:* cases with disturbance of consciousness, delirium, psychosis, severe aphasia, or major sensorimotor impairment precluding neuropsychological testing. Also excluded are systemic disorders or other brain diseases that in and of themselves could account for deficits in memory and cognition.
2.	CDV*,* defined by the presence of focal signs on neurologic examination consistent with stroke (with or without history of stroke), and evidence of relevant CVD by brain imaging (CT or MRI) including multiple large vessel infarcts or a single strategically placed infarct*,* as well as multiple basal ganglia and white matter lacunes, or extensive periventricular white matter lesions, or combinations thereof.
3.	Relationship between the above two disorders, manifested or inferred by the presence of one or more of the following: • onset of dementia within 3 months following a recognized stroke; and/or • abrupt deterioration in cognitive functions; and/or • fluctuating, stepwise progression of cognitive deficits.
II	**Clinical features for probable VaD**
1.	Early presence of gait disturbance.
2.	History of unsteadiness and frequent, unprovoked falls.
3.	Early urinary frequency, urgency, and other urinary symptoms not explained by urologic disease.
4.	Pseudobulbar palsy.
5.	Personality and mood changes, abulia, depression, emotional incontinence, or other subcortical deficits including psychomotor retardation and abnormal executive function.
III	**Exclusion criteria for VaD**
1.	Early onset of memory deficit and progressive worsening of memory deficit and progressive worsening of memory and other cognitive functions such as language, motor skills, and perception, in the absence of corresponding focal lesions on brain imaging.
2.	Absence of focal neurological signs, other than cognitive disturbance.
3.	Absence of cerebrovascular lesions on brain CT or MRI.
IV	**Clinical diagnosis of possible VaD**
	Meets criteria for dementia [3] with focal neurologic signs in patients in whom brain imaging studies to confirm definite CVD are missing; or in the absence of clear temporal relationship between dementia and stroke; or in patients with subtle onset and variable course of cognitive deficits and evidence of relevant CVD.

Abbreviations: CT = computed tomography; CVD = cerebrovascular disease; MRI = magnetic resonance imaging; VaD = vascular dementia;

1.1.6 Mixed dementia

Mixed dementia is characterized by coexisting pathologies where both pathologies are estimated to contribute to the clinical syndrome. Coexisting pathologies (hereafter referred to as dual pathology) have been demonstrated in up to 75% of all autopsied cases, especially in advanced age [60]. However, the clinical diagnosis of mixed dementia can be very complex and covers a wide spectrum of dual pathologies and concurrent mixed disease-specific clinical presentations, from clinical presentations with one predominant pathology and minor contributions from other pathologies, to clinical presentations with equally contributing pathologies [24]. Currently, there are no well-established diagnostic criteria for coexisting pathologies other than mixed AD. The

diagnostic criteria for mixed AD is based on the presence of current disease-specific clinical features and biomarker evidence for both pathologies (AD pathology and either CVD or LB pathology) [24]. The diagnostic criteria for mixed AD are summarized in Table 5.

Table 5. Diagnostic criteria for mixed AD [24].

A	**Clinical and biomarker evidence of AD (both are required)**
	• Amnestic syndrome of the hippocampal type or one of the clinical phenotypes of atypical AD. • Decreased Aβ42 together with increased T-tau or P-tau in CSF, or increased tracer retention on amyloid PET.
B	**Clinical and biomarker evidence of mixed pathology**
	For CVD (both are required) • Documented history of stroke, or focal neurological features, or both. • MRI evidence of one or more of the following: corresponding vascular lesions, small vessel disease, strategic lacunar infarcts, or cerebral hemorrhages. For DLB (both are required) • One of the following: extrapyramidal signs, early hallucinations, or cognitive fluctuations. • Abnormal DAT imaging.

Abbreviations: Aβ42 = amyloid beta 1-42; AD = Alzheimer's disease; CSF = cerebrospinal fluid; CVD = cerebrovascular disease; DAT = dopamine transporter; DLB = dementia with Lewy bodies; MRI = magnetic resonance imaging; p-tau = phosphorylated tau at threonine 181; PET = positron emission tomography; t-tau = total tau;

1.2 Biomarkers in clinical diagnosis of dementia

The clinical practice for diagnosing dementia has gradually shifted from a solely clinical-based diagnosis to a biomarker-supported diagnosis as biomarkers have become widely available in clinical practice.

Biomarkers are either physiological, biochemical, or anatomic parameters which can objectively measure specific features of the disease-related pathophysiological processes in-vivo [61]. Although there is a large range of potentially useful biomarkers, the most well-established biomarkers for clinical use include neuroimaging and CSF AD biomarkers. Subsequently, these biomarkers have been incorporated across the disease spectrum of AD in the proposed research criteria [3,24–26]. In addition, neuroimaging biomarkers are included as supportive features in the recent diagnostic criteria for VaD, DLB, and FTD [34,51,52,58,62].

The three most commonly used biomarkers for clinical diagnosis of dementia and other relevant neuroimaging biomarkers are presented in the following sections.

1.2.1 Magnetic resonance imaging

MRI is the preferred structural imaging modality as it is more sensitive with regards to visualizing subtle vascular and atrophy changes compared to CT [14,63]. Accordingly, MRI has become a

routine part of the clinical work-up of dementia to exclude alternative causes of dementia, detect CVD, and recognize focal patterns of atrophy to support the diagnosis of dementia [15]. In addition, MRI is considered a topographic downstream biomarker with proven evidence of correlation between cortical atrophy and neurofibrillary tangle Braak staging [29,64].

Cerebral atrophy can be detected prior to clinical manifestations, and distinctive imaging features are supportive for specific subtypes of dementias [3,24,50–52], although a certain degree of overlap may occur.

In patients with AD, the cerebral atrophy initially involves the medial temporal lobe, predominantly hippocampus and entorhinal cortex, followed by changes in the posterior cingulate cortex (PCC), precuneus, and the temporoparietal association neocortex [65]. Although atrophy in medial temporal lobe including hippocampus correlates with AD pathology and is regarded as an imaging biomarker of AD [3,16,66], atrophy in this region is also common in other dementias, such as DLB and FTD [63].

There is no characteristic atrophy pattern for DLB [14], although, recognition of relative spared medial temporal lobe has been suggested to support the differentiating of DLB from AD [34].

Patients with FTD have more severe atrophy in the frontal lobe and anterior temporal pole together with relative preserved temporoparietal association neocortex compared to patients with AD, and this anterior-posterior gradient of atrophy can support the distinction between FTD and AD [67]. Predominant left-sided posterior frontoinsular atrophy is often seen in PNFA, whereas more pronounced atrophic changes in anterior temporal lobe is typically found in semantic dementia [52].

There are no specific atrophy patterns for VaD, although a lesser extent of cerebral atrophy may be present in patients with VaD [63]. On the other hand, MRI is sensitive to detect various vascular pathologies, which is required for a clinical diagnosis of probable VaD [58]. Although the presence of vascular lesions are specific for VaD, they are also present to a lesser degree in healthy elderly controls and in patients with AD and FTD [68,69].

Currently, visual imaging assessment is the most commonly used method in clinical settings, although an established algorithm for identifying and evaluating diagnostical relevant imaging features is lacking [70]. Several visual rating scales have been developed to assess global and focal atrophy for integration in visual imaging assessment, because they are both fast to perform and easy to apply on routine acquired images. A few scales, such as the MTA scale to assess medial temporal atrophy [71], the GCA scale to assess global cortical atrophy [72], and the Fazekas scale to rate

white matter hyperintensities [56,73], are extensively used in both research and clinical settings [74]. However, their disadvantages include interrater variability.

More advanced methods such as volumetric quantification of brain structures and automatic classifier algorithms including voxel-based morphometry (VBM) and tensor-based morphometry (TBM) are objective and have been proposed to improve differential diagnosis of dementia in clinical settings. However, these methods are both time-consuming and require extensive training and dedicated software. Furthermore, a standard operation procedure for metrics (image acquisition and preprocessing, measurement, and determination of reliable abnormality thresholds) is needed before these methods can be sufficiently integrated in clinical setting as results can vary across scanners and metrices [66,75].

1.2.2 Cerebrospinal fluid biomarkers

The CSF circulates in the subarachnoid space surrounding the brain and spinal cord, and accordingly biochemical changes in the brain are reflected in the CSF. The three core CSF biomarkers for AD hereafter referred to as CSF AD biomarkers are the Aβ42 which is a 42 amino acid long Aβ peptide reflecting cortical amyloid deposition; t-tau reflecting cortical neuronal loss; and p-tau reflecting cortical tangle formation [27].

Concentrations of CSF Aβ42 are fully abnormal more than 5-10 years prior to clinical symptoms of dementia with AD, whereas CSF t-tau and p-tau are considered as later markers of the degenerative process and become gradually more abnormal as the clinical manifestation becomes evident [10,76] (Figure 2).

The biomarkers have a high diagnostic accuracy to identify AD at the MCI stage with sensitivity and specificity of 85–90% [22]. Consequently, the biomarkers are recommended as addition to the diagnostic evaluation of patients suspected of AD if the diagnosis is uncertain or the clinical presentation is atypical [3]. In addition, the biomarkers can also to some extent be useful as exclusion criteria in the differential diagnosis of other neurodegenerative disorders [51,58,77–79].

Nevertheless, some important factors should be considered when interpreting the CSF AD biomarkers in clinical practice. First of all, the specificities of the CSF AD biomarkers for AD are not optimal, because abnormal concentrations are also found in other dementia disorders such as FTD, DLB, and VaD [27]. This may, however, reflect the presence of mixed pathology, which is a common finding at autopsy [80]. Moreover, the prevalence of abnormal CSF AD biomarkers is high in elderly cognitively intact individuals because prevalence of preclinical AD increases with age

[81,82]. Another issue is the considerable variabilities in measurements of these markers between laboratories, which has hampered the consensus on standardized, established cutoffs [83,84]. Despite these issues, the CSF AD biomarkers have reached a prominent role in the early and differential diagnosis of AD in clinical practice.

Figure 2. Temporal ordering of CSF AD biomarkers.

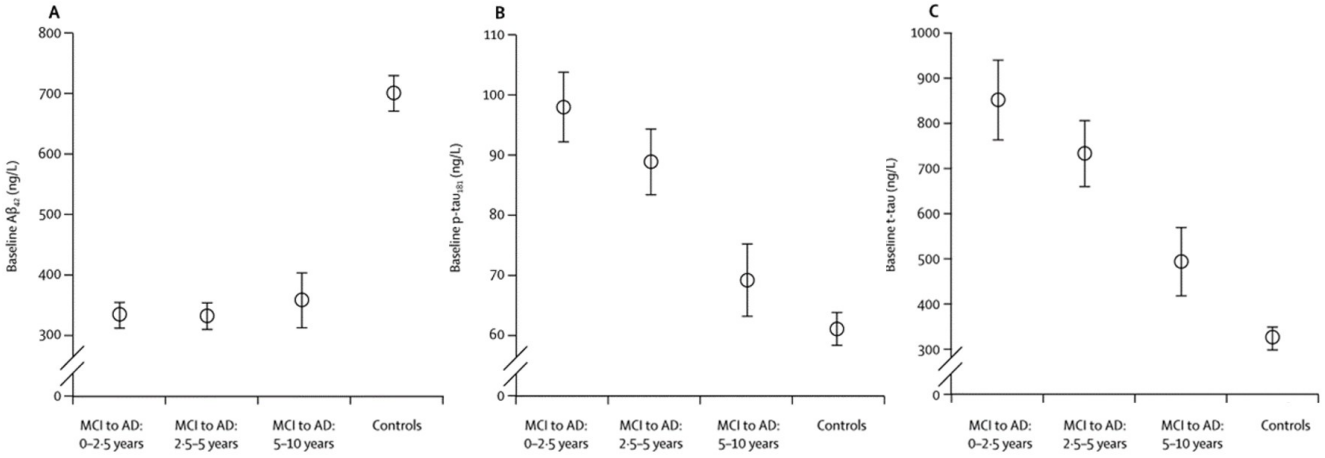

Mean baseline concentrations of (A) CSF Aβ42, (B) p-tau, and (C) t-tau stratified into patients with MCI converting to AD within 0–2.5 years (n=28), 2.5–5 years (n=32), or 5–10 years (n=12). Biomarker concentrations in a cognitively healthy control group are also given. Concentrations of Aβ42 did not differ between any of the MCI groups. Concentrations of t-tau and p-tau were significantly lower in late converters (5–10 years) than in very early converters (0–2.5 years). The error bars show standard errors.
Abbreviations: Aβ42 = beta-amyloid 1-42; AD = Alzheimer's disease; MCI = mild cognitive impairment; p-tau = phosphorylated tau at threonine 181; t-tau = total tau;
Reprinted from The Lancet Neurology, 12; Jack Jr CR, Knopman DS, Jagust WJ, Petersen RC, Weiner MW, Aisen PS, Shaw LM, Vemuri P, Wiste HJ, Weigand SD, Lesnick TG, Pankratz VS, Donohue MC, Trojanowski JQ; Tracking pathophysiological processes in Alzheimer's disease: An updated hypothetical model of dynamic biomarkers; 207-216, 2013, with permission from Elsevier.

1.2.3 2-[^{18}F]fluoro-2-deoxy-D-glucose positron emission tomography

2-[^{18}F]FDG-PET has become widely available for clinical use and is a well-established method in differential diagnosis of dementia [15,85]. 2-[^{18}F]FDG is a radiolabeled glucose analogue measured by PET to reflect cerebral glucose metabolism in-vivo. Cerebral glucose hypometabolism is a marker of neurodegeneration [11]. Thus, 2-[^{18}F]FDG-PET is considered a marker of neuronal injury demonstrating both the topographic extent of the neuronal dysfunction and the disease severity [29].

Previous studies have shown that addition of 2-[^{18}F]FDG-PET to the diagnostic evaluation improved the diagnostic accuracy when compared to both final clinical evaluation and pathological diagnosis [86,87]. Accordingly, current guidelines recommend that 2-[^{18}F]FDG-

PET can be added as a supportive biomarker in clinical settings, if clinical diagnosis is uncertain after standard diagnostic assessment including structural imaging [14,15,85]. Several previous studies have found that 2-[^{18}F]FDG-PET can be used to distinguish neurodegenerative dementias from other forms of cognitive dysfunction and detection of distinctive disease patterns of hypometabolism can support the diagnosis of AD, FTD, and DLB [3,15,24,34,51,52,85].

In patients with AD, the initial hypometabolic pattern typically involves the temporoparietal regions including the precuneus and the PCC, followed at a later stage by dorsolateral prefrontal cortex; whereas, the sensorimotor and visual cortices, basal ganglia and cerebellum remain relatively preserved [11,88] (Figure 3B). MCI subjects that converts to AD typically have an AD-like pattern of hypometabolism, although with less severe hypometabolism [89]. However, temporoparietal hypometabolism is not specific for AD, and is also seen in a variety of other disorders such as CVD, clinical variants of FTD, and DLB [11,29].

Patients with DLB have a more prominent occipital hypometabolism particularly in the primary visual cortex, whereas the parietotemporal hypometabolism is somewhat similar to AD [90,91]. In addition, many DLB patients have a relatively spared PCC, which is termed the cingulate island sign (CIS) (Figure 3C+D). CIS is defined as relatively sparing of the PCC relative to precuneus and cuneus [92]. CIS can differentiate DLB from AD with high accuracy [92–96]. CIS and occipital hypometabolism on 2-[^{18}F]FDG-PET are both proposed as supportive DLB biomarkers in the updated diagnostic criteria for DLB [34]. However, occipital hypometabolism are also seen in patients with PD, PDD, and posterior cortical atrophy [97,98], and CIS has been suggested to be more specific for DLB than occipital hypometabolism [92,93,99,100].

Patients with FTD have early and more severe frontal and anterior temporal hypometabolism with preserved uptake in PCC compared to AD [101] (Figure 3E). Furthermore, the clinical variants of FTD have characteristic patterns of hypometabolism which are typically asymmetric, that is patients with PNFA predominantly have a pattern of left posterior frontoinsular hypometabolism; patients with semantic dementia usually have a pattern of left anterior temporal hypometabolism; whereas patients with bvFTD predominantly have frontal and anterior temporal hypometabolism [51,52].

Patients with VaD have no characteristic patterns of hypometabolism on 2-[^{18}F]FDG-PET, but lower metabolism has been demonstrated in subcortical VaD compared to AD in mainly the primary cortices, middle temporal gyrus, anterior cingulate gyrus, deep grey nuclei, and cerebellum [102].

Figure 3. 2-[^{18}F]FDG-PET images and statistical surface projections.

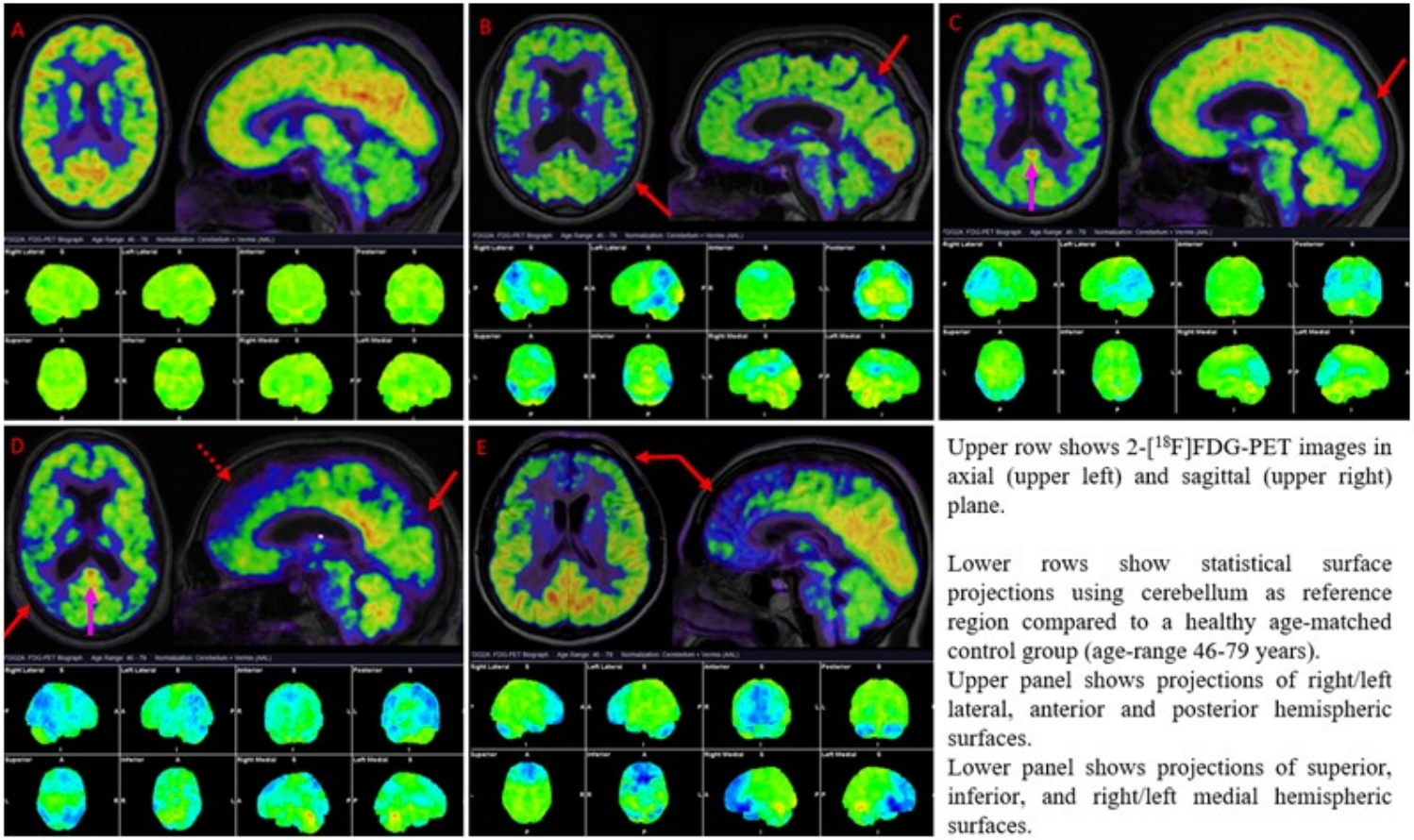

Upper row shows 2-[^{18}F]FDG-PET images in axial (upper left) and sagittal (upper right) plane.

Lower rows show statistical surface projections using cerebellum as reference region compared to a healthy age-matched control group (age-range 46-79 years).
Upper panel shows projections of right/left lateral, anterior and posterior hemispheric surfaces.
Lower panel shows projections of superior, inferior, and right/left medial hemispheric surfaces.

A Healthy elderly control with normal cerebral metabolic uptake. **B.** AD patient with moderate-to-severe temporoparietal hypometabolism (red arrows). **C.** DLB patient with moderate parietotemporal and occipital hypometabolism (red arrow) and CIS (pink arrow). **D.** DLB patient with moderate-to-severe parietotemporal and occipital hypometabolism (red arrow) with involvement of frontal cortices (red dotted arrow) and CIS (pink arrow). **E.** FTD patient with severe frontotemporal hypometabolism (red arrows).
Abbreviations: AD = Alzheimer's disease; CIS = cingulate island sign; DLB = dementia with Lewy bodies; FTD = Frontotemporal dementia; 2-[^{18}F]FDG-PET = 2-[^{18}F]fluoro-2-deoxy-D-glucose positron emission tomography;
Images courtesy of professor Ian Law and Otto Mølby Henriksen, Department of Clinical Physiology, Nuclear Medicine and PET, Rigshospitalet.

The standard procedure to evaluate 2-[^{18}F]FDG-PET images is visual assessment by a nuclear medicine physician [103], which requires adequate training and experience. Consequently, centres without advanced expertise in visual assessment may have reduced clinical value of 2-[^{18}F]FDG-PET.

Several fully and semi-automatic tools have been developed to assist the visual assessment by providing statistical brain mappings of regional glucose metabolic abnormalities as compared against a reference group of healthy controls [104]. However, standard operating procedures for 2-[^{18}F]FDG-PET metrics are essential for implementation in clinical routine. A large meta-analysis study on imaging AD biomarkers concluded that diagnostic accuracy was highly dependent on how the biomarker was measured and evaluated, particularly for 2-[^{18}F]FDG-PET [75].

1.2.4 Other biomarkers

Other commonly used biomarkers include amyloid PET, DAT imaging, and tau PET. DAT imaging is a well-established neuroimaging biomarkers, whereas amyloid PET and tau PET are still developing technologies that are mainly available in specialized clinical centres.

DAT imaging has a high sensitivity to detect presynaptic dopaminergic dysfunction in-vivo, which is a distinctive feature for patients with parkinsonism [105]. Reduced DAT uptake in the basal ganglia demonstrated by SPECT or PET is clinically useful in distinguishing DLB from AD with a high sensitivity (78%) and specificity (90%) [42]. Consequently, DAT imaging has been included as an indicative biomarker in the diagnostic criteria for DLB [34]. Although DAT imaging cannot distinguish DLB from other nigrostriatal disorders that are associated with dopaminergic dysfunction, such as PDD, vascular parkinsonism with dementia, multiple system atrophy (MSA), progressive supranuclear palsy (PSP), corticobasal degeneration (CBD), or FTD with parkinsonism [106,107]. Furthermore, about 20% of probable DLB cases have a normal or inconclusive DAT imaging, and therefore does a negative DAT scan not exclude a diagnosis of DLB [108].

Amyloid PET uses Aβ-specific tracers to enable in-vivo detection of fibrillar Aβ in neuritic plaques [109,110]. Amyloid PET has a high accuracy to distinguish disorders with a prominent amyloid deposition from those without, such as FTD [111]. Nevertheless, cerebral amyloidosis is a necessary but not exclusive condition for AD, as the prevalence of cerebral amyloidosis increases with age in cognitively normal individuals [112]. Furthermore, a high percentage of

patients with other dementia disorders also have cerebral amyloidosis as seen in patients with DLB [113].

Tau PET is a promising method to assess tau neurofibrillary tangle deposition in-vivo [114], which is a pathologic hallmark of AD [22] and many other neurodegenerative disorders known as tauopathies [115]. Several tau PET studies have demonstrated that the topographic tau binding is consistent with the pathologic Braak neurofibrillary tangle stage in AD [116–118]. The emerging role of tau PET is also acknowledged in the A/T/N classification, where tau PET is included as a tau biomarker for AD [29]. The clinical utility of tau PET needs to be investigated further, and extensive tracer development is ongoing with regards to e.g. reduction of off-target binding which has been a problem especially in first-generation tracers [115].

1.3 Clinical challenges in differential diagnosis of dementia

Clinical diagnosis of dementia can be challenging due to a great degree of overlap in clinical symptoms and pathologies [9,33,80,119,120]. Furthermore, despite the emerging role of available biomarkers over the last decades, biomarkers for non-AD dementia such as DLB and FTD are less developed [75,121]. Consequently, a substantial number of patients with dementia are still unrecognized or misdiagnosed, the latter is especially related to difficulties of distinguishing AD from DLB and FTD [23,36,41,122–124].

The clinical decision-making process can be very complex, as conflicting or inconclusive results can complicate interpretation of diagnostic test results. Moreover, factors such as age, educational level, and comorbidities should also be taken into consideration in the diagnostic evaluation. In general, there is limited knowledge of how to both weigh, combine and interpret biomarkers across the spectrum of dementia diseases, although a greater understanding of these issues are valuable in the clinical decision-making process [75,90,121,125]. The clinicians must consider if an ancillary diagnostic test is needed and weigh the cost and benefits including the efficacy, experience and access to apply and interpret the biomarker appropriately as well as factors such as suitability of the biomarker, especially in elderly, frail patients.

The current knowledge of the performance of the biomarkers is predominantly based on the performance of a single modality marker in differentiating between two homogenous diagnostic groups, for the most part involving comparison of a subtype of dementia with healthy elderly controls [121]. However, in clinical practice the common clinical challenge is to identify the

specific subtype of dementia rather than to distinguish whether a patient has dementia or is cognitively intact. In addition, the clinical value of biomarkers is outlined in general terms and lack recommendations for how to prioritize and weigh the biomarkers in differential diagnosis of dementia. This emphasizes the need for further research to optimize and validate the added value of biomarkers in decision-making of dementia.

1.4 Disease state index classifier

There is a growing amount of extensive and complex patient data-driven in part on the one hand by the desire for earlier diagnosis where the patients have more subtle symptoms, and on the other hand the increasing availability of biomarkers and diagnostic tests. Consequently, clinicians face a major challenge of getting a comprehensive overview of the available patient data, which potentially results in underutilization of important diagnostic information. This issue has led to the development of clinical data-driven decision support models that are useful for efficiently integrating biomarkers and diagnostic tests from extensive, heterogenous patient data in an objective and systematic way to assist clinicians in decision-making [126].

In the PredictND project, a consortium of collaborators from four European memory clinics and various research partners focused on developing and validating a data-driven decision support tool, that is the PredictND tool, to support clinicians in earlier and more objective evaluation of biomarkers in the diagnosis of dementia [127,128]. In addition, the PredictND project aimed at developing methods for segmenting and extracting features of brain structures on MR scans [129–131]. The clinical value of the PredictND tool along with the developed image analysis methods was evaluated in terms of effect on improving diagnostic accuracy and confidence of the diagnosis in a clinical setting.

The PredictND tool is composed of the disease state index (DSI) classifier, which is an ensemble classifier that uses a data-driven statistical model to compute a scalar index value, i.e. the DSI value, as an estimation of the similarity of an undiagnosed patient to a disease state. The classifier extracts data from a large quantity of training data from patients with known diagnosis to derive an algorithm that is specific for each disease state. This algorithm can be applied to an undiagnosed patient to estimate patient-specific DSI values for each disease state as an indication of which disease state most closely resemble the undiagnosed patient [128,132].

The DSI describes the ability of each biomarker or diagnostic test to distinguish between two disease states, e.g. AD and DLB (the relevance value) and the extent to which the biomarker or

diagnostic test resembles one of the disease states (fitness value). The DSI value for each biomarker or diagnostic test is weighed by the relevance to obtain a composite DSI value. An "overall" DSI value is obtained by combining composite DSI values for each biomarker or diagnostic test [128].
To support clinical decision-making, the classifier can provide a visual representation of all available data from an undiagnosed patient in the disease state fingerprint (DSF) to give the clinician an overview of the contribution of each biomarkers and diagnostic tests to the computed DSI [128,133]. In the DSF, the DSI value is presented as a numeric value, whereas the fitness value is indicated by box color (e.g. red color indicates similarity AD, whereas blue color indicates similarity to DLB) and the relevance is indicated by the box size. An example of the DSF are shown in Figure 4.
The classifier can cope with many different combinations of variables such as demographic data, cognitive tests, CSF AD and neuroimaging biomarkers [130,134,135]. Moreover, the classifier can deal with missing data without requiring any imputation.

Previous DSI classifier studies have demonstrated high diagnostic accuracies for AD, VaD, and controls using different combinations of cognitive tests, CSF and MRI biomarkers (AUC > 70%), whereas the diagnostic sensitivity for FTD and in particular DLB was suboptimal with many cases being misclassified as AD [130,132,134,135]. However, the addition of 2-[^{18}F]FDG-PET biomarkers may enhance the classification accuracy for FTD and DLB in the DSI classifier considering that 2-[^{18}F]FDG-PET is included as a supportive biomarker for both AD, DLB, and FTD [3,34,50–52]. Until now, studies based on the DSI classifier have not included 2-[^{18}F]FDG-PET data.

Figure 4. Screenshot of the PredictND tool.

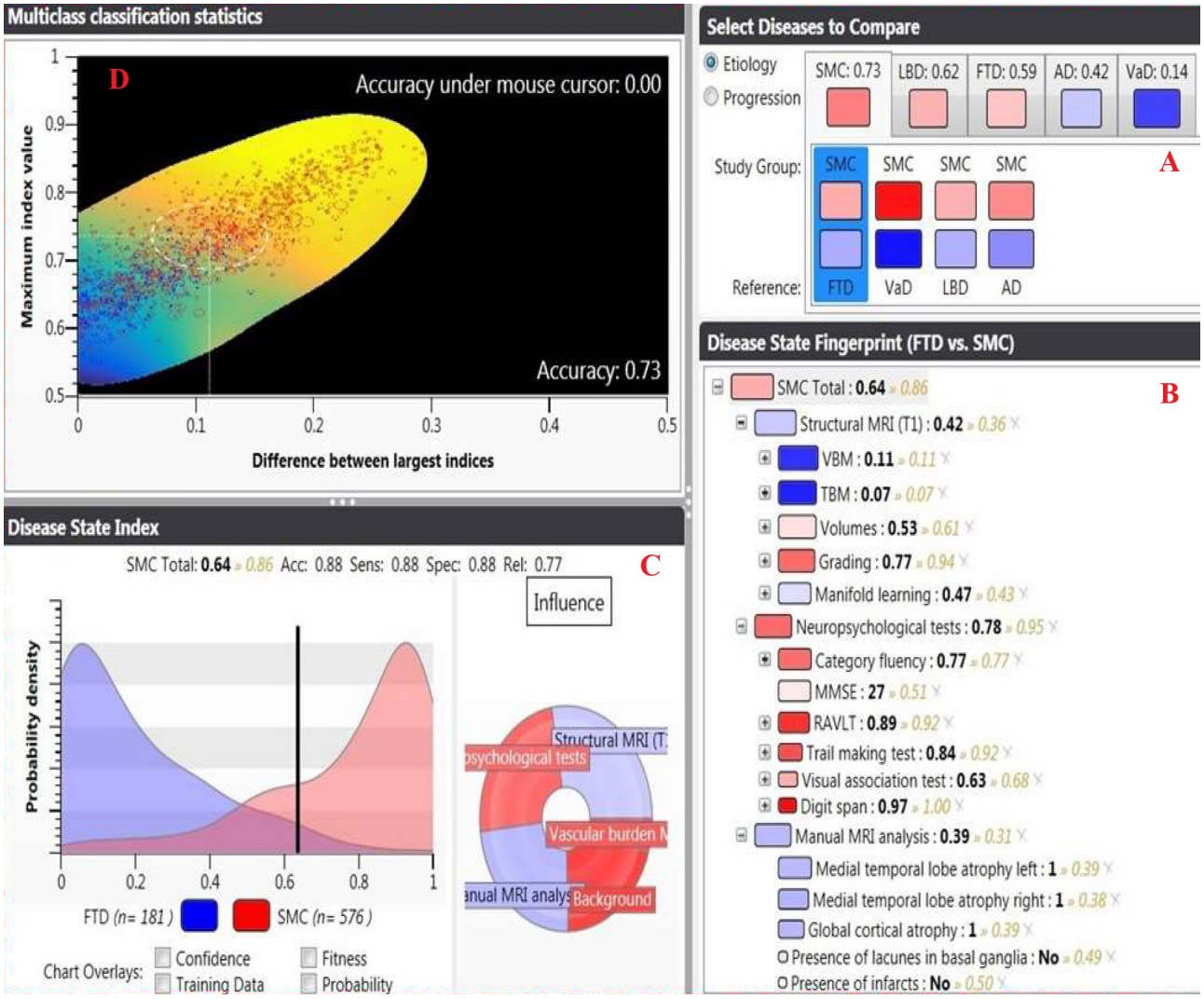

A. Visualization of the "overall" DSI value for the five disease states (SMC, LBD, FTD, AD, and VaD). B. Visualization of the DSF for FTD vs. SMC with weighted contribution of individual and combined biomarkers and diagnostic tests. C. Visualization of the relative influence of the individual biomarker or diagnostic test on the DSI classification as compared to the training data. D. Visualization of the "overall" classification.

Abbreviations: AD = Alzheimer's disease; DSF = disease state fingerprint; DSI = disease state index; FTD = Frontotemporal dementia; LBD = dementia with Lewy bodies; MRI = magnetic resonance imaging; SMC = subjective memory complaint; VaD = vascular dementia;

2. Objectives and hypothesis

The overall objective of this PhD project was to optimize the clinical value of 2-[^{18}F]FDG-PET by proposing three disease-specific 2-[^{18}F]FDG-PET biomarkers and to evaluate the added value of 2-[^{18}F]FDG-PET against commonly used biomarkers in the differential diagnosis of dementia.

Study I

The objective was to compare the added clinical value of CSF AD biomarkers and 2-[^{18}F]FDG-PET in a routine clinical setting with regards to diagnosis, prognosis, and patient management in patients suspected of having AD.

Hypothesis: CSF AD biomarkers have a higher clinical impact on diagnosis, prognosis and patient management in patients with AD compared in comparison to 2-[^{18}F]FDG-PET.

Study II

The objective was to develop a visual rating scale for CIS on 2-[^{18}F]FDG-PET and to validate the diagnostic accuracy in patients with DLB +/- dual pathology and patients with AD.

Hypothesis: The visual rating scale for CIS can differentiate patients with DLB +/- dual pathology from patients with AD.

Study III

The objective was to evaluate the value of 2-[^{18}F]FDG-PET biomarkers when added to commonly used diagnostic tests (cognitive tests, CSF and MRI biomarkers) in the differential diagnosis of dementia using a data-driven decision model.

Hypothesis: 2-[^{18}F]FDG-PET biomarkers will improve the diagnostic accuracy for patients with DLB and FTD.

3. Materials and methods

3.1 Study participants

The study participants were included from two independent cohorts:

3.1.1 The PredictND cohort

For this project, a subgroup from the PredictND study, referred to as the PredictND cohort, was included. In the PredictND study, a prospective cohort consisting of 779 participants was enrolled from four European memory clinics between March 2015 and June 2016 [127]. The participants were included if they were suspected of having cognitive complaints due to neurodegenerative disease (ND) and had a baseline mini-mental state examination (MMSE) score ≥ 18; a clinical dementia rating (CDR) global score ≤ 1.0 and had undergone a T1-weighted MRI ≥ 1.5 Tesla. The participants were excluded if they had excessive alcohol intake and/or substance abuse within the last 2 years or had a psychiatric or brain disorder diagnosis that could have caused the cognitive impairment.

The PredictND cohort consisted of 144 participants from the PredictND study who also had a 2-[^{18}F]FDG-PET scan at baseline (119 participants from the Danish Dementia Research Centre at Copenhagen University Hospital, Rigshospitalet, Copenhagen, Denmark (RH) and 25 participants from the Department of Gerontology and Geriatrics at "S. Maria della Misericordia" Hospital, Perugia, Italy (PER)). Flow chart for the PredictND cohort is shown in Figure 5.

At baseline, all participants underwent a standardized diagnostic program including medical history, physical and neurological examinations, cognitive testing with a neuropsychological test battery, blood screening and an MRI. On clinical indication, the standard diagnostic program was supplemented with ancillary investigations, such as further neuropsychological testing, CSF AD biomarkers, 2-[^{18}F]FDG-PET, DAT-SPECT, and amyloid PET.

After 12 months, the subjects had a standardized clinical follow-up visit including of a clinical interview with the patient, assessment of MMSE and CDR, and determination of a clinical follow-up diagnosis and disease course (progressed or stable). This follow-up diagnosis was used as reference diagnosis.

Figure 5. Flow chart for the PredictND cohort.

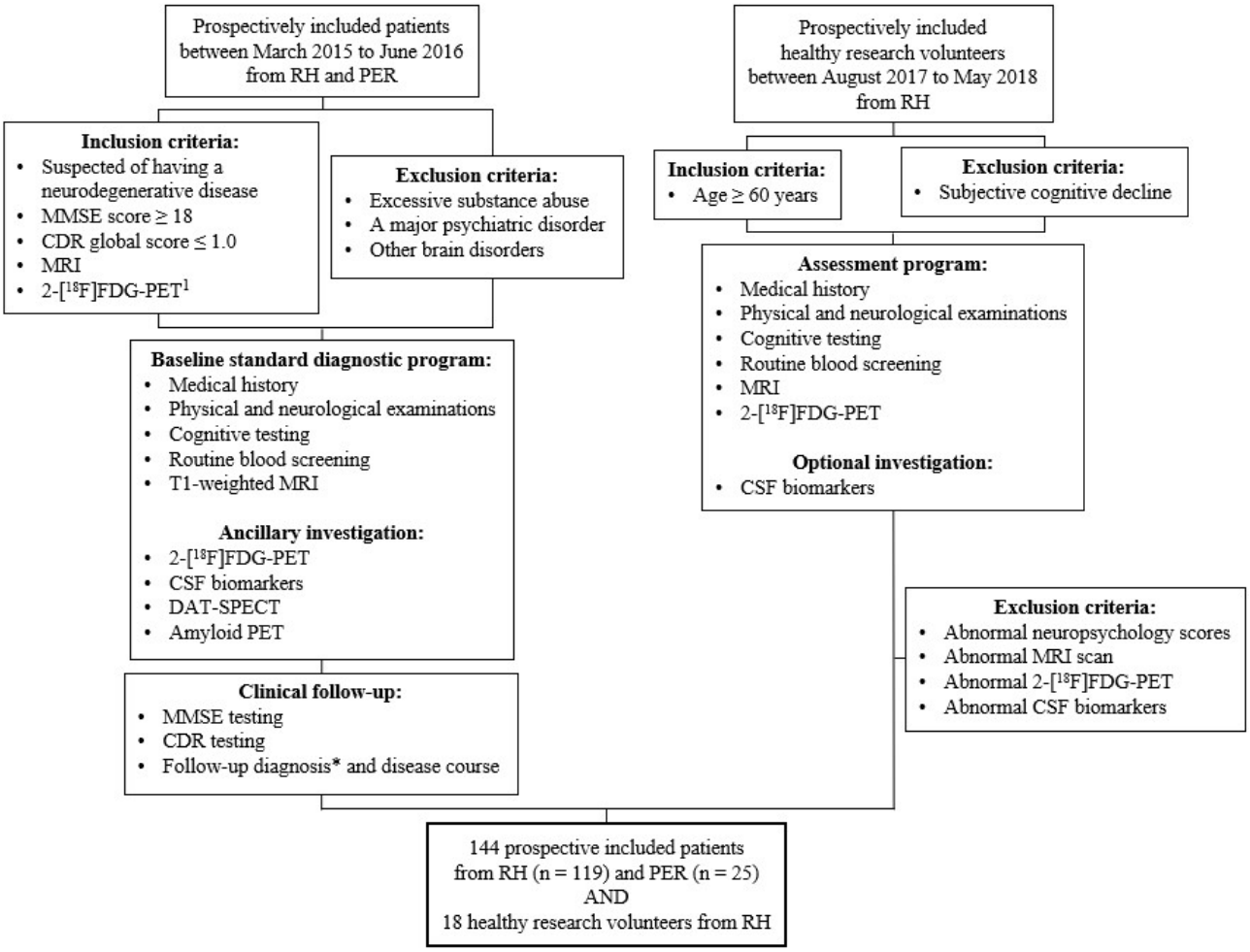

[1]Specific inclusion criteria for this study cohort.
*Follow-up diagnosis was made by an experienced dementia specialist according to clinical diagnostic criteria [3,24,37,50,57,105,136–139].
Abbreviations: Aβ = amyloid beta; CDR = clinical dementia rating; CSF = cerebrospinal fluid; DAT-SPECT = dopamine transporter single photon emission computed tomography; MMSE = mini-mental state examination; MRI = magnetic resonance imaging; n = number; PER = section of Gerontology and Geriatrics, University of Perugia and "S. Maria della Misericordia" Hospital of Perugia, Perugia, Italy; RH = memory clinic, Copenhagen University Hospital, Rigshospitalet, Copenhagen, Denmark; 2-[^{18}F]FDG-PET = 2-[^{18}F]fluoro-2-deoxy-D-glucose positron emission tomography;

Furthermore, a prospective cohort of 18 healthy research volunteers was enrolled between August 2017 and May 2018 from the memory clinic at RH as part of the PredictND study. Subjects were included if they were > 60 years old and excluded if they had subjective cognitive decline.

All volunteers underwent an assessment program included medical history, physical and neurological examinations, cognitive testing with a neuropsychological test battery, blood screening, an MRI, and a 2-[^{18}F]FDG-PET. CSF AD biomarkers was collected by lumbar puncture as an optional ancillary investigation.

The exclusion criteria were abnormal performance on neuropsychological assessment and/or abnormal MRI, 2-[^{18}F]FDG-PET and CSF AD biomarkers.

3.1.2 The COP cohort

The COP cohort consisted of 144 retrospectively identified patients diagnosed with AD, DLB, FTD, VaD, or SCD between 2009 and 2018 at four Danish memory clinics in the greater Copenhagen area (RH, Glostrup Hospital (GLO), Bispebjerg Hospital (BBH), and Roskilde Hospital (ROS)). Flow chart for the COP cohort is shown in Figure 6.

At baseline, all patients underwent a standard diagnostic program including medical history, physical and neurological examinations, cognitive testing with MMSE, routine blood screening, and an MRI. On clinical indication, the standard diagnostic program was supplemented with ancillary investigations, such as further neuropsychological testing, CSF AD biomarkers, 2-[^{18}F]FDG-PET, DAT-SPECT, and amyloid PET. The included patients had a minimum of clinical baseline data consisting of assessment with MMSE, an MRI, and a 2-[^{18}F]FDG-PET.
The clinical diagnosis was confirmed by an experienced dementia specialist based on all available clinical patient data including diagnostic test results from baseline to the most recent clinical follow-up. The confirmed diagnosis was used as reference diagnosis.

3.1.3 Diagnostic criteria for reference diagnosis

The syndrome diagnosis was established according to the clinical diagnostic criteria: the diagnosis of MCI was based on the Petersen and the national institute on aging-Alzheimer's association (NIA-AA) criteria for MCI [18,25,140], and the diagnosis of dementia was based on the NIA-AA criteria for all-cause dementia [3]. The diagnosis of SCD was based on the subjective cognitive decline initiative criteria for SCD [17], when the criteria for MCI and dementia were not met [3,18,25,140]

The etiological diagnosis was established according to the clinical diagnostic criteria: the NIA-AA criteria for AD [3]; the DLB consortium criteria for DLB [105]; the working group on frontotemporal dementia and Pick's disease criteria for FTD [50]; the national institute of neurological disorders and stroke and the association internationale pour la recherche et l-enseignement en neurosciences criteria for VaD [57]; the NIA-AA and the international working group 2 criteria for mixed AD [3,24]; the Relkin criteria for idiopathic normal pressure hydrocephalus (NPH) [136]; the movement disorder society criteria for PDD [37]; the national

Figure 6. Flow chart for the COP cohort.

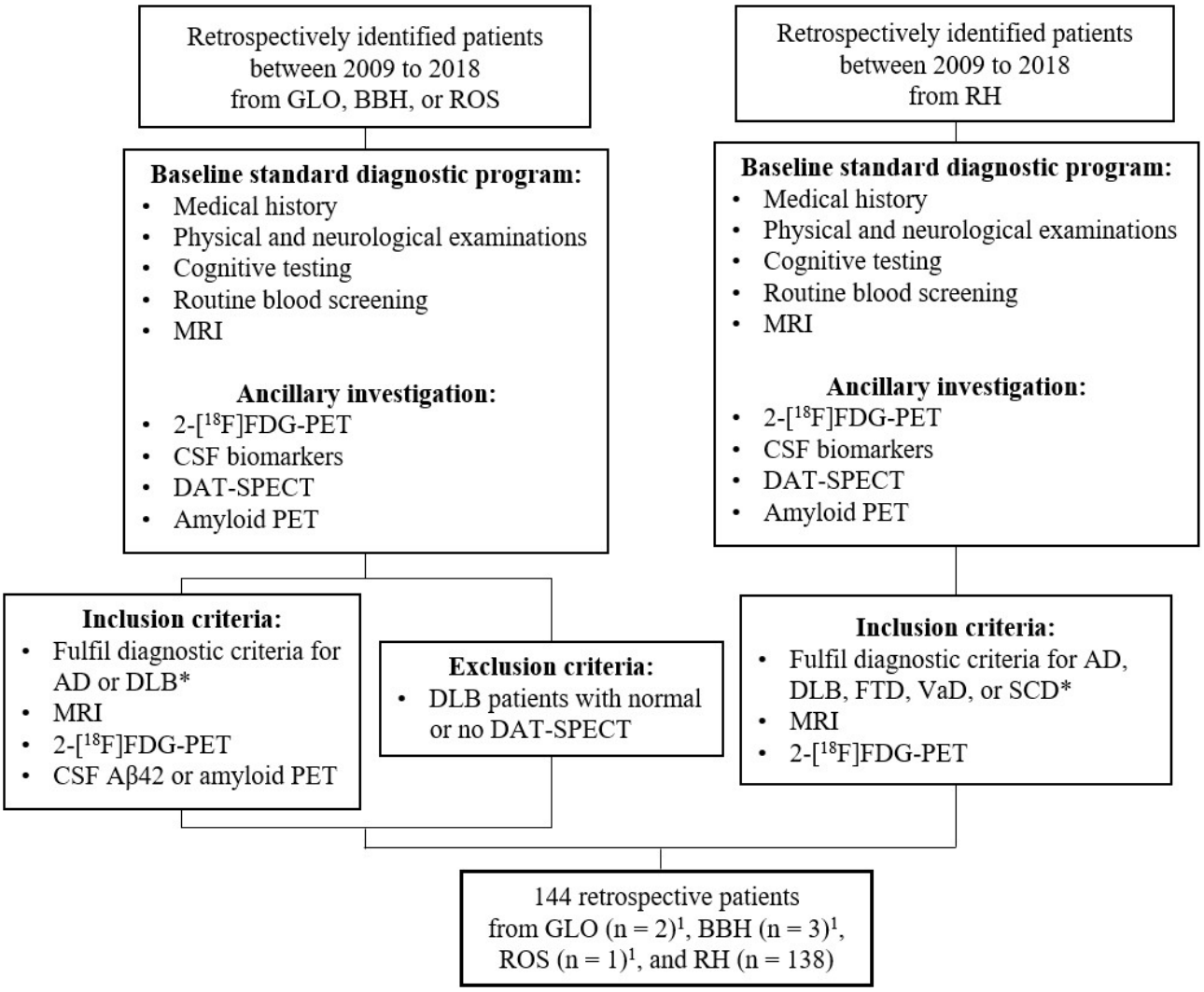

[1]Patients were exclusively included for study II.
* Reviewed by an experienced dementia specialist according to clinical diagnostic criteria [3,17,50–52,57,58,105]
Abbreviations: Aβ42 = amyloid beta 1-42; AD = Alzheimer's disease; BBH = memory clinic, Copenhagen University Hospital, Bispebjerg Hospital, Copenhagen, Denmark; CSF = cerebrospinal fluid; DAT-SPECT = dopamine transporter single photon emission computed tomography; DLB = dementia with Lewy bodies; FTD = frontotemporal dementia; GLO = memory clinic, Glostrup Hospital, Copenhagen, Denmark; MRI = magnetic resonance imaging; n = number; RH = memory clinic, Copenhagen University Hospital, Rigshospitalet, Copenhagen, Denmark; ROS = memory clinic, Department of Neurology, Zealand University Hospital, Roskilde, Denmark; SCD = subjective cognitive decline; VaD = vascular dementia; 2-[18F]FDG-PET = 2-[18F]fluoro-2-deoxy-D-glucose positron emission tomography;

institute of neurological disorders and stroke and the society for PSP criteria for PSP [137]; the Gilman criteria for MSA [138]; and the Riley & Lang criteria for CBD [139].

3.2 Study populations for each study

Flow chart for the study populations for each study is shown in Figure 7.

Figure 7. Flow chart for study I, II, and III.

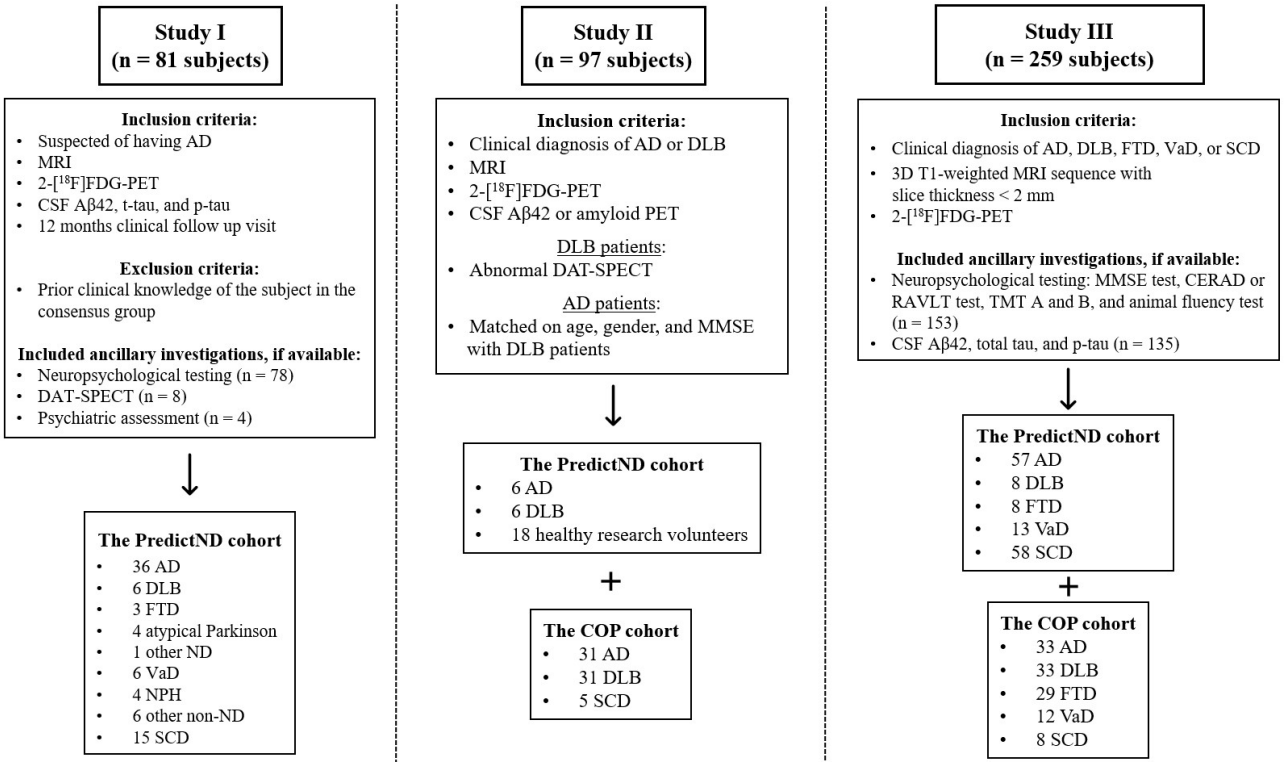

Abbreviations: Aβ42 = amyloid beta 1-42; AD = Alzheimer's disease; CERAD = consortium to establish a registry for Alzheimer's disease; CSF = cerebrospinal fluid; CT = computed tomography; DAT-SPECT = dopamine transporter single photon emission computed tomography; DLB = dementia with Lewy bodies; FTD = frontotemporal dementia; MMSE = mini-mental state examination; MRI = magnetic resonance imaging; NPH = normal pressure hydrocephalus; n = number; ND = neurodegenerative disease; p-tau = phosphorylated tau at threonine 181; PET = positron emission tomography; RAVLT = Rey auditory verbal learning task; SCD = subjective cognitive decline; TMT = trail making test; VaD = vascular dementia; 2-[^{18}F]FDG-PET = 2-[^{18}F]fluoro-2-deoxy-D-glucose positron emission tomography;

3.2.1 Study population for study I

The study population for study I consisted of 81 subjects suspected of having AD from the PredictND cohort.

The subjects were included, if they had an MRI, a 2-[^{18}F]FDG-PET, and measurement of CSF AD biomarkers. The subjects were excluded if the clinicians in the consensus group had prior clinical knowledge of the subject.

Ancillary investigations of neuropsychological testing, DAT-SPECT, and psychiatric assessment were included if available.

3.2.2 Study population for study II

The study population for study II consisted of 37 patients with DLB matched on age, gender, and MMSE with 37 patients with AD and 23 healthy, elderly controls from the PredictND and COP cohorts.

The dementia patients were included, if they had a structural scan, a 2-[^{18}F]FDG-PET image, and determination of the brain Aβ status, i.e. measurement of CSF Aβ42 or amyloid PET imaging. Additionally, patients with DLB also needed to have an abnormal DAT-SPECT scan to be included in the study.

The healthy elderly controls were included, if they had a structural scan and a 2-[^{18}F]FDG-PET. Measurements of CSF Aβ42 were included if available.

3.2.3 Study population for study III

The study population of study III consisted of 259 subjects diagnosed with either AD, DLB, FTD, VaD, or SCD from the PredictND and COP cohorts.

The subjects were included, if they had a 3D T1-weighted MRI sequence with a slice thickness < 2 mm and a 2-[^{18}F]FDG-PET. Ancillary investigations of neuropsychological testing (MMSE test, consortium to establish a registry for Alzheimer's disease (CERAD) or Rey auditory verbal learning task (RAVLT) test, trail making test (TMT) A and B, and animal fluency test) and measurements of CSF Aβ42, t-tau, and p-tau were included if available.

3.3 Diagnostic tests

3.3.1 Cognitive tests

The cognitive test scores were included when available. Global cognitive functioning was assessed with the MMSE [141]. The Addenbrooke's cognitive examination (ACE) test battery was used to assess memory, language, and visuospatial functioning [142]. In the PredictND cohort, evaluation of dementia staging was assessed with the CDR scale [143].

All participants from the PredictND cohort underwent a comprehensive neuropsychological test battery including the MMSE as well as the TMT A and B, and the animal fluency test for assessment of language and executive functioning [144,145]. For assessment of episodic memory, the CERAD word list and delayed recall were used in RH [146], whereas the RAVLT immediate and delayed recall were used in PER [147]. To compare the episodic memory test

scores, z-scores for CERAD and RAVLT tests were standardized to the baseline mean and standard deviation.

3.3.2 Cerebrospinal fluid biomarkers for Alzheimer's disease

The CSF AD biomarker measures of Aβ42, t-tau, and p-tau was performed on clinical indication and included when available. The CSF AD biomarkers were obtained by lumbar puncture and CSF was drained into polypropylene tubes and analysed locally according to standard operating procedures. CSF concentrations of Aβ42, t-tau, and p-tau were measured using commercially available enzyme-linked immunosorbent assays (Innotest, Fujirebio, Europe, Ghent, Belgium).
The local clinic-based cut-points for CSF AD biomarkers were used to define abnormal CSF values: Aβ42 values < 550 pg/mL, p-tau > 80 pg/mL, and t-tau > 400 pg/mL [148]. An abnormal concentration of CSF Aβ42 is indicated by Aβ+, whereas a normal concentration of CSF Aβ42 is indicated by Aβ−.

3.3.3 Neuroimaging

The MRI was acquired on clinical 1.0, 1.5 or 3.0 Tesla scanner systems. The three-dimensional T1-weighted gradient echo sequence and the fast fluid-attenuated inversion recovery (FLAIR) sequence were used for tissue-segmentation when available.
Visual assessment of the MRI was performed by an experience neuroradiologist and described in a written clinical MRI rapport as part of the routine clinical work-up.

2-[^{18}F]FDG-PET images were performed on clinical GE Medical, Philips, and Siemens PET scanners according to the international practice guideline [103].
Visual assessment of 2-[^{18}F]FDG-PET image was performed by an experienced nuclear medicine physician and described in a written clinical 2-[^{18}F]FDG-PET rapport as part of the routine clinical work-up.

The DAT-SPECT images were performed according to the international practice guideline [149]. Visual interpretation of the DAT-SPECT image was performed by an experienced nuclear medicine physician and described in a clinical written DAT-SPECT image report as part of the clinical work-up. Reduced symmetric or asymmetric tracer uptake in putamen and/or caudate nucleus was defined as abnormal, supported by the semiquantitative analysis of the specific binding ratio of striatum, caudate nucleus, and putamen relative to occipital cortex and the putamen/caudate nucleus uptake ratio [149,150].

The amyloid PET images were acquired according to the international practice guidelines [151]. Visual interpretation of the amyloid PET image was performed by an experienced nuclear medicine physician and described in a clinical written amyloid PET image report as part of the clinical work-up. Visual interpretation of increased tracer uptake in at least two cortical AD specific regions at the level of or above white matter supported by cortex-to-cerebellar grey matter uptake ratio > 1.5 was defined as abnormal [151]. An abnormal amyloid PET image was indicated as Aβ+, whereas a normal amyloid PET was indicated as Aβ−.

3.4 Study design for study I

The diagnostic consensus evaluation was done in a three-step incremental process by two blinded, experienced dementia specialists (either BBA and KSF or SGH and KSF) as shown in Figure 8. In the first step, the evaluation was based on the standard diagnostic program without CSF AD biomarkers and 2-[^{18}F]FDG-PET. In the second step, the result of the first biomarker (randomized to either CSF AD biomarkers or 2-[^{18}F]FDG-PET) was added, and finally in the third step, the result of the second biomarker was added. After a minimum of six months, the same two clinicians evaluated the same patients in the three-step incremental process with addition of the biomarkers in reverse order.

Figure 8. Flow diagram of the three-step incremental evaluation.

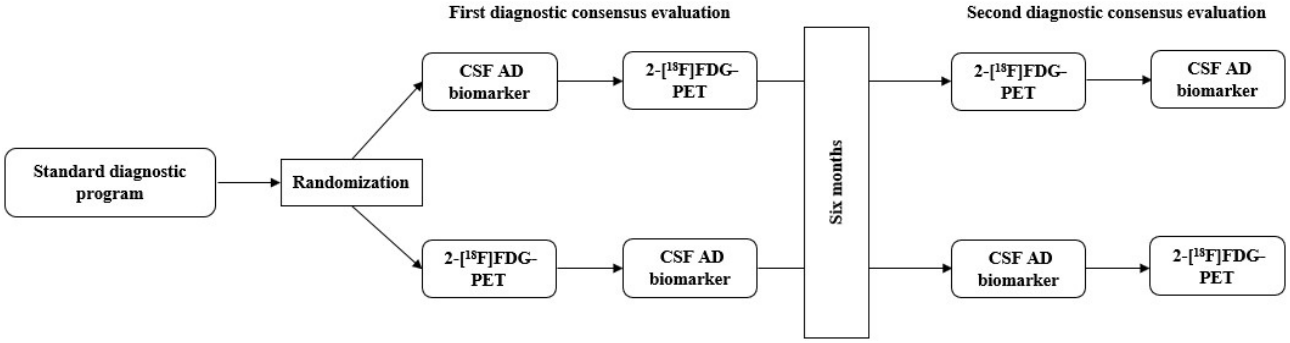

The three-step incremental diagnostic consensus evaluation was done by two blinded dementia specialists. In the first step, the evaluation was based solely on the standard diagnostic program. In the second step, the first biomarker was added (randomized to either CSF AD biomarkers or 2-[^{18}F]FDG-PET), and in the third step, the second biomarker was added. After 6 months, the same clinicians evaluated the same patients in the three-step incremental process with addition of the biomarkers in reverse order.
Abbreviations: AD = Alzheimer's disease; CSF = cerebrospinal fluid; standard diagnostic program = medical history, physical and neurological examinations, cognitive testing, routine blood screening, and MRI; 2-[^{18}F]FDG-PET = 2-[^{18}F]fluoro-2-deoxy-D-glucose positron emission tomography;
Figure from Gjerum et al., Manuscript, study I.

All clinical data were presented as anonymized case reports of each patient from the baseline visit, including clinical notes, result of cognitive tests and blood samples, and clinical written

MRI reports. The CSF AD biomarkers and 2-[^{18}F]FDG-PET images were presented separately in clinical written reports. The clinicians could inspect the images upon request.

At each step the clinicians reached a consensus decision on (1) baseline etiological diagnosis and confidence in diagnosis reported as a numeric rating scale (NRS) score between 0-100, (2) prediction of disease course after 12 months reported as stable or progressed and confidence in prediction of disease course reported as a NRS score between 0-100, (3) change in antidementia medication, for instance cholinesterase inhibitors, (4) change in psychosocial interventions including case manager, speech therapy, and physiotherapy, and (5) need for ancillary investigations, for instance CSF AD biomarkers, 2-[^{18}F]FDG-PET image, or other supplementary investigations such as DAT-SPECT, amyloid PET image, EEG, neuropsychologic assessment, and psychiatric assessment.

3.5 Analysis for study II

3.5.1 Analysis of quantitative CIS ratio

The three-dimensional T1-weighted gradient echo sequence was segmented using FreeSurfer (version 5.3.0) [152] to generate region of interests (ROIs) of PCC, precuneus, cuneus, and cerebellar grey matter for each hemisphere based on the Desikan-Killiany Atlas. The segmented MRI was fused with 2-[^{18}F]FDG-PET image to generate mean uptake volumes for the obtained ROIs. Only non-partial volume corrected PET data was used, as partial volume corrected by the Symmetric Geometric Transfer Matrix method [153] was not sufficiently robust. The mean standardized uptake value (SUV) of each region was normalized to cerebellum. In each hemisphere the ratio for the mean SUV in the PCC ROI was divided by the mean SUV in the combined precuneus plus cuneus ROIs, the quantitative CIS ratio was derived by averaging the ratios for each hemisphere [92].

3.5.2 Development and scoring of the visual CIS scale

The visual CIS scale was developed and adjusted to the final version by two experienced nuclear medicine physicians (IL and OH) based upon 2-[^{18}F]FDG-PET images from a training cohort of five DLB patients and ten AD patients with a wide range of CIS presentations.

A standardized reading approach was used for scoring of the visual CIS scale: 2-[^{18}F]FDG-PET image was displayed superimposed on the structural scan on a clinical workstation using SyngoVia (SyngoVia, MI Neurology, Siemens Healthcare, Erlangen, Germany). The image was

displayed in “PET Rainbow” in the three-way orthogonal view approximately along AC-PC plane with both sagittal and axial planes through PCC, precuneus, and cuneus with windowing adjusted to basal ganglia red and cerebellum green-to-yellow with red hues as shown in Figure 9. The visual CIS scoring was based on both sagittal and axial views.

Figure 9. Standardized reading approach for scoring of the visual CIS scale.

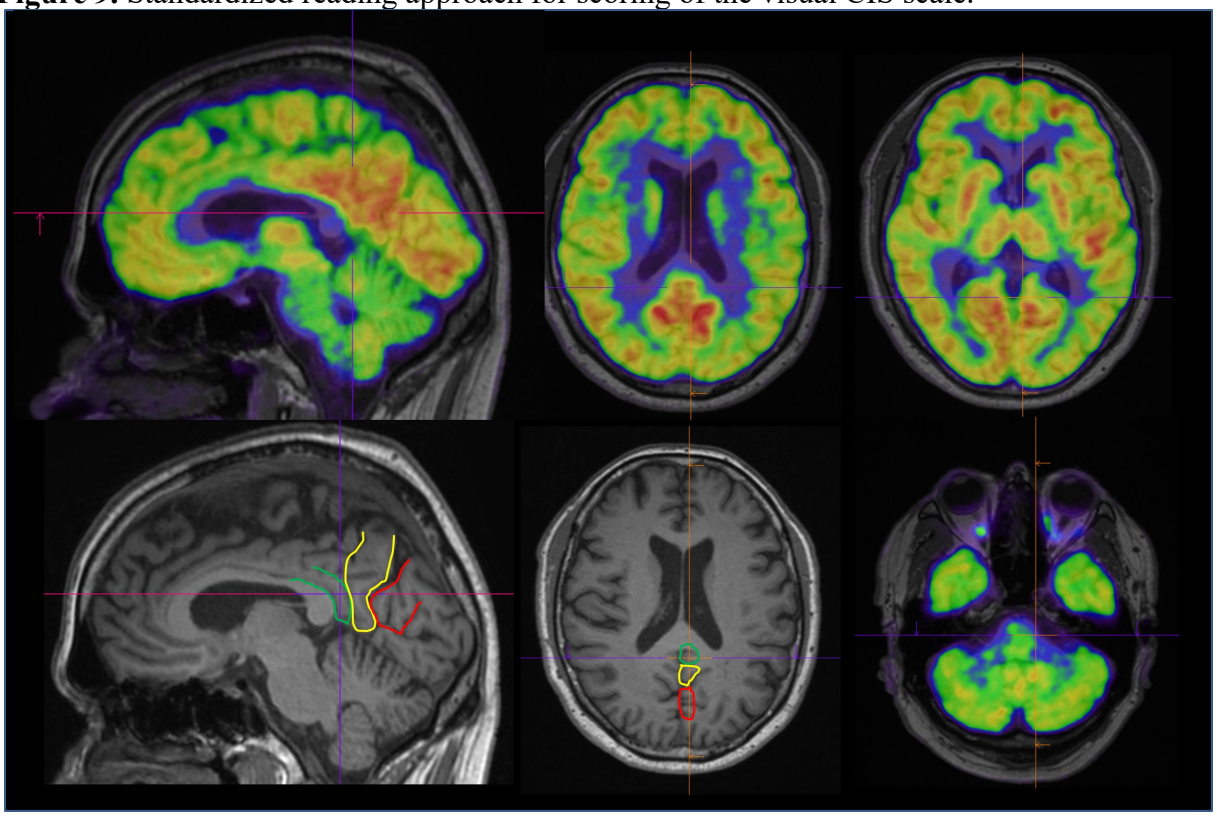

The MRI and 2-[^{18}F]FDG-PET image are displayed in saggital and axial plane in SyngoVia with orientation through PCC (green), precuneus (yellow) and cuneus (red).
Abbreviations: MRI = magnetic resonance imaging; PCC = posterior cingulate cortex; 2-[^{18}F]FDG-PET = 2-[^{18}F]fluoro-2-deoxy-D-glucose positron emission tomography;
Figure from Journal of the Neurological Sciences, 410; Gjerum L, Frederiksen KS, Henriksen OM, Law I, Anderberg L, Andersen BB, Bjerregaard E, Hejl A-M, Høgh P, Hasselbalch SG; A visual rating scale for cingulate island sign on ^{18}F-FDG-PET to differentiate dementia with Lewy bodies and Alzheimer's disease; 116645, 2020, with permission from Elsevier.

Scoring of the visual CIS scale was performed in the following order:

First, the degree of hypometabolism in PCC, precuneus, and cuneus for each hemisphere was classified as “none”, “mild”, or “moderate-to-severe”.

Second, the rating of CIS was based on the degree of hypometabolism in PCC, precuneus, and cuneus and the visual interpretation of the presence of CIS including the influence of central and cortical atrophy. CIS was rated for each hemisphere according to the following criteria:

0 = absent (PCC similar or lower than precuneus and cuneus)

1 = intermediate (e.g. PCC hypometabolic, but less than precuneus and cuneus, or only precuneus lower than PCC)

2 = present (typically PCC normal and both precuneus and cuneus lower)

The rating was changed to 0, if the uptake in precuneus or cuneus was reduced due to adjacent leukoaraiosis or ischemia on the structural scan.

Finally, the ratings from each hemisphere were summed to a visual CIS score.

For clinical operationalization the visual CIS score was classified as:

Score 0 = "no CIS"

Score 1-2 = "possible CIS"

Score 3-4 = "definite CIS"

Three examples of scorings of the visual CIS scale are shown in Figure 10.

3.5.3 Visual assessment of 2-[^{18}F]FDG-PET images

The visual assessment of 2-[^{18}F]FDG-PET images was performed in the following order: First, scoring of the visual CIS scale, then assessment of occipital hypometabolism, and finally determination of the forced diagnosis.

The visual interpretation was performed individually by two experienced nuclear medicine physicians (IL and OMH), who were blinded to all clinical data. In case of disagreements a consensus evaluation was performed between the two readers.

The evaluation of occipital hypometabolism and forced diagnosis was based upon the standardized reading approach in SyngoVia including the statistical surface projection comparisons. The occipital hypometabolism was assessed in lateral and medial occipital cortices and rated as "present" or "absent". The evaluation of the forced diagnosis was based on the overall visual interpretation of 2-[^{18}F]FDG-PET image including typical features of DLB (predominant occipital involvement with no or minimal involvement of frontal or anterior temporal cortex) and typical features of AD (anterior temporal, mesial temporal, or AD-like parietotemporal hypometabolism with occipital sparing). The readers were forced to determine a diagnosis of the most likely etiology ("DLB", "AD", "other abnormal", or "normal").

Figure 10. 2-[^{18}F]FDG-PET images with examples of the visual CIS-scores.

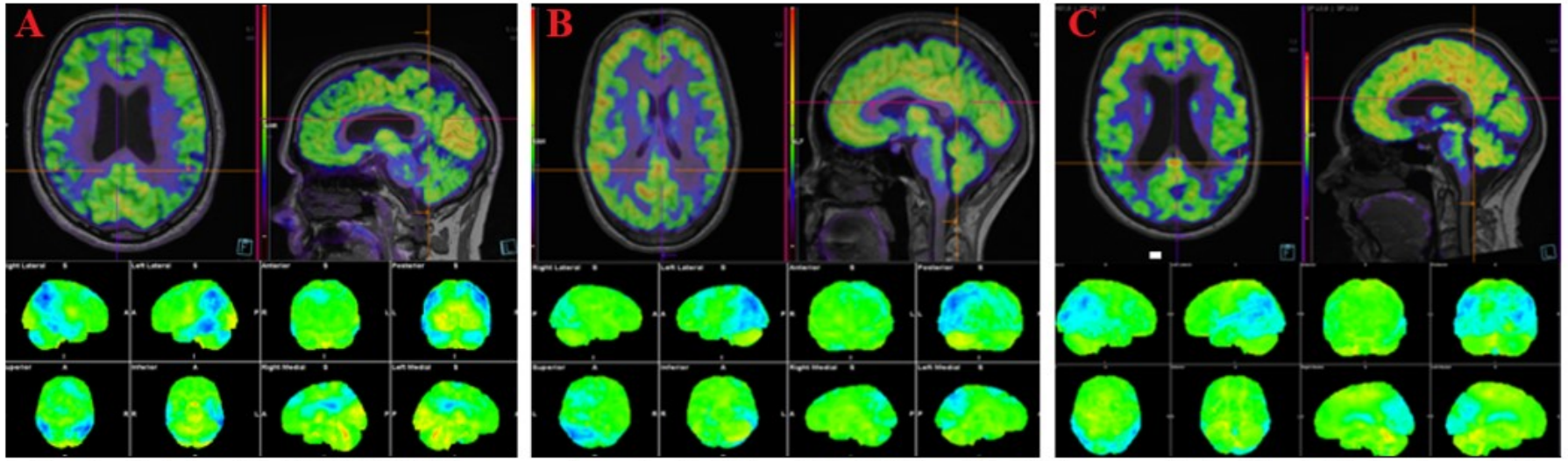

Axial and sagittal view of the 2-[^{18}F]FDG-PET image superimposed on the high-resolution 3D T1-weighted MRI sequence (top) and the statistical surface projections (right/left lateral and anterior/posterior view) using cerebellum as reference region compared to a healthy age-matched control group (bottom).
A. 71-years old male diagnosed with AD with MMSE score 25 and a positive Aβ biomarker. Visual CIS score = 0.
B. 66-years old female diagnosed with DLB with MMSE score 29 and a positive Aβ biomarker. Visual CIS score (R+L) = 1 (0 + 1).
C. 75-years old female diagnosed with DLB with MMSE score 29 and a negative Aβ biomarker. Visual CIS score (R+L) = 4 (2 + 2).
Abbreviations: Aβ = amyloid beta; AD = Alzheimer's disease; CIS = cingulate island sign; DLB = dementia with Lewy bodies; L = left; MMSE = mini-mental state examination; MRI = magnetic resonance imaging; R = right; 2-[^{18}F]FDG-PET = 2-[^{18}F]fluoro-2-deoxy-D-glucose positron emission tomography;
Modified figure from Journal of the Neurological Sciences, 410; Gjerum L, Frederiksen KS, Henriksen OM, Law I, Anderberg L, Andersen BB, Bjerregaard E, Hejl A-M, Høgh P, Hasselbalch SG; A visual rating scale for cingulate island sign on ^{18}F-FDG-PET to differentiate dementia with Lewy bodies and Alzheimer's disease; 116645, 2020, with permission from Elsevier.

3.6 Analysis for study III

3.6.1 Analysis of MRI biomarkers

The three-dimensional T1-weighted gradient echo sequence with slice thickness < 2 mm was used to derive the volumetric and morphometric biomarkers in the DSI classifier [129,130]. Volumes of 133 brain regions were extracted from the segmented T1-weighted image by a fully automatic multi-atlas segmentation algorithm [129] based on the Neuromorphometric atlases (Neuromorphometrics Inc, Massachusetts, USA).

Volumes of 10 clinically relevant regions were included as MRI biomarkers: Hippocampus, temporal pole, whole cortex, frontal cortex, temporal cortex, medial temporal cortex, parietal cortex, occipital cortex, lateral ventricle, and inferior lateral ventricle.

Additionally, four MRI biomarkers were derived from the segmented T1-weighted images: The anterior vs. posterior index (API-MRI) was derived as a z-score ratio between the segmented volumes of temporal and frontal lobe regions, and the segmented volumes of parietal and occipital lobe regions [154].

The two morphometric indices were used to quantify atrophy of the brain tissue. The VBM computed differences in local grey matter concentrations [155], whereas the TBM computed differences in local volumes [156]. Specific patterns of locations with significant differences in the local concentrations or volumes were defined for each pairwise diagnostic group, and the global VBM and TBM indices indicated the similarity of a patient image to these reference patterns [130].

The ROI-based grading measured the similarities of intensities within the ROIs to a reference image database of subjects with known diagnoses [131].

The vascular changes were quantified by segmentation of white matter hyperintensities and cortical and lacunar infarcts on FLAIR sequences [157]. The vascular burden was estimated as the summed volume of white matter hyperintensities and cortical infarcts combined with the weighted volume of lacunar infarcts [130].

3.6.2 Analysis of 2-[^{18}F]FDG-PET biomarkers

2-[^{18}F]FDG-PET image was co-registered to the segmented MRI to generate uptake values from the segmented brain regions on 2-[^{18}F]FDG-PET, i.e. 2-[^{18}F]FDG-PET ROIs. The mean uptake value of each 2-[^{18}F]FDG-PET ROI was normalized to the cerebellum.

Volumes of 12 clinically relevant regions were included as 2-[^{18}F]FDG-PET biomarkers: Anterior cingulate gyrus, calcarine cortex, middle cingulate gyrus, posterior cingulate gyrus, precuneus, precentral gyrus, whole cortex, frontal cortex, temporal cortex, medial temporal cortex, parietal cortex, and occipital cortex. 2-[^{18}F]FDG-PET biomarkers based on previous 2-[^{18}F]FDG-PET studies demonstrating specific disease patterns of hypometabolism as hallmarks for AD, FTD, and DLB, respectively [3,34,50–52,158–163]. In addition, three 2-[^{18}F]FDG-PET biomarkers were derived from the segmented 2-[^{18}F]FDG-PET image. The API-PET was defined as a z-scored ratio between the mean uptake in frontal and temporal lobe regions, and the mean uptake in parietal and occipital lobe regions, and is similar to and uses the same regions as the API-MRI [154]. The occipital vs. temporal index was derived as the uptake in occipital lobe region divided by the uptake in temporal lobe region. The biomarker was proposed to improve differentiating between AD and DLB, where the temporal region is often affected in AD and the occipital region is often affected in DLB, respectively [3,34]. The CIS ratio was derived as the uptake in PCC divided by the summed uptake in precuneus and cuneus [92].

3.6.3 Data analysis in the DSI classifier

The DSI classifier is composed of two components: fitness and relevance [128]. Fitness is calculated for a biomarker or test result of the subject as $f(x) = FN(x)/(FN(x)+FP(x)$, where FN is the false-negative error rate, and FP is the false-positive error rate in the reference data when using the biomarker or test result value x as a cut-off value in classification. Relevance is defined as the goodness of a biomarker or test result as sensitivity+specificity-1.

A DSI value is calculated as a weighted average of fitness values: $DSI = \Sigma (\text{relevance} \cdot \text{fitness})/\Sigma \text{ relevance}$.

The volumetric imaging biomarkers were corrected for intracranial volume, age, and sex using the methods proposed in [164,165], while the other features were corrected for age and sex [165].

3.7 Statistical analysis

An overview of the statistical analyses for each study is shown in Table 6.

The differences between diagnostic groups were assessed with Kruskal-Wallis tests followed by Mann-Whitney post-hoc tests or one-way ANOVA tests followed by post-hoc unpaired t-tests for continuous variables, and Pearson's or Fischer's Chi-square test for count variables,

where appropriate. The post-hoc tests were Bonferroni corrected in study I and III and Tukey corrected in study II.

The balanced accuracy (bal. acc.) was calculated as the average of sensitivity and specificity for the cut-off score or pairwise comparison, and was computed to adjust the results for the imbalance number in the disease groups in the dataset [166].

Table 6. Overview of the statistical analyses for each study.

Statistical analyses	Study I	Study II	Study III
Kruskal-Wallis, one-way ANOVA, and Chi-square tests with post-hoc Bonferroni corrections	X		X
Kruskal-Wallis, one-way ANOVA, and Chi-square test with post-hoc Tukey corrections		X	
McNemar's test	X		
Linear mixed model with post-hoc Bonferroni corrections	X		
Cohens weighted Kappa		X	
Spearman's correlation with false discovery rate corrections		X	
Sensitivity and specificity		X	
Bal. acc. and AUC		X	X
10-fold cross-validation			X

Abbreviations: AUC = area under the curve; bal. acc = balanced accuracy;

In study I, McNemar's test was used to evaluate the paired comparison between the baseline diagnoses, prediction of disease course, change in antidementia medication and psychosocial interventions, and need for further investigations. A linear mixed model with post-hoc Bonferroni corrections was used to estimate the effect of adding the two biomarkers individually on confidence for diagnosis.

In study II, the interrater agreement was quantified by Cohen's weighted Kappa. The Spearman's correlation analysis was applied for comparing the quantitative CIS ratio values and the visual CIS scores, and for verifying the correlations between visual CIS score, MMSE score, age, education, and symptom duration for all subjects and DLB patients. For the latter, the Spearman correlation results were corrected by false discovery rate correction. The diagnostic accuracy for each binary disease group comparison was reported as sensitivity, specificity, bal. acc., and area under the curve (AUC). The optimal cut-off was established by maximizing the Youden index [167].

In study III, the 10-fold cross-validation approach was applied using the whole study population data (n = 259). The accuracy of each individual diagnostic test and each or combined diagnostic test group for pairwise comparisons was reported as bal. acc. and AUC based on the DSI values.

To obtain the optimal sets of diagnostic tests for each pairwise comparison, a feature selection method was applied to include only a subset of relevant diagnostic tests and exclude redundant or irrelevant diagnostic tests. The diagnostic tests with the highest accuracy were added one by one until the overall AUC did not increase as previously described [135]. The feature selection was first performed using complete cross-validation to produce unbiased classification results. After that, the feature selection was applied to all data without cross-validation to produce single optimal feature set to show which features typically were selected.

The statistical analyses were performed using SAS Studio software, version 9.4 (SAS Institute Inc., Cary, NC, USA). A MATLAB toolbox was used in the DSI analyses [168]. The analyses were performed in MATLAB, version R2015b (MathWorks, Natick, MA).
A two-sided p-value < 0.05 was considered indicative of statistical significance.

3.8 Ethical considerations

All participants in the PredictND cohort gave a written informed consent as part of the inclusion in the PredictND study. The study was approved by the local Medical Ethical Committees: The Regional Committee on Medical Research Ethics of the Capital Region of Denmark (Approval no.: H-1-2014-126) and Italy (Approval no.: CEAS 2381/14). The Data Processing Agreement was approved by the Data Protection Agency in Denmark (Journal no.: 2012-58-0004).

The study of subjects from the COP cohort was approved by the Danish Patient Safety Authority (no. 3-3013-2703/1). Data was extracted from the Danish Clinical registries with approval from the Danish Clinical Quality Program – National Clinical Registries (DANDEM-2017-11-21). The Data Processing Agreement was approved by the Data Protection Agency in Denmark (Journal no.: 2012-58-0004).

4. Results

The main findings for each study are presented in the following sections. For further details, please see Study manuscripts for Study I-III.

4.1 Results for study I

For this study, 81 subjects (36 AD, 6 DLB, 3 FTD, 4 atypical Parkinson, 1 with other ND, 6 VaD, 4 NPH, 6 with other non-ND, and 15 SCD) were included. Based on the reference diagnosis, the subjects were divided into four groups: AD (AD, atypical AD, mixed AD); other ND (DLB, FTD, PSP, MSA, CBD, and other ND); non-ND (VaD, NPH, and other non-ND); and SCD.

As shown in Table 7, seven patients were additionally classified correct after adding CSF AD biomarkers to the standard diagnostic program as compared to adding 2-[^{18}F]FDG-PET (66 vs. 59 patients, p = 0.09) due to a better recognition of AD and non-ND. The impact on diagnostic confidence was similar for adding the two biomarkers individually, apart from a significant increase in diagnostic confidence for correctly diagnosed AD after adding CSF

Table 7. Added value of CSF AD biomarkers and 2-[^{18}F]FDG-PET on diagnosis and diagnostic confidence.

Diagnosis, n (%)	All patients		AD		Other ND		Non-ND		SCD	
	Cor.	Incor.	Cor.	Incor.	Cor.	Incor.	Cor.	Incor.	Cor.	Incor.
Standard program + CSF AD biomarkers	66 (81)	15 (19)	35 (97)	1 (3)	8 (57)	6 (43)	8 (50)	8 (50)	15 (100)	0
Standard program + 2-[^{18}F]FDG-PET	59 (73)	22 (27)	32 (89)	4 (11)	8 (57)	6 (43)	5 (31)	11 (69)	14 (93)	1 (7)
Diagnostic confidence, mean NRS score ±SD										
Standard program + CSF AD biomarkers	81±14	71±16	88±11*	85	79±16	72±15	66±14	69±18	76±11	NA
Standard program + 2-[^{18}F]FDG-PET	81±13	65±12	83±11	63±18	81±17	69±14	67±11	65±9	80±14	50

*Statistical significantly different from 2-[^{18}F]FDG-PET ($p < 0.05$).
Abbreviations: AD = Alzheimer's disease; Cor. = correct; CSF = cerebrospinal fluid; Incor. = incorrect; n = number; ND = neurodegenerative disease; NA = not applicable; NRS = numeric rating scale; SCD = subjective cognitive decline; SD = standard deviation; standard program = standard diagnostic program including medical history, physical and neurological examinations, cognitive testing, routine blood screening, and MRI; 2-[^{18}F]FDG-PET = 2-[^{18}F]fluoro-2-deoxy-D-glucose positron emission tomography;
Modified table from Gjerum et al., Manuscript, study I.

AD biomarkers compared to adding 2-[^{18}F]FDG-PET (mean NRS scores: 88±11 vs. 83±11, p = 0.04).

The clinical impact of adding the two biomarkers individually to a standard diagnostic program was similar for predicting disease course after 12 months (36 correctly classified patients for CSF AD biomarkers vs. 33 correctly classified patients for 2-[^{18}F]FDG-PET, p = 0.32). Moreover, the impact on the clinicians' confidence in the predicted disease course was similar for the two biomarkers.

For correctly classified patients, the impact of adding CSF AD biomarkers and 2-[^{18}F]FDG-PET individually to a standard diagnostic program was similar for change in anti-dementia medication (13 vs. 11 patients, p = 0.66) and psychosocial interventions (12 vs. 16 patients, p = 0.41) as shown in Table 8. After adding CSF AD biomarkers to the standard diagnostic program 24 patients (30%) changed to no need for ancillary investigations compared to 17 patients (21%) after adding 2-[^{18}F]FDG-PET (p = 0.21). The total number of correctly classified AD patients with need for ancillary investigations was significantly reduced after adding CSF AD biomarkers to a standard diagnostic program compared to adding 2-[^{18}F]FDG-PET (19 vs. 8 patients, p = 0.007).

Table 8. Impact of CSF AD biomarkers and 2-[^{18}F]FDG-PET on patient management.

According to FU diagnosis	All patients		AD		Other ND		Non-ND		SCD	
	Cor.	Incor.	Cor.	Incor.	Cor.	Incor.	Cor.	Incor.	Cor.	Incor.
Change in anti-dementia medication, n (%)										
Standard program + CSF AD biomarkers	13 (16)	2 (2)	12 (33)	0	0	0	1 (6)	2 (13)	0	0
Standard program + 2-[^{18}F]FDG-PET	11 (14)	3 (4)	10 (28)	1 (3)	0	1 (7)	1 (6)	1 (6)	0	0
Change in psychosocial interventions, n (%)										
Standard program + CSF AD biomarkers	12 (18)	2 (2)	11 (31)	0	0	0	0	2 (13)	0	0
Standard program + 2-[^{18}F]FDG-PET	16 (20)	5 (6)	11 (31)	1 (3)	2 (14)	1 (7)	3 (19)	3 (19)	0	0
Reduced need for ancillary investigations, n (%)										
Standard program + CSF AD biomarkers	24 (30)	3 (4)	19 (53) *	0	0	1 (7)	2 (13)	2 (13)	3 (20)	0
Standard program + 2-[^{18}F]FDG-PET	17 (21)	1 (1)	8 (22)	0	1 (7)	1 (7)	0	0	6 (40)	0

*Statically significant difference as compared 2-[^{18}F]FDG-PET (p < 0.05).
Abbreviations: AD = Alzheimer's disease; Cor. = correct; CSF = cerebrospinal fluid; FU = follow-up; Incor. = incorrect; n = number; ND = neurodegenerative disease; SCD = subjective cognitive decline; standard program = standard diagnostic program including medical history, physical and neurological examinations, cognitive testing, routine blood screening, and MRI; 2-[^{18}F]FDG-PET = 2-[^{18}F]fluoro-2-deoxy-D-glucose positron emission tomography;
Table from Gjerum et al., Manuscript, study I.

4.2. Results for study II

For this study, 97 subjects (37 DLB, 37 AD, and 23 controls) were included, but due to poor quality of three 2-[^{18}F]FDG-PET images, two patients with DLB and one patient with AD were excluded.

There were no significant differences in the baseline demographics between the two dementia groups (DLB and AD) after exclusion of the three patients, as shown in Table 9.

Table 9. Baseline demographics for study II.

	AD	DLB	Controls
Subjects, n	36	35	23
Female, n (%)	11 (30.6%)	10 (28.6%)	8 (34.8%)
Age, mean years ±SD	70.6 ±6.3	69.9 ±6.8	68.7 ±6.1
MMSE, mean score ±SD	25.8 ±2.9*	26.3 ±3.2*	29.3 ±1.2
Education, mean years ±SD	13.5 ±2.8	12.8 ±2.8*	14.5 ±2.4
Symptom duration, mean years ±SD	3.1 ±3.1	2.9 ±2.8	NA

*Statistical significantly different from controls ($p < 0.05$).

Abbreviations: AD = Alzheimer's disease; DLB = dementia with Lewy bodies; MMSE = mini-mental state examination; n = number; NA = not applicable; SD = standard deviation;

Modified table from Journal of the Neurological Sciences, 410; Gjerum L, Frederiksen KS, Henriksen OM, Law I, Anderberg L, Andersen BB, Bjerregaard E, Hejl A-M, Høgh P, Hasselbalch SG; A visual rating scale for cingulate island sign on ^{18}F-FDG-PET to differentiate dementia with Lewy bodies and Alzheimer's disease; 116645, 2020, with permission from Elsevier.

The interrater agreement of the visual CIS scores between the two readers was moderate-to-high (Cohen's weighted Kappa coefficient, $\kappa = 0.73$, 95% CI 0.63-0.83). The quantitative CIS ratio analysis was performed in the 77 subjects with a high-resolution 3D T1-weighted MRI sequence. The correlation between the visual CIS scores and the quantitative CIS ratio values was moderate (Spearman's correlation coefficient, $r = 0.60$, 95% CI 0.44-0.73; $p < 0.0001$).

The median visual CIS score was significantly higher for DLB patients and the DLB subgroups (DLB Aβ− and DLB Aβ+) compared to both AD patients and controls ($p < 0.05$). Whereas, the median visual CIS score was higher for DLB Aβ− patients compared to DLB Aβ+ patients reaching a trend level ($p = 0.06$) (Table 10).

As shown in Table 11, a cut-off score ≥ 2 on the visual CIS scale had a sensitivity of 51%, a specificity of 92%, and a bal. acc. of 72% for DLB vs. AD, whereas a cut-off value of ≥ 0.98 on the quantitative CIS ratio had a sensitivity of 88%, a specificity of 67%, and a bal. acc. of 77%. For DLB Aβ− vs. AD, a cut-off score of 4 on the visual CIS scale had a sensitivity of 63%, a specificity of 97%, and a bal. acc. of 80%, whereas a cut-off value of

Table 10. Visual CIS scores.

	AD	DLB	Controls	DLB Aβ−	DLB Aβ+
Median score [IQR]	0 [0.5]	2 [4]*	0 [0]	4 [4]*‡	1 [2.5]*

*Statistical significantly different from AD and controls ($p < 0.05$).
‡ Different from DLB Aβ+ at trend level ($p = 0.06$).
Abbreviations: Aβ = amyloid beta; AD = Alzheimer's disease; CIS = cingulate island sign; DLB = dementia with Lewy bodies; IQR = interquartile range;
Modified table from Journal of the Neurological Sciences, 410; Gjerum L, Frederiksen KS, Henriksen OM, Law I, Anderberg L, Andersen BB, Bjerregaard E, Hejl A-M, Høgh P, Hasselbalch SG; A visual rating scale for cingulate island sign on ^{18}F-FDG-PET to differentiate dementia with Lewy bodies and Alzheimer's disease; 116645, 2020, with permission from Elsevier.

≥ 1.04 on the quantitative CIS ratio had a sensitivity of 86%, a specificity of 87%, and a bal. acc. of 86%. When comparing the performance of the two methods by an AUC analysis, there were no significant difference, although the quantitative CIS ratio had a slightly better performance compared to the visual CIS scale.

Table 11. Diagnostic accuracy of the visual CIS scale and quantitative CIS ratio.

DLB versus AD	Sens.	Spec.	Bal. acc.	AUC (95% CI)
Visual CIS score ≥ 2	51%	92%	72%	0.77 (0.64-0.89)
Quantitative CIS ratio value ≥ 0.98	88%	67%	77%	0.82 (0.70-0.94)
DLB Aβ− versus AD				
Visual CIS score = 4	63%	97%	80%	0.85 (0.71-0.99)
Quantitative CIS ratio value ≥ 1.04	86%	87%	86%	0.88 (0.77-0.98)
DLB Aβ+ versus AD				
Visual CIS score ≥ 1	56%	75%	66%	0.65 (0.45-0.85)
Quantitative CIS ratio value ≥ 0.99	80%	77%	78%	0.74 (0.54-0.94)
DLB Aβ− versus DLB Aβ+				
Visual CIS score = 4	60%	81%	70%	0.73 (0.52-0.93)
Quantitative CIS ratio value ≥ 1.04	86%	50%	68%	0.66 (0.43-0.90)

Abbreviations: Aβ = amyloid beta; AD = Alzheimer's disease; AUC = area under the curve; bal. acc. = balanced accuracy; CI = confidence interval; CIS = cingulate island sign; DLB = dementia with Lewy bodies; Sens. = sensitivity; Spec. = specificity;
Modified table from Journal of the Neurological Sciences, 410; Gjerum L, Frederiksen KS, Henriksen OM, Law I, Anderberg L, Andersen BB, Bjerregaard E, Hejl A-M, Høgh P, Hasselbalch SG; A visual rating scale for cingulate island sign on ^{18}F-FDG-PET to differentiate dementia with Lewy bodies and Alzheimer's disease; 116645, 2020, with permission from Elsevier.

4.3 Results for study III

For this study, 259 subjects (90 AD, 41 DLB, 37 FTD, 25 VaD, and 66 SCD) were included. The pairwise comparison for each diagnostic test was presented as bal. acc. and AUC as shown in Table 12. Overall, the episodic memory tests had a high classification accuracy for distinguishing subjects with SCD from the dementia groups (bal. acc. ranging from 71%-91%), whereas CSF AD biomarkers had a good accuracy for distinguishing AD from the other groups (bal. acc. ranging from 73%-84%), except CSF Aβ42 for AD vs. DLB (bal. acc.

of 50%). MRI biomarkers of vascular burden had a good accuracy for distinguishing VaD from the other groups (bal. acc. of 80%-89%). 2-[^{18}F]FDG-PET biomarker occipital vs. temporal index had a high accuracy for distinguishing AD vs. DLB compared to the two supportive biomarkers for DLB, occipital hypometabolism and CIS (bal. acc.: occipital vs. temporal index: 79% vs. occipital hypometabolism: 62% vs. CIS: 67%). For AD vs. FTD, the CSF AD biomarkers and API-PET had a high accuracy, whereas API-MRI had a lower accuracy (bal. acc.: CSF AD biomarkers: 79%-83% vs. API-PET: 76% vs. API-MRI: 64%).

Table 12. The pairwise comparison of individual diagnostic tests.

Bal. acc./AUC	AD vs. DLB	AD vs. FTD	AD vs. VaD	AD vs. SCD	DLB vs. FTD	DLB vs. VaD	DLB vs. SCD	FTD vs. VaD	FTD vs. SCD	VaD vs. SCD
Cognitive tests										
MMSE	59/58	39/36	55/54	85/89	56/59	56/54	71/79	52/53	79/88	83/89
Memory (learning)	48/59	62/62	50/46	91/97	43/39	61/63	88/93	71/60	90/90	87/94
Memory (recall)	64/68	66/67	59/58	89/96	51/51	56/49	85/92	64/54	84/89	81/90
CSF										
Aβ42	50/50	79/82	78/86	83/89	79/77	75/81	81/84	57/57	60/63	57/55
t-tau	77/80	83/84	80/83	84/88	58/56	61/55	61/58	29/27	33/35	35/33
p-tau	73/76	83/90	82/88	78/88	63/66	69/63	64/57	11/4	51/62	20/21
MRI										
Frontal cortex	59/62	55/58	57/59	71/74	63/69	68/69	59/64	41/34	70/78	72/77
Temporal cortex	57/64	46/43	66/71	84/90	56/61	52/56	75/82	54/64	75/85	74/76
Medial temporal cortex	58/61	51/51	60/66	80/91	45/51	38/38	80/85	54/56	75/84	75/83
Parietal cortex	48/48	56/63	54/58	68/74	59/67	50/48	68/74	68/72	62/65	76/81
Occipital cortex	59/65	52/45	60/61	61/63	59/64	46/51	68/75	49/49	51/55	60/65
API-MRI	62/63	64/70	56/58	61/64	76/79	41/35	44/43	72/78	74/82	34/32
Vascular burden	45/46	51/50	82/89	63/69	59/59	80/85	64/70	83/89	67/69	89/93
2-[^{18}F]FDG-PET										
Frontal cortex	47/43	58/59	42/40	74/79	58/63	44/41	72/78	55/56	76/85	72/77
Temporal cortex	56/57	55/58	61/67	80/86	45/42	56/60	80/86	56/58	76/80	67/73
Medial temporal cortex	62/62	63/69	57/59	75/83	76/80	66/71	82/89	55/57	68/71	70/72
Parietal cortex	72/74	65/67	38/36	66/70	78/86	73/80	80/89	65/60	39/36	63/64
Occipital cortex	62/68	58/58	59/67	70/78	71/76	44/37	63/62	68/74	74/81	62/62
API-PET	75/81	76/86	59/62	47/43	92/97	83/90	82/87	74/80	79/88	60/61
Occipital vs. Temporal index	79/85	54/60	63/65	70/75	83/90	70/76	63/71	64/74	73/83	62/60
CIS ratio	67/79	54/51	62/63	71/77	71/77	64/70	57/59	55/61	75/77	67/68

The colors correspond to the bal. acc. for the pairwise comparison. Bal. acc. 85%–100% are highlighted in dark green. The gradually lighter shades of green indicate lower bal. acc. with white being at or below 50. Both bal. acc. and AUC are reported as percentage values (%).

Abbreviations: Aβ42 = amyloid beta 1-42; AD = Alzheimer's disease; API = Anterior vs. posterior index; AUC = area under the curve; bal. acc. = balanced accuracy; CIS = cingulate island sign; CSF = cerebrospinal fluid; DLB = dementia with Lewy bodies; 2-[^{18}F]FDG-PET = 2-[^{18}F]fluoro-2-deoxy-D-glucose positron emission tomography; FTD = frontotemporal dementia; MMSE = mini-mental state examination; MRI = magnetic resonance imaging; p-tau = phosphorylated tau at threonine 181; ROC = receiver operating characteristic; SCD = subjective cognitive decline; VaD = vascular dementia;

Table from Gjerum et al., Manuscript, study III.

The accuracies of the individual and combined groups of diagnostic tests for pairwise comparison are presented in Table 13. The addition of 2-[^{18}F]FDG-PET biomarkers to cognitive tests, CSF and MRI biomarkers considerably improved the classification accuracy for all pairwise comparisons of DLB to other dementias (bal. acc.: DLB vs. AD from 64% to 77%; DLB vs. FTD from 71% to 92%; and DLB vs. VaD from 71% to 84%).

Table 13. The pairwise comparison of individual and combined diagnostic test groups.

Bal. acc./AUC	**AD vs. DLB**	**AD vs. FTD**	**AD vs. VaD**	**AD vs. SCD**	**DLB vs. FTD**	**DLB vs. VaD**	**DLB vs. SCD**	**FTD vs. VaD**	**FTD vs. SCD**	**VaD vs. SCD**
Cognitive tests	56/60	62/58	47/51	94/97	57/60	53/62	84/88	58/59	83/89	82/87
CSF	76/78	90/94	85/84	85/93	79/80	68/75	81/82	28/32	55/51	47/49
MRI	62/69	74/78	80/86	83/90	65/73	76/83	78/83	73/86	85/91	84/89
2-[^{18}F]FDG-PET	76/84	76/87	63/72	82/87	92/97	83/90	80/90	72/75	77/90	75/80
Cognitive tests + CSF	70/73	90/94	85/84	94/97	74/75	66/71	84/88	58/59	83/89	82/87
Cognitive tests + MRI	50/54	68/79	80/85	94/97	74/76	73/79	85/89	73/85	84/91	92/92
Cognitive tests + 2-[^{18}F]FDG-PET	78/84	77/87	64/68	94/97	92/97	87/89	86/88	63/71	80/88	82/87
CSF + MRI	70/73	90/94	84/82	87/93	75/81	75/80	83/89	73/85	85/91	86/88
CSF + 2-[^{18}F]FDG-PET	80/88	90/94	85/84	85/93	92/97	83/88	84/89	70/74	77/90	75/80
MRI + 2-[^{18}F]FDG-PET	77/85	78/86	80/88	85/93	92/97	82/90	85/91	83/86	86/93	90/90
Cognitive tests + CSF + MRI	64/64	90/94	84/82	94/97	71/75	71/77	85/89	73/84	84/91	92/92
Cognitive tests + CSF + 2-[^{18}F]FDG-PET	76/85	90/94	85/84	94/97	92/97	87/91	86/88	64/71	80/88	82/87
Cognitive tests + MRI + 2-[^{18}F]FDG-PET	80/83	80/86	80/86	94/97	92/97	82/90	86/89	83/85	80/90	92/92
CSF + MRI + 2-[^{18}F]FDG-PET	75/85	90/94	81/81	92/94	92/97	82/90	85/91	83/86	86/93	89/88
Cognitive tests + CSF + MRI + 2-[^{18}F]FDG-PET	77/87	90/94	81/81	94/97	92/97	84/90	86/89	83/85	80/90	92/92

The colors correspond to the bal. acc. for the pairwise comparison. Bal. acc. 85%–100% are highlighted in dark green. The gradually lighter shades of green indicate lower bal. acc. with white being at or below 50. Both bal. acc. and AUC are reported as percentage values (%).
Abbreviations: AD = Alzheimer's disease; AUC = area under the curve; bal. acc. = balanced accuracy; CSF = cerebrospinal fluid; DLB = dementia with Lewy bodies; FTD = frontotemporal dementia; MRI = magnetic resonance imaging; ROC = receiver operating characteristic; SCD = subjective cognitive decline; VaD = vascular dementia; 2-[^{18}F]FDG-PET = 2-[^{18}F]fluoro-2-deoxy-D glucose positron emission tomography;
Table from Gjerum et al., Manuscript, study III.

Furthermore, 2-[^{18}F]FDG-PET biomarkers combined with CSF and MRI biomarkers had a high performance for distinguishing FTD from the other dementia groups (bal. acc. ranging from 83%-92%), whereas combined 2-[^{18}F]FDG-PET and MRI biomarkers were useful to distinguish VaD from the other dementia groups (bal. acc. ranging from 80%-90%).

5. Discussion

5.1 Summary of key findings:

This PhD project had three main findings. First, the clinical value of adding CSF AD biomarkers to a standard diagnostic program was higher for corroborating the AD diagnosis compared to adding 2-[^{18}F]FDG-PET in patients suspected of having AD. Second, the visual CIS scale was able to differentiate patients with DLB from patients with AD and controls, and the presence of Aβ pathology seemed to influence the degree of CIS in patients with DLB. Third, 2-[^{18}F]FDG-PET biomarkers, particularly API-PET and occipital vs. temporal index, improved the classification accuracy for both FTD and DLB as compared to AD using a DSI classifier.

These key findings will be discussed in the following sections. For further details, please see Study manuscripts for Study I-III.

5.2 Comparison of clinical value of CSF AD biomarkers and 2-[^{18}F]FDG-PET

The CSF AD biomarkers have a well-established, supportive role for the diagnosis of AD [3,121], whereas the clinical value of differentiating AD from other non-AD neurodegenerative dementias such as DLB and FTD are less established. On the other hand, 2-[^{18}F]FDG-PET is a promising supportive biomarker in the differential diagnosis of neurodegenerative disorders by demonstrating specific patterns of hypometabolism in both AD, FTD, and DLB [3,24,34,51,52]. However, the knowledge of the clinical added value of one biomarker over another in clinical practice is less established.

In study I, the clinical value of adding 2-[^{18}F]FDG-PET and CSF AD biomarkers individually to a standard diagnostic program including MRI was comparable with regards to diagnosis, prognosis, and patient management. Although CSF AD biomarkers potentially had a higher clinical value in confirming the AD diagnosis as indicated by a higher diagnostic confidence and a more reduced need for ancillary investigations for AD patients compared to 2-[^{18}F]FDG-PET. This was somewhat expected as CSF AD biomarkers have a more established role as supportive biomarker for in subjects suspected of having AD.

However, it was rather unexpected that 2-[^{18}F]FDG-PET had a limited clinical value for other ND diagnoses including DLB and FTD considering that disease-specific metabolic

patterns have been shown to distinguish between AD, DLB, and FTD on 2-[^{18}F]FDG-PET [3,24,34,51,52]. Moreover, a previous study found a specificity greater than 95% in the differential diagnosis of AD towards other dementias based on 2-[^{18}F]FDG-PET diagnosis in a study cohort of early-onset AD and other dementias (mean age (SD): 60 ±4 years) [169].

The lower diagnostic accuracy for 2-[^{18}F]FDG-PET in this study may be caused by an overlap of the AD-like patterns of temporoparietal hypometabolism between AD and CVD [29]. Moreover, the lack of distinct, hypometabolic patterns for non-ND cases including VaD and NPH, which amounted to almost 20% of this study cohort. Finally, the findings of 2-[^{18}F]FDG-PET images were given in a clinical written 2-[^{18}F]FDG-PET rapport as part of the routine clinical work-up, which may be less sensitive to subtle disease-specific patterns compared to quantitative methods.

5.3 The visual CIS scale

The CIS on 2-[^{18}F]FDG-PET is a supportive biomarker for DLB [34], and previous studies have demonstrated that the CIS ratio is higher in DLB patients compared to AD patients using various quantitative methods [92–96,99]. A previous study by Lim et al. found that visual assessment of CIS had a higher diagnostic accuracy compared to the quantitative CIS ratio in distinguishing DLB patients from AD patients [92]. However, there are no established visual criteria for the degree of CIS, even though visual rating of other neuroimaging biomarkers and modalities are commonly used and has proven to be a fast, reliable and reproducible method in clinical practice [74,170,171].

In this study, the proposed visual CIS scale was able to distinguish DLB patients and AD patients with a sensitivity of 52% and a sensitivity of 92% using a cut-off visual CIS score ≥ 2. In comparison, Lim et al. found that a visual assessment of CIS (dichotomized rating – absent or present) had a specificity of 100% and a sensitivity ranging from 62% to 86% for distinguishing DLB from AD [92]. The lower diagnostic accuracy may be explained by the inclusion of study population with a more uncharacteristic presentation considering that the included dementia patients had examinations with supplemental diagnostic test (determination of Aβ status and DAT-SPECT scan) on clinical indication.

Another finding was that coexisting Aβ pathology in DLB patients seemed to influence the degree of CIS. This was indicated by the finding of DLB Aβ− patients with the highest median visual CIS score, followed by DLB Aβ+ patients, lastly the AD patients, although

the difference only reached a trend level ($p = 0.06$) between DLB Aβ+ patients and DLB Aβ− patients. On the other hand, the association between CIS and coexisting Aβ pathology was not substantiated using the quantitative CIS ratio in this study and two previous studies consisting of a smaller study of 10 DLB patients [172] and a larger study of 39 DLB patients [93]. The differences between the findings for the visual CIS scale and the quantitative CIS ratios could not fully be explained by metrics variations, although this may to some extent have an impact [75]. However, the finding that Aβ pathology may influence the presence of CIS needs to be elucidated in further studies.

The visual CIS scale had a similar diagnostic accuracy compared to the quantitative CIS ratio in distinguishing DLB patients from AD patients, but from a clinical perspective a visual rating scale is advantageous compared to a quantitative method for several reasons. Using a quantitative method to assess CIS is time-consuming and the diagnostic accuracy depends on the acquisition and processing of the MRI and 2-[^{18}F]FDG-PET image and usage of specific software, which may vary across centres [75]. In contrast, a visual rating scale for CIS can be implemented as a fast-diagnostic adjunct to the standard visual 2-[^{18}F]FDG-PET image evaluation across centres without additional software. Moreover, the implementation of the visual CIS scale in a routine practice is potentially valuable considering that visual features such as cingulate hypometabolism appear to be underreported and missed on the clinical interpretation of 2-[^{18}F]FDG-PET scans of patients with DLB [173].

5.4 Evaluation of 2-[^{18}F]FDG-PET in the DSI classifier

Previous studies have demonstrated the usefulness of the DSI classifier in the differential diagnosis of dementia using different combinations of cognitive tests, CSF AD biomarkers, and automatic and visual MRI quantification features [130,132,134,135]. However, the diagnostic sensitivity for DLB and FTD was suboptimal with many cases being misclassified as AD. Until now, the DSI classifier has not included 2-[^{18}F]FDG-PET data.

In study III, 2-[^{18}F]FDG-PET biomarkers improved the classification accuracy for DLB and FTD, both individually and combined with cognitive tests, CSF and MRI biomarkers. Particularly, the two proposed disease-specific 2-[^{18}F]FDG-PET biomarkers, the API-PET and the occipital vs. temporal index.

The API-PET was included to demonstrate a specific pattern of reduced metabolism in frontotemporal regions and relative preserved metabolism in posterior region as seen in

many FTD patients [11,51,174]. The API-PET is similar to and uses the same regions as API-MRI, which has demonstrated a good classification accuracy for differentiating FTD from AD [135,154]. When comparing the API-PET and the API-MRI for differentiating FTD from the other groups, the API-PET had higher balanced accuracies ranging from 74% to 92% in comparison to the API-MRI with balanced accuracies ranging from 64% to 76%, suggesting that 2-[^{18}F]FDG-PET may outperform MRI with regards to specific FTD patterns.

The occipital vs. temporal index was included to improve the differentiation of DLB from AD. This 2-[^{18}F]FDG-PET biomarker was the diagnostic tests with the highest diagnostic accuracy for pairwise comparison of AD vs. DLB (AUC of 85%), and the feature outperformed both occipital hypometabolism (AUC of 68%) and CIS ratio (AUC of 79%). The accuracies of occipital hypometabolism and CIS ratio were lower than expected as previous 2-[^{18}F]FDG-PET studies have found accuracies between 73%-97% for occipital hypometabolism [92,95,163,175–179] and an accuracy of 92% for the CIS ratio in differentiating DLB from AD [95]. The lower accuracy in this study may reflect that the included patients may have a more uncharacteristic presentation due to selection bias, where 2-[^{18}F]FDG-PET was used as a supplemental diagnostic test for patients with an uncertain diagnosis after disclosure of standard diagnostic tests such as MRI and cognitive tests. Moreover, differences in the quantitative analyses may also have an impact on the performance [75].

5.5 Strengths and limitations

The three studies focused on developing three disease-specific 2-[^{18}F]FDG-PET biomarkers and evaluating the clinical impact of 2-[^{18}F]FDG-PET. This approach has several methodological considerations, which are described in the following.

5.5.1 Strengths

The strengths of the studies were the inclusion of a relatively large study population examined with a comprehensive standard diagnostic program and confirmation of the clinical diagnosis by experienced dementia specialists. In addition, the setting in the three studies reflected a clinically relevant setting by including study participants that were representative of a mixed memory clinic population rather than a homogenous research population. Moreover, the included data represented commonly used diagnostic tests in a routine memory clinic setting, and the ancillary investigations with 2-[^{18}F]FDG-PET and

CSF AD biomarkers were performed on a clinical indication reflecting the recommended use.

In study II, the included DLB patients had an abnormal DAT-SPECT, which is an indicative biomarker of DLB [34]. In study III, all available diagnostic tests were included, and cases with incomplete data were not excluded as the DSI classifier can deal with missing data.

5.5.2 Limitations

Some limitations must be considered for the three studies. One limitation for the three studies and for other similar studies is the absence of a neuropathologic validation diagnosis. Even though the reference diagnosis was based on all available clinical patient data at follow-up and established on the clinical diagnostic criteria by experienced dementia specialists, there is a risk of misclassification. Clinicopathological studies have found a correlation between clinical and neuropathological diagnoses of 70% to 90% for AD, whereas the correlation was significantly lower varying between 40% and 75% for DLB, FTD, and VaD [23,41,123,180,181]. Furthermore, mixed pathologies have been identified as one of the most common neuropathologic diagnosis, particularly in older persons with dementia [68], which is difficult to determine clinically. However, in study II, the included DLB patients had an abnormal DAT-SPECT and determination of the brain Aβ status to account for the clinicopathological spectrum of DLB [33].

Another limitation is the risk of circular evidence considering that the clinical reference diagnosis was supported and reinforced by the available diagnostic tests and biomarkers. However, in study III, the derived automatic neuroimaging biomarkers were not used for clinical diagnosis. Moreover, due to the limited availability of FTD and DLB cases, cross-validation was used in study III, which may lead to an overfit of the results in the absence of an individual validation cohort. On the other hand, the objective of this study was to explore the clinical impact of commonly used diagnostic tests and 2-[^{18}F]FDG-PET biomarkers in the differential diagnosis of dementia and obtain information about their relative performance, and not to get precise accuracy estimates.

Additionally, like other clinical-based patients cohort studies where the supplementary diagnostic tests are performed on clinical indication, the three studies explicitly include subjects with examination of 2-[^{18}F]FDG-PET imaging leading to a potential selection bias. Another potential selection bias concerns that most of the subjects were included

from RH, which is a tertiary memory clinic with a higher proportion of patients with complex clinical presentations. Consequently, it may be the case that the findings to some extent reflect sample-specific characteristics and hence are difficult to generalize. On the other hand, the use of 2-[^{18}F]FDG-PET is specifically recommended in the cases where diagnosis remains unclear after standard diagnostic work-up, and therefore this is the clinical relevant subgroup to evaluate the impact of 2-[^{18}F]FDG-PET [85].

Finally, some limitations regarding metrics should also be mentioned. First, the evaluation and interpretation of the biomarkers were deliberately based on clinical routine procedures and locally determined cut-points, which may however, lessen the generalization to other centres in the absence of a standardized operating procedure for the biomarkers [75]. Moreover, several different scanners were used given that the clinical diagnostic work-up was performed across several centres, which lead to exclusion of some subjects in study III due to specific criteria for MRI. However, the different scanners did not have an impact on the other studies considering that visual assessment of neuroimaging including visual ratings has the advantage of being robust for scanner differences.

6. Conclusions and perspectives for further research

2-[^{18}F]FDG-PET has achieved an emerging role in clinical settings and become an established biomarker in the identification and differential diagnosis of dementia. However, the clinical value of 2-[^{18}F]FDG-PET in the diagnosis of dementia in the clinical decision-making is not completely clarified. Furthermore, there is a limited knowledge on how to weigh and prioritize the biomarkers to optimize the clinical diagnosis of dementia.

The main findings and perspectives were:

- Overall, 2-[^{18}F]FDG-PET provided diagnostically useful information in the differential diagnosis of dementia, although the diagnostic value seemed to depend on the diagnostic groups and metrics. The addition of disease-specific 2-[^{18}F]FDG-PET biomarkers were promising features to increase the diagnostic classification accuracy for DLB and FTD as compared to AD. Diagnosing DLB and FTD can be challenging due to the sparse disease-specific biomarkers, and complicated by a clinical and pathological overlap with other subtypes of dementia. However, using disease-specific 2-[^{18}F]FDG-PET biomarkers may be valuable for clinicians in decision-making to improve the differential diagnosis of dementia.
- The main finding in study I was that CSF AD biomarkers seemed to have a higher clinical impact on corroborating the diagnosis of AD in comparison to 2-[^{18}F]FDG-PET. This was demonstrated by a slightly higher diagnostic classification accuracy together with a higher diagnostic confidence and a more reduced need for ancillary investigations for correctly classified AD when adding CSF AD biomarkers as compared to adding 2-[^{18}F]FDG-PET. Furthermore, the addition of 2-[^{18}F]FDG-PET to CSF AD biomarkers were of limited value. The finding adds some knowledge to the first choice of the two supportive biomarkers in the diagnostic algorithm, as most memory clinics have implemented a stepwise approach of the diagnostic work-up.
- The main findings in study II were that the visual CIS scale was relatively robust and applicable to evaluate the presence of CIS from clinically acquired 2-[^{18}F]FDG-PET images, and DLB patients had a significantly higher visual CIS

score compared to AD patients. In perspective, the visual CIS scale can be integrated as a fast and easy-applicable part of the routine visual assessment of 2-[^{18}F]FDG-PET images to provide diagnostic useful information to support the differentiation of DLB from AD.

- The main findings in study III were that the proposed disease-specific 2-[^{18}F]FDG-PET biomarkers, that is the API-PET and occipital vs. temporal index, improved the classification accuracy for both FTD and DLB, especially as compared to AD using the DSI classifier. Moreover, specific combinations of biomarkers and diagnostic tests were valuable to differentiate specific subtypes of dementia. In perspective, the additional information from 2-[^{18}F]FDG-PET and addition of disease-specific 2-[^{18}F]FDG-PET biomarkers may support clinicians in the differential diagnosis of dementia.

In conclusion, the addition of 2-[^{18}F]FDG-PET is valuable in the clinical decision-making, especially the addition of disease-specific 2-[^{18}F]FDG-PET biomarkers have a significant clinical impact in identifying DLB and FTD.

Future studies are needed to validate the novel disease-specific 2-[^{18}F]FDG-PET biomarkers, that is the visual CIS scale and the automated API-PET and occipital vs. temporal index, in larger, prospective mixed memory cohorts. Moreover, the visual CIS scale should also be assessed by less experienced readers. And it should also be further investigated if the degree of CIS is associated with the presence of Aβ pathology in DLB patients as this is not completely clarified.

Furthermore, future studies should compare the clinical value of 2-[^{18}F]FDG-PET and CSF AD biomarkers in a larger study with less experienced clinicians, in addition to an evaluation of the cost vs. benefit to optimize the biomarkers in diagnosis of dementia disorders.

Finally, it should be assessed further if data-driven diagnostic tools such as the DSI classifier supports the clinicians in prioritization and weighing of the biomarkers in the diagnostic work-up.

7. References

[1] Nichols E, Szoeke CEI, Vollset SE, Abbasi N, Abd-Allah F, Abdela J, Aichour MTE, Akinyemi RO, Alahdab F, Asgedom SW, Awasthi A, Barker-Collo SL, Baune BT, Béjot Y, Belachew AB, Bennett DA, Biadgo B, Bijani A, Bin Sayeed MS, Brayne C, Carpenter DO, Carvalho F, Catalá-López F, Cerin E, Choi JYJ, Dang AK, Degefa MG, Djalalinia S, Dubey M, Duken EE, Edvardsson D, Endres M, Eskandarieh S, Faro A, Farzadfar F, Fereshtehnejad SM, Fernandes E, Filip I, Fischer F, Gebre AK, Geremew D, Ghasemi-Kasman M, Gnedovskaya E V., Gupta R, Hachinski V, Hagos TB, Hamidi S, Hankey GJ, Haro JM, Hay SI, Irvani SSN, Jha RP, Jonas JB, Kalani R, Karch A, Kasaeian A, Khader YS, Khalil IA, Khan EA, Khanna T, Khoja TAM, Khubchandani J, Kisa A, Kissimova-Skarbek K, Kivimäki M, Koyanagi A, Krohn KJ, Logroscino G, Lorkowski S, Majdan M, Malekzadeh R, März W, Massano J, Mengistu G, Meretoja A, Mohammadi M, Mohammadi-Khanaposhtani M, Mokdad AH, Mondello S, Moradi G, Nagel G, Naghavi M, Naik G, Nguyen LH, Nguyen TH, Nirayo YL, Nixon MR, Ofori-Asenso R, Ogbo FA, Olagunju AT, Owolabi MO, Panda-Jonas S, Passos VM d. A, Pereira DM, Pinilla-Monsalve GD, Piradov MA, Pond CD, Poustchi H, Qorbani M, Radfar A, Reiner RC, Robinson SR, Roshandel G, Rostami A, Russ TC, Sachdev PS, Safari H, Safiri S, Sahathevan R, Salimi Y, Satpathy M, Sawhney M, Saylan M, Sepanlou SG, Shafieesabet A, Shaikh MA, Sahraian MA, Shigematsu M, Shiri R, Shiue I, Silva JP, Smith M, Sobhani S, Stein DJ, Tabarés-Seisdedos R, Tovani-Palone MR, Tran BX, Tran TT, Tsegay AT, Ullah I, Venketasubramanian N, Vlassov V, Wang YP, Weiss J, Westerman R, Wijeratne T, Wyper GMA, Yano Y, Yimer EM, Yonemoto N, Yousefifard M, Zaidi Z, Zare Z, Vos T, Feigin VL, Murray CJL (2019) Global, regional, and national burden of Alzheimer's disease and other dementias, 1990–2016: a systematic analysis for the Global Burden of Disease Study 2016. *Lancet Neurol.* **18**, 88–106.

[2] Prince M, Comas-Herrera A, Knapp M, Guerchet M, Karagiannidou M (2016) *World Alzheimer Report 2016 Improving healthcare for people living with dementia. Coverage, Quality and costs now and in the future*,, London.

[3] McKhann GM, Knopman DS, Chertkow H, Hyman BT, Jack Jr CR, Kawas CH,

Klunk WE, Koroshetz WJ, Manly JJ, Mayeux R, Mohs RC, Morris JC, Rossor MN, Scheltens P, Carrillo MC, Thies B, Weintraub S, Phelps CH (2011) The diagnosis of dementia due to Alzheimer's disease: Recommendations from the National Institute on Aging-Alzheimer's Association workgroups on diagnostic guidelines for Alzheimer's disease. *Alzheimer's Dement.* **7**, 263–269.

[4] World Health Organization (1992) *ICD-10 Classification of Mental and Behavioural Disorders. Clinical descriptions and diagnostic guidelines*,, Geneva.

[5] World Health Organization (2012) Dementia: a public health priority. *Dementia* 112.

[6] Livingston G, Sommerlad A, Orgeta V, Costafreda SG, Huntley J, Ames D, Ballard C, Banerjee S, Burns A, Cohen-mansfield J, Cooper C, Fox N, Gitlin LN, Howard R, Kales HC, Larson EB, Ritchie K, Rockwood K, Sampson EL, Samus Q, Schneider LS, Selbæk G, Teri L, Mukadam N (2017) Dementia prevention, intervention, and care. *Lancet* **6736**, 1–62.

[7] Waldemar G, Dubois B, Emre M, Georges J, McKeith IG, Rossor M, Scheltens P, Tariska P, Winblad B (2007) Recommendations for the diagnosis and management of Alzheimer's disease and other disorders associated with dementia: EFNS guideline. *Eur. J. Neurol.* **14**, 1–27.

[8] Badhwar A, McFall GP, Sapkota S, Black SE, Chertkow H, Duchesne S, Masellis M, Li L, Dixon RA, Bellec P (2019) A Multiomics Approach to Heterogeneity in Alzheimer′s Disease: Focused Review and Roadmap. *Brain* 1–17.

[9] Kapasi A, DeCarli C, Schneider JA (2017) Impact of multiple pathologies on the threshold for clinically overt dementia. *Acta Neuropathol.* **134**, 1–16.

[10] Jack CR, Knopman DS, Jagust WJ, Petersen RC, Weiner MW, Aisen PS, Shaw LM, Vemuri P, Wiste HJ, Weigand SD, Lesnick TG, Pankratz VS, Donohue MC, Trojanowski JQ (2013) Tracking pathophysiological processes in Alzheimer's disease: An updated hypothetical model of dynamic biomarkers. *Lancet Neurol.* **12**, 207–216.

[11] Bohnen NI, Djang DSW, Herholz K, Anzai Y, Minoshima S (2012) Effectiveness and Safety of 18F-FDG PET in the Evaluation of Dementia: A Review of the Recent Literature. *J. Nucl. Med.* **53**, 59–71.

[12] Morbelli S, Garibotto V, Van De Giessen E, Arbizu J, Chételat G, Drezgza A, Hesse S, Lammertsma AA, Law I, Pappata' S, Payoux P, Pagani M (2015) A Cochrane

review on brain [18F]FDG PET in dementia: limitations and future perspectives. *Eur. J. Nucl. Med. Mol. Imaging* **42**, 1487–1491.

[13] National Collaborating Centre for Mental Health (2007) *Dementia: The NICE-SCIE guideline on supporting people with dementia and their carers in health and social care*.

[14] Sorbi S, Hort J, Erkinjuntti T, Fladby T, Gainotti G, Gurvit H, Nacmias B, Pasquier F, Popescu BO, Rektorova I, Religa D, Rusina R, Rossor M, Schmidt R, Stefanova E, Warren JD, Scheltens P (2012) EFNS-ENS Guidelines on the diagnosis and management of disorders associated with dementia. *Eur. J. Neurol.* **19**, 1159–1179.

[15] Filippi M, Agosta F, Barkhof F, Dubois B, Fox N, Frisoni G, Jack C, Johannsen P, Miller B, Nestor P, Scheltens P, Sorbi S, Teipel S, Thompson P, Wahlund L (2012) EFNS task force: The use of neuroimaging in the diagnosis of dementia. *Eur. J. Neurol.* **19**, 1487–1501.

[16] Dubois B, Feldman HH, Jacova C, Dekosky ST, Barberger-gateau P, Cummings J, Delacourte A, Galasko D, Gauthier S, Jicha G, Meguro K, Brien JO, Pasquier F, Robert P, Rossor M, Salloway S, Stern Y, Visser PJ, Scheltens P (2007) Research criteria for the diagnosis of Alzheimer's disease: revising the NINCDS-ADRDA criteria. *Lancet Neurol.* **6**, 634–646.

[17] Jessen F, Amariglio RE, van Boxtel M, Breteler M, Ceccaldi M, Chételat G, Dubois B, Dufouil C, Ellis KA, van der Flier WM, Glodzik L, van Harten AC, de Leon MJ, McHugh P, Mielke MM, Molinuevo JL, Mosconi L, Osorio RS, Perrotin A, Petersen RC, Rabin LA, Rami L, Reisberg B, Rentz DM, Sachdev PS, de la Sayette V, Saykin AJ, Scheltens P, Shulman MB, Slavin MJ, Sperling RA, Stewart R, Uspenskaya O, Vellas B, Visser PJ, Wagner M (2014) A conceptual framework for research on subjective cognitive decline in preclinical Alzheimer's disease. *Alzheimer's Dement.* **10**, 844–52.

[18] Petersen R, Doody R, Kurz A, Mohs R, Morris J, Rabins P, Ritchie K, Rossor M, Thal L, Winblad B (2001) Current concepts in Mild Cognitive Impairment. *Arch. Neurol.* **58**, 1985–1992.

[19] Portet F, Ousset PJ, Visser PJ, Frisoni GB, Nobili F, Scheltens P, Vellas B, Touchon J (2006) Mild cognitive impairment (MCI) in medical practice: A critical review of the concept and new diagnostic procedure. Report of the MCI Working Group of the European Consortium on Alzheimer's Disease. *J. Neurol. Neurosurg. Psychiatry* **77**,

714–718.

[20] Knopman DS, Boeve BF, Petersen RC (2003) Essentials of the Proper Diagnoses of Mild Cognitive Impairment, Dementia, and Major Subtypes of Dementia. *Mayo Clin. Proc.* **78**, 1290–1308.

[21] Cummings JL, Isaacson RS, Schmitt FA, Velting DM (2015) A practical algorithm for managing Alzheimer's disease: what, when, and why? *Ann. Clin. Transl. Neurol.* **2**, 307–323.

[22] Scheltens P, Blennow K, Breteler MMB, Strooper B De, Frisoni GB, Salloway S, Flier WM Van Der (2016) Alzheimer's disease. *Lancet* **6736**, 1–13.

[23] Knopman D, Dekosky S, Cummings J, Chui H, Corey-Bloom J, Relkin N, Small G, Miller B, Stevens J (2001) Practice Parameter: Diagnosis of Dementia (an Evidence-Based Review). *Neurology* **56**, 1143–1153.

[24] Dubois B, Feldman HH, Jacova C, Hampel H, Molinuevo JLJL, Blennow K, Dekosky ST, Gauthier S, Selkoe D, Bateman R, Cappa S, Crutch S, Engelborghs S, Frisoni GB, Fox NC, Galasko D, Habert MO, Jicha GA, Nordberg A, Pasquier F, Rabinovici G, Robert P, Rowe C, Salloway S, Sarazin M, Epelbaum SS, de Souza LC, Vellas B, Visser PJ, Schneider L, Stern Y, Scheltens P, Cummings JL (2014) Advancing research diagnostic criteria for Alzheimer's disease: The IWG-2 criteria. *Lancet Neurol.* **13**, 614–629.

[25] Albert MS, DeKosky ST, Dickson D, Dubois B, Feldman HH, Fox NC, Gamst A, Holtzman DM, Jagust WJ, Petersen RC, Snyder PJ, Carillo MC, Thies B, Phelps CH (2011) The diagnosis of mild cognitive impairment due to Alzheimer's disease: Recommendations from the National Institute on Aging-Alzheimer's Association workgroups on diagnostic guidelines for Alzheimer's disease. *Alzheimer's Dement.* **7**, 270–279.

[26] Sperling RAR., Aisen PS, Beckett LALA, Bennett DADA, Craft S, Fagan AMAM, Iwatsubo T, Jack CRCRJ, Kaye J, Montine TJ, Park DCDC, Reiman EMEM, Rowe CCC, Siemers E, Stern Y, Yaffe K, Carrillo MC, Thies B, Morrison-Bogorad M, Wagster M V, Phelps CH, Wegster MV, and Phelps CH (2011) Toward defining the preclinical stages of Alzheimer's disease: Recommendations from the National Institute on Aging- Alzheimer's Association workgroups on diagnostic guidelines for Alzheimer's disease. *Alzheimer's Dement.* **7**, 280–292.

[27] Jack CR, Albert MS, Knopman DS, McKhann GM, Sperling RA, Carrillo MC,

Thies B, Phelps CH (2011) Introduction to the recommendations from the National Institute on Aging-Alzheimer's Association workgroups on diagnostic guidelines for Alzheimer's disease. *Alzheimer's Dement.* **7**, 257–262.

[28] Jack CRJ, Bennett DA, Blennow K, Carillo MC, Dunn B, Haeberlein SB, Holtzman DM, Jagust W, Jessen F, Karlawish J, Molinuevo JL, Montine T, Phelps C, Rankin KP, Rowe CC, Scheltens P, Siemers E, Snyder HM, Sperling R (2018) NIA-AA Research Framework: Toward a biological definition of Alzheimer's disease. *Alzheimers Dement* **14**, 535–562.

[29] Jack CR, Bennett DA, Blennow K, Carrillo MC, Feldman HH, Frisoni GB, Hampel HJ, Jagust WJ, Johnson KA, Knopman DS, Petersen RC, Scheltens P, Sperling RA, Dubois B (2016) A/T/N: An unbiased descriptive classification scheme for Alzheimer disease biomarkers. *Neurology* **87**, 539–547.

[30] Walker Z, Possin KL, Boeve BF, Aarsland D (2015) Lewy body dementias. *Lancet* **386**, 1683–1697.

[31] Duda JE (2004) Pathology and neurotransmitter abnormalities of dementia with Lewy bodies. *Dement. Geriatr. Cogn. Disord.* **17**, 3–14.

[32] Lippa CF, Duda JE, Grossman M, Hurtig HI, Aarsland D, Boeve BF, Brooks DJ, Dickson DW, Dubois B, Emre M, Fahn S, Farmer JM, Galasko D, Galvin JE, Goetz CG, Growdon JH, Gwinn-Hardy KA, Hardy J, Heutink P, Iwatsubo T, Kosaka K, Lee VMY, Leverenz JB, Masliah E, McKeith IG, Nussbaum RL, Olanow CW, Ravina BM, Singleton AB, Tanner CM, Trojanowski JQ, Wszolek ZK (2007) DLB and PDD boundary issues: Diagnosis, treatment, molecular pathology, and biomarkers. *Neurology* **68**, 812–819.

[33] McKeith I, Taylor J-P, Thomas A, Donaghy P, Kane J (2016) Revisiting DLB Diagnosis: A Consideration of Prodromal DLB and of the Diagnostic Overlap With Alzheimer Disease. *J. Geriatr. Psychiatry Neurol.* **29**, 249–253.

[34] McKeith IG, Boeve BF, Dickson DW, Halliday G, Taylor J-P, Weintraub D, Aarsland D, Galvin J, Attems J, Ballard CG, Bayston A, Beach TG, Blanc F, Bohnen N, Bonanni L, Bras J, Brundin P, Burn D, Chen-Plotkin A, Duda JE, El-Agnaf O, Feldman H, Ferman TJ, Ffytche D, Fujishiro H, Galasko D, Goldman JG, Gomperts SN, Graff-Radford NR, Honig LS, Iranzo A, Kantarci K, Kaufer D, Kukull W, Lee VMY, Leverenz JB, Lewis S, Lippa C, Lunde A, Masellis M, Masliah E, McLean P, Mollenhauer B, Montine TJ, Moreno E, Mori E, Murray M,

O'Brien JT, Orimo S, Postuma RB, Ramaswamy S, Ross OA, Salmon DP, Singleton A, Taylor A, Thomas A, Tiraboschi P, Toledo JB, Trojanowski JQ, Tsuang D, Walker Z, Yamada M, Kosaka K (2017) Diagnosis and management of dementia with Lewy bodies Fourth consensus report of the DLB Consortium. *Neurology* **89**, 1–13.

[35] Weisman, D; McKeith I (2007) Dementia with Lewy bodies. *Semin. Neurol. Neurol.* **27**, 42–47.

[36] Barker WW, Luis CA, Kashuba A, Luis M, Harwood DG, Loewenstein D, Waters C, Jimison P, Shepherd E, Sevush S, Graff-Radford N, Newland D, Todd M, Miller B, Gold M, Heilman K, Doty L, Goodman I, Robinson B, Pearl G, Dickson D, Duara R (2002) Relative frequencies of Alzheimer disease, Lewy body, vascular and frontotemporal dementia, and hippocampal sclerosis in the State of Florida Brain Bank. *Alzheimer Dis. Assoc. Disord.* **16**, 203–212.

[37] Emre M, Aarsland D, Brown R, Burn DJ, Duyckaerts C, Mizuno Y, Broe GA, Cummings J, Dickson DW, Gauthier S, Goldman J, Goetz C, Korczyn A, Lees A, Levy R, Litvan I, McKeith I, Olanow W, Poewe W, Quinn N, Sampaio C, Tolosa E, Dubois B (2007) Clinical diagnostic criteria for dementia associated with Parkinson's disease. *Mov. Disord.* **22**, 1689–1707.

[38] Olichney J, Galasko D, Salmon D, Hofstetter C, Hansen L, Katzman R, Thal L (1998) Cognitive decline is faster in Lewy body variant than in Alzheimer's disease. *Neurology* **51**, 351–357.

[39] Heyman A, Fillenbaum GG, Gearing M, Mirra SS, Welsh-Bohmer KA, Peterson B, Pieper C (1999) Comparison of Lewy body variant of Alzheimer's disease with pure Alzheimer's disease: Consortium to establish a registry for Alzheimer's disease, part XIX. *Neurology* **52**, 1839–1844.

[40] Mueller C, Ballard C, Corbett A, Aarsland D (2017) The prognosis of dementia with Lewy bodies. *Lancet Neurol.* **16**, 390–398.

[41] Nelson PT, Jicha GA, Kryscio RJ, Abner EL, Schmitt FA, Cooper G, Xu LO, Smith CD, Markesbery WR (2010) Low sensitivity in clinical diagnoses of dementia with Lewy bodies. *J. Neurol.* **257**, 359–366.

[42] McKeith I, O'Brien J, Walker Z, Tatsch K, Booij J, Darcourt J, Padovani A, Giubbini R, Bonuccelli U, Volterrani D, Holmes C, Kemp P, Tabet N, Meyer I, Reininger C (2007) Sensitivity and specificity of dopamine transporter imaging with

123I-FP-CIT SPECT in dementia with Lewy bodies: a phase III, multicentre study. *Lancet Neurol.* **6**, 305–313.

[43] Yoshita M, Arai H, Arai H, Arai T, Asada T, Fujishiro H, Hanyu H, Iizuka O, Iseki E, Kashihara K, Kosaka K, Maruno H, Mizukami K, Mizuno Y, Mori E, Nakajima K, Nakamura H, Nakano S, Nakashima K, Nishio Y, Orimo S, Samuraki M, Takahashi A, Taki J, Tokuda T, Urakami K, Utsumi K, Wada K, Washimi Y, Yamasaki J, Yamashina S, Yamada M (2015) Diagnostic accuracy of123I-meta-iodobenzylguanidine myocardial scintigraphy in dementia with lewy bodies: A multicenter study. *PLoS One* **10**, 1–14.

[44] Boeve BF, Silber MH, Ferman TJ, Lin SC, Benarroch EE, Schmeichel AM, Ahlskog JE, Caselli RJ, Jacobson S, Sabbagh M, Adler C, Woodruff B, Beach TG, Iranzo A, Gelpi E, Santamaria J, Tolosa E, Singer C, Mash DC, Luca C, Arnulf I, Duyckaerts C, Schenck CH, Mahowald MW, Dauvilliers Y, Graff-Radford NR, Wszolek ZK, Parisi JE, Dugger B, Murray ME, Dickson DW (2013) Clinicopathologic correlations in 172 cases of rapid eye movement sleep behavior disorder with or without a coexisting neurologic disorder. *Sleep Med.* **14**, 754–762.

[45] Rizzo G, Arcuti S, Copetti M, Alessandria M, Savica R, Fontana A, Liguori R, Logroscino G (2018) Accuracy of clinical diagnosis of dementia with Lewy bodies: A systematic review and meta-analysis. *J. Neurol. Neurosurg. Psychiatry* **89**, 358–366.

[46] Bang J, Spina S, Miller BL (2015) Frontotemporal dementia. *Lancet* **386**, 1672–1682.

[47] Vieira RT, Caixeta L, Machado S, Silva AC, Nardi AE, Arias-Carrión O, Carta MG (2013) Epidemiology of early-onset dementia: a review of the literature. *Clin. Pract. Epidemiol. Ment. Heal.* **9**, 88–95.

[48] Josephs KA, Hodges JR, Snowden JS, MacKenzie IR, Neumann M, Mann DM, Dickson DW (2011) Neuropathological background of phenotypical variability in frontotemporal dementia. *Acta Neuropathol.* **122**, 137–153.

[49] Mann DMA, Snowden JS (2017) Frontotemporal lobar degeneration: Pathogenesis, pathology and pathways to phenotype. *Brain Pathol.* **27**, 723–736.

[50] McKhann GM (2001) Clinical and Pathological Diagnosis of Frontotemporal Dementia. *Arch. Neurol.* **58**, 1803.

[51] Rascovsky K, Hodges JR, Knopman D, Mendez MF, Kramer JH, Neuhaus J, Van

Swieten JC, Seelaar H, Dopper EGP, Onyike CU, Hillis AE, Josephs KA, Boeve BF, Kertesz A, Seeley WW, Rankin KP, Johnson JK, Gorno-Tempini ML, Rosen H, Prioleau-Latham CE, Lee A, Kipps CM, Lillo P, Piguet O, Rohrer JD, Rossor MN, Warren JD, Fox NC, Galasko D, Salmon DP, Black SE, Mesulam M, Weintraub S, Dickerson BC, Diehl-Schmid J, Pasquier F, Deramecourt V, Lebert F, Pijnenburg Y, Chow TW, Manes F, Grafman J, Cappa SF, Freedman M, Grossman M, Miller BL (2011) Sensitivity of revised diagnostic criteria for the behavioural variant of frontotemporal dementia. *Brain* **134**, 2456–2477.

[52] Gorno-Tempini ML, Hillis AE, Weintraub S, Kertesz A, Mendez M, Cappa SF, Ogar JM, Rohrer JD, Black S, Boeve BF, Manes F, Dronkers NF, Vandenberghe R, Roscovsky K, Patterson K, Miller BI, Knopman DS, Hodges JR, Mesulam MM, Grossman M (2011) Classification of primary progressive aphasia and its variants. *Neurology* **76**, 1006–1014.

[53] Meeter LH, Kaat LD, Rohrer JD, Van Swieten JC (2017) Imaging and fluid biomarkers in frontotemporal dementia. *Nat. Rev. Neurol.* **13**, 406–419.

[54] O'Brien JT, Thomas A (2015) Vascular dementia. *Lancet* **386**, 1698–1706.

[55] Dichgans M, Leys D (2017) Vascular Cognitive Impairment. *Circ. Res.* **120**, 573–591.

[56] O'Brien JT, Erkinjuntti T, Reisberg B, Roman G, Sawada T, Pantoni L, Bowler J V., Ballard C, DeCarli C, Gorelick PB, Rockwood K, Burns A, Gauthier S, DeKosky ST (2003) Vascular cognitive impairment. *Lancet Neurol.* **2**, 89–98.

[57] Román GC, Tatemichi TK, Erkinjuntti T, Cummings JL, Masdeu JC, Garcia JH, Amaducci L, Orgogozo J-M, Brun A, Hofman A, Moody DM, O'Brien MD, Yamaguchi T, Grafman J, Drayer BP, Bennett DA, Fisher M, Ogata J, Kokmen E, Bermejo F, Wolf PA, Gorelick PB, Bick KL, Pajeau AK, Bell MA, DeCarli C, Culebras A, Korczyn AD, Bogousslavsky J, Hartmann A, Scheinberg P (1993) Vascular dementia: diagnostic criteria for research studies. Report of the NINDS-AIREN International Workshop. *Neurology* **43**, 250–260.

[58] Sachdev P, Kalaria R, O'Brien J, Skoog I, Alladi S, Black S, Blacker D, Blazer D, Chen C, Chui H, Ganguli M, Jellinger K, Jeste D, Pasquier F, Paulsen J, Prins N, Rockwood K, Roman G, Scheltens P (2014) Diagnostic criteria for vascular cognitive disorders: a VASCOG statement. *Alzheimer Dis. Assoc. Disord.* **28**, 206–218.

[59] Román GC, Erkinjuntti T, Wallin A, Pantoni L, Chui HC (2002) Subcortical ischaemic vascular dementia. *Lancet Neurol.* **1**, 426–436.

[60] Brenowitz WD, Hubbard RA, Keene CD, Hawes SE, Longstreth WT, Woltjer RL, Kukull WA (2016) Mixed neuropathologies and estimated rates of clinical progression in a large autopsy sample. *Alzheimer's Dement.* 1–9.

[61] Atkinson AJ, Colburn WA, DeGruttola VG, DeMets DL, Downing GJ, Hoth DF, Oates JA, Peck CC, Schooley RT, Spilker BA, Woodcock J, Zeger SL (2001) Biomarkers and surrogate endpoints: Preferred definitions and conceptual framework. *Clin. Pharmacol. Ther.* **69**, 89–95.

[62] Mendez MF, Ghajarania M, Perryman KM (2002) Posterior cortical atrophy: Clinical characteristics and differences compared to Alzheimer's disease. *Dement. Geriatr. Cogn. Disord.* **14**, 33–40.

[63] Harper L, Barkhof F, Scheltens P, Schott JM, Fox NC (2014) An algorithmic approach to structural imaging in dementia. *J. Neurol. Neurosurg. Psychiatry* **85**, 692–698.

[64] Clifford RJ, Knopman D, Jagust W, Petersen R, Weiner M, Aisen P, Shaw L, Vemuri P, Wiste H, Weigand S, Lesnick T, Pankratz V, Donohue M, Trojanowski J (2013) Update on hypothetical model of Alzheimer's disease biomarkers. *Lancet Neurol.* **12**, 207–216.

[65] Jagust W (2018) Imaging the evolution and pathophysiology of Alzheimer disease. *Nat. Rev. Neurosci.* **19**, 687–700.

[66] ten Kate M, Barkhof F, Boccardi M, Visser PJ, Jack CRJ, Lovblad K-O, Frisoni GB, Scheltens P (2017) Clinical validity of medial temporal atrophy as a biomarker for Alzheimer's disease in the context of a structured 5-phase development framework. *Neurobiol. Aging* **52**, 167–182.

[67] Rabinovici GD, Seeley WW, Kim EJ, Gorno-Tempini ML, Rascovsky K, Pagliaro T a, Allison SC, Halabi C, Kramer JH, Johnson JK, Weiner MW, Forman MS, Trojanowski JQ, Dearmond SJ, Miller BL, Rosen HJ (2008) Distinct MRI atrophy patterns in autopsy-proven Alzheimer's disease and frontotemporal lobar degeneration. *Am. J. Alzheimers. Dis. Other Demen.* **22**, 474–488.

[68] Schneider JA, Arvanitakis Z, Bang W, Bennett DA (2007) Mixed brain pathologies account for most dementia cases in community-dwelling older persons. *Neurology* **69**, 2197–2204.

[69] Gold G, Bouras C, Canuto A, Bergallo MF, Herrmann FR, Hof PR, Mayor PA, Michel JP, Giannakopoulos P (2002) Clinicopathological validation study of four sets of clinical criteria for vascular dementia. *Am. J. Psychiatry* **159**, 82–87.

[70] Harper L, Fumagalli GG, Barkhof F, Scheltens P, O'Brien JT, Bouwman F, Burton EJ, Rohrer JD, Fox NC, Ridgway GR, Schott JM (2016) MRI visual rating scales in the diagnosis of dementia: Evaluation in 184 post-mortem confirmed cases. *Brain* **139**, 1211–1225.

[71] Scheltens P, Leys D, Barkhof F, Huglo D, Weinstein HC, Vermersch P, Kuiper M, Steinling M, Wolters EC, Valk J (1992) Atrophy of medial temporal lobes on MRI in 'probable' Alzheimer's disease and normal ageing: diagnostic value and neuropsychological correlates. *J. Neurol. Neurosurgery, Psychiatry* **55**, 967–972.

[72] Pasquier F, Leys D, Weerts JGE, Mounier-Vehier F, Barkhof F, Scheltens P (1996) Inter-and Intraobserver Reproducibility of Cerebral Atrophy Assessment on MRI Scans with Hemispheric Infarcts. *Eur Neurol* **36**, 268–272.

[73] Fazekas F, Chawluk JB, Alavi A, Hurtig HI, Zimmerman RA (1987) MR signal abnormalities at 1.5 T in Alzheimer's dementia and normal aging. *Am. J. Roentgenol.* **149**, 351–356.

[74] Vernooij MW, Pizzini FB, Schmidt R, Smits M, Yousry TA, Bargallo N, Frisoni GB, Haller S, Barkhof F (2019) Dementia imaging in clinical practice: a European-wide survey of 193 centres and conclusions by the ESNR working group. *Neuroradiology* **61**, 633–642.

[75] Frisoni GB, Bocchetta M, Chételat G, Rabinovici GD, De Leon MJ, Kaye J, Reiman EM, Scheltens P, Barkhof F, Black SE, Brooks DJ, Carrillo MC, Fox NC, Herholz K, Nordberg A, Jack CR, Jagust WJ, Johnson KA, Rowe CC, Sperling RA, Thies W, Wahlund LO, Weiner MW, Pasqualetti P, DeCarli C (2013) Imaging markers for Alzheimer disease: Which vs how. *Neurology* **81**, 487–500.

[76] Buchhave P, Minthon L, Zetterberg H, Wallin ÅK, Blennow K, Hansson O (2012) Cerebrospinal fluid levels of β-amyloid 1-42, but not of tau, are fully changed already 5 to 10 years before the onset of Alzheimer dementia. *Arch. Gen. Psychiatry* **69**, 98–106.

[77] Ewers M, Mattsson N, Minthon L, Molinuevo JL, Antonell A, Popp J, Jessen F, Herukka SK, Soininen H, Maetzler W, Leyhe T, Bürger K, Taniguchi M, Urakami K, Lista S, Dubois B, Blennow K, Hampel H (2015) CSF biomarkers for the

differential diagnosis of Alzheimer's disease: A large-scale international multicenter study. *Alzheimer's Dement.* **11**, 1306–1315.

[78] Paterson RW, Slattery CF, Poole T, Nicholas JM, Magdalinou NK, Toombs J, Chapman MD, Lunn MP, Heslegrave AJ, Foiani MS, Weston PSJ, Keshavan A, Rohrer JD, Rossor MN, Warren JD, Mummery CJ, Blennow K, Fox NC, Zetterberg H, Schott JM (2018) Cerebrospinal fluid in the differential diagnosis of Alzheimer's disease: Clinical utility of an extended panel of biomarkers in a specialist cognitive clinic. *Alzheimer's Res. Ther.* **10**, 1–11.

[79] Schoonenboom N, Reesink F, Verwey N, Kester M, Teunissen C, van de Ven P, Pijnenburg Y, Blankenstein M, Rozemuller A, Scheltens P, van der Flier W (2012) Cerebrospinal fluid markers for differential dementia diagnosis in a large memory clinic cohort. *Neurology* **78**, 47–54.

[80] Blennow K, de Leon MJ, Zetterberg H (2006) Alzheimer's disease. *Lancet* **368**, 387–403.

[81] Shaw LM, Arias J, Blennow K, Galasko D, Luis J, Salloway S, Schindler S, Carrillo MC, Hendrix JA, Ross A, Illes J, Ramus C, Fifer S (2018) Appropriate use criteria for lumbar puncture and cerebrospinal fluid testing in the diagnosis of Alzheimer's disease. *Alzheimer's Dement.* 1–17.

[82] Mattsson N, Rosen E, Hansson O, Andreasen N, Parnetti L, Jonsson M, Herukka SK, van der Flier WM, Blankenstein MA, Ewers M, Rich K, Kaiser E, Verbeek MM, Rikkert MO, Tsolaki M, Mulugeta E, Aarsland D, Visser PJ, Schroeder J, Marcusson J, de Leon M, Hampel H, Scheltens P, Wallin A, Eriksdotter-Jonhagen M, Minthon L, Winblad B, Blennow K, Zetterberg H (2012) Age and diagnostic performance of Alzheimer disease CSF biomarkers. *Neurology* **78**, 468–476.

[83] Frisoni GB, Boccardi M, Barkhof F, Blennow K, Cappa S, Chiotis K, Démonet JF, Garibotto V, Giannakopoulos P, Gietl A, Hansson O, Herholz K, Jack CR, Nobili F, Nordberg A, Snyder HM, Ten Kate M, Varrone A, Albanese E, Becker S, Bossuyt P, Carrillo MC, Cerami C, Dubois B, Gallo V, Giacobini E, Gold G, Hurst S, Lönneborg A, Lovblad KO, Mattsson N, Molinuevo JL, Monsch AU, Mosimann U, Padovani A, Picco A, Porteri C, Ratib O, Saint-Aubert L, Scerri C, Scheltens P, Schott JM, Sonni I, Teipel S, Vineis P, Visser PJ, Yasui Y, Winblad B (2017) Strategic roadmap for an early diagnosis of Alzheimer's disease based on biomarkers. *Lancet Neurol.* **16**, 661–676.

[84] Hort J, O'Brien JT, Gainotti G, Pirttila T, Popescu BO, Rektorova I, Sorbi S, Scheltens P (2010) EFNS guidelines for the diagnosis and management of Alzheimer's disease. *Eur. J. Neurol.* **17**, 1236–1248.

[85] Nobili F, Arbizu J, Bouwman F, Drzezga A, Agosta F, Nestor P, Walker Z, Boccardi M (2018) European Association of Nuclear Medicine and European Academy of Neurology recommendations for the use of brain 18F-Fluorodeoxyglucose Positron Emission Tomography in neurodegenerative cognitive impairment and dementia: Delphi consensus. *Eur. J. Neurol.* 1–17.

[86] Jagust W, Reed B, Mungas D, Ellis W, DeCarli C (2007) What does fluorodeoxyglucose PET imaging add to a clinical diagnosis of dementia? *Neurology* **69**, 871–877.

[87] Foster NL, Heidebrink JL, Clark CM, Jagust WJ, Arnold SE, Barbas NR, DeCarli CS, Scott Turner R, Koeppe RA, Higdon R, Minoshima S (2007) FDG-PET improves accuracy in distinguishing frontotemporal dementia and Alzheimer's disease. *Brain* **130**, 2616–2635.

[88] Ishii K (2014) PET approaches for diagnosis of dementia. *Am. J. Neuroradiol.* **35**, 2030–2038.

[89] Arbizu J, Festari C, Altomare D, Walker Z, Bouwman F, Rivolta J, Orini S, Barthel H, Agosta F, Drzezga A, Nestor P, Boccardi M, Frisoni GB, Nobili F (2018) Clinical utility of FDG-PET for the differential diagnosis in MCI. *Eur J Nucl Med Mol Imaging*.

[90] Nestor PJ, Altomare D, Festari C, Drzezga A, Rivolta J, Walker Z, Bouwman F, Orini S, Law I, Agosta F, Arbizu J, Boccardi M, Nobili F, Frisoni GB (2018) Clinical utility of FDG-PET for the differential diagnosis among the main forms of dementia. *Eur. J. Nucl. Med. Mol. Imaging* 1–17.

[91] Sinha N, Firbank M, O'Brien J (2012) Biomarkers in dementia with Lewy bodies: A review. *Int. J. Geriatr. Psychiatry* **27**, 443–453.

[92] Lim SM, Katsifis A, Villemagne VL, Best R, Jones G, Saling M, Bradshaw J, Merory J, Woodward M, Hopwood M, Rowe CC (2009) The 18F-FDG PET Cingulate Island Sign and Comparison to 123I-b-CIT SPECT for Diagnosis of Dementia with Lewy Bodies. *J. Nucl. Med.* **50**, 1638–1645.

[93] Graff-Radford J, Murray ME, Lowe VJ, Boeve BF, Ferman TJ, Przybelski SA, Lesnick TG, Senjem ML, Gunter JL, Smith GE, Knopman DS, Jack Jr CR, Dickson

DW, Petersen RC, Kejal K (2014) Dementia with Lewy bodies: Basis of cingulate island sign. *Neurology* **83**, 801–809.

[94] Iizuka T, Kameyama M (2016) Cingulate island sign on FDG-PET is associated with medial temporal lobe atrophy in dementia with Lewy bodies. *Ann. Nucl. Med.* **30**, 421–429.

[95] Kantarci K, Lowe VJ, Boeve BF, Weigand SD, Senjem ML, Przybelski SA, Dickson DW, Parisi JE, Knopman DS, Smith GE, Ferman TJ, Petersen RC, Jack Jr CR (2012) Multimodality imaging characteristics of dementia with Lewy bodies. *Neurobiol. Aging* **33**, 2091–2105.

[96] O'Brien JT, Firbank MJ, Davison C, Barnett N, Bamford C, Donaldson C, Olsen K, Herholz K, Williams D, Lloyd J (2014) 18F-FDG PET and perfusion SPECT in the diagnosis of Alzheimer and Lewy body dementias. *J. Nucl. Med.* **55**, 1959–65.

[97] Johansen KK, White LR, Sando SB, Aasly JO (2010) Biomarkers: Parkinson disease with dementia and dementia with Lewy bodies. *Parkinsonism Relat. Disord.* **16**, 307–315.

[98] Tang-Wai DF, Graff-Radford NR, Boeve BF, Dickson DW, Parisi JE, Crook R, Caselli RJ, Knopman DS, Petersen RC (2004) Clinical, genetic, and neuropathologic characteristics of posterior cortical atrophy. *Neurology* **63**, 1168–1174.

[99] Whitwell JL, Graff-Radford J, Singh TD, Drubach DA, Senjem ML, Spychalla AJ, Tosakulwong N, Lowe VJ, Josephs KA (2017) 18 F-FDG PET in Posterior Cortical Atrophy and Dementia with Lewy Bodies. *J. Nucl. Med.* **58**, 632–638.

[100] Imamura T, Ishii K, Sasaki M, Kitagaki H, Yamaji S, Hirono N, Shimomura T, Hashimoto M, Tanimukai S, Kazui H, Mori E (1997) Regional cerebral glucose metabolism in dementia with Lewy bodies and Alzheimer's disease: A comparative study using positron emission tomography. *Neurosci. Lett.* **235**, 49–52.

[101] Whitwell JL, Jack CR (2007) Neuroimaging in Dementia. *Neurol. Clin.* **25**, 843–857.

[102] Kerrouche N, Herholz K, Mielke R, Holthoff V, Baron JC (2006) 18FDG PET in vascular dementia: Differentiation from Alzheimer's disease using voxel-based multivariate analysis. *J. Cereb. Blood Flow Metab.* **26**, 1213–1221.

[103] Varrone A, Asenbaum S, Borght TV, Booij J, Nobili F, Någren K, Darcourt J, Kapucu ÖL, Tatsch K, Bartenstein P, Van Laere K (2009) EANM procedure guidelines for PET brain imaging using [18F]FDG, version 2. *Eur. J. Nucl. Med.*

Mol. Imaging **36**, 2103–2110.

[104] Nobili F, Festari C, Altomare D, Agosta F, Orini S, Van Laere K, Arbizu J, Bouwman F, Drzezga A, Nestor P, Walker Z, Boccardi M (2018) Automated assessment of FDG-PET for differential diagnosis in patients with neurodegenerative disorders. *Eur. J. Nucl. Med. Mol. Imaging* **45**, 1557–1566.

[105] McKeith IG, Dickson DW, Lowe J, Emre M, O'Brien JT, Feldman H, Cummings J, Duda JE, Lippa C, Perry EK, Aarsland D, Arai H, Ballard CG, Boeve B, Burn DJ, Costa D, Del Ser T, Dubois B, Galasko D, Gauthier S, Goetz CG, Gomez-Tortosa E, Halliday G, Hansen LA, Hardy J, Iwatsubo T, Kalaria RN, Kaufer D, Kenny RA, Korczyn A, Kosaka K, Lee VMY, Lees A, Litwan I, Londos E, Lopez OL, Minoshima S, Mizuno Y, Molina JA, Mukaetova-Ladinska EB, Pasquier F, Perry RH, Schulz JB, Trojanowski JQ, Yamada M (2005) Diagnosis and management of dementia with Lewy bodies: Third report of the DLB Consortium. *Neurology* **65**, 1863–1872.

[106] Sedaghat F, Gotzamani-Psarrakou A, Dedousi E, Arnaoutoglou M, Psarrakos K, Baloyannis I, Dimitriadis AS, Baloyannis SJ (2007) Evaluation of dopaminergic function in frontotemporal dementia using 123I-FP-CIT single photon emission computed tomography. *Neurodegener. Dis.* **4**, 382–385.

[107] Colloby SJ, Williams ED, Burn DJ, Lloyd JJ, McKeith IG, O'Brien JT (2005) Progression of dopaminergic degeneration in dementia with Lewy bodies and Parkinson's disease with and without dementia assessed using 123I-FP-CIT SPECT. *Eur. J. Nucl. Med. Mol. Imaging* **32**, 1176–1185.

[108] O'Brien JT, McKeith IG, Walker Z, Tatsch K, Booij J, Darcourt J, Marquardt M, Reininger C (2009) Diagnostic accuracy of 123I-FP-CIT SPECT in possible dementia with Lewy bodies. *Br. J. Psychiatry* **194**, 34–39.

[109] Klunk WE, Engler H, Nordberg A, Wang Y, Blomqvist G, Holt DP, Bergström M, Savitcheva I, Huang GF, Estrada S, Ausén B, Debnath ML, Barletta J, Price JC, Sandell J, Lopresti BJ, Wall A, Koivisto P, Antoni G, Mathis CA, Långström B (2004) Imaging Brain Amyloid in Alzheimer's Disease with Pittsburgh Compound-B. *Ann. Neurol.* **55**, 306–319.

[110] Clark CM, Schneider JA, Bedell BJ, Beach TG, Bilker WB, Mintun MA, Pontecorvo MJ, Hefti F, Carpenter AP, Flitter ML, Krautkramer MJ, Kung HF, Coleman RE, Doraiswamy PM, Fleisher AS, Sabbagh MN, Sadowsky CH, Reiman

PEM, Zehntner SP, Skovronsky DM (2011) Use of florbetapir-PET for imaging β-amyloid pathology. *JAMA - J. Am. Med. Assoc.* **305**, 275–283.

[111] Rabinovici GD, Rosen HJ, Alkalay A, Kornak J, Furst AJ, Agarwal N, Mormino EC, O'Neil JP, Janabi M, Karydas A, Growdon ME, Jang JY, Huang EJ, DeArmond SJ, Trojanowski JQ, Grinberg LT, Gorno-Tempini ML, Seeley WW, Miller BL, Jagust WJ (2011) Amyloid vs FDG-PET in the differential diagnosis of AD and FTLD. *Neurology* **77**, 2034–2042.

[112] Jansen WJ, Ossenkoppele R, Knol DL, Tijms BM, Scheltens P, Verhey FRJ, Visser PJ (2015) Prevalence of Cerebral Amyloid Pathology in Persons Without Dementia A Meta-analysis. **313**, 1924–1938.

[113] Rik Ossenkoppele, PhD, Willemijn J. Jansen, MSc, Gil D. Rabinovici, MD, Dirk L. Knol, PhD, Wiesje M. van der Flier, PhD, Bart N. M. van Berckel, MD, PhD, Philip Scheltens, MD, PhD, and Pieter Jelle Visser, MD P on behalf of the APSG (2015) Prevalence of Amyloid PET Positivity in Dementia Syndromes: A Meta-analysis. *JAMA* **313**, 1939–1949.

[114] Villemagne VL, Fodero-Tavoletti MT, Masters CL, Rowe CC (2015) Tau imaging: Early progress and future directions. *Lancet Neurol.* **14**, 114–124.

[115] Leuzy A, Chiotis K, Lemoine L, Gillberg PG, Almkvist O, Rodriguez-Vieitez E, Nordberg A (2019) Tau PET imaging in neurodegenerative tauopathies—still a challenge. *Mol. Psychiatry*.

[116] Cho H, Choi JY, Hwang MS, Kim YJ, Lee HM, Lee HS, Lee JH, Ryu YH, Lee MS, Lyoo CH (2016) In vivo cortical spreading pattern of tau and amyloid in the Alzheimer disease spectrum. *Ann. Neurol.* **80**, 247–258.

[117] Johnson KA, Schultz A, Betensky RA, Becker JA, Sepulcre J, Rentz D, Mormino E, Chhatwal J, Amariglio R, Papp K, Marshall G, Albers M, Mauro S, Pepin L, Alverio J, Judge K, Philiossaint M, Shoup T, Yokell D, Dickerson B, Gomez-Isla T, Hyman B, Vasdev N, Sperling R (2016) Tau PET imaging in aging and early Alzheimer's disease. *Ann Neurol* **79**, 110–119.

[118] Schöll M, Lockhart SN, Schonhaut DR, O'Neil JP, Janabi M, Ossenkoppele R, Baker SL, Vogel JW, Faria J, Schwimmer HD, Rabinovici GD, Jagust WJ (2016) PET Imaging of Tau Deposition in the Aging Human Brain. *Neuron* **89**, 971–982.

[119] Sweeney MD, Montagne A, Sagare AP, Nation DA, Schneider LS, Chui HC, Harrington MG, Pa J, Law M, Wang DJJ, Jacobs RE, Doubal FN, Ramirez J, Black

SE, Nedergaard M, Benveniste H, Dichgans M, Iadecola C, Love S, Bath PM, Markus HS, Salman RA, Allan SM, Quinn TJ, Kalaria RN, Werring DJ, Carare RO, Touyz RM, Williams SCR, Moskowitz MA, Katusic ZS, Lutz SE, Lazarov O, Minshall RD, Rehman J, Davis TP, Wellington CL, González HM, Yuan C, Lockhart SN, Hughes TM, Chen CLH, Sachdev P, O'Brien JT, Skoog I, Pantoni L, Gustafson DR, Biessels GJ, Wallin A, Smith EE, Mok V, Wong A, Passmore P, Barkof F, Muller M, Breteler MMB, Román GC, Hamel E, Seshadri S, Gottesman RF, van Buchem MA, Arvanitakis Z, Schneider JA, Drewes LR, Hachinski V, Finch CE, Toga AW, Wardlaw JM, Zlokovic B V. (2019) Vascular dysfunction—The disregarded partner of Alzheimer's disease. *Alzheimer's Dement.* **15**, 158–167.

[120] Gaugler JE, Ascher-Svanum H, Roth DL, Fafowora T, Siderowf A, Beach TG (2013) Characteristics of patients misdiagnosed with Alzheimer's disease and their medication use: An analysis of the NACC-UDS database. *BMC Geriatr.* **13**,.

[121] Simonsen AH, Herukka SK, Andreasen N, Baldeiras I, Bjerke M, Blennow K, Engelborghs S, Frisoni GB, Gabryelewicz T, Galluzzi S, Handels R, Kramberger MG, Kulczyńska A, Molinuevo JL, Mroczko B, Nordberg A, Oliveira CR, Otto M, Rinne JO, Rot U, Saka E, Soininen H, Struyfs H, Suardi S, Visser PJ, Winblad B, Zetterberg H, Waldemar G (2017) Recommendations for CSF AD biomarkers in the diagnostic evaluation of dementia. *Alzheimer's Dement.* **13**, 274–284.

[122] McKeith IG (2006) Consensus guidelines for the clinical and pathologic diagnosis of dementia with Lewy bodies (DLB): Report of the consortium on DLB international workshop. *J. Alzheimer's Dis.* **9**, 417–423.

[123] Brunnström H, Englund E (2009) Clinicopathological concordance in dementia diagnostics. *Am. J. Geriatr. Psychiatry* **17**, 664–670.

[124] Beach TG, Monsell SE, Phillips LE, Kukull W (2012) Accuracy of the Clinical Diagnosis of Alzheimer Disease at National Institute on Aging Alzheimer Disease Centers, 2005-2010. *J Neuropathol Exp. Neurol.* **71**, 266–273.

[125] Bloudek LM, Spackman DE, Blankenburg M, Sullivan SD (2011) Review and meta-analysis of biomarkers and diagnostic imaging in Alzheimer's disease. *J. Alzheimer's Dis.* **26**, 627–645.

[126] Oxtoby NP, Alexander DC (2017) Imaging plus X: Multimodal models of neurodegenerative disease. *Curr. Opin. Neurol.* **30**, 371–379.

[127] Bruun M, Frederiksen KS, Rhodius-meester HFM, Baroni M, Gjerum L,

Koikkalainen J, Urhemaa T, Tolonen A, Gils M Van, Tong T, Guerrero R, Rueckert D, Dyremose N, Andersen BB, Simonsen AH, Lemstra A, Hallikainen M, Kurl S, Herukka S-K, Remes AM, Waldemar G, Soininen H, Mecocci P, Flier WM Van Der, Hasselbalch SG (2019) Impact of a Clinical Decision Support Tool on Dementia Diagnostics in Memory Clinics: The PredictND Validation Study. *Curr. Alzheimer Res.* **16**, 91–101.

[128] Mattila J, Koikkalainen J, Virkki A, Van Gils M, Lötjönen J (2012) Design and application of a generic clinical decision support system for multiscale data. *IEEE Trans. Biomed. Eng.* **59**, 234–240.

[129] Lötjönen JM, Wolz R, Koikkalainen JR, Thurfjell L, Waldemar G, Soininen H, Rueckert D (2010) Fast and robust multi-atlas segmentation of brain magnetic resonance images. *Neuroimage* **49**, 2352–2365.

[130] Koikkalainen J, Rhodius-Meester H, Tolonen A, Barkhof F, Tijms B, Lemstra AW, Tong T, Guerrero R, Schuh A, Ledig C, Rueckert D, Soininen H, Remes AM., Waldemar G, Hasselbalch S, Mecocci P, van der Flier W, Lötjönen J, Rhodius-Meester, Hanneke; Tolonen A, Barkhof F, Tijms B, Lemstra AW., Tong T, Guerrero R, Schuh A, Ledig C, Rueckert D, Soininen H, Remes AM., Waldemar G, Hasselbalch S, Mecocci P, van der Flier W, Lötjönen J (2016) Differential diagnosis of neurodegenerative diseases using structural MRI data. *NeuroImage Clin.* **11**, 435–449.

[131] Tong T, Wolz R, Coupé P, Hajnal J V., Rueckert D (2013) Segmentation of MR images via discriminative dictionary learning and sparse coding: Application to hippocampus labeling. *Neuroimage* **76**, 11–23.

[132] Tolonen A, Rhodius-Meester HFM, Bruun M, Koikkalainen J, Barkhof F, Lemstra AW, Koene T, Scheltens P, Teunissen CE, Tong T, Guerrero R, Schuh A, Ledig C, Baroni M, Rueckert D, Soininen H, Remes AM, Waldemar G, Hasselbalch SG, Mecocci P, van der Flier WM, Lötjönen J (2018) Data-driven differential diagnosis of dementia using multiclass disease state index classifier. *Front. Aging Neurosci.* **10**, 1–11.

[133] Mattila J, Koikkalainen J, Virkki A, Simonsen A, Van Gils M, Waldemar G, Soininen H, Lötjönen J (2011) A disease state fingerprint for evaluation of Alzheimer's disease. *J. Alzheimer's Dis.* **27**, 163–176.

[134] Tong T, Ledig C, Guerrero R, Schuh A, Koikkalainen J, Tolonen A, Rhodius H,

Barkhof F, Tijms B, Lemstra AW, Soininen H, Remes AM, Waldemar G, Hasselbalch S, Mecocci P, Baroni M, Lötjönen J, Flier W van der, Rueckert D (2017) Five-class differential diagnostics of neurodegenerative diseases using random undersampling boosting. *NeuroImage Clin.* **15**, 613–624.

[135] Bruun M, Rhodius-meester HFM, Koikkalainen J, Baroni M, Gjerum L, Lemstra AW, Barkhof F, Remes AM, Urhemaa T, Tolonen A, Rueckert D, Gils M Van, Frederiksen KS, Waldemar G, Scheltens P, Mecocci P, Soininen H, Jyrki L (2018) Evaluating combinations of diagnostic tests to discriminate different dementia types. *Alzheimer's Dement. Diagnosis, Assess. Dis. Monit.* **10**, 1–10.

[136] Relkin N, Marmarou A, Klinge P, Bergsneider M, Black PM (2005) Diagnosing idiopathic normal-pressure hydrocephalus. *Neurosurgery* **57**, S2-4-S2-16.

[137] Litvan I (2001) Diagnosis and management of progressive supranuclear palsy. *Semin Neurol* **21**, 41–48.

[138] Gilman S, Wenning GK, Low P a, Brooks DJ, Mathias CJ, Trojanowski JQ, Wood NW, Colosimo C, Dürr A, Fowler CJ, Kaufmann H, Klockgether T, Lees AJ, Poewe WH, Quinn NP, Revesz T, Robertson D, Sandroni P, Seppi K, Vidailhet M (2008) Second consensus statement on the diagnosis of multiple system atrophy. *Neurology* **71**, 670–6.

[139] Riley D, Lang A (2000) Clinical diagnostic criteria. *Adv. Neurol.* **82**, 29–34.

[140] Petersen RC, Smith GE, Waring SC, Ivnik RJ, Tangalos EG, Kokmen E (1999) Mild Cognitive Impairment: Clinical characterization and outcome. *Arch. Neurol.* **56**, 303–308.

[141] Folstein M, Folstein S, McHugh P (1975) 'Mini-mental state' - A practical method for grading the cognitive state of patients for the clinician. *J. Psychiatr. Res.* **12**, 189–198.

[142] Mathuranath P, Nestor P, Berrios G, Rakowicz W, Hodges J (2000) A brief cognitive test battery to differentiate Alzheimer's disease and frontotemporal dementia. *Neurology* **55**, 1613–1620.

[143] Morris J (1993) The clinical dementia rating (CDR): Current version and scoring rules. *Neurology* **43**, 2412–2414.

[144] Reitan R (1958) Validity of the Trail Making Test as an indicator of organic brain damage. *Percept Mot Ski.* **8**, 271–276.

[145] Van Der Elst W, Van Boxtel MPJ, Van Breukelen GJP, Jolles J (2006) Normative

data for the Animal, Profession and Letter M Naming verbal fluency tests for Dutch speaking participants and the effects of age, education, and sex. *J. Int. Neuropsychol. Soc.* **12**, 80–89.

[146] Morris J, Heyman A, Mohs R, Hughes J, van Belle G, Fillenbaum G, Mellits E, Clark C (1989) The Consortium to Establish a Registry for Alzheimer's Disease (CERAD). Part I. Clinical and neuropsychological assessment of Alzheimer's disease. *Neurology* **39**, 1159–1165.

[147] Schmidt M (1996) *Rey auditory verbal learning test: A handbook*, Los Angeles, CA: Western Psychological Services.

[148] Zwan MD, Rinne JO, Hasselbalch SG, Nordberg A, Lleó A, Herukka S-K, Soininen H, Law I, Bahl JMC, Carter SF, Fortea J, Blesa R, Teunissen CE, Bouwman FH, Van Berckel BNM, Visser PJ (2016) Use of amyloid-PET to determine cutpoints for CSF markers. *Neurology* **86**, 50–58.

[149] Darcourt J, Booij J, Tatsch K, Varrone A, Borght TV, Kapucu ÖL, Någren K, Nobili F, Walker Z, Van Laere K (2010) EANM procedure guidelines for brain neurotransmission SPECT using 123 I-labelled dopamine transporter ligands, version 2. *Eur. J. Nucl. Med. Mol. Imaging* **37**, 443–450.

[150] McCleery J, Morgan S, Bradley KM, Noel-Storr AH, Ansorge O, Hyde C (2015) Dopamine transporter imaging for the diagnosis of dementia with Lewy bodies. *Cochrane database Syst. Rev.* **1**,.

[151] Minoshima S, Drzezga AE, Barthel H, Bohnen N, Djekidel M, Lewis DH, Mathis CA, McConathy J, Nordberg A, Sabri O, Seibyl JP, Stokes MK, Van Laere K (2016) SNMMI Procedure Standard/EANM Practice Guideline for Amyloid PET Imaging of the Brain 1.0. *J. Nucl. Med.* **57**, 1316–1322.

[152] Fischl B (2012) FreeSurfer. *Neuroimage* **62**, 774–781.

[153] Greve DN, Salat DH, Bowen SL, Izquierdo-Garcia D, Schultz AP, Catana C, Becker JA, Svarer C, Knudsen G, Sperling RA, Johnson KA (2016) Different partial volume correction methods lead to different conclusions: An 18 F-FDG-PET study of aging. *Neuroimage* **15**, 334–343.

[154] Bruun M, Koikkalainen J, Rhodius-meester HFM, Baroni M, Gjerum L, Gils M Van, Soininen H, Remes AM, Hartikainen P, Waldemar G, Mecocci P, Barkhof F, Pijnenburg Y, Flier WM Van Der, Hasselbalch SG, Lötjönen J, Frederiksen KS (2019) Detecting frontotemporal dementia syndromes using MRI biomarkers.

NeuroImage Clin. **22**, 1–9.

[155] Ashburner J, Friston KJ (2000) Voxel-Based Morphometry - The Methods. *Neuroimage* **11**, 805–821.

[156] Ashburner J, Hutton C, Frackowiak R, Johnsrude I, Price C, Friston K (1998) Identifying global anatomical differences: Deformation-based morphometry. *Hum. Brain Mapp.* **6**, 348–357.

[157] Wang Y, Catindig JA, Hilal S, Soon HW, Ting E, Wong TY, Venketasubramanian N, Chen C, Qiu A (2012) Multi-stage segmentation of white matter hyperintensity, cortical and lacunar infarcts. *Neuroimage* **60**, 2379–2388.

[158] Herholz K, Salmon E, Perani D, Baron JC, Holthoff V, Frölich L, Schönknecht P, Ito K, Mielke R, Kalbe E, Zündorf G, Delbeuck X, Pelati O, Anchisi D, Fazio F, Kerrouche N, Desgranges B, Eustache F, Beuthien-Baumann B, Menzel C, Schröder J, Kato T, Arahata Y, Henze M, Heiss WD (2002) Discrimination between Alzheimer dementia and controls by automated analysis of multicenter FDG PET. *Neuroimage* **17**, 302–316.

[159] Davison CM, O'Brien JT (2014) A comparison of FDG-PET and blood flow SPECT in the diagnosis of neurodegenerative dementias: A systematic review. *Int. J. Geriatr. Psychiatry* **29**, 551–561.

[160] Dukart J, Mueller K, Horstmann A, Barthel H, Möller HE, Villringer A, Sabri O, Schroeter ML (2011) Combined evaluation of FDG-PET and MRI improves detection and differentiation of dementia. *PLoS One* **6**,.

[161] Rice L, Bisdas S (2017) The diagnostic value of FDG and amyloid PET in Alzheimer's disease - A systematic review. *Eur. J. Radiol.* **94**, 16–24.

[162] Jagust WJ, Landau SM, Shaw LM, Trojanowski JQ, Koeppe RA, Reiman EM, Foster NL, Petersen RC, Weiner MW, Price JC, Mathis CA (2009) Relationships between biomarkers in aging and dementia. *Neurology* **73**, 1193–1199.

[163] Minoshima S, Foster NL, Sima AAF, Frey KA, Albin RL, Kuhl DE (2001) Alzheimer's Disease versus Dementia with Lewy Bodies: Cerebral Metabolic Distinction with Autopsy Confirmation. *Ann. Neurol.* **50**, 358–365.

[164] Buckner RL, Head D, Parker J, Fotenos AF, Marcus D, Morris JC, Snyder AZ (2004) A unified approach for morphometric and functional data analysis in young, old, and demented adults using automated atlas-based head size normalization: Reliability and validation against manual measurement of total intracranial volume.

Neuroimage **23**, 724–738.

[165] Cole T, Green P (1992) Smoothing reference centile curves: the LMS method and penalized likelihood. *Stat. Med.* **11**, 1305–1319.

[166] Brodersen KH, Ong CS, Stephan KE, Buhmann JM (2010) The balanced accuracy and its posterior distribution. *2010 20th Int. Conf. Pattern Recognit.* 3121–3124.

[167] Youden WJ (1950) Index for rating diagnostic tests. *Cancer* **3**, 32–35.

[168] Cluitmans L, Mattila J, Runtti H, Van Gils M, Lötjönen J (2013) A MATLAB toolbox for classification and visualization of heterogenous multi-scale human data using the disease state fingerprint method. In *pHealth 2013* IOS Press, 2013, pp. 77–82.

[169] Panegyres PK, Rogers JM, McCarthy M, Campbell A, Wu JS (2009) Fluorodeoxyglucose-positron emission tomography in the differential diagnosis of early-onset dementia: A prospective, community-based study. *BMC Neurol.* **9**, 1–9.

[170] Wahlund L-O, Westman E, van Westen D, Wallin A, Shams S, Cavallin L, Larsson E-M (2017) Imaging biomarkers of dementia: recommended visual rating scales with teaching cases. *Insights Imaging* **8**, 79–90.

[171] Høgh P, Teller AS, Hasselbalch S, Waldemar G (2007) Visual rating and ROI-based parametric analysis of rCBF SPECT in patients with mild or questionable dementia: A comparative study. *Dement. Geriatr. Cogn. Disord.* **24**, 429–433.

[172] Ishii K, Hosokawa C, Hyodo T, Sakaguchi K, Usami K, Shimamoto K, Hosono M, Yamazoe Y, Murakami T (2015) Regional glucose metabolic reduction in dementia with Lewy bodies is independent of amyloid deposition. *Ann. Nucl. Med.* **29**, 78–83.

[173] Hamed M, Schraml F, Wilson J, Galvin J, Sabbagh MN (2018) Occipital and Cingulate Hypometabolism are Significantly Under-Reported on 18-Fluorodeoxyglucose Positron Emission Tomography Scans of Patients with Lewy Body Dementia. *J Alzheimers Dis Park.* **8**, 1–12.

[174] Neary D, Snowden JS, Gustafson L, Passant U, Stuss D, Black S, Freedman M, Kertesz A, Robert P., Albert M, Boone M, Miller B., Cummings J, Benson D. (1998) Frontotemporal lobar degeneration: A consensus on clinical diagnoistic criteria. *Neurology* **51**, 1546–1554.

[175] Caminiti SP, Sala A, Iaccarino L, Beretta L, Pilotto A, Gianolli L, Iannaccone S, Magnani G, Padovani A, Ferini-Strambi L, Perani D (2019) Brain glucose metabolism in Lewy body dementia: Implications for diagnostic criteria.

Alzheimer's Res. Ther. **11**, 1–14.

[176] Ishii K, Imamura T, Sasaki M, Yamaji S, Sakamoto S, Kitagaki H, Hashimoto M, Hirono N, Shimomura T, Mori E (1998) Regional cerebral glucose metabolism in dementia with Lewy bodies and Alzheimer's disease. *Neurology* **51**, 125–130.

[177] Kono AKA, Ishii K, Sofue K, Miyamoto N, Sakamoto S, Mori E (2007) Fully automatic differential diagnosis system for dementia with Lewy bodies and Alzheimer's disease using FDG-PET and 3D-SSP. *Eur. J. Nucl. Med. Mol. Imaging* **34**, 1490–1497.

[178] Mosconi L, Tsui WHWH, Herholz K, Pupi A, Drzezga A, Lucignani G, Reiman EMEM, Holthoff V, Kalbe E, Sorbi S, Diehl-Schmid J, Perneczky R, Clerici F, Caselli R, Beuthien-Baumann B, Kurz A, Minoshima S, de Leon MJMMJ (2008) Multicenter Standardized 18F-FDG PET Diagnosis of Mild Cognitive Impairment, Alzheimer's Disease, and Other Dementias. *J. Nucl. Med.* **49**, 390–398.

[179] Higuchi M, Tashiro M, Arai H, Okamura N, Hara S, Higuchi S, Itoh M, Shin R, Trojanowski J, Sasaki H (2000) Glucose Hypometabolism and Neuropathological Correlates in Brains of Dementia with Lewy Bodies. *Exp. Neurol.* **162**, 247–256.

[180] Schneider JA, Arvanitakis Z, Leurgans SE, Bennett DA (2009) The neuropathology of probable Alzheimer disease and mild cognitive impairment. *Ann. Neurol.* **66**, 200–208.

[181] Mendez MF, Joshi A, Tassniyom K, Teng E, Shapira JS (2013) Clinicopathologic differences among patients with behavioral variant frontotemporal dementia. *Neurology* **80**, 561–568.

8. Study manuscripts

Study I

Comparison of the added clinical value of 2-[^{18}F]FDG-PET and cerebrospinal fluid biomarkers in patients suspected of Alzheimer's disease.

Comparison of the added clinical value of 2-[^{18}F]FDG-PET and cerebrospinal fluid biomarkers in patients suspected of Alzheimer's disease.

Le Gjerum[a], Birgitte Bo Andersen[a], Marie Bruun[a], Anja Hviid Simonsen[a], Otto Mølby Henriksen[b], Ian Law[b], Steen Gregers Hasselbalch[a], and Kristian Steen Frederiksen[a].

[a]Department of Neurology, Danish Dementia Research Centre, Rigshospitalet, University of Copenhagen, Copenhagen, Denmark
[b]Department of Clinical Physiology, Nuclear Medicine & PET, Rigshospitalet, University of Copenhagen, Copenhagen, Denmark

Corresponding author:
Kristian Steen Frederiksen,
Department of Neurology,
Danish Dementia Research Centre,
Rigshospitalet,
University of Copenhagen,
Blegdamsvej 9, DK-2100 Copenhagen, Denmark,
Office phone: +45 35 45 69 11,
E-mail: kristian.steen.frederiksen@regionh.dk

ABSTRACT

BACKGROUND The two biomarkers 2-[^{18}F]FDG-PET and cerebrospinal fluid biomarkers are both recommended to support the diagnosis of Alzheimer's disease. However, there is a lack of knowledge for the comparison of the two biomarkers in a routine clinical setting.

OBJECTIVE The aim of this study was to compare the clinical value of adding 2-[^{18}F]FDG-PET and cerebrospinal fluid biomarkers to a standard program.

METHOD Eighty-one patients suspected of having Alzheimer's disease were include from the Copenhagen Memory Clinic. As part of the clinical work-up all patients had a standard program examination including MRI and ancillary investigations with 2-[^{18}F]FDG-PET and cerebrospinal fluid biomarkers. A three-step incremental evaluation was done by two blinded dementia specialists to reach consensus decision on diagnosis, prediction of disease course, and change in patient management. Confidence in the decision was measure on a numeric rating scale (0-100). A clinical follow up after 12 months was used as reference for diagnosis and disease course.

RESULTS The two biomarkers had a similar clinical value across all diagnosis when added individually to the standard program. However, for the correctly diagnosed patient with Alzheimer's disease cerebrospinal fluid biomarkers had a significantly higher impact on diagnostic confidence (mean scores±SD: 88±11 vs. 83±11, p=.04) and a reduced need for ancillary investigations (19 vs. 8 patients, p=.007) compared to 2-[^{18}F]FDG-PET.

CONCLUSION The two biomarkers had similar clinical value across all diagnosis, but cerebrospinal fluid biomarkers seemed to have more significant value in corroborating the

INTRODUCTION

Correct diagnosis of dementia can be challenging due to clinical heterogeneity as well as a considerable clinical overlap between various subtypes of dementia. The use of biomarkers are recommended as a supplement in the clinical evaluation to improve the diagnostic accuracy [1,2].

Brain imaging with positron emission tomography using 2-[^{18}F]fluoro-2-deoxy-D-glucose as tracer (2-[^{18}F]FDG-PET) is a biomarker of neurodegeneration [3]. Distinct patterns of hypometabolism in Alzheimer's disease (AD), frontotemporal dementia (FTD), and dementia with Lewy bodies (DLB) are seen on 2-[^{18}F]FDG-PET. Therefore, 2-[^{18}F]FDG-PET is included in the supportive criteria for both AD, FTD, and DLB [3–7]. In addition, previous studies have suggested that 2-[^{18}F]FDG-PET may facilitate an earlier detection of neurodegeneration compared to magnetic resonance imaging (MRI), considering hypometabolism on 2-[^{18}F]FDG-PET often precede atrophy on MRI [8–12].

AD biomarkers measured in cerebrospinal fluid (CSF), i.e. beta-amyloid 1-42 (Aβ42), total tau, and phosphorylated tau at threonine 181 (p-tau), reflect both specific AD pathology as well as neurodegeneration [13]. In addition, the CSF AD biomarkers can also to some extent be useful to determine the possibility of AD for the differential diagnostic evaluation [4,14–17].

2-[^{18}F]FDG-PET and CSF AD biomarkers are both recommended as ancillary investigations to the diagnostic evaluation of patients suspected of AD, if the diagnosis is uncertain or the clinical presentation is atypical [7,18–20]. Furthermore, there is a growing attention on the clinical value of neuroimaging and CSF biomarkers as potential markers of disease progression, which may be useful in clinical practice for counselling and supporting patients and caregivers, as well as outcome measures for clinical trials [21].

Currently, few studies have directly compared the diagnostic value of 2-[^{18}F]FDG-PET and CSF AD biomarkers [22–25]. Hence, conclusions regarding the added value of one biomarker over another in clinical practice are unclear.

The objective of the study was to carry out a head-to-head comparison of the added clinical value of 2-[^{18}F]FDG-PET and CSF AD biomarkers to a standard program on diagnosis, prognosis, and patient management. This was examined in patients suspected of AD with diagnostic uncertainty in a specialized memory clinic setting.

METHODS

Study population

In this study, we included 81 patients suspected of having AD from the PredictND study, who were referred to the Copenhagen memory clinic, Copenhagen University Hospital, Rigshospitalet, Copenhagen, Denmark between March 2015 and June 2016. The Copenhagen memory clinic is a specialized multidisciplinary clinic that offers diagnostic evaluation and treatment of dementia disorders on secondary and tertiary referrals from general practitioners, neurologists, psychiatrists and other hospitals.

The main inclusion criteria for the PredictND study was suspicion of having cognitive complaints due to neurodegenerative disease (ND), a mini-mental state examination (MMSE) score ≥ 18, a clinical dementia rating (CDR) global score ≤ 1.0, and no major brain disorders, psychiatric disorders or excessive substance abuse [26]. In the PredictND study, the participants were followed with a standardized clinical follow-up for at least 12 months.

To be eligible for inclusion in the present study, subjects had to have both 2-[^{18}F]FDG-PET image and measurement of CSF AD biomarkers. The patients were excluded if the clinicians in the consensus group had prior clinical knowledge of the patient (Flow diagram of the study population is shown in Supplementary Figure 1A).

All participants gave written informed consent, and the study was approved by the Danish National Committee on Health Research (no. H-1-2014-126).

Clinical examinations and supplementary investigations

All patients in the study underwent a standard program for dementia including medical history, physical and neurological examinations, cognitive testing (i.e. MMSE [27] and Addenbrooke's cognitive examination (ACE) [28]), routine blood screening, and MRI. 2-[^{18}F]FDG-PET and CSF AD biomarkers were added to the standard program on clinical indication, when the diagnosis was uncertain. In this specialized memory clinic, 2-[^{18}F]FDG-PET was commonly added as first choice biomarker, whereas CSF AD biomarkers were added on clinical indication for AD if the diagnosis was uncertain.

Additional investigations of dopamine transporter single photon emission computed tomography (DAT-SPECT) (n=8), neuropsychological assessment (n=78) and psychiatric assessment (n=4) were performed if clinically indicated. A subgroup of the patients underwent amyloid PET imaging (n=8), but this information was not used in the diagnostic evaluation.

Magnetic resonance imaging

MRI was performed on a clinical 1.5 or 3.0 Tesla system. The scan included a three-dimensional T1-weighted magnetization-prepared rapid acquisition gradient echo sequence and a T2-weighted fluid attenuation inversion recovery sequence. Each scan was evaluated by an experienced neuroradiologist in a written report as part of the clinical routine.

Cerebrospinal fluid

The CSF AD biomarkers (Aβ42, total tau, and p-tau) were analysed with enzyme-linked immunosorbent assay using commercially available kits (Innotest, Fujirebio, Europe, Ghent, Belgium). CSF AD biomarkers were considered as abnormal based on the local clinical cut-off-values for each biomarker, i.e. Aβ42 values <550 pg/mL, p-tau levels >80 pg/mL, and t-tau >400 pg/mL [29].

^{18}F-fluorodeoxyglucose positron emission tomography

PET images were acquired using clinical PET/CT or PET/MRI systems after an intravenous bolus of 200-300 MBq 2-[^{18}F]FDG as a 10 min static scan during the 40-60 min post-injection time window. The 2-[^{18}F]FDG-PET image was co-registered to the structural scan (i.e. low-dose CT, non-enhanced diagnostic CT or MRI) in a clinical standardized reading approach in SyngoVia (SyngoVia, MI Neurology, Siemens Healthcare, Erlangen, Germany). The PET image was analysed using clinically routine quantification methods, i.e. the statistical parametric mapping and statistical surface projects were performed using Scenium in comparison with a database of healthy subjects together with a visual inspection. The 2-[^{18}F]FDG-PET image was evaluated by an experienced nuclear medicine physician in a written report as part of the clinical routine.

Study design

As shown in Figure 1, the evaluation was done in a three-step incremental process by two blinded, experienced dementia specialists (either BBA and KSF or SGH and KSF). In the first step, the evaluation was based on the standard program without CSF AD biomarkers and 2-[^{18}F]FDG-PET. In the second step, results of the first biomarker (randomized to either CSF AD biomarkers or 2-[^{18}F]FDG-PET) was added, and finally in the third step, the result of the second biomarker was added. Imaging results were presented as written reports, but upon request the clinicians could inspect the images. After a minimum of six months, the same two clinicians evaluated the same patients in the three-step incremental process with addition of 2-[^{18}F]FDG-PET and CSF AD biomarkers in reverse order.

Figure 1. Flow diagram of the three-step incremental evaluation.

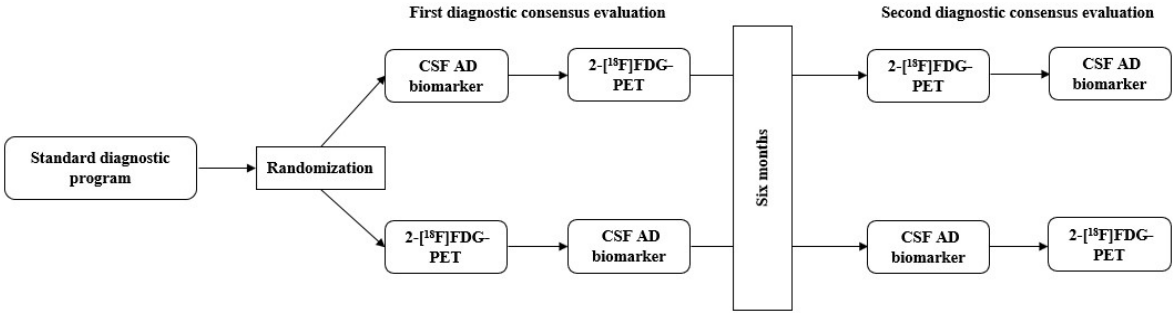

Abbreviations: AD: Alzheimer's disease; CSF: cerebrospinal fluid; standard program: medical history, physical and neurological examinations, cognitive testing, routine blood screening, and MRI; 2-[^{18}F]FDG-PET: 2-[^{18}F]fluoro-2-deoxy-D-glucose positron emission tomography;
The three-step incremental diagnostic consensus evaluation was done by two blinded dementia specialists. In the first step, the evaluation was based solely on the standard program. In the second step, the first biomarker was added (randomized to either CSF AD biomarkers or 2-[^{18}F]FDG-PET), and in the third step, the second biomarker was added. After 6 months, the same clinicians evaluated the same patients in the three-step incremental process with addition of the biomarkers in reverse order.

At each step the clinicians reached a consensus decision on (1) baseline etiological diagnosis and confidence in the diagnosis reported as a numeric rating scale (NRS) score between 0-100; (2) prediction of disease course after 12 months reported as stable or progressed and confidence in the prediction of disease course reported as a NRS score between 0-100; (3) change in antidementia medication, for instance cholinesterase inhibitors; (4) change in psychosocial interventions including case manager, speech therapy, and physiotherapy; and (5) need for ancillary investigations, for instance CSF AD biomarkers, 2-[^{18}F]FDG-PET, or other supplementary investigations such as DAT-SPECT, PET amyloid scan, electroencephalography, neuropsychologic assessment, and psychiatric assessment.

The reference diagnosis and disease course were determined by an experienced dementia specialist based on the clinical impression at a 12 months follow-up visit including clinical interview with the patient, assessment of MMSE and CDR, and all available clinical patient data as described in [26].

Diagnostic criteria

The patients were diagnosed with subjective cognitive decline (SCD), if cognitive complaints were present without confirmed objective cognitive impairment, and the criteria for MCI and dementia were not met [30]. The remainder of patients were diagnosed with a syndrome diagnosis of either MCI or dementia based on the National Institute on Aging-Alzheimer's Association criteria [7,31]. The patients were divided into groups based on the underlying etiological diagnosis: AD according to established

diagnostic criteria [3,7], other ND (DLB, FTD, atypical parkinsonism, and other ND) according to established diagnostic criteria [32–38]), non-ND (VaD, normal pressure hydrocephalus (NPH), and other non-ND according to established diagnostic criteria [17,39]), and SCD.

Data analysis

Differences in baseline values between groups were assessed using one-way ANOVA tests followed by post-hoc unpaired t-tests, Kruskal-Wallis tests followed by post-hoc Mann-Whitney tests for pairwise comparison, or Chi-square tests followed by post-hoc pairwise comparison, where appropriate. All post-hoc tests were Bonferroni corrected.

The accuracies of diagnosis and prediction of disease course were evaluated by comparing the baseline consensus evaluation to the reference evaluation at 12 months follow-up.

McNemar's test was used to evaluate the paired comparison between the baseline diagnoses, prediction of disease course, change in antidementia medication and psychosocial interventions, and need for further investigations. One-way ANOVA tests were used to evaluate the impact of biomarkers on continuous variables (confidence for diagnosis and disease course).

A linear mixed model with post-hoc Bonferroni corrections was used to estimate the effect of adding the two biomarkers individually and combined on confidence for diagnosis.

Statistical analysis was performed using SAS Studio software, version 9.4 (SAS Institute Inc., Cary, NC, USA). A two-sided p-value<.05 was considered indicative of statistical significance.

RESULTS

Study population

At 12 months clinical follow-up, the 81 patients received the following diagnoses: AD (n=36), DLB (n=6), FTD (n=3), atypical Parkinson (n=4), other ND (n=1), VaD (n=6), NPH (n=4), other non-ND (n=6), and SCD (n=15).

Baseline demographics according to the reference diagnosis at 12 months follow-up are presented in Table 1. The subjects with SCD were younger than patients with AD and non-ND. As expected, the subjects with SCD had a higher mean MMSE score than patients with AD, and the AD group had lower median Aβ42 values and higher median tau values than all other groups.

Table 1. Baseline demographics.

	AD	Other ND	Non-ND	SCD
Patients, n	36	14	16	15
Female, n (%)	21 (58)	6 (43)	6 (38)	7 (47)
Age, mean years ±SD	70.2±9.4[a]	69.1±9.7	72.6±7.7[a]	62.8±7.4
Education, mean years ±SD	13.7±3.0	11.4±2.1	13.6±3.0	13.1±2.7
Symptom duration, mean years ±SD	2.3±1.9	3.2±4.0	2.2±1.6	2.9±2.7
CDR global score, n (0/0.5/1.0)	7/17/12	1/6/7[a]	2/9/5	5/10/0
MMSE, mean score ±SD	26.1±2.8[a]	26.2±2.8	27.3±2.7	28.7±1.9
ACE, mean score ±SD	77.7±10.3[a]	76.1±9.3[a]	82.7±10.2	90.8±6.5
CSF Aβ42, median volume pg/mL [IQR]	521 [149]	866 [500][b]	918 [448][b]	804 [454][b]
CSF total tau, median volume pg/mL [IQR]	556 [370]	240 [173][b]	322 [281][b]	194 [206][b]
CSF p-tau, median volume pg/mL [IQR]	73 [36]	38 [28][b]	49 [38][b]	40 [35][b]

Abbreviations: Aβ42: amyloid beta 1-42; ACE: Addenbrooke's cognitive examination; AD: Alzheimer's disease; CDR: clinical dementia rating; CSF: cerebrospinal fluid; IQR: interquartile range; MCI: mild cognitive impairment; MMSE: mini-mental state examination; n: number; ND: neurodegenerative disease; p-tau: phosphorylated tau at threonine 181; SD: standard deviation; SCD: subjective cognitive decline;
[a] Statically significant difference as compared to SCD.
[b] Statically significant difference as compared to AD.

Clinical impact of 2-[^{18}F]FDG-PET and CSF AD biomarkers on diagnosis

As shown in Table 2, 59 patients (73%) were correctly classified after adding 2-[^{18}F]FDG-PET to the standard program with a high accuracy for AD (89%) and SCD (93%), but a low-to-moderate accuracy for other ND (57%) and non-ND (31%). The diagnostic confidence for the correctly classified patients across all diagnoses, as well as for the specific diagnostic groups of AD, other ND, and SCD were moderate-to-high (≥80) after adding 2-[^{18}F]FDG-PET to the standard program.

In comparison, 66 patients (81%) were correctly classified after adding CSF AD biomarkers to the standard program with a nearly perfect accuracy for AD (97%) and SCD (100%), but a low-to-moderate accuracy for the other ND (57%) and non-ND (50%). The diagnostic confidence for the correctly classified patients across all diagnoses as well as for the specific diagnostic group of AD were moderate-to-high (≥80) after adding CSF AD biomarkers to the standard program.

A direct comparison between the two biomarkers showed that adding CSF AD biomarkers led to an additional seven patients being correctly classified as compared to adding 2-[^{18}F]FDG-PET (66 vs. 59 patients, p=.09) due to a better recognition of AD and non-ND. The impact on diagnostic confidence was similar, except for a significant increase in diagnostic confidence for correctly diagnosed AD after adding CSF AD biomarkers compared to adding 2-[^{18}F]FDG-PET (mean NRS scores: 88±11 vs. 83±11, p=.04).

Table 2. The added value of 2-[^{18}F]FDG-PET and CSF AD biomarkers on diagnosis and confidence in diagnosis.

Diagnosis, n (%)	All patients		AD		Other ND		Non-ND		SCD	
	Cor.	Incor.	Cor.	Incor.	Cor.	Incor.	Cor.	Incor.	Cor.	Incor.
Standard program	55 (68)	26 (32)	35 (97)	1 (3)	7 (50)	7 (50)	1 (6)	15 (94)	12 (80)	3 (20)
Standard program + 2-[^{18}F]FDG-PET	59 (73)	22 (27)	32 (89)	4 (11)	8 (57)	6 (43)	5 (31)	11 (69)	14 (93)	1 (7)
Standard program + CSF AD biomarkers	66 (81) [a]	15 (19)	35 (97)	1 (3)	8 (57)	6 (43)	8 (50) [a]	8 (50)	15 (100)	0
Standard program + both biomarkers	66 (81) [a]	15 (19)	35 (97)	1 (3)	7 (50)	7 (50)	9 (56) [a]	7 (44)	15 (100)	0
Diagnostic confidence, mean NRS score ±SD										
Standard program	76±9	64±10	74±8	50	81±14	64±11	60	66±10	79±9	55±5
Standard program + 2-[^{18}F]FDG-PET	81±13 [ab]	65±12 [b]	83±11 [ab*]	63±18	81±17	69±14	67±11	65±9	80±14	50
Standard program + CSF AD biomarkers	81±14 [ab]	71±16	88±11 [ab]	85	79±16	72±15	66±14	69±18	76±11	NA
Standard program + both biomarkers	86±13 [a]	75±15 [a]	93±7[a]	95	88±14	72±17	69±16	75±12	80±12	NA

Abbreviations: AD: Alzheimer's disease; Cor.: correct; CSF: cerebrospinal fluid; Incor.: incorrect; n: number; ND: neurodegenerative disease; NA: not applicable; NRS: numeric rating scale; SD: standard deviation; SCD: subjective cognitive decline; standard program: medical history, physical and neurological examinations, cognitive testing, routine blood screening, and MRI; 2-[^{18}F]FDG-PET: 2-[^{18}F]fluoro-2-deoxy-D-glucose positron emission tomography;

[a] Statically significant difference as compared to standard program.

[b] Statically significant difference as compared to both biomarkers.

*Statically significant difference as compared to CSF AD biomarkers.

The combined addition of both biomarkers did not improve diagnostic accuracy, but significantly improved the diagnostic confidence for all correctly classified patients across all diagnoses as well as for the specific diagnostic group of AD when compared to adding 2-[^{18}F]FDG-PET and CSF AD biomarkers individually.

We used a linear mixed model to assess the relationship between adding one or both biomarkers to the standard program and diagnostic confidence. We found that adding 2-[^{18}F]FDG-PET and CSF AD biomarkers, increased the diagnostic confidence significantly

regardless of whether the diagnosis was correct or incorrect. The increase in diagnostic confidence did not differ when adding 2-[^{18}F]FDG-PET compared to adding CSF AD biomarkers (β(SE) 3(1), p=.41). Moreover, the diagnostic confidence increased significantly for correctly classified cases compared to incorrectly classified cases (β(SE) 4(2), p=.03).

Clinical value of 2-[^{18}F]FDG-PET and CSF AD biomarkers on predicting disease course

At 12 months follow-up, 37 (56%) of the patients with either MCI or dementia remained stable and 29 (44%) had progressed. More than half (55%) of the patients with either MCI or dementia with an abnormal CSF Aβ42 value remained stable at 12 months follow-up (Supplementary Table 1A).

The total number of patients that was correctly classified with regards to disease course was comparable after adding CSF AD biomarkers and 2-[^{18}F]FDG-PET individually (36 vs. 33 patients, p=.32), and the impact of biomarkers on the clinicians' confidence in the predicted disease course was similar (Table 3).

Table 3. The added value of 2-[^{18}F]FDG-PET and CSF AD biomarkers on disease course and confidence in disease course.

	MCI		Dementia	
Disease course, n (%)	Correct	Incorrect	Correct	Incorrect
Standard program	5 (45)	6 (55)	32 (58)	23 (42)
Standard program + 2-[^{18}F]FDG-PET	5 (45)	6 (55)	28 (51)	27 (49)
Standard program + CSF AD biomarkers	5 (45)	6 (55)	31 (56)	24 (44)
Disease course confidence, mean NRS score ±SD				
Standard program	59±7	57±8	65±12	70±9
Standard program + 2-[^{18}F]FDG-PET	60±7	52±5 *	74±13[a]	71±13
Standard program + CSF AD biomarkers	61±13	64±10	71±11	74±9

Abbreviations: AD: Alzheimer's disease; CSF: cerebrospinal fluid; MCI: mild cognitive impairment; n: number; NRS: numeric rating scale; SD: standard deviation; standard program: medical history, physical and neurological examinations, cognitive testing, routine blood screening, and MRI; 2-[^{18}F]FDG-PET: 2-[^{18}F]fluoro-2-deoxy-D-glucose positron emission tomography;

[a] Statically significant difference as compared to standard program.

*Statically significant difference as compared CSF AD biomarkers.

Impact of CSF AD biomarkers and 2-[^{18}F]FDG-PET on patient management

Based on the evaluation with the standard program, the clinicians recommended that 16 patients initiated anti-dementia medication, 21 patients were recommended initiation of psychosocial interventions, and 75 patient needed ancillary investigations as shown in Table 4.

For correctly classified patients, the impact of adding 2-[^{18}F]FDG-PET and CSF AD biomarkers individually was similar for change in anti-dementia medication (11 vs. 13 patients, p=.66) and psychosocial interventions (16 vs. 12 patients, p=.41). After adding 2-[^{18}F]FDG-PET to the standard program 17 patients (21%) changed to no need for ancillary investigations compared to 24 patients (30%) after adding CSF AD biomarkers (p=.21). However, the total number of correctly classified AD patients with need for ancillary investigations was significantly reduced after adding CSF AD biomarkers compared to adding 2-[^{18}F]FDG-PET to the standard program (19 vs. 8 patients, p=.007).

The clinicians predominantly requested examination of the other biomarker (2-[^{18}F]FDG-PET or CSF AD biomarkers) for the remaining patients with recommendations of ancillary investigations after addition of the first biomarker.

Table 4. Impact of 2-[^{18}F]FDG-PET and CSF AD biomarkers on patient management.

According to FU diagnosis	All patients		AD		Other ND		Non-ND		SCD	
	Cor.	Incor.	Cor.	Incor.	Cor.	Incor.	Cor.	Incor.	Cor.	Incor.
Change in anti-dementia medication, n (%)										
Standard program + 2-[^{18}F]FDG-PET	11 (14)	3 (4)	10 (28)	1 (3)	0	1 (7)	1 (6)	1 (6)	0	0
Standard program + CSF AD biomarkers	13 (16)	2 (2)	12 (33)	0	0	0	1 (6)	2 (13)	0	0
Change in psychosocial interventions, n (%)										
Standard program + 2-[^{18}F]FDG-PET	16 (20)	5 (6)	11 (31)	1 (3)	2 (14)	1 (7)	3 (19)	3 (19)	0	0
Standard program + CSF AD biomarkers	12 (18)	2 (2)	11 (31)	0	0	0	0	2 (13)	0	0
Reduced need for ancillary investigations, n (%)										
Standard program + 2-[^{18}F]FDG-PET	17 (21)	1 (1)	8 (22) *	0	1 (7)	1 (7)	0	0	6 (40)	0
Standard program + CSF AD biomarkers	24 (30)	3 (4)	19 (53)	0	0	1 (7)	2 (13)	2 (13)	3 (20)	0

Abbreviations: AD: Alzheimer's disease; Cor.: correct; CSF: cerebrospinal fluid; FU: follow-up; Incor.: incorrect; n: number; ND: neurodegenerative disease; SCD: subjective cognitive decline; standard program: medical history, physical and neurological examinations, cognitive testing, routine blood screening, and MRI; 2-[^{18}F]FDG-PET: 2-[^{18}F]fluoro-2-deoxy-D-glucose positron emission tomography;
*Statically significant difference as compared CSF AD biomarkers.

DISCUSSION

In this study, we compared the clinical value of two commonly used supportive biomarkers, 2-[^{18}F]FDG-PET and CSF AD biomarkers. The evaluation was performed in patients suspected of having AD in a clinically relevant added value setting. We found a comparable clinical value of adding 2-[^{18}F]FDG-PET and CSF AD biomarkers individually to the standard program on diagnosis, prognosis, and patient management.

However, CSF AD biomarkers had a significantly higher impact on diagnostic confidence and a reduced need for ancillary investigations compared to 2-[^{18}F]FDG-PET for the correctly diagnosed patient with AD.

A few studies have compared the diagnostic value of 2-[^{18}F]FDG-PET and CSF AD biomarkers, and overall found a high accuracy for the two biomarkers in the differential diagnosis of AD. However, there were some divergence regarding the performance of the biomarkers. Two studies found higher accuracies for 2-[^{18}F]FDG-PET in diagnosing AD compared to CSF AD biomarkers [23,25], whereas one study concluded the opposite [24], and one study found that the accuracy of the biomarkers were dependent on disease stage [22]. The discrepancies may be due to different factors, such as the differences in the included population and variance in operating procedures and biomarker measurement methods. The variance in the measurement methods for neuroimaging biomarkers is to some extent related to the lack of a clear definition of normal and abnormal outcomes. In addition, none of the above-mentioned studies evaluated the impact of the biomarkers on clinical decision-making.

In this study, we intended to compare the clinical impact of 2-[^{18}F]FDG-PET and CSF AD biomarkers as applied in a routine clinical setting, i.e. the PET images were analysed using clinical routine quantification methods together with visual inspection. We found a slightly higher accuracy for CSF AD biomarkers due to a higher diagnostic classification accuracy of AD and non-ND patients. Remarkably, the addition of 2-[^{18}F]FDG-PET was of limited clinical added value to other ND diagnoses such as DLB and FTD, although specific metabolic patterns have been shown to distinguish between AD, DLB, and FTD [3,5–7,19,30]. In comparison, a previous study found a specificity greater than 95% in the differential diagnosis of AD towards other dementias based on 2-[^{18}F]FDG-PET diagnosis in a study cohort of early-onset AD and other dementias (mean age of 60±4 years) [41].
The lower diagnostic accuracy for 2-[^{18}F]FDG-PET in our study may be caused by an overlap of the AD-like patterns of temporoparietal hypometabolism between AD and cerebrovascular disease [13] and the lack of distinct, hypometabolic patterns for non-ND including VaD and NPH.
Moreover, the accuracy for AD diagnosis by using the standard program alone was very good (97%), indicating that the evaluation was performed by highly experienced clinicians [42]. Nevertheless, the addition of the biomarkers significantly increased the diagnostic confidence for correctly classified AD patient, suggesting that the predominantly clinical

value of adding either 2-[^{18}F]FDG-PET and CSF AD biomarkers was to confirm this diagnosis.

In our study, we did not find any change in the accuracy nor diagnostic confidence when combining CSF AD biomarkers and 2-[^{18}F]FDG-PET, except for an increase in diagnostic confidence for correctly classified AD patients. Hence suggesting that the impact of adding an additional biomarker is marginal, when the diagnostic confidence is already high. This is in line with the recommendations for 2-[^{18}F]FDG-PET [19,43,44] and corroborated by previous studies demonstrating that the clinical impact of 2-[^{18}F]FDG-PET was highest when prior diagnostic confidence was low [45–47].

2-[^{18}F]FDG-PET and CSF AD biomarkers both had an equally low accuracy in predicting the disease course. This finding was somewhat unexpected, since previous studies have identified different regional patterns of hypometabolism on 2-[^{18}F]FDG-PET [48–56] and abnormal level of CSF AD biomarkers [57–61] as predictors of cognitive decline in dementia and conversion from MCI to dementia. A few studies have compared 2-[^{18}F]FDG-PET and CSF AD biomarkers head-to-head as predictors of cognitive decline and conversion to dementia in MCI patients. Overall, the studies found that CSF AD biomarkers were highly sensitive for cognitive decline, whereas 2-[^{18}F]FDG-PET was superior to predict conversion to dementia with AD based on biomarker positivity [62–64]. However, these findings may not be very applicable to our study as most of our cohort consisted of patients with dementia.

The low accuracy of both biomarkers to predict disease course may be caused by various factors. The most important factors could be that a follow-up of 12 months may be too short to encompass the complexity of progression and biomarker abnormality for the clinicians, and that our patient population may be too small and heterogenous to pick up predictive power on a group level [65]. Finally, the definitions of how to evaluate cognitive decline is variable and difficult to compare across studies [18].

Our third finding was that the impact of 2-[^{18}F]FDG-PET and CSF AD biomarkers on patient management was similar regarding changes in anti-dementia medication and psychosocial interventions. In line with previous studies, the clinicians were more likely to suggest initiation of anti-dementia medication after adding a biomarker [45,46,67]. A previous study reported that the addition of CSF AD biomarkers had consequences for 13% of patients regarding patient management specified as clinical trials, intensive follow-

up and imaging studies [68], but apart from that the knowledge of the impact of CSF AD biomarkers on patients management is very limited [18].

A few studies have evaluated the impact of 2-[^{18}F]FDG-PET on patient management and found that changes in anti-dementia medication varied from 17% to 32 % of the patients and the request for ancillary investigations were reduced for 42% of the patients after disclosure of the 2-[^{18}F]FDG-PET [45,46,67]. However, the changes in patient management are dependent on the performance of the clinicians before the biomarkers are added. In our study, the clinicians had a high accuracy in diagnosing AD patients and therefore the changes may be bigger in a study with less experienced clinicians. In our study, nevertheless adding CSF AD biomarkers significantly reduced the need for ancillary investigations for correct diagnosed AD patients compared to adding 2-[^{18}F]FDG-PET, which underlines the role of CSF AD biomarker in confirming the AD diagnosis.

The findings in this study are in line with the existing studies that indicate that both 2-[^{18}F]FDG-PET and CSF AD biomarkers have a clinical value in diagnosing patients suspected of dementia. Furthermore, our finding of slightly higher clinical value of adding CSF AD biomarkers in patients suspected of AD, adds some knowledge to the first choice of two common biomarkers in diagnostic algorithm, as most memory clinics have implemented a stepwise approach of the diagnostic work-up. However, it may be the case that our findings reflect sample-specific characteristics. Future studies should compare the clinical impact of 2-[^{18}F]FDG-PET and CSF AD biomarkers in a larger study with less experienced clinicians, in addition to an evaluation of the cost-effectiveness and patients experience with the biomarkers to optimize the clinical utility of biomarkers.

There are some limitations to our study. First, evaluations and interpretations of biomarkers were deliberately based on clinical routine procedures and locally determined cut-points, which may however, lessen the generalization to other centres in the absence of a standardized clinical application of the biomarkers. Also, patients in this study were included based on the clinical indication for 2-[^{18}F]FDG-PET and CSF AD biomarkers, which clearly induces a selection bias. On the other hand, our study population consisted of patients with diagnostic uncertainty and need for further investigations with biomarkers, which is the clinically relevant subgroup to investigate the clinical value of adding the biomarkers. Furthermore, there is a potential risk of circularity as the results of 2-[^{18}F]FDG-PET and CSF AD biomarkers were included as part of the follow-up clinical evaluation. Finally, it must be noted that our study was performed in a tertiary center with

experienced clinicians, which may result in a higher prevalence of abnormal biomarkers and clinical atypical presentations compared to less specialized centres.
The strength of the study was that the diagnostic process including added value of biomarkers reflected a routine clinical setting. Moreover, we included patients from a memory clinic instead of a selected research population, and the patients had a clinical indication for ancillary investigation with 2-[^{18}F]FDG-PET and CSF AD biomarkers.

To conclude, we found that CSF AD biomarkers may have a more significant clinical impact on corroborating the diagnosis of AD if the patient is suspected of having AD. This was demonstrated by a slightly higher diagnostic classification accuracy together with a higher diagnostic confidence and more reduced need for ancillary investigations for correctly classified AD as compared to adding 2-[^{18}F]FDG-PET. The combined addition of both biomarkers was of limited value.

ACKNOWLEDGEMENTS

Data collection and sharing for the project was funded under the 7th Framework Program by the European Commission (Grant agreement ID: 611005).
This work was supported by the Danish Alzheimer's Association Research Fund and the Absalon Foundation of 1st May 1978.

CONFLICT OF INTERESTS

All authors declare no competing interests.

REFERENCES

[1] Waldemar G, Phung KTT, Alistair B, Georges J, Hansen FR, Iliffe S, Marking C, Rikkert MO, Selmes J, Stoppe G, Sartorius N (2007) Access to diagnostic evaluation and treatment for dementia in Europe. *Int. J. Geriatr. Psychiatry* **22**, 47–54.

[2] Sorbi S, Hort J, Erkinjuntti T, Fladby T, Gainotti G, Gurvit H, Nacmias B, Pasquier F, Popescu BO, Rektorova I, Religa D, Rusina R, Rossor M, Schmidt R, Stefanova E, Warren JD, Scheltens P (2012) EFNS-ENS Guidelines on the diagnosis and management of disorders associated with dementia. *Eur. J. Neurol.* **19**, 1159–1179.

[3] Dubois B, Feldman HH, Jacova C, Hampel H, Molinuevo JLJL, Blennow K, Dekosky ST, Gauthier S, Selkoe D, Bateman R, Cappa S, Crutch S, Engelborghs S, Frisoni GB, Fox NC, Galasko D, Habert MO, Jicha GA, Nordberg A, Pasquier F, Rabinovici G, Robert P, Rowe C, Salloway S, Sarazin M, Epelbaum SS, de Souza LC, Vellas B, Visser PJ, Schneider L, Stern Y, Scheltens P, Cummings JL (2014) Advancing research diagnostic criteria for Alzheimer's disease: The IWG-2 criteria. *Lancet Neurol.* **13**, 614–629.

[4] Rascovsky K, Hodges JR, Knopman D, Mendez MF, Kramer JH, Neuhaus J, Van Swieten JC, Seelaar H, Dopper EGP, Onyike CU, Hillis AE, Josephs KA, Boeve BF, Kertesz A, Seeley WW, Rankin KP, Johnson JK, Gorno-Tempini ML, Rosen H, Prioleau-Latham CE, Lee A, Kipps CM, Lillo P, Piguet O, Rohrer JD, Rossor MN, Warren JD, Fox NC, Galasko D, Salmon DP, Black SE, Mesulam M, Weintraub S, Dickerson BC, Diehl-Schmid J, Pasquier F, Deramecourt V, Lebert F, Pijnenburg Y, Chow TW, Manes F, Grafman J, Cappa SF, Freedman M, Grossman M, Miller BL (2011) Sensitivity of revised diagnostic criteria for the behavioural variant of frontotemporal dementia. *Brain* **134**, 2456–2477.

[5] Gorno-Tempini ML, Hillis AE, Weintraub S, Kertesz A, Mendez M, Cappa SF, Ogar JM, Rohrer JD, Black S, Boeve BF, Manes F, Dronkers NF, Vandenberghe R, Roscovsky K, Patterson K, Miller BI, Knopman DS, Hodges JR, Mesulam MM, Grossman M (2011) Classification of primary progressive aphasia and its variants. *Neurology* **76**, 1006–1014.

[6] McKeith IG, Boeve BF, Dickson DW, Halliday G, Taylor J-P, Weintraub D, Aarsland D, Galvin J, Attems J, Ballard CG, Bayston A, Beach TG, Blanc F, Bohnen N, Bonanni L, Bras J, Brundin P, Burn D, Chen-Plotkin A, Duda JE, El-

Agnaf O, Feldman H, Ferman TJ, Ffytche D, Fujishiro H, Galasko D, Goldman JG, Gomperts SN, Graff-Radford NR, Honig LS, Iranzo A, Kantarci K, Kaufer D, Kukull W, Lee VMY, Leverenz JB, Lewis S, Lippa C, Lunde A, Masellis M, Masliah E, McLean P, Mollenhauer B, Montine TJ, Moreno E, Mori E, Murray M, O'Brien JT, Orimo S, Postuma RB, Ramaswamy S, Ross OA, Salmon DP, Singleton A, Taylor A, Thomas A, Tiraboschi P, Toledo JB, Trojanowski JQ, Tsuang D, Walker Z, Yamada M, Kosaka K (2017) Diagnosis and management of dementia with Lewy bodies Fourth consensus report of the DLB Consortium. *Neurology* **89**, 1–13.

[7] McKhann GM, Knopman DS, Chertkow H, Hyman BT, Jack Jr CR, Kawas CH, Klunk WE, Koroshetz WJ, Manly JJ, Mayeux R, Mohs RC, Morris JC, Rossor MN, Scheltens P, Carrillo MC, Thies B, Weintraub S, Phelps CH (2011) The diagnosis of dementia due to Alzheimer's disease: Recommendations from the National Institute on Aging-Alzheimer's Association workgroups on diagnostic guidelines for Alzheimer's disease. *Alzheimer's Dement.* **7**, 263–269.

[8] Chételat G, Desgranges B, Landeau B, Mézenge F, Poline JB, De La Sayette V, Viader F, Eustache F, Baron JC (2008) Direct voxel-based comparison between grey matter hypometabolism and atrophy in Alzheimer's disease. *Brain* **131**, 60–71.

[9] Moodley KK, Perani D, Minati L, Anthony Della Rosa P, Pennycook F, Dickson JC, Barnes A, Elisa Contarino V, Michopoulou S, D'Incerti L, Good C, Fallanca F, Giovanna Vanoli E, Ell PJ, Chan D (2015) Simultaneous PET-MRI studies of the concordance of atrophy and hypometabolism in syndromic variants of Alzheimer's disease and frontotemporal dementia: An extended case series. *J. Alzheimer's Dis.* **46**, 639–653.

[10] La Joie R, Perrotin A, Barré L, Hommet C, Mézenge F, Ibazizene M, Camus V, Abbas A, Landeau B, Guilloteau D, de La Sayette V, Eustache F, Desgranges B, Chételat G (2012) Region-specific hierarchy between atrophy, hypometabolism, and 2-amyloid (Aβ) load in Alzheimer's disease dementia. *J. Neurosci.* **32**, 16265–16273.

[11] Whitwell JL, Jack CR (2007) Neuroimaging in Dementia. *Neurol. Clin.* **25**, 843–857.

[12] Jack CR, Knopman DS, Jagust WJ, Shaw LM, Aisen PS, Weiner MW, Petersen RC, Trojanowski JQ (2010) Hypothetical Pathological Cascade in Alheimer's Disease.

Lancet Neurol. **9**, 1–20.

[13] Jack CR, Bennett DA, Blennow K, Carrillo MC, Feldman HH, Frisoni GB, Hampel HJ, Jagust WJ, Johnson KA, Knopman DS, Petersen RC, Scheltens P, Sperling RA, Dubois B (2016) A/T/N: An unbiased descriptive classification scheme for Alzheimer disease biomarkers. *Neurology* **87**, 539–547.

[14] Ewers M, Mattsson N, Minthon L, Molinuevo JL, Antonell A, Popp J, Jessen F, Herukka SK, Soininen H, Maetzler W, Leyhe T, Bürger K, Taniguchi M, Urakami K, Lista S, Dubois B, Blennow K, Hampel H (2015) CSF biomarkers for the differential diagnosis of Alzheimer's disease: A large-scale international multicenter study. *Alzheimer's Dement.* **11**, 1306–1315.

[15] Paterson RW, Slattery CF, Poole T, Nicholas JM, Magdalinou NK, Toombs J, Chapman MD, Lunn MP, Heslegrave AJ, Foiani MS, Weston PSJ, Keshavan A, Rohrer JD, Rossor MN, Warren JD, Mummery CJ, Blennow K, Fox NC, Zetterberg H, Schott JM (2018) Cerebrospinal fluid in the differential diagnosis of Alzheimer's disease: Clinical utility of an extended panel of biomarkers in a specialist cognitive clinic. *Alzheimer's Res. Ther.* **10**, 1–11.

[16] Schoonenboom N, Reesink F, Verwey N, Kester M, Teunissen C, van de Ven P, Pijnenburg Y, Blankenstein M, Rozemuller A, Scheltens P, van der Flier W (2012) Cerebrospinal fluid markers for differential dementia diagnosis in a large memory clinic cohort. *Neurology* **78**, 47–54.

[17] Sachdev P, Kalaria R, O'Brien J, Skoog I, Alladi S, Black S, Blacker D, Blazer D, Chen C, Chui H, Ganguli M, Jellinger K, Jeste D, Pasquier F, Paulsen J, Prins N, Rockwood K, Roman G, Scheltens P (2014) Diagnostic criteria for vascular cognitive disorders: a VASCOG statement. *Alzheimer Dis. Assoc. Disord.* **28**, 206–218.

[18] Simonsen AH, Herukka SK, Andreasen N, Baldeiras I, Bjerke M, Blennow K, Engelborghs S, Frisoni GB, Gabryelewicz T, Galluzzi S, Handels R, Kramberger MG, Kulczyńska A, Molinuevo JL, Mroczko B, Nordberg A, Oliveira CR, Otto M, Rinne JO, Rot U, Saka E, Soininen H, Struyfs H, Suardi S, Visser PJ, Winblad B, Zetterberg H, Waldemar G (2017) Recommendations for CSF AD biomarkers in the diagnostic evaluation of dementia. *Alzheimer's Dement.* **13**, 274–284.

[19] Nobili F, Arbizu J, Bouwman F, Drzezga A, Agosta F, Nestor P, Walker Z, Boccardi M (2018) European Association of Nuclear Medicine and European

Academy of Neurology recommendations for the use of brain 18F-Fluorodeoxyglucose Positron Emission Tomography in neurodegenerative cognitive impairment and dementia: Delphi consensus. *Eur. J. Neurol.* 1–17.

[20] National Institute for Health and Care Excellence (2018) *Dementia: Assessment, management and support for people living with dementia and their carers*.

[21] O'Brien JT, Holmes C, Jones M, Jones R, Livingston G, McKeith I, Mittler P, Passmore P, Ritchie C, Robinson L, Sampson EL, Taylor J-P, Thomas A, Burns A (2017) Clinical practice with anti-dementia drugs: A revised (third) consensus statement from the British Association for Psychopharmacology. *J. Psychopharmacol.* **31**, 147–168.

[22] Morinaga A, Ono K, Ikeda T, Ikeda Y, Shima K, Noguchi-Shinohara M, Samuraki M, Yanase D, Yoshita M, Iwasa K, Mastunari I, Yamada M (2010) A comparison of the diagnostic sensitivity of MRI, CBF-SPECT, FDG-PET and cerebrospinal fluid biomarkers for detecting Alzheimer's disease in a memory clinic. *Dement. Geriatr. Cogn. Disord.* **30**, 285–292.

[23] Yakushev I, Bartenstein P, Siessmeier T, Hiemke C, Scheurich A, Lotz J, Fellgiebel A, Müller MJ (2010) Cerebrospinal fluid tau protein levels and 18F-fluorodeoxyglucose positron emission tomography in the differential diagnosis of Alzheimer's disease. *Dement. Geriatr. Cogn. Disord.* **30**, 245–253.

[24] Walhovd KB, Fjell AM, Brewer J, McEvoy LK, Fennema-Notestine C, Hagler DJ, Jennings RG, Karow D, Dale AM (2010) Combining MR Imaging, Positron-Emission Tomography, and CSF Biomarkers in the Diagnosis and Prognosis of Alzheimer Disease. *Am. J. Neuroradiol.* **31**, 347–354.

[25] Perani D, Cerami C, Caminiti SP, Santangelo R, Coppi E, Ferrari L, Pinto P, Passerini G, Falini A, Iannaccone S, Cappa SF, Comi G, Gianolli L, Magnani G (2016) Cross-validation of biomarkers for the early differential diagnosis and prognosis of dementia in a clinical setting. *Eur. J. Nucl. Med. Mol. Imaging* **43**, 499–508.

[26] Bruun M, Frederiksen KS, Rhodius-meester HFM, Baroni M, Gjerum L, Koikkalainen J, Urhemaa T, Tolonen A, Gils M Van, Tong T, Guerrero R, Rueckert D, Dyremose N, Andersen BB, Simonsen AH, Lemstra A, Hallikainen M, Kurl S, Herukka S-K, Remes AM, Waldemar G, Soininen H, Mecocci P, Flier WM Van Der, Hasselbalch SG (2019) Impact of a Clinical Decision Support Tool on

Dementia Diagnostics in Memory Clinics: The PredictND Validation Study. *Curr. Alzheimer Res.* **16**, 91–101.

[27] Folstein M, Folstein S, McHugh P (1975) 'Mini-mental state' - A practical method for grading the cognitive state of patients for the clinician. *J. Psychiatr. Res.* **12**, 189–198.

[28] Mathuranath P, Nestor P, Berrios G, Rakowicz W, Hodges J (2000) A brief cognitive test battery to differentiate Alzheimer's disease and frontotemporal dementia. *Neurology* **55**, 1613–1620.

[29] Zwan MD, Rinne JO, Hasselbalch SG, Nordberg A, Lleó A, Herukka S-K, Soininen H, Law I, Bahl JMC, Carter SF, Fortea J, Blesa R, Teunissen CE, Bouwman FH, Van Berckel BNM, Visser PJ (2016) Use of amyloid-PET to determine cutpoints for CSF markers. *Neurology* **86**, 50–58.

[30] Jessen F, Amariglio RE, van Boxtel M, Breteler M, Ceccaldi M, Chételat G, Dubois B, Dufouil C, Ellis KA, van der Flier WM, Glodzik L, van Harten AC, de Leon MJ, McHugh P, Mielke MM, Molinuevo JL, Mosconi L, Osorio RS, Perrotin A, Petersen RC, Rabin LA, Rami L, Reisberg B, Rentz DM, Sachdev PS, de la Sayette V, Saykin AJ, Scheltens P, Shulman MB, Slavin MJ, Sperling RA, Stewart R, Uspenskaya O, Vellas B, Visser PJ, Wagner M (2014) A conceptual framework for research on subjective cognitive decline in preclinical Alzheimer's disease. *Alzheimer's Dement.* **10**, 844–52.

[31] Albert MS, DeKosky ST, Dickson D, Dubois B, Feldman HH, Fox NC, Gamst A, Holtzman DM, Jagust WJ, Petersen RC, Snyder PJ, Carillo MC, Thies B, Phelps CH (2011) The diagnosis of mild cognitive impairment due to Alzheimer's disease: Recommendations from the National Institute on Aging-Alzheimer's Association workgroups on diagnostic guidelines for Alzheimer's disease. *Alzheimer's Dement.* **7**, 270–279.

[32] McKhann GM (2001) Clinical and Pathological Diagnosis of Frontotemporal Dementia. *Arch. Neurol.* **58**, 1803.

[33] Rizzo G, Arcuti S, Copetti M, Alessandria M, Savica R, Fontana A, Liguori R, Logroscino G (2018) Accuracy of clinical diagnosis of dementia with Lewy bodies: A systematic review and meta-analysis. *J. Neurol. Neurosurg. Psychiatry* **89**, 358–366.

[34] Emre M, Aarsland D, Brown R, Burn DJ, Duyckaerts C, Mizuno Y, Broe GA,

Cummings J, Dickson DW, Gauthier S, Goldman J, Goetz C, Korczyn A, Lees A, Levy R, Litvan I, McKeith I, Olanow W, Poewe W, Quinn N, Sampaio C, Tolosa E, Dubois B (2007) Clinical diagnostic criteria for dementia associated with Parkinson's disease. *Mov. Disord.* **22**, 1689–1707.

[35] Litvan I (2001) Diagnosis and management of progressive supranuclear palsy. *Semin Neurol* **21**, 41–48.

[36] Gilman S, Wenning GK, Low P a, Brooks DJ, Mathias CJ, Trojanowski JQ, Wood NW, Colosimo C, Dürr A, Fowler CJ, Kaufmann H, Klockgether T, Lees AJ, Poewe WH, Quinn NP, Revesz T, Robertson D, Sandroni P, Seppi K, Vidailhet M (2008) Second consensus statement on the diagnosis of multiple system atrophy. *Neurology* **71**, 670–6.

[37] Riley D, Lang A (2000) Clinical diagnostic criteria. *Adv. Neurol.* **82**, 29–34.

[38] McKeith IG, Dickson DW, Lowe J, Emre M, O'Brien JT, Feldman H, Cummings J, Duda JE, Lippa C, Perry EK, Aarsland D, Arai H, Ballard CG, Boeve B, Burn DJ, Costa D, Del Ser T, Dubois B, Galasko D, Gauthier S, Goetz CG, Gomez-Tortosa E, Halliday G, Hansen LA, Hardy J, Iwatsubo T, Kalaria RN, Kaufer D, Kenny RA, Korczyn A, Kosaka K, Lee VMY, Lees A, Litwan I, Londos E, Lopez OL, Minoshima S, Mizuno Y, Molina JA, Mukaetova-Ladinska EB, Pasquier F, Perry RH, Schulz JB, Trojanowski JQ, Yamada M (2005) Diagnosis and management of dementia with Lewy bodies: Third report of the DLB Consortium. *Neurology* **65**, 1863–1872.

[39] Relkin N, Marmarou A, Klinge P, Bergsneider M, Black PM (2005) Diagnosing idiopathic normal-pressure hydrocephalus. *Neurosurgery* **57**, S2-4-S2-16.

[40] Sperling RAR., Aisen PS, Beckett LALA, Bennett DADA, Craft S, Fagan AMAM, Iwatsubo T, Jack CRCRJ, Kaye J, Montine TJ, Park DCDC, Reiman EMEM, Rowe CCC, Siemers E, Stern Y, Yaffe K, Carrillo MC, Thies B, Morrison-Bogorad M, Wagster M V, Phelps CH, Wegster MV, and Phelps CH (2011) Toward defining the preclinical stages of Alzheimer's disease: Recommendations from the National Institute on Aging- Alzheimer's Association workgroups on diagnostic guidelines for Alzheimer's disease. *Alzheimer's Dement.* **7**, 280–292.

[41] Panegyres PK, Rogers JM, McCarthy M, Campbell A, Wu JS (2009) Fluorodeoxyglucose-positron emission tomography in the differential diagnosis of early-onset dementia: A prospective, community-based study. *BMC Neurol.* **9**, 1–9.

[42] Mayeux R, Reitz C, Brickman AM, Haan MN, Manly JJ, Glymour MM, Weiss CC, Yaffe K, Middleton L, Hendrie HC, Warren LH, Hayden KM, Welsh-Bohmer KA, Breitner JCS, Morris JC (2011) Operationalizing diagnostic criteria for Alzheimer's disease and other age-related cognitive impairment - Part 1. *Alzheimer's Dement.* **7**, 15–34.

[43] Bohnen NI, Djang DSW, Herholz K, Anzai Y, Minoshima S (2012) Effectiveness and Safety of 18F-FDG PET in the Evaluation of Dementia: A Review of the Recent Literature. *J. Nucl. Med.* **53**, 59–71.

[44] Nestor PJ, Altomare D, Festari C, Drzezga A, Rivolta J, Walker Z, Bouwman F, Orini S, Law I, Agosta F, Arbizu J, Boccardi M, Nobili F, Frisoni GB (2018) Clinical utility of FDG-PET for the differential diagnosis among the main forms of dementia. *Eur. J. Nucl. Med. Mol. Imaging* 1–17.

[45] Elias A, Woodward M, Rowe CC (2014) Management impact of FDG-PET in dementia: Results from a tertiary center memory clinic. *J. Alzheimer's Dis.* **42**, 885–892.

[46] Laforce R, Buteau JP, Paquet N, Verret L, Houde M, Bouchard RW (2010) The value of PET in mild cognitive impairment, typical and atypical/unclear dementias: A retrospective memory clinic study. *Am. J. Alzheimers. Dis. Other Demen.* **25**, 324–332.

[47] Ossenkoppele R, Prins ND, Pijnenburg YAL, Lemstra AW, van der Flier WM, Adriaanse SF, Windhorst AD, Handels RLH, Wolfs CAG, Aalten P, Verhey FRJ, Verbeek MM, van Buchem MA, Hoekstra OS, Lammertsma AA, Scheltens P, van Berckel BNM (2013) Impact of molecular imaging on the diagnostic process in a memory clinic. *Alzheimer's Dement.* **9**, 414–421.

[48] Silverman DHS, Small GW, Chang CY, Lu CS, Kung De Aburto MA, Chen W, Czernin J, Rapoport SI, Pietrini P, Alexander GE, Schapiro MB, Jagust WJ, Hoffman JM, Welsh-Bohmer KA, Alavi A, Clark CM, Salmon E, de Leon MJ, Mielke R, Cummings JL, Kowell AP, Gambhir SS, Hoh CK, Phelps ME (2001) Positron Emission Tomography in Evaluation of Dementia: Regional Brain Metabolism and Long-term Outcome. *J. Am. Med. Assoc.* **286**, 2120–2127.

[49] Mosconi L, Perani D, Sorbi S, Herholz K, Nacmias B, Holthoff V, Salmon E, Baron J, Cristofaro MTR De, Padovani A, Borroni B, Franceschi M, Bracco L, Pupi A (2004) MCI conversion to dementia and the APOE genotype: A prediction study

with FDG-PET. *Neurology*.

[50] Drzezga A, Lautenschlager N, Siebner H, Riemenschneider M, Willoch F, Minoshima S, Schwaiger M, Kurz A (2003) Cerebral metabolic changes accompanying conversion of mild cognitive impairment into alzheimer's disease: A PET follow-up study. *Eur. J. Nucl. Med. Mol. Imaging* **30**, 1104–1113.

[51] Chetelat G, Desgranges B, de la Sayette V, Viader F, Eustache F, Baron J-C (2003) Mild cognitive impairment: Can FDG-PET predict who is to rapidly convert to Alzheimer's disease? *Neurology* **60**, 1374–1377.

[52] Herholz K, Carter S, Jones M (2007) Positron emission tomography imaging in dementia. *Br. J. Radiol.* **80**, S160-167.

[53] Jagust W (2006) Positron emission tomography and magnetic resonance imaging in the diagnosis and prediction of dementia. *Alzheimers. Dement.* **2**, 36–42.

[54] Pagani M, Nobili F, Morbelli S, Arnaldi D, Giuliani A, Öberg J, Girtler N, Brugnolo A, Picco A, Bauckneht M, Piva R, Chincarini A, Sambuceti G, Jonsson C, De Carli F (2017) Early identification of MCI converting to AD: a FDG PET study. *Eur. J. Nucl. Med. Mol. Imaging* **44**, 2042–2052.

[55] Dukart J, Sambataro F, Bertolino A (2015) Accurate prediction of conversion to Alzheimer's disease using imaging, genetic, and neuropsychological biomarkers. *J. Alzheimer's Dis.* **49**, 1143–1159.

[56] Landau SM, Harvey D, Madison CM, Reiman EM, Foster NL, Aisen PS, Petersen RC, Shaw LM, Trojanowski JQ, Jack CR, Weiner MW, Jagust WJ (2010) Comparing predictors of conversion and decline in mild cognitive impairment. *Neurology* **75**, 230–238.

[57] Jensen M, Schröder J, Blomberg M, Engvall B, Pantel J, Ida N, Basun H, Wahlund LO, Werle E, Jauss M, Beyreuther K, Lannfelt L, Hartmann T (1999) Cerebrospinal fluid Aβ42 is increased early in sporadic Alzheimer's disease and declines with disease progression. *Ann. Neurol.* **45**, 504–511.

[58] Kester MI, Van Der Vlies AE, Blankenstein MA, Pijnenburg YAL, Van Elk EJ, Scheltens P, Van Der Flier WM (2009) CSF biomarkers predict rate of cognitive decline in Alzheimer disease. *Neurology* **73**, 1353–1358.

[59] Vos SJB, Verhey F, Frölich L, Kornhuber J, Wiltfang J, Maier W, Peters O, Rüther E, Nobili F, Morbelli S, Frisoni GB, Drzezga A, Didic M, Van Berckel BNM, Simmons A, Soininen H, Kłoszewska I, Mecocci P, Tsolaki M, Vellas B, Lovestone

S, Muscio C, Herukka SK, Salmon E, Bastin C, Wallin A, Nordlund A, De Mendonça A, Silva D, Santana I, Lemos R, Engelborghs S, Van Der Mussele S, Freund-Levi Y, Wallin ÅK, Hampel H, Van Der Flier W, Scheltens P, Visser PJ (2015) Prevalence and prognosis of Alzheimer's disease at the mild cognitive impairment stage. *Brain* **138**, 1327–1338.

[60] Hansson O, Zetterberg H, Buchlave P, Londos E, Blennow K, Minthon L (2006) Association between CSF biomarkers and incipient Alzheimer's disease in patients with mild cognitive impairment: A follow-up study. *Lancet Neurol.* **5**, 228–234.

[61] Mattsson N, Insel PS, Donohue M, Jagust W, Sperling R, Aisen P, Weiner MW (2015) Predicting reduction of cerebrospinal fluid β-Amyloid 42 in Cognitively healthy controls. *JAMA Neurol.* **72**, 554–560.

[62] Fellgiebel A, Scheurich A, Bartenstein P, Müller MJ (2007) FDG-PET and CSF phospho-tau for prediction of cognitive decline in mild cognitive impairment. *Psychiatry Res. - Neuroimaging* **155**, 167–171.

[63] Jagust WJ, Bandy D, Chen K, Foster NL, Landau SM, Mathis CA, Price JuC, Reiman EM, Skovronsky D, Koeppe RA (2010) The ADNI PET Core. *Alzheimer's Dement.* **6**, 221–229.

[64] Prestia A, Caroli A, Flier WM Van Der, Teunissen CE, Wall AE, Carter SF, Schöll M (2013) Prediction of dementia in MCI patients based on core diagnostic markers for Alzheimer disease. *Brain* 1–9.

[65] Van Der Flier WM, Scheltens P (2018) Amsterdam dementia cohort: Performing research to optimize care. *J. Alzheimer's Dis.* **62**, 1091–1111.

[66] Jack CR, Knopman DS, Jagust WJ, Petersen RC, Weiner MW, Aisen PS, Shaw LM, Vemuri P, Wiste HJ, Weigand SD, Lesnick TG, Pankratz VS, Donohue MC, Trojanowski JQ (2013) Tracking pathophysiological processes in Alzheimer's disease: An updated hypothetical model of dynamic biomarkers. *Lancet Neurol.* **12**, 207–216.

[67] Motara H, Olusoga T, Russell G, Jamieson S, Ahmed S, Brindle N, Pillai A, Scarsbrook AF, Patel CN, Chowdhury FU (2017) Clinical impact and diagnostic accuracy of 2-[18F]-fluoro-2-deoxy-D-glucose positron-emission tomography/computed tomography (PET/CT) brain imaging in patients with cognitive impairment: a tertiary centre experience in the UK. *Clin. Radiol.* **72**, 63–73.

[68] Duits FH, Prins ND, Lemstra AW, Pijnenburg YALL, Bouwman FH, Teunissen CE, Scheltens P, Van Der Flier WM (2015) Diagnostic impact of CSF biomarkers for Alzheimer's disease in a tertiary memory clinic. *Alzheimer's Dement.* **11**, 523–532.

Supplementary material.

Figure 1A. Flow diagram of the study population.

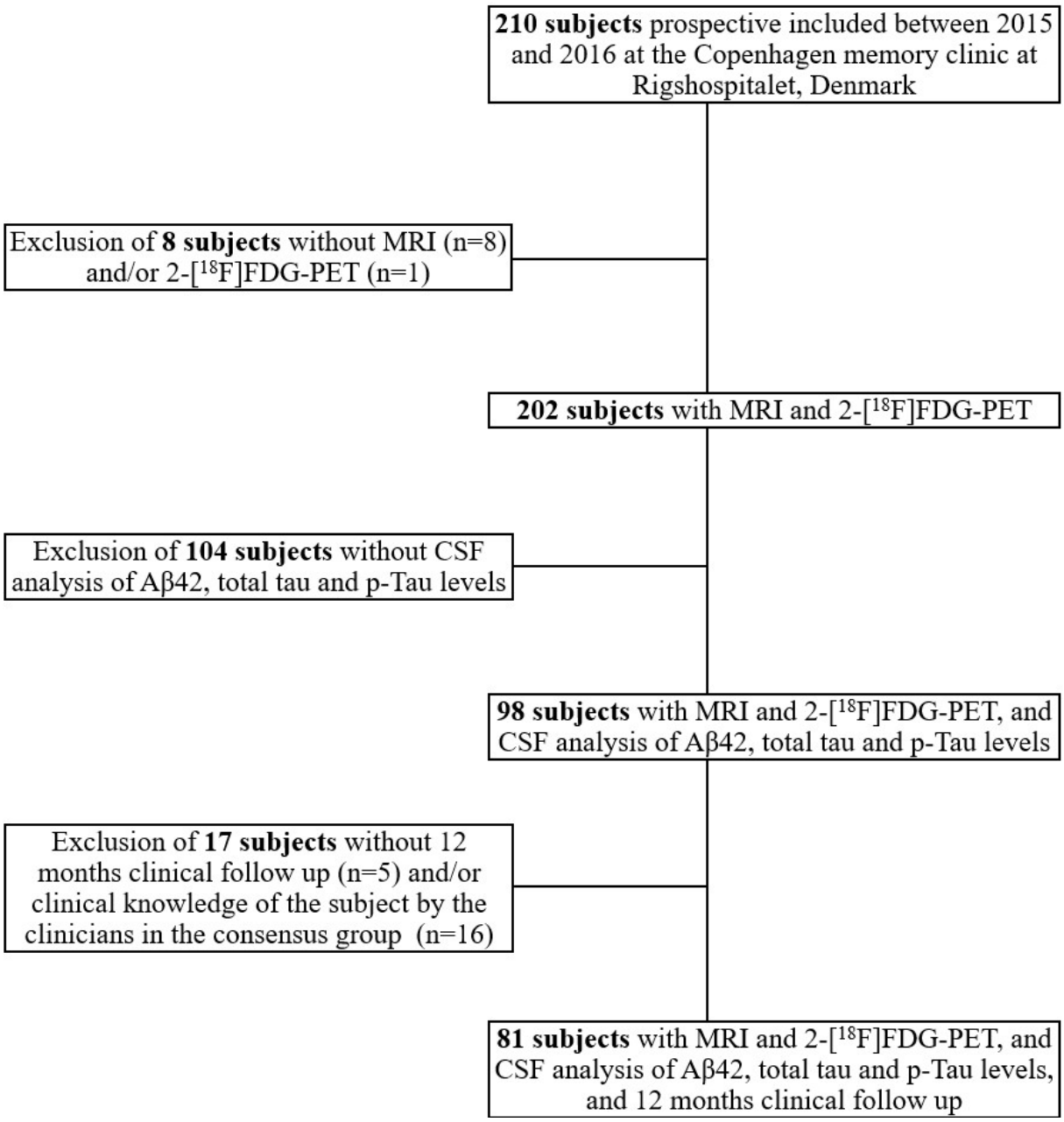

Abbreviations: Aβ42: amyloid beta 1-42; CSF: cerebrospinal fluid; MRI: magnetic resonance imaging; n: number; p-tau: phosphorylated tau at threonine 181; 2-[^{18}F]FDG-PET: 2-[^{18}F]fluoro-2-deoxy-D-glucose positron emission tomography;

Table 1A. Distribution of disease course for CSF AD biomarkers and 2-[^{18}F]FDG-PET based on positivity/negativity to CSF Aβ42 for dementia and MCI patients.

CSF Aβ42	Positive (n=29)		Negative (n=37)	
Disease course, n (%)	Stable	Progression	Stable	Progression
12 months clinical follow-up (reference)	**16 (55)**	**13 (45)**	**21 (57)**	**16 (43)**
Standard program	5 (17)	24 (83)	7 (19)	30 (81)
Standard program + 2-[^{18}F]FDG-PET	5 (17)	24 (83)	7 (19)	30 (81)
Standard program + CSF AD biomarkers	1 (3)	28 (97)	8 (35)	29 (65)
Standard program + both biomarkers	1 (3)	28 (97)	11 (30)	26 (70)

Abbreviations: AD: Alzheimer's disease; CSF: cerebrospinal fluid; n: number; standard program: medical history, physical and neurological examinations, cognitive testing, routine blood screening, and MRI; 2-[^{18}F]FDG-PET: 2-[^{18}F]fluoro-2-deoxy-D-glucose positron emission tomography;

Study II

A visual rating scale for cingulate island sign on ^{18}F-FDG-PET to differentiate dementia with Lewy bodies and Alzheimer's disease.

Reprinted from Journal of the Neurological Sciences, 410; Gjerum L, Frederiksen KS, Henriksen OM, Law I, Anderberg L, Andersen BB, Bjerregaard E, Hejl A-M, Høgh P, Hasselbalch SG; A visual rating scale for cingulate island sign on ^{18}F-FDG-PET to differentiate dementia with Lewy bodies and Alzheimer's disease; 116645, 2020, with permission from Elsevier.
The publication is available at Elsevier through
http://dx.doi.org/10.1016/j.jns.2019.116645

Journal of the Neurological Sciences 410 (2020) 116645

Contents lists available at ScienceDirect

Journal of the Neurological Sciences

journal homepage: www.elsevier.com/locate/jns

A visual rating scale for cingulate island sign on 18F-FDG-PET to differentiate dementia with Lewy bodies and Alzheimer's disease

Le Gjerum[a,*], Kristian Steen Frederiksen[a], Otto Mølby Henriksen[b], Ian Law[b], Lasse Anderberg[b], Birgitte Bo Andersen[a], Eva Bjerregaard[a], Anne-Mette Hejl[c], Peter Høgh[d,e], Steen Gregers Hasselbalch[a]

[a] Department of Neurology, Danish Dementia Research Centre, Rigshospitalet, University of Copenhagen, Blegdamsvej 9, DK-2100 Copenhagen, Denmark
[b] Department of Clinical Physiology, Nuclear Medicine & PET, Rigshospitalet, University of Copenhagen, Blegdamsvej 9, DK-2100 Copenhagen, Denmark
[c] Department of Neurology, Bispebjerg Hospital, University of Copenhagen, Bispebjerg Bakke 23, DK-2400 Copenhagen, Denmark
[d] Regional Dementia Research Center, Department of Neurology, Zealand University Hospital, Sygehusvej 10, DK-4000 Roskilde, Denmark
[e] Department of Clinical Medicine, University of Copenhagen, Blegdamsvej 3B, DK-2200 Copenhagen, Denmark

II

ARTICLE INFO

Keywords:
Cingulate island sign
FDG-PET
Dementia with Lewy bodies
Alzheimer's disease
Dual pathology
Visual rating scale

ABSTRACT

Valid diagnosis of dementia with Lewy bodies (DLB) is essential to establish appropriate treatment and care. However, the diagnostic accuracy is complicated by clinical and pathological overlap with Alzheimer's disease (AD). Cingulate island sign (CIS), defined as sparing of posterior cingulate cortex (PCC) relative to precuneus and cuneus on 18F-fluoro-deoxy-glucose positron emission tomography (18F-FDG-PET), is included in the revised diagnostic DLB criteria. There are no guidelines for the visual grading of CIS, although visual rating is a fast-applicable method in a clinical setting.

The objective was to develop a robust visual CIS scale and evaluate the performance in differentiating DLB with and without amyloid beta pathology (Aβ+/−), and AD.

18F-FDG-PET scans from 35 DLB patients, 36 AD patients, and 23 healthy controls were rated according to a visual CIS scale based on specific reading criteria. The visual CIS scale was validated against a quantitative CIS ratio derived from a region of interest analysis of PCC, precuneus, and cuneus.

DLB patients had a significantly higher visual CIS score compared to AD patients, and controls.

A cut-off visual CIS score of 4 significantly differentiated DLB Aβ− patients from DLB Aβ+ patients.

In conclusion, the visual CIS scale is clinically useful to differentiate DLB from AD. The degree of CIS may be related to Aβ pathology in DLB patients.

1. Introduction

Dementia with Lewy bodies (DLB), which is pathologically characterized by accumulation of Lewy bodies (LB), is the second most common cause of neurodegenerative dementia after Alzheimer's disease (AD) [24]. Early and accurate diagnosis of DLB is essential to enable appropriate treatment and care, in addition to identify and manage clinical features including motor and psychiatric symptoms, severe autonomic dysfunction and hazardous antipsychotic sensitivity [26]. A valid diagnosis is also central for predicting the prognosis of the disease and planning clinical trials, but the diagnostic process may be complicated by substantial overlap in clinical and neuropsychological features between AD and DLB [23]. Furthermore, the frequent occurrence of pathological heterogeneity in DLB patients, particularly coexisting AD pathology, i.e. amyloid beta (Aβ) plaques and tau tangles, can contribute to diverse clinical presentations [33,34]. Aβ pathology in patients with DLB has been associated with faster cognitive decline and shorter survival compared to the DLB patients with pure LB pathology

Abbreviations: Aβ, amyloid beta; AD, Alzheimer's disease; AUC, area under the curve; CI, confidence interval; CIS, cingulate island sign; CSF, cerebrospinal fluid; CT, computed tomography; DAT, dopamine transporter; DLB, dementia with Lewy bodies; LB, Lewy bodies; MMSE, mini mental state examination; MRI, magnetic resonance imaging; PCC, posterior cingulate cortex; PET, positron emission tomography; ROI, region of interest; SPECT, single photon emission computed tomography; SUV, standardized uptake value; 11C-PiB, 11C-Pittsburgh compound B; 123I-FP-CIT, 123I-2β-carbomethoxy-3β-(4-iodophenyl)-N-(3-fluoropropyl)-nortropane; 18F-FDG, 18F-fluoro-deoxy-glucose

* Corresponding author.
E-mail addresses: le.gjerum@regionh.dk (L. Gjerum), steen.gregers.hasselbalch@regionh.dk (S.G. Hasselbalch).

https://doi.org/10.1016/j.jns.2019.116645
Received 15 October 2019; Received in revised form 17 December 2019; Accepted 21 December 2019
Available online 24 December 2019

[6,16]. These findings underline the clinical relevance of identifying coexisting Aβ pathology in DLB patients.

Functional neuroimaging has become a commonly used supplement to the clinical diagnosis of dementia [36], and has also been introduced in the diagnostic criteria for both DLB and AD [26,27]. Several studies have demonstrated occipital hypometabolism as a supportive feature to distinguish DLB patients from AD patients on positron emission tomography (PET) imaging using 18F-fluoro-deoxy-glucose as tracer (18F-FDG-PET) [1,18,19,29].

Cingulate island sign (CIS) is another identified feature on 18F-FDG-PET to support the diagnosis of DLB, and has been found to be more specific than occipital hypometabolism for DLB [21]. CIS is defined as preserved metabolism of the posterior cingulate cortex (PCC) relative to reduced metabolism in the precuneus and the cuneus, and is included in the updated diagnostic DLB criteria [26]. The CIS ratio, defined as the measure of FDG uptake in the PCC divided by the sum of the uptake in the precuneus and the cuneus, is higher in DLB patients compared to AD patients as demonstrated by a semi-quantitative method [11,15,19,21,31]. A quantitative method can be time consuming, requires standardized acquisition and analysis of both the 18F-FDG-PET and the structural scan, i.e. either computed tomography (CT) or magnetic resonance imaging (MRI), and the specific software may only be accessible in expert centres. Of interest, a dichotomous visual interpretation of CIS (present or absent) had a higher diagnostic accuracy compared to the quantitative CIS ratio in distinguishing DLB patients from AD patients [21]. However, there are no established visual criteria for the degree of CIS, even though visual rating of other imaging biomarkers and modalities are commonly used and has proven to be a fast, reliable and reproducible method in clinical practice [14,36,37]. The application of a standardized method to classify and interpret the presence of CIS may enhance the utilization of relevant diagnostic information, along with improving the diagnostic accuracy of DLB. Furthermore, a visual rating scale can easily be implemented into the clinical practice across centres and assist the less experienced nuclear medicine physicians.

The objectives of this study were (1) to develop a robust visual rating scale for the presence of CIS on 18F-FDG-PET (the visual CIS scale); (2) to evaluate the reproducibility and the accuracy of the visual CIS scale to differentiate DLB patients and AD patients; (3) to compare the performance of the visual CIS scale to a quantitative method for CIS (the quantitative CIS ratio) and 18F-FDG-PET visual features of occipital involvement and forced diagnosis; (4) to examine whether coexisting Aβ pathology influenced the presence of CIS for the DLB patients.

2. Materials and methods

2.1. AD and DLB study population

The study population consisted of retrospectively identified patients with a clinical diagnosis of DLB according to the DLB criteria [25] and AD according to the AD criteria [27] diagnosed from 2011 to 2017 at four Danish memory clinics in the greater Copenhagen area (Rigshospitalet, Glostrup Hospital, Bispebjerg Hospital, and Roskilde Hospital).

The dementia diagnoses were confirmed according to the established clinical criteria by an experienced dementia specialist (SGH, AH, or PH) based on patient files from baseline to the most recent clinical follow up and all available examination results (except the 18F-FDG-PET findings).

All eligible patients had a structural scan, i.e. either CT or MRI, a 18F-FDG-PET scan, and determination of the brain Aβ status, i.e. either measurement of Aβ 1–42 (Aβ42) in the cerebrospinal fluid (CSF) or PET imaging using the ligand 11C-Pittsburgh compound B (11C-PIB-PET).

For patients with DLB an abnormal 123I-2β-carbomethoxy-3β-(4-iodophenyl)-N-(3-fluoropropyl)-nortropane (123I-FP-CIT) dopamine transporter single photon emission computed tomography (123I-FP-CIT-DAT-SPECT) scan was also required.

Thirty-seven patients with a clinical diagnosis of DLB and 37 patients with a clinical diagnosis of AD matched on age, sex, and MMSE were included.

The retrospective use of clinical data was approved by the Danish Patient Safety Authority (no. 3-3013-2703/1).

2.2. Healthy controls

A group of 23 healthy elderly controls aged over 60 years with normal MRI and 18F-FDG-PET results, and normal neuropsychology scores from the Memory Clinic at Rigshospitalet was also included. The controls consisted of 18 healthy research volunteers and five subjects with subjective cognitive decline in whom dementia and neurodegenerative disease had been ruled out. All controls had no evidence of brain amyloid accumulation, i.e. normal concentration of Aβ42 in CSF, except three of the healthy research volunteers who did not undergo assessment of brain amyloid.

All healthy research volunteers gave a written informed consent, and the inclusion was approved by the Danish National Committee on Health Research (no. H-1-2014-126).

2.3. Clinical examinations

All patients and controls underwent a standardized diagnostic dementia assessment including medical history, physical and neurological examinations, cognitive testing (i.e. Mini mental state examination (MMSE) and Addenbrooke's cognitive examination), routine blood screening, and a structural scan, i.e. either CT or MRI.

The dementia patients were followed up longitudinally as part of the standard clinical routine, and 93% of the patients were followed for at least 12 months.

2.4. Assessment of brain amyloid

The brain amyloid accumulation was determined by either Aβ42 in CSF ($n = 76$), 11C-PIB-PET imaging ($n = 5$), or both ($n = 10$). If the Aβ biomarkers were incongruent ($n = 5$) the result of the 11C-PIB-PET image determined the Aβ status.

The CSF was collected by lumbar puncture in polypropylene tubes, and Aβ42 was analysed with the enzyme-linked immunosorbent assay (ELISA) using the commercially available kit (Innotest, Fujirebio, Europe, Ghent, Belgium). An abnormal Aβ42 (< 550 pg/mL) was indicated as Aβ+, whereas a normal Aβ42 was indicated as Aβ− [40].

2.5. Imaging

Imaging was performed over a seven-year period at different hospitals using a range of scanner systems. General aspects of MRI, 123I-FP-CIT-DAT-SPECT, 11C-PIB-PET, and 18F-FDG-PET imaging are summarized in subsection 2.5.1–2.5.5. Imaging details are provided in Appendix A.

2.5.1. Acquisition of MRI

MRI was performed on a clinical 1.5 or 3.0 Tesla system. A high-resolution 3D T1 weighted MRI sequence suitable for tissue segmentation was available in 77 subjects. A semi-quantitative CIS ratio analysis of the high-resolution 3D T1 weighted MRI sequence was performed as describe in subsection 2.5.5.1.

2.5.2. Analysis of 123I-FP-CIT-DAT-SPECT

A visual interpretation of reduced symmetric or asymmetric tracer uptake in putamen and/or caudate nucleus was defined as abnormal, supported by the semiquantitative analysis of the specific binding ratio of striatum, caudate nucleus, and putamen relative to occipital cortex and the putamen/caudate nucleus uptake ratio [5,22].

2.5.3. Analysis of 11C-PiB-PET

A visual interpretation of increased tracer uptake in at least two cortical AD specific regions at the level of or above white matter supported by cortex-to-cerebellar grey matter uptake ratio > 1.5 was defined as abnormal [28]. An abnormal 11C-PiB-PET was indicated as Aβ+, whereas a normal 11C-PiB-PET was indicated as Aβ− .

2.5.4. Acquisition of 18F-FDG-PET

The PET imaging was performed according to the international practice guideline [35]. PET images were acquired using clinical PET/CT or PET/MRI systems after an intravenous bolus of 200–300 MBq 18F-FDG as a 10 min static scan during the 40–60 min post-injection time window. All images were reconstructed using CT based attenuation correction [2].

2.5.5. Analysis of 18F-FDG-PET

2.5.5.1. Analysis of quantitative CIS ratio. The high-resolution 3D T1 weighted MRI sequence was segmented using FreeSurfer (version 5.3.0) [8] to generate region of interests (ROIs) of PCC, precuneus, cuneus, and cerebellar grey matter for each hemisphere based on the Desikan-Killiany Atlas. The 18F-FDG-PET image of each patient was fused to the segmented MRI and the mean ROI values were obtained. Only non-partial volume corrected PET data was used, as partial volume corrected by the Symmetric Geometric Transfer Matrix method [12] was not Please insert hyphen: "suf- < br > ficiently"sufficiently robust. The mean standardized uptake value (SUV) of each region was normalized to cerebellum. In each hemisphere the ratio for the mean SUV in the PCC ROI was divided by the mean SUV in the combined precuneus plus cuneus ROIs, the quantitative CIS ratio was derived by averaging the ratios for each hemisphere [21].

2.5.5.2. Standardized reading approach for the visual interpretation. A clinical standardized reading approach in SyngoVia (SyngoVia, MI Neurology, Siemens Healthcare, Erlangen, Germany) of the 18F-FDG-PET scan co-registered to the structural scan (i.e. low-dose CT, non-enhanced diagnostic CT or MRI) was performed.

The visual interpretation of the 18F-FDG-PET scan was performed in the following order: First, scoring of the visual CIS scale, then rating of occipital hypometabolism, and finally assessment of the forced diagnosis. Rating of CIS was based on visual evaluation only, whereas evaluation of occipital hypometabolism and forced diagnosis was supported by the statistical surface projections from a normal database supplied by the software vendor (age 46–75 years) using cerebellum as a reference region.

Two experienced nuclear medicine physicians (IL and OMH) blinded to all clinical data visually assessed all the 18F-FDG-PET scans. In case of disagreement a consensus evaluation was performed between the two readers.

2.5.5.3. Development of the visual CIS-scale. To define the degree of CIS for the visual scale, we evaluated 18F-FDG-PET images from five DLB patients and ten AD patients with a wide range of CIS presentations. Based on the evaluations of the 18F-FDG-PET images, the visual CIS scale was developed and adjusted to the final version by two experienced nuclear medicine physicians (IL and OMH).

2.5.5.4. Standardized reading approach for the visual CIS-scale. A standard reading approach was used to standardize the 18F-FDG-PET images and optimize the visualization of the CIS region (Fig. 1):

- the 18F-FDG-PET scan was displayed on a clinical workstation using SyngoVia with the PET image superimposed on the structural scan.
- the scan was displayed in "PET Rainbow" and windowing adjusted to basal ganglia red and cerebellum green/yellow with red hues.
- three-way orthogonal view approximately along AC-PC plane with both sagittal and axial planes through PCC, precuneus, and cuneus.

The visual CIS scoring was based on both sagittal and axial views.

2.5.5.5. Scoring of the visual CIS scale. First, the degree of hypometabolism in PCC, precuneus, and cuneus was classified for each hemisphere as "none", "mild", or "moderate-to-severe".

Secondly, the presence of CIS was based on the degree of hypometabolism in PCC, precuneus, and cuneus together with a visual, interpretation of CIS including influence of central or cortical atrophy, and rated for each hemisphere according to the following criteria:

0 = absent (PCC similar or lower than precuneus and cuneus).
1 = intermediate (e.g. PCC hypometabolic, but less than precuneus and cuneus, or only precuneus lower than PCC).
2 = present (typically PCC normal and both precuneus and cuneus lower).

If the activity uptake in precuneus or cuneus was considered reduced because of adjacent leukoaraiosis or ischemia on the available structural scan the rating was changed to 0.

Finally, the ratings from each hemisphere were summed to a visual CIS score. Three examples of scorings of the visual CIS scale are giving in Fig. 2.

For clinical operationalization the visual CIS score was classified as:

Score 0 = "no CIS".
Score 1–2 = "possible CIS".
Score 3–4 = "definite CIS".

2.5.5.6. Occipital hypometabolism. Occipital hypometabolism was assessed in lateral and medial occipital cortices and rated as "present" or "absent".

2.5.5.7. Forced diagnosis. This approach was adopted to mimic the usual reading approach of a nuclear medicine physician. The forced diagnosis was based on the overall visual interpretation of the 18F-FDG-PET scan including typical features of DLB (predominant occipital involvement with no or minimal involvement of frontal or anterior temporal cortex) and typical features of AD (anterior temporal, mesial temporal, or AD like parietotemporal hypometabolism with occipital sparing). The readers were asked to give a forced diagnosis of the most likely aetiology ("DLB", "AD", "other abnormal", or "normal").

2.6. Statistical analysis

Differences between groups were assessed with Kruskal-Wallis tests followed by Mann-Whitney post-hoc tests or one-way ANOVA tests followed by Tukey post-hoc tests for continuous variables, and Pearson's or Fischer's Chi-square test for count variables, where appropriate.

The interrater agreement was quantified by Cohen's weighted Kappa. The Spearman's correlation analysis was applied for comparing the quantitative CIS ratio values and the visual CIS scores, and for verifying the correlations between visual CIS score, MMSE score, age, education, and symptom duration for all subjects and DLB patients. For the latter, the Spearman correlation results were corrected by false discovery rate (FDR) correction. The diagnostic accuracy for each binary disease group comparison was reported as sensitivity, specificity, balanced accuracy, and area under the receiver-operator characteristic curve (AUC). Balanced accuracy is defined as the average of sensitivity and specificity for the cut-off score, and compensates for the imbalanced number in the disease groups [4].

The optimal cut-off was established by maximizing the Youden index. Youden index is defined as the sum of sensitivity and specificity minus one [39].

Statistical analysis was performed using SAS Studio software, version 9.4 (SAS Institute Inc., Cary, NC, USA) and GraphPad Prism 8.0.0

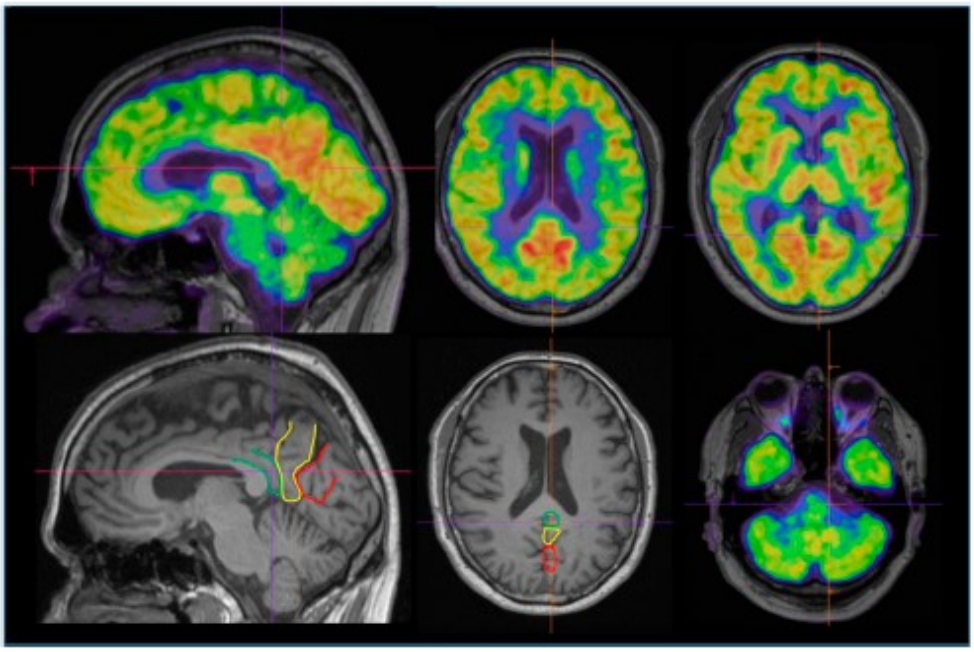

Fig. 1. Standardized reading approach of 18F-FDG-PET.
Abbreviations: MRI = magnetic resonance imaging; PCC = posterior cingulate cortex; 18F-FDG-PET = 18F-fluoro-deoxy-glucose positron emission tomography; MRI and 18F-FDG-PET image displayed in saggital and axial plane in Scenium with orientation through PCC (green), precuneus (yellow) and cuneus (red).

for Windows (GraphPad Software, San Diego, California USA). A two-sided p-value < .05 was considered indicative of statistical significance.

3. Results

3.1. Baseline characteristics

Two patients with a clinical diagnosis of DLB and one patient with a clinical diagnosis of AD were excluded during the visual assessment of the 18F-FDG-PET scans due to poor quality. The flow diagram of the study population is shown in (Appendix B, Fig. B.1). Demographics are shown in Table 1. There were no significant differences in the baseline demographics between the two dementia groups (DLB patients and AD patients) or the DLB subgroups (DLB Aβ− patients and DLB Aβ+ patients). The controls had a significantly higher MMSE score than all dementia groups (AD, DLB Aβ− patients and DLB Aβ+ patients) and

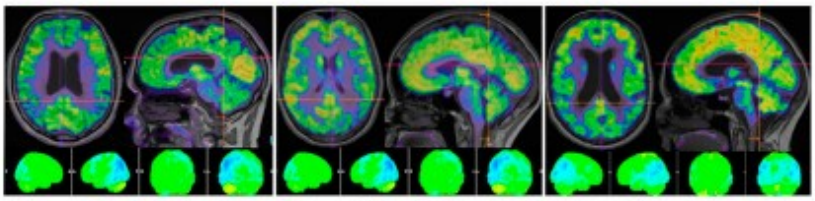

		71-years old male diagnosed with AD with MMSE-score 25 and a positive Aβ-biomarker	66-years old female diagnosed with DLB with MMSE-score 29 and a positive Aβ-biomarker	75-years old female diagnosed with DLB with MMSE-score 29 and a negative Aβ-biomarker
Degree of hypometabolism (R/L)	PCC	moderate-to-severe/mild	none/mild	none/none
	Precuneus	moderate-to-severe/mild	none/mild	moderate-to-severe/moderate-to-severe
	Cuneus	none/none	none/moderate-to-severe	moderate-to-severe/moderate-to-severe
Visual CIS score (R+L)		0 (0+0)	1 (0+1)	4 (2+2)
Classification of CIS		No CIS	Possible CIS	Definite CIS
Quantitative CIS ratio		0.95	1.17	1.16

Fig. 2. 18F-FDG-PET images with examples of the visual CIS-score and quantitative CIS ratio.
Abbreviations: Aβ = amyloid beta; AD = Alzheimer's disease; CIS = cingulate island sign; DLB = dementia with Lewy bodies; L = left; MMSE = Mini-Mental State Examination; PCC = posterior cingulate cortex; R = right; 18F-FDG-PET = 18F-fluoro-deoxy-glucose positron emission tomography; Axial and sagittal view of the PET image superimposed on the high-resolution 3D T1 weighted MRI sequence (top) and the statistical surface (right lateral, left lateral, anterior, and posterior view) projections using cerebellum as a reference region compared to a healthy age-matched control group (bottom).

Table 1
Baseline demographics.

	AD	Controls	DLB	DLB Aβ−	DLB Aβ+
Subjects, n	36	23	35	19	16
Female, n (%)	11 (30.6%)	8 (34.8%)	10 (28.6%)	4 (21.0%)	6 (37.5%)
Age, mean years ± SD	70.6 ± 6.3	68.7 ± 6.1	69.9 ± 6.8	68.0 ± 8.3	72.1 ± 3.5*
MMSE, mean score ± SD	25.8 ± 2.9*	29.3 ± 1.2	26.3 ± 3.2*	26.1 ± 3.3*	26.6 ± 3.1*
Education, mean years ± SD	13.5 ± 2.8	14.5 ± 2.4	12.8 ± 2.8*	13.0 ± 2.7	12.6 ± 3.0
Symptom duration, mean years ± SD	3.1 ± 3.1	NA	2.9 ± 2.8	2.3 ± 2.2	3.6 ± 3.4

Abbreviations: Aβ = amyloid beta; AD = Alzheimer's disease; DLB = dementia with Lewy bodies; MMSE = Mini-Mental State Examination; n = number; NA = not applicable; SD = standard deviation;
* Differ significantly from Controls ($p < .05$).

longer education in years compared to DLB patients.

3.2. Reliability of the visual CIS scale

According to Cohen's weighted kappa, the interrater agreement of the visual CIS score between the two readers was 0.73 (95% CI 0.63;0.83). The two readers had disagreement of the visual CIS scores in 26 of 97 cases, of which 61% was of one grade, 35% was of two grades, 4% (1 case) was of three grades. The distribution of the visual CIS scores between the two readers are shown in Appendix C, Table C.1.

The quantitative CIS ratio analysis was performed in the 77 subjects with a high-resolution 3D T1 weighted MRI sequence. The correlation of the visual CIS score with the quantitative CIS ratio value was moderate-to-strong (Spearman's correlation coefficient, $r = 0.60$, 95% CI 0.44–0.73; $p < .0001$) (Fig. 3).

3.3. DLB patients and AD patients

Table 2 shows that the median visual CIS score was significantly higher for DLB patients in comparison to AD patients, and controls. In line with this, the mean quantitative CIS ratio was significantly higher for DLB patients compared to AD patients and controls. Most of the AD patients (75%) and controls (87%) were evaluated to have "no CIS" based on the classification of the visual CIS score in comparison to a minority of the DLB patients (26%).

An optimal cut-off score on the visual CIS scale of ≥2 had a sensitivity of 51% and a specificity of 92% in differentiating DLB patients and AD patients, yielding a balanced accuracy of 72% (Table 3). In comparison, the optimal cut-off value of ≥0.98 on the quantitative CIS ratio separated DLB patients and AD patients with a higher sensitivity of 88% and a lower specificity of 67%, yielding a balanced accuracy of 77%. When comparing the performance of the two methods by an AUC analysis, we observed no significant difference ($p = .45$) in differentiating DLB patients and AD patients, although the latter method had a slightly better performance. Also, the visual CIS scale did not differ in performance when compared with visual interpretation of occipital hypometabolism and forced diagnosis for distinguishing DLB patients and AD patients (Table 3).

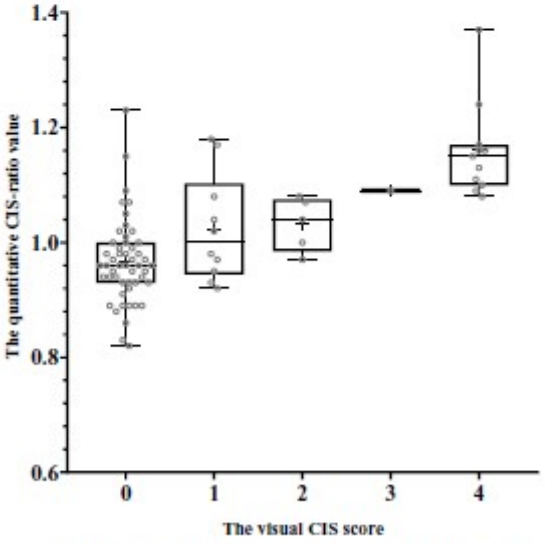

Fig. 3. Correlation of the visual CIS score and the quantitative CIS ratio value. Abbreviations: CIS = cingulate island sign; Boxplot graph with the boxes corresponding to median values with indications of the 25th and 75th percentiles, and the whiskers show the minimum and maximum values. The + indicates the mean. All the subjects are plotted as ○. The Spearman's correlation coefficient of all five groups on the visual CIS score (0, 1, 2, 3, and 4) and the quantitative CIS ratio was $r = 0.60$ (95% CI 0.44–0.73, $p < .0001$).

3.4. Amyloid positive and amyloid negative DLB patients

The DLB Aβ− patients had the highest median visual CIS score of 4, followed by DLB Aβ+ patients with a median score of 1, and lastly the AD patients with a median score of 0. However, the visual CIS score were only significant different between the AD patients and the DLB subgroups, although the difference between DLB Aβ+ patients and DLB Aβ− patients reached a trend level of $p = .06$. A significant larger proportion of the DLB Aβ− patients (58%) was classified with "definite CIS", when compared both to DLB Aβ+ patients (25%) and to AD patients (3%) (Table 2).

As shown in Table 3, an optimal cut-off score of 4 on the visual CIS scale distinguish DLB Aβ− patients from the DLB Aβ+ patients and AD patients with a balanced accuracy of 70% and 80% respectively. When applying the Fishers exact test, the proportion of DLB Aβ− patients with a visual CIS score 4 was significantly higher compared to the DLB Aβ+ patients and AD patients. Whereas, the proportion of DLB Aβ+ patients with an optimal cut-off score ≥1 was significantly higher than the AD patients.

No significant differences were observed between the visual CIS scale and the quantitative CIS ratio for separating the diagnostic groups.

3.5. Clinical correlations

Box plot of MMSE scores across CIS scores (Appendix D, Fig. D.1) and Kruskal-Wallis test ($p = .55$) did not indicate an association of MMSE with visual CIS score.

Furthermore, the pairwise correlations between the visual CIS score and MMSE score, age, education, and symptom duration for all subjects and DLB patients were investigated with a Spearman correlation analysis both for all subjects and for DLB patients (Appendix D, Table D.1 and D.2). The visual CIS score was not significant correlated with any clinical variable, neither for all subjects or for DLB patients.

Table 2
The visual CIS scale and the quantitative CIS ratio.

	AD	Controls	DLB	DLB Aβ−	DLB Aβ+
Subjects, n	36	23	35	19	16
Visual CIS score					
0/1/2/3/4, n	27/6/2/0/1	20/1/2/0/0	12/5/3/1/14	5/2/0/1/11	7/3/2/1/3
Median score (IQR)	0 (0.5)	0 (0)	2 (4)*	4 (4)*,‡	1 (2.5)*
Visual CIS classification					
No CIS/Possible CIS/Definite CIS, n	27/8/1	20/3/0	12/8/15*	5/3/11*	7/5/4*
Quantitative CIS ratio					
Mean value ± SD	0.98 ± 0.08	0.96 ± 0.07	1.09 ± 0.10*	1.11 ± 0.10*	1.05 ± 0.09

Abbreviations: Aβ = amyloid beta; AD = Alzheimer's disease; CIS = cingulate island sign; DLB = dementia with Lewy bodies; IQR = interquartile range; n = number; SD = standard deviation;

* Differ significantly from AD and controls ($p < .05$).

‡ Trend difference from DLB Aβ + ($p = .06$).

Table 3
Diagnostic accuracy of the visual CIS scale, quantitative CIS ratio and 18F-FDG-PET visual features.

	DLB versus AD			
	Sens.	Spec.	Bal. acc.	AUC (95% CI)
Visual CIS score ≥ 2	51.4%	91.7%	71.6%	0.77 (0.64–0.89)
Quantitative CIS ratio value ≥ 0.98	87.5%	66.7%	77.1%	0.82 (0.70–0.94)
Occipital hypometabolism	54.3%	91.7%	73.0%	0.74 (0.63–0.85)
Forced diagnosis	51.4%	94.4%	72.9%	0.78 (0.66–0.90)
	DLB Aβ− versus AD			
	Sens.	Spec.	Bal. acc.	AUC (95% CI)
Visual CIS score = 4	63.2%	97.2%	80.2%	0.85 (0.71–0.99)
Quantitative CIS ratio value ≥ 1.04	85.7%	86.7%	86.2%	0.88 (0.77–0.98)
	DLB Aβ+ versus AD			
	Sens.	Spec.	Bal. acc.	AUC (95% CI)
Visual CIS score ≥ 1	56.3%	75.0%	65.6%	0.65 (0.45–0.85)
Quantitative CIS ratio value ≥ 0.99	80.0%	76.7%	78.3%	0.74 (0.54–0.94)
	DLB Aβ− versus DLB Aβ+			
	Sens.	Spec.	Bal. acc.	AUC (95% CI)
Visual CIS score = 4	57.9%	81.3%	69.6%	0.73 (0.52–0.93)
Quantitative CIS ratio value ≥ 1.04	85.7%	50.0%	67.9%	0.66 (0.43–0.90)

Abbreviations: Aβ = amyloid beta; AD = Alzheimer's disease; AUC = the area under the receiver operating characteristic curve; Bal. acc. = balanced accuracy; CI = confidence interval; CIS = cingulate island sign; DLB = dementia with Lewy bodies; Sens. = sensitivity; Spec. = specificity; 18F-FDG-PET = 18F-fluoro-deoxy-glucose positron emission tomography.

4. Discussion

CIS is a supportive marker of DLB on 18F-FDG-PET, and is useful in the discrimination of DLB from AD [26], however, a visual rating scale for CIS has been lacking. With this study we aimed to develop a robust visual rating scale from clinically acquired 18F-FDG-PET scans to detect the degree of CIS. We found an acceptable interrater agreement with most disagreements amounting to a single grade in the low-grade group, and a moderate-to-strong correlation with the quantitative CIS ratio, suggesting that the visual CIS scale is useful in a clinical setting as an aid in assessment of CIS.

Furthermore, we found significant differences between the groups median visual CIS scores in both the diagnostic groups analysis (DLB, AD, and controls) and the subgroups analysis (DLB Aβ−, DLB Aβ+, and AD). Notably, a cut-off visual CIS score of 4 could significantly differentiate the DLB Aβ− patients from the DLB Aβ+ patients, which reflects that the degree of CIS may be associated with Aβ pathology in DLB patients.

The original study introducing visual interpretation of CIS for differentiating DLB from AD by Lim et al. found CIS to be highly specific for DLB with a specificity of 100% and a sensitivity ranging from 62% to 86% [21]. The higher diagnostic accuracy in the prior study compared to our findings may be due to a restricted dichotomized rating of CIS in a relatively small study cohort of 14 DLB patients and 10 AD patients, together with only 29% of DLB patients having AD pathology. In contrast, we aimed to characterize the degree of CIS in the pathological heterogenous DLB patients considering previous studies have demonstrated higher CIS ratio in DLB patients compared to AD patients [11,15,19,21,31] together with over half of pathologically confirmed DLB cases have coexisting AD pathology [3,10].

We evaluated the performance of the visual CIS scale against a quantitative CIS method as the presence of CIS has mainly been demonstrated by various quantitative methods [11,15,19,21,31,38]. In accordance with the previous studies, we found a significantly higher quantitative CIS ratio for the DLB patients compared to the AD patients and controls (Table 2). The visual CIS scale had a similar diagnostic accuracy compared to the quantitative CIS ratio in distinguishing DLB patients from AD patients, but from a clinical perspective a visual rating scale is advantageous compared to a quantitative method for several reasons. A quantitative method can be time consuming, the actual value depends on both the acquisition and processing of the 18F-FDG-PET and MRI, and the specific software used may only be accessible in expert centres. A cut-off value may thus only be applicable to a specific setup in a single centre. In contrast, a visual rating scale for CIS can be implemented as a fast-diagnostic adjunct to the standard visual 18F-FDG-PET scan evaluation without additional software.

The visual CIS scale was also compared to another relevant 18F-FDG-PET feature (occipital hypometabolism) and to an overall visual evaluation of the 18F-FDG-PET image including typical and atypical features of DLB and AD (forced diagnosis). The performance for these 18F-FDG-PET visual features in distinguishing DLB from AD were consistent with two previous studies of similar ratings [21,31], and comparable to the visual CIS scale. This suggests that the visual CIS scale may supplement or even replace more resource demanding techniques performed by experienced nuclear medicine physicians.

Finally, we examined if the presence of CIS was influenced by concurrent Aβ pathology in DLB patients. Comparable to previous studies [7,20], we found that nearly half (46%) of the patient with a clinical diagnosis of DLB had an abnormal Aβ biomarker (Aβ+). Two previous studies consisting of a smaller study of 10 DLB patients [17]

and a larger study of 39 DLB patients [11] with determination of the brain Aβ status by 11C-PIB-PET found no association between a quantitative method of CIS and Aβ accumulation. Likewise, we found no significant differences between the DLB Aβ− patients and DLB Aβ+ patients for the quantitative CIS ratio. However, we found that the DLB Aβ− patients had the highest score on the visual CIS scale in comparison to the DLB Aβ+ patients with intermediate values (Table 2) as an indication of coexisting Aβ pathology may diminish the presence of CIS, although the difference only reached a trend level of $p = .06$.

Additionally, a cut-off visual CIS score of 4 discriminated the DLB Aβ− patients from DLB Aβ+ patients with a balanced accuracy of 70%, and this finding corroborate that Aβ pathology might be a possible confounding factor associated with the presence of CIS in DLB patients, which is relevant to include in the interpretation of CIS.

In general, the visual CIS scale distinguishes the diagnostic groups (DLB and AD) and the subgroups (DLB Aβ−, DLB Aβ+, and AD) with high specificities, but only moderate sensitivities. This may be explained by various potentially confounding circumstances. Previous studies have suggested that CIS may be influenced by the severity of cognitive impairment [11,30], however, in line with a previous study [15], we did not find a relationship between CIS and MMSE. The implementation of the visual CIS scale in a routine practice is potentially valuable considering that visual features including cingulate hypometabolism seemed to be underreported and missed on the clinical interpretation of FDG-PET scans of patients with DLB [13].

Combining the visual CIS scale on 18F-FDG-PET with visual assessment of atrophy pattern on MRI [32] could potentially increase the accuracy of DLB diagnosis and could be explored in future studies. Furthermore, the visual CIS scale should preferably be evaluated in a larger mixed memory cohort with unknown diagnosis and by less experienced readers.

Some limitations should be considered. In this study, the diagnosis of DLB and AD lacked pathological confirmation, but the reference diagnosis was based on reconfirmed diagnosis by an experienced dementia specialist (SGH, AH, and PH) according to the current DLB diagnostic criteria [25] and AD research criteria [27], and based on all available data including clinical follow up for at least 12 months for the majority of the patients.

Another limitation is the selection criteria, considering that we only included DLB patients with an Aβ biomarker and a 123I-FP-CIT-DAT-SPECT and AD patients with an Aβ biomarker, respectively, which are considered as supplementary disease biomarkers if the diagnosis is questionable in our clinics. Consequently, our study population may consist of patients with a more heterogenous clinical presentation, which may diminish the diagnostic accuracy. A final limitation is the use of different scanners given that the diagnostic workup for the study population was performed across several centres. On the other hand, visual ratings are in general more robust for scanner differences and should be applicable without consideration of the scanner.

Among the strengths of this study is the relatively large sample size with a comprehensive diagnostic evaluation program together with explicitly including DLB patients with an abnormal 123I-FP-CIT-DAT-SPECT. The latter is an indicative biomarker of DLB [26].

In conclusion, our study demonstrated that the visual CIS scale was robust and clinical applicable to evaluate the presence of CIS, which may help to improve the accuracy of clinical diagnosis of DLB. Furthermore, the degree of CIS may be associated with the presence of Aβ pathology in DLB patients. In perspective, the validity of the visual CIS scale should be evaluated in a larger mixed memory cohort and by less experienced readers.

Funding

This work was supported by the Rigshospitalet research board [R129-A5325].

Declaration of Competing Interest

All authors declare no conflicts of interest.

Acknowledgment

The authors wish to thank the Department of Clinical Physiology, Nuclear Medicine & PET, Rigshospitalet, Denmark, and in particular Oriol Puig Calvo for obtaining the 18F-FDG-PET scans of the healthy research volunteers, and Lisbeth Marner and Karine Madsen for valuable help with development of the visual CIS scale.

The authors wish to thank the Department of Neurology, Danish Dementia Research Centre, Rigshospitalet, Denmark, and in particular Asmus Vogel for assessing the neuropsychological tests of the healthy research volunteers.

Appendix A

A.1. Imaging details

A.1.1. MRI

MRI were acquired using a 1.5 Tesla GE Medical (Optima MR450w, Signa Hde, or Signa HDxt) ($n = 19$), 1.5 or 3 Tesla Philips (Achieva) ($n = 4$), or 1.5 or 3 Tesla Siemens (Aera, Avanto, Biograph, Espree, Trio, or Verio) ($n = 74$)

A.1.2. 123I-FP-CIT-DAT-SPECT

The DAT-SPECT imaging was performed according to the international practice guideline [5]. DAT-SPECT images were acquired using Triple-head IRIX camera (Philips Medical) ($n = 27$), PRISM 3000XP (Marconi, Philips) ($n = 5$), or Infina Hawkeye (GE) or Syngo Symbia T2 (Siemens) ($n = 4$)

In general, the SPECT image was acquired on either brain dedicated SPECT or general SPECT/CT systems 180–240 min after an intravenous bolus of 200 MBq 123I-FP-CIT.

A.1.3. 11C-PIB-PET

The PET imaging was performed according to the international practice guideline [28]. PET images were acquired using a Siemens Biograph mCT PET/CT scanner (Siemens Healthcare, Erlangen, Germany) ($n = 15$). In general, a 20–30 min static PET acquisition was performed on a standard PET/CT system 40 min after an intravenous bolus of 150–400 MBq 11C-PiB. After spatial normalization, images were analysed using clinical workstations, SyngoVia (SyngoVia, MI Neurology, Siemens Healthcare, Erlangen, Germany). The activity uptake in AD specific ROIs was defined [9], and uptake values calculated relative to cerebellar grey matter. The uptake was assessed after co-registration to the structural scan

A.1.4. 18F-FDG-PET

Imaging details are summarized in Table A.1

Table A.1
Imaging details for 18F-FDG-PET.

Subjects (n)	Scanner	Reconstruction method	Matrix size
2	GE Medical (Discovery MI)	QCFX or VPFXS	256 × 256
6	Philips (Gemini)	LOR-RAMLA or 3D-RAMLA	128 × 128
89	Siemens (Biograph mCT, Biograph mMR, or Somatom, 1094)	OSEM	336 × 336, 344 × 344, or 400 × 400

Abbreviations: n = numbers; 18F-FDG-PET = 18F-fluoro-deoxy-glucose positron emission tomography.

Appendix B

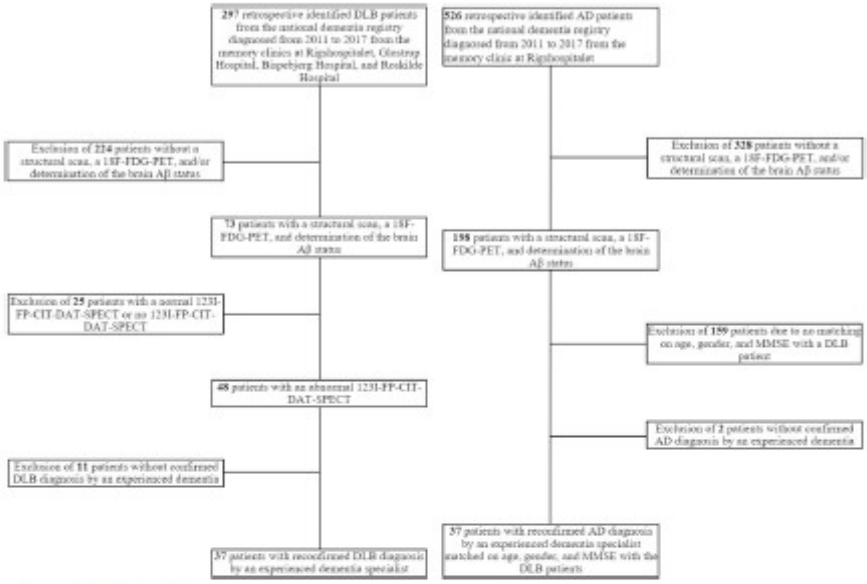

Fig. B.1. Flow diagram of the study population
Retrospective cohort study design and study flow diagram.

Appendix C

Table C.1
Distribution of the visual CIS scores between the two readers.

	Visual CIS score	Reader 1					Total
		0	1	2	3	4	
Reader 2	0	49	2	3	0	0	54
	1	5	3	2	0	1	11
	2	2	0	5	0	0	7
	3	0	3	4	0	3	10
	4	0	0	1	0	11	12
	Total	56	8	15	0	15	94

Abbreviations: CIS = cingulate island sign.

Appendix D

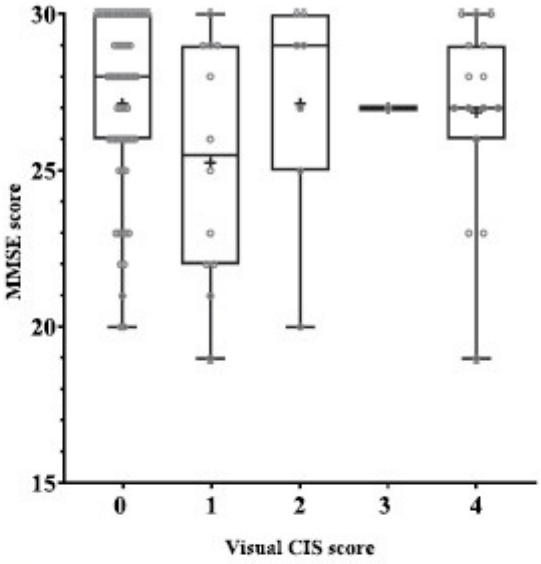

Fig. D.1. Boxplot for visual CIS score and MMSE score.
Abbreviations: CIS = cingulate island sign; MMSE = mini-mental state examination. Boxplot graph with the boxes corresponding to median values with indications of the 25th and 75th percentiles, and the whiskers show the minimum and maximum values. The + indicates the mean. All the subjects are plotted as ○.
Overall comparison of all five groups on the visual CIS score (0, 1, 2, 3, and 4) and MMSE score with the Kruskal-Wallis tests (p = .55).

Table D.1
Correlation analysis between visual CIS score, MMSE score, age, education, and symptom duration for all subjects.

Correlation coefficient (r)	Visual CIS score	MMSE, score	Age, years	Education, years	Symptom duration, years
Visual CIS score	1.0	−0.08	−0.007	−0.11	0.12
MMSE, score	−0.08	1.0	−0.18	0.26*	−0.32*
Age, years	−0.007	−0.18	1.0	−0.06	−0.04
Education, years	−0.11	0.26*	−0.06	1.0	−0.26*

Abbreviations: CIS = cingulate island sign; FDG = false discovery rate; MMSE = Mini-Mental State Examination.
* $p < .05$ (FDR corrected).

Table D.2
Correlation analysis between visual CIS score, MMSE score, age, education, and symptom duration for DLB group.

Correlation coefficient (r)	Visual CIS score	MMSE, score	Age, years	Education, years	Symptom duration, years
Visual CIS score	1.0	0.21	0.02	0.13	−0.10
MMSE, score	0.21	1.0	−0.17	0.12	−0.02
Age, years	0.02	−0.17	1.0	−0.31	0.07
Education, years	0.13	0.12	−0.31	1.0	−0.15

Abbreviations: CIS = cingulate island sign; MMSE = Mini-Mental State Examination.

References

[1] R.L. Albin, S. Minoshima, C.J. D'Amato, K.A. Frey, D.A. Kuhl, A.A.F. Sima, Fluoro-deoxyglucose positron emission tomography in diffuse Lewy body disease, Neurology 47 (1996) 462–466.
[2] F.L. Andersen, C.N. Ladefoged, T. Beyer, S.H. Keller, A.E. Hansen, L. Højgaard, A. Kjær, I. Law, S. Holm, Combined PET/MR imaging in neurology: MR-based attenuation correction implies a strong spatial bias when ignoring bone, NeuroImage 84 (2014) 206–216. Available at https://doi.org/10.1016/j.neuroimage.2013.08.042.
[3] W.W. Barker, et al., Relative frequencies of Alzheimer disease, Lewy body, vascular and frontotemporal dementia, and hippocampal sclerosis in the State of Florida Brain Bank, Alzheimer Dis. Assoc. Disord. 16 (2002) 203–212.
[4] K.H. Brodersen, C.S. Ong, K.E. Stephan, J.M. Buhmann, The balanced accuracy and its posterior distribution. 2010, 20th Int Conf Pattern Recognit, 2010, pp. 3121–3124.
[5] J. Darcourt, J. Booij, K. Tatsch, A. Varrone, T.V. Borght, Ö. Kapucu, K. Någren, F. Nobili, Z. Walker, K. Van Laere, EANM procedure guidelines for brain neurotransmission SPECT using 123 I-labelled dopamine transporter ligands, version 2, Eur. J. Nucl. Med. Mol. Imaging 37 (2010) 443–450.
[6] P. Donaghy, A.J. Thomas, J.T. O'Brien, Amyloid PET imaging in Lewy body disorders, Am J Geriatr Psychiatry 23 (2015) 23–37. Available at https://doi.org/10.1016/j.jagp.2013.03.001.
[7] P. Edison, C.C. Rowe, J.O. Rinne, S. Ng, I. Ahmed, N. Kemppainen, V.L. Villemagne, G. O'Keefe, K. Någren, K.R. Chaudhury, C.L. Masters, D.J. Brooks, Amyloid load in

Parkinson's disease dementia and Lewy body dementia measured with [11C]PIB positron emission tomography, J. Neurol. Neurosurg. Psychiatry 79 (2008) 1331–1338.
[8] B. Fischl, FreeSurfer, NeuroImage 62 (2012) 774–781.
[9] A.S. Fleisher, K. Chen, X. Liu, A. Roontiva, P. Thiyyagura, N. Ayutyanont, A.D. Joshi, C.M. Clark, M.A. Mintun, M.J. Pontecorvo, P.M. Doraiswamy, K.A. Johnson, D.M. Skovronsky, E.M. Reiman, Using positron emission tomography and florbetapir F 18 to image cortical amyloid in patients with mild cognitive impairment or dementia due to Alzheimer disease, Arch. Neurol. 68 (2011) 1404–1411.
[10] H. Fujishiro, E. Iseki, S. Higashi, K. Kasanuki, N. Murayama, T. Togo, O. Katsuse, H. Uchikado, N. Aoki, K. Kosaka, H. Arai, K. Sato, Distribution of cerebral amyloid deposition and its relevance to clinical phenotype in Lewy body dementia, Neurosci Lett 486 (2010) 19–23. Available at https://doi.org/10.1016/j.neulet.2010.09.036.
[11] J. Graff-Radford, M.E. Murray, V.J. Lowe, B.F. Boeve, T.J. Ferman, S.A. Przybelski, T.G. Lesnick, M.L. Senjem, J.L. Gunter, G.E. Smith, D.S. Knopman, C.R. Jack Jr., D.W. Dickson, R.C. Petersen, K. Kantarci, Dementia with Lewy bodies: basis of cingulate island sign, Neurology 83 (2014) 801–809.
[12] D.N. Greve, D.H. Salat, S.L. Bowen, D. Izquierdo-Garcia, A.P. Schultz, C. Catana, J.A. Becker, C. Svarer, G. Knudsen, R.A. Sperling, K.A. Johnson, Different partial volume correction methods lead to different conclusions: an 18 F-FDG-PET study of aging, NeuroImage 15 (2016) 334–343.
[13] M. Hamed, F. Schrami, J. Wilson, J. Galvin, M.N. Sabbagh, Occipital and cingulate hypometabolism are significantly under-reported on 18-Fluorodeoxyglucose positron emission tomography scans of patients with Lewy body dementia, J Alzheimers Dis Park 8 (2018) 1–12.
[14] P. Høgh, A.S. Teller, S. Hasselbalch, G. Waldemar, Visual rating and ROI-based parametric analysis of rCBF SPECT in patients with mild or questionable dementia: a comparative study, Dement. Geriatr. Cogn. Disord. 24 (2007) 429–433.
[15] T. Iizuka, M. Kameyama, Cingulate island sign on FDG-PET is associated with medial temporal lobe atrophy in dementia with Lewy bodies, Ann. Nucl. Med. 30 (2016) 421–429.
[16] D.J. Irwin, S.X. Xie, D. Coughlin, N. Nevler, R.S. Akhtar, C.T. McMillan, E.B. Lee, D.A. Wolk, D. Weintraub, A. Chen-Plotkin, J.E. Duda, M. Spindler, A. Siderowf, H.I. Hurtig, L.M. Shaw, M. Grossman, J.Q. Trojanowski, CSF tau and β-amyloid predict cerebral synucleinopathy in autopsied Lewy body disorders, Neurology 90 (2018) 1038–1046.
[17] K. Ishii, C. Hosokawa, T. Hyodo, K. Sakaguchi, K. Usami, K. Shimamoto, M. Hosono, Y. Yamazoe, T. Murakami, Regional glucose metabolic reduction in dementia with Lewy bodies is independent of amyloid deposition, Ann. Nucl. Med. 29 (2015) 78–83.
[18] K. Ishii, T. Imamura, M. Sasaki, S. Yamaji, S. Sakamoto, H. Kitagaki, M. Hashimoto, N. Hirono, T. Shimomura, E. Mori, Regional cerebral glucose metabolism in dementia with Lewy bodies and Alzheimer's disease, Neurology 51 (1998) 125–130.
[19] K. Kantarci, V.J. Lowe, B.F. Boeve, S.D. Weigand, M.L. Senjem, S.A. Przybelski, D.W. Dickson, J.E. Parisi, D.S. Knopman, G.E. Smith, T.J. Ferman, R.C. Petersen, C.R. Jack Jr., Multimodality imaging characteristics of dementia with Lewy bodies, Neurobiol. Aging 33 (2012) 2091–2105.
[20] K. Kantarci, C. Yang, J.A. Schneider, M.L. Senjem, D.A. Reyes, V.J. Lowe, L.L. Barnes, N.T. Aggarwal, D.A. Bennett, G.E. Smith, R.C. Petersen, C.R. Jack Jr., B.F. Boeve, Ante mortem amyloid imaging and β-amyloid pathology in a case with dementia with Lewy bodies, Neurobiol Aging 33 (2012) 878–885. Available at https://doi.org/10.1016/j.neurobiolaging.2010.08.007.
[21] S.M. Lim, A. Katsifis, V.L. Villemagne, R. Best, G. Jones, M. Saling, J. Bradshaw, J. Merory, M. Woodward, M. Hopwood, C.C. Rowe, The 18F-FDG PET Cingulate Island sign and comparison to 123I-b-CIT SPECT for diagnosis of dementia with Lewy bodies, J. Nucl. Med. 50 (2009) 1638–1645.
[22] J. McCleery, S. Morgan, K.M. Bradley, A.H. Noel-Storr, O. Ansorge, C. Hyde, Dopamine transporter imaging for the diagnosis of dementia with Lewy bodies, Cochrane Database Syst. Rev. (2015) 1.
[23] I. McKeith, J.-P. Taylor, A. Thomas, P. Donaghy, J. Kane, Revisiting DLB diagnosis: a consideration of prodromal DLB and of the diagnostic overlap with Alzheimer disease, J. Geriatr. Psychiatry Neurol. 29 (2016) 249–253. Available at https://doi.org/10.1177/0891988716656083.
[24] I.G. McKeith, et al., Consensus guidelines for the clinical and pathologic diagnosis of dementia with Lewy bodies (DLB): report of the consortium on DLB international workshop, Neurology 47 (1996) 1113–1124.
[25] I.G. McKeith, et al., Diagnosis and management of dementia with Lewy bodies: third report of the DLB consortium, Neurology 65 (2005) 1863–1872.
[26] I.G. McKeith, et al., Diagnosis and management of dementia with Lewy bodies fourth consensus report of the DLB consortium, Neurology 89 (2017) 1–13.
[27] G.M. McKhann, D.S. Knopman, H. Chertkow, B.T. Hyman, C.R. Jack Jr., C.H. Kawas, W.E. Klunk, W.J. Koroshetz, J.J. Manly, R. Mayeux, R.C. Mohs, J.C. Morris, M.N. Rossor, P. Scheltens, M.C. Carrillo, B. Thies, S. Weintraub, C.H. Phelps, The diagnosis of dementia due to Alzheimer's disease: Recommendations from the National Institute on Aging-Alzheimer's Association workgroups on diagnostic guidelines for Alzheimer's disease, Alzheimer's Dement 7 (2011) 263–269. Available at: https://doi.org/10.1016/j.jalz.2011.03.005.
[28] S. Minoshima, A.E. Drzezga, H. Barthel, N. Bohnen, M. Djekidel, D.H. Lewis, C.A. Mathis, J. McConathy, A. Nordberg, O. Sabri, J.P. Seibyl, M.K. Stokes, K. Van Laere, SNMMI procedure standard/EANM practice guideline for amyloid PET imaging of the brain 1.0, J. Nucl. Med. 57 (2016) 1316–1322.
[29] S. Minoshima, N.L. Foster, A.A.F. Sima, K.A. Frey, R.L. Albin, D.E. Kuhl, Alzheimer's disease versus dementia with Lewy bodies: cerebral metabolic distinction with autopsy confirmation, Ann. Neurol. 50 (2001) 358–365.
[30] S. Morbelli, et al., Metabolic patterns across core features in dementia with Lewy bodies, Ann. Neurol. 85 (2019) 715–725.
[31] J.T. O'Brien, M.J. Firbank, C. Davison, N. Barnett, C. Bamford, C. Donaldson, K. Olsen, K. Herholz, D. Williams, J. Lloyd, 18F-FDG PET and perfusion SPECT in the diagnosis of Alzheimer and Lewy body dementias, J. Nucl. Med. 55 (2014) 1959–1965. Available at http://www.ncbi.nlm.nih.gov/pubmed/25453043.
[32] K. Oppedal, et al., A signature pattern of cortical atrophy in dementia with Lewy bodies: a study on 333 patients from the European DLB consortium, Alzheimers Dement. 15 (2019) 400–409.
[33] J.A. Schneider, Z. Arvanitakis, W. Bang, D.A. Bennett, Mixed brain pathologies account for most dementia cases in community-dwelling older persons, Neurology 69 (2007) 2197–2204.
[34] I. van Steenoven, D. Aarsland, D. Weintraub, E. Londos, F. Blanc, W.M. van der Flier, C.E. Teunissen, B. Mollenhauer, T. Fladby, M.G. Kramberger, L. Bonanni, A.W. Lemstra, Cerebrospinal fluid Alzheimer's disease biomarkers across the spectrum of Lewy body diseases: results from a large multicenter cohort, J. Alzheimers Dis. 54 (2016) 287–295.
[35] A. Varrone, S. Asenbaum, T.V. Borght, J. Booij, F. Nobili, K. Någren, J. Darcourt, Ö. Kapucu, K. Tatsch, P. Bartenstein, K. Van Laere, EANM procedure guidelines for PET brain imaging using [18F]FDG, version 2, Eur. J. Nucl. Med. Mol. Imaging 36 (2009) 2103–2110.
[36] M.W. Vernooij, F.B. Pizzini, R. Schmidt, M. Smits, T.A. Yousry, N. Bargallo, G.B. Frisoni, S. Haller, F. Barkhof, Dementia imaging in clinical practice: a European-wide survey of 193 centres and conclusions by the ESNR working group, Neuroradiology 61 (2019) 633–642.
[37] L.-O. Wahlund, E. Westman, D. van Westen, A. Wallin, S. Shams, L. Cavallin, E.-M. Larsson, Imaging biomarkers of dementia: recommended visual rating scales with teaching cases, Insights Imaging 8 (2017) 79–90. Available at https://doi.org/10.1007/s13244-016-0521-6.
[38] J.L. Whitwell, J. Graff-Radford, T.D. Singh, D.A. Drubach, M.L. Senjem, A.J. Spychalla, N. Tosakulwong, V.J. Lowe, K.A. Josephs, 18 F-FDG PET in posterior cortical atrophy and dementia with Lewy bodies, J. Nucl. Med. 58 (2017) 632–638. Available at https://doi.org/10.2967/jnumed.116.179903.
[39] W.J. Youden, Index for rating diagnostic tests, Cancer 3 (1950) 32–35.
[40] M.D. Zwan, J.O. Rinne, S.G. Hasselbalch, A. Nordberg, A. Lleó, S.-K. Herukka, H. Soininen, I. Law, J.M.C. Bahl, S.F. Carter, J. Fortea, R. Blesa, C.E. Teunissen, F.H. Bouwman, B.N.M. Van Berckel, P.J. Visser, Use of amyloid-PET to determine cutpoints for CSF markers, Neurology 86 (2016) 50–58.

Study III

Evaluating 2-[^{18}F]FDG-PET in differential diagnosis of dementia using a data-driven decision model.

Reprinted from NeuroImage: Clinical, 27; Gjerum L, Frederiksen KS, Henriksen OM, Law I, Bruun M, Simonsen AH, Mecocci P, Baroni M, Dottorini ME, Koikkalainen J, Lötjönen J, Hasselbalch SG; Evaluating 2-[^{18}F]FDG-PET in differential diagnosis of dementia using a data-driven decision model; 102267, 2020, with permission from Elsevier.
The publication is available at Elsevier through
https://doi.org/10.1016/j.nicl.2020.102267

NeuroImage: Clinical 27 (2020) 102267

Contents lists available at ScienceDirect

NeuroImage: Clinical

journal homepage: www.elsevier.com/locate/ynicl

Evaluating 2-[^{18}F]FDG-PET in differential diagnosis of dementia using a data-driven decision model

Le Gjerum[a], Kristian Steen Frederiksen[a], Otto Mølby Henriksen[b], Ian Law[b], Marie Bruun[a], Anja Hviid Simonsen[a], Patrizia Mecocci[c], Marta Baroni[c], Massimo Eugenio Dottorini[d], Juha Koikkalainen[e], Jyrki Lötjönen[e], Steen Gregers Hasselbalch[a,*]

[a] Department of Neurology, Danish Dementia Research Centre, Rigshospitalet, University of Copenhagen, Copenhagen, Denmark
[b] Department of Clinical Physiology, Nuclear Medicine & PET, Rigshospitalet, University of Copenhagen, Copenhagen, Denmark
[c] Institute of Gerontology and Geriatrics, University of Perugia, Perugia, Italy
[d] Department of Diagnostic Imaging, Nuclear Medicine Unit, Perugia General Hospital, Perugia, Italy
[e] Combinostics Ltd., Tampere, Finland

ARTICLE INFO

Keywords:
2-[^{18}F]FDG-PET
Computer-assisted diagnosis
Neurodegenerative disease
Clinical decision support system
Differential dementia diagnosis
Alzheimer's disease
Frontotemporal dementia
Vascular dementia
Dementia with Lewy bodies

ABSTRACT

2-[^{18}F]fluoro-2-deoxy-D-glucose positron emission tomography (2-[^{18}F]FDG-PET) has an emerging supportive role in dementia diagnostic as distinctive metabolic patterns are specific for Alzheimer's disease (AD), dementia with Lewy bodies (DLB) and frontotemporal dementia (FTD). Previous studies have demonstrated that a data-driven decision model based on the disease state index (DSI) classifier supports clinicians in the differential diagnosis of dementia by using different combinations of diagnostic tests and biomarkers. Until now, this model has not included 2-[^{18}F]FDG-PET data.

The objective of the study was to evaluate 2-[^{18}F]FDG-PET biomarkers combined with commonly used diagnostic tests in the differential diagnosis of dementia using the DSI classifier.

We included data from 259 subjects diagnosed with AD, DLB, FTD, vascular dementia (VaD), and subjective cognitive decline from two independent study cohorts. We also evaluated three 2-[^{18}F]FDG-PET biomarkers (anterior vs. posterior index (API-PET), occipital vs. temporal index, and cingulate island sign) to improve the classification accuracy for both FTD and DLB.

We found that the addition of 2-[^{18}F]FDG-PET biomarkers to cognitive tests, CSF and MRI biomarkers considerably improved the classification accuracy for all pairwise comparisons of DLB (balanced accuracies: DLB vs. AD from 64% to 77%; DLB vs. FTD from 71% to 92%; and DLB vs. VaD from 71% to 84%). The two 2-[^{18}F]FDG-PET biomarkers, API-PET and occipital vs. temporal index, improved the accuracy for FTD and DLB, especially as compared to AD. Moreover, different combinations of diagnostic tests were valuable to differentiate specific subtypes of dementia.

In conclusion, this study demonstrated that the addition of 2-[^{18}F]FDG-PET to commonly used diagnostic tests provided complementary information that may help clinicians in diagnosing patients, particularly for differentiating between patients with FTD, DLB, and AD.

III

Abbreviations: Aβ42, beta-amyloid 1-42; AD, Alzheimer's disease; API, anterior vs. posterior index; AUC, area under the receiver-operator characteristic curve; bal. acc., balanced accuracy; CERAD, consortium to establish a registry for Alzheimer's disease; CSF, cerebrospinal fluid; DDRC, Danish Dementia Research Centre; DLB, dementia with Lewy bodies; DSI, disease state index; 2-[^{18}F]FDG-PET, 2-[^{18}F]fluoro-2-deoxy-D-glucose positron emission tomography; FLAIR, fluid-attenuated inversion recovery; FTD, frontotemporal dementia; MMSE, mini-mental state examination; MRI, magnetic resonance imaging; p-tau, phosphorylated tau; RAVLT, Rey auditory verbal learning task; ROI, region of interest; SCD, subjective cognitive decline; TBM, tensor-based morphometry; TMT, trail making test; VaD, vascular dementia; VBM, voxel-based morphometry; WMH, white matter hyperintensity

* Corresponding author: Department of Neurology, Danish Dementia Research center, Rigshospitalet, University of Copenhagen, Blegdamsvej 9, DK-2100 Copenhagen, Denmark.
E-mail address: steen.gregers.hasselbalch@regionh.dk (S.G. Hasselbalch).

https://doi.org/10.1016/j.nicl.2020.102267
Received 13 January 2020; Received in revised form 6 April 2020; Accepted 8 April 2020
Available online 24 April 2020

1. Introduction

The most common causes of dementia are Alzheimer's disease (AD), vascular dementia (VaD), dementia with Lewy bodies (DLB), and frontotemporal dementia (FTD) (Livingston et al., 2017; World Health Organization, 2012). Correct clinical dementia diagnosis is essential to establish proper treatment, support and care (National Collaborating center for Mental Health, 2007).

Clinical decision support systems are emerging to assist clinicians for earlier and accurate diagnosis of dementia by providing a systematic and objective overview of comprehensive patient data (Bruun et al., 2019a; Kawamoto et al., 2005; Klöppel et al., 2008; Mattila et al., 2011).

The use of biomarkers, such as total tau, phosphorylated tau (p-tau) and amyloid beta 1–42 (Aβ42) from cerebrospinal fluid (CSF) and magnetic resonance imaging (MRI), have improved the differential diagnosis of dementia and have been included in the clinical diagnostic criteria (Gorno-Tempini et al., 2011; McKeith et al., 2017; McKhann et al., 2011; Rascovsky et al., 2011; Sachdev et al., 2014). Nevertheless, DLB and FTD remain particularly difficult to identify due to shared clinical and pathological features with other subtypes of dementia, especially AD (McKeith et al., 2016; Mendez et al., 2013; Ossenkoppele et al., 2015; Schneider et al., 2007; Thomas et al., 2018). Most of the previous biomarker studies have focused on the ability to differentiate AD from other dementias, and moreover, biomarkers for other subtypes of dementia are less evolved (Jack et al., 2016).

2-[^{18}F]fluoro-2-deoxy-D-glucose positron emission tomography (2-[^{18}F]FDG-PET) imaging is considered a sensitive imaging modality for neuronal degeneration in dementia and has shown potential to support the diagnosis of dementia at an early stage (Bloudek et al., 2011; Hort et al., 2010). Various subtypes of dementia have characteristic patterns of regional hypometabolism (Nobili et al., 2018), and 2-[^{18}F]FDG-PET is included as a supportive biomarker in the diagnostic criteria of AD, DLB, and FTD (Gorno-Tempini et al., 2011; McKeith et al., 2017; McKhann, 2001; McKhann et al., 2011; Rascovsky et al., 2011).

Data-driven diagnostic tools are useful for analysing heterogenous multimodality data of complex diseases such as dementia. Previous studies have demonstrated that a data-driven decision model based on the disease state index (DSI) classifier (Mattila et al., 2012) is a promising method for clinical decision support in the differential diagnosis of dementia by using different combinations of cognitive tests, CSF biomarkers, and automatic and visual MRI quantification features (Bruun et al., 2018; Koikkalainen et al., 2016; Tong et al., 2017). Until now, this model has not included 2-[^{18}F]FDG-PET data.

The objective of the study was to evaluate 2-[^{18}F]FDG-PET biomarkers combined with commonly used diagnostic tests (cognitive tests, CSF and MRI biomarkers) in the differential diagnosis of dementia using the DSI classifier.

2. Methods

2.1. Study population

We included data from 259 subjects diagnosed from 2009 to 2018 with either AD, DLB, FTD, VaD, or subjective cognitive decline (SCD) from two independent study cohorts (a subgroup from the PredictND study cohort and a Danish Dementia Research center (DDRC) cohort). The subjects were eligible for inclusion if a 3D T1-weighted MRI sequence with a slice thickness < 2 mm and 2-[^{18}F]FDG-PET images were available.

The PredictND study cohort consisted of 779 prospectively enrolled subjects from four European memory clinics (Bruun et al., 2019b). We included a subgroup from the PredictND study cohort consisting of 119 subjects from the Copenhagen Memory Clinic, Copenhagen University Hospital, Rigshospitalet, Copenhagen, Denmark and 25 subjects from the Section of Gerontology and Geriatrics, University of Perugia and "S. Maria della Misericordia" Hospital of Perugia, Perugia, Italy.

The DDRC cohort consisted of 115 retrospectively identified subjects from the clinical database at the Copenhagen Memory Clinic, Copenhagen University Hospital, Rigshospitalet, Copenhagen, Denmark.

All diagnoses were confirmed by experienced dementia specialists according to the following established diagnostic criteria: the NIA-AA criteria for AD (McKhann et al., 2011), the DLB consortium criteria for DLB (McKeith et al., 2005), the work group on FTD and Pick's Disease criteria for FTD (Gorno-Tempini et al., 2011; McKhann, 2001; Rascovsky et al., 2011), and the NINDS-AIREN criteria for VaD (Román et al., 1993). Subjects were diagnosed with SCD when the cognitive complaint was present without confirmed objective cognitive impairment, and the criteria for mild cognitive impairment and dementia were not met (Albert et al., 2011; McKhann et al., 2011).

The study was approved by the local Medical Ethical Committees: The Regional Committee on Medical Research Ethics of the Capital Region of Denmark (Approval no.: H-1–2014–126) and Italy (Approval no.: CEAS 2381/14).

2.2. Clinical assessment and auxiliary investigations

All subjects were referred to the memory clinics due to suspicion of a neurodegenerative disease. At baseline, all subjects were assessed with a standard diagnostic dementia program including medical history, physical and neurological examinations, cognitive testing, routine blood screening, and MRI. On a clinical diagnostic indication, the standard diagnostic dementia program was supplemented with diagnostic tests such as CSF biomarkers, 2-[^{18}F]FDG-PET, dopamine transporter single photon emission computed tomography, and amyloid PET.

As a minimum all included subjects had an MRI with 3D T1-weighted sequence, an 2-[^{18}F]FDG-PET scan, and a mini-mental state examination (MMSE) test. Sixty-seven percent had additional cognitive test data other than MMSE, 51% percent had CSF biomarkers of Aβ42, total tau, and p-tau, and 98% had an MRI with fluid-attenuated inversion recovery (FLAIR) sequence (distribution of the diagnostic test for each diagnostic group are listed in Table A.1 in Supplementary material).

2.3. Cognitive tests

The standard cognitive test battery consisted of the MMSE test for assessment of global cognitive functioning, the consortium to establish a registry for Alzheimer's disease (CERAD) test or the Rey auditory verbal learning task (RAVLT) test for assessment of episodic memory, and the trail making test (TMT) A and B, and the animal fluency test for assessment of language and executive functioning.

To compare the episodic memory test scores, we standardized the CERAD test to the RAVLT test using z-scoring as previously described (Bruun et al., 2018).

2.4. Cerebrospinal fluid biomarkers

The CSF biomarkers, Aβ42, total tau, and p-tau, were analysed with enzyme-linked immunosorbent assay (ELISA) using commercially available kits (Innotest, Fujirebio, Europe, Ghent, Belgium).

2.5. Magnetic resonance imaging

MRI were performed on clinical 1.0, 1.5, or 3.0 Tesla scanners. We derived the volumetric and morphometric biomarkers from the 3D T1-weighted MRI sequence (Koikkalainen et al., 2016; Lötjönen et al., 2010). The volumes of 133 brain regions were defined using a multi-atlas segmentation method (Lötjönen et al., 2010) based on the manually segmented Neuromorphometric atlases (Neuromorphometrics Inc, Massachusetts, USA) (Region of interests for MRI are listed

in Table B.1 in Supplementary material).

Ten MRI biomarkers of clinically relevant regions were extracted from the volumetric features, together with the anterior vs. posterior index (API-MRI), defined as a z-scored ratio between the volumes of temporal and frontal lobe regions, and the volumes of parietal and occipital lobe regions (Bruun et al., 2019c).

Furthermore, we derived two morphometric indices by comparing specific volumetric patterns between two study groups (Koikkalainen et al., 2016). The voxel-based morphometry (VBM) index was estimated using measures of the local concentration of gray matter (Ashburner and Friston, 2000), whereas the tensor-based morphometry (TBM) index was estimated using measures of changes in the local volume (Ashburner et al., 1998).

The region of interest (ROI) based grading was estimated by measuring the similarities of intensities of the T1-weighted image within the ROIs to an image database of subjects with known diagnoses (Tong et al., 2013)

The vascular burden from FLAIR images was estimated from the summed volume of white matter hyperintensity (WMH), cortical infarcts, and the weighted volume of lacunar infarcts by a segmentation method described in (Koikkalainen et al., 2016; Wang et al., 2012).

2.6. 2-[^{18}F]fluoro-2-deoxy-D-glucose positron emission tomography

The 2-[^{18}F]FDG-PET images were acquired using GE Medical, Philips, and Siemens PET scanners. The 2-[^{18}F]FDG-PET image was co-registered to the segmented MRI to generate uptake values from the segmented brain regions on 2-[^{18}F]FDG-PET, i.e. 2-[^{18}F]FDG-PET ROIs. The mean uptake value of each 2-[^{18}F]FDG-PET ROI was normalized to the cerebellum.

We selected 12 clinically relevant regions (anterior cingulate gyrus, calcarine cortex, middle cingulate gyrus, posterior cingulate gyrus, precuneus, precentral gyrus, frontal cortex, temporal cortex, parietal cortex, occipital cortex, medial temporal cortex, and whole cortex) as 2-[^{18}F]FDG-PET biomarkers based on previous 2-[^{18}F]FDG-PET studies demonstrating characteristic patterns of hypometabolism which have been well documented in patients with AD, FTD, and DLB, respectively (Davison and O'Brien, 2014; Dukart et al., 2011; Gorno-Tempini et al., 2011; Herholz et al., 2002; Jagust et al., 2009; McKeith et al., 2017; McKhann, 2001; McKhann et al., 2011; Minoshima et al., 2001; Rascovsky et al., 2011; Rice and Bisdas, 2017).

Moreover, three 2-[^{18}F]FDG-PET biomarkers were derived from the segmented 2-[^{18}F]FDG-PET image. The API-PET was defined as a z-scored ratio between the mean uptake in frontal and temporal lobe regions, and the mean uptake in parietal and occipital lobe regions, and is similar to and uses the same regions as the API-MRI (Bruun et al., 2019c). The occipital vs. temporal index was derived as the uptake in occipital lobe region divided by the uptake in temporal lobe region. The biomarker was proposed to improve differentiating between AD and DLB, where the temporal region is often affected in AD and the occipital region is often affected in DLB, respectively (McKeith et al., 2017; McKhann et al., 2011). Cingulate island sign is a supportive DLB biomarker on 2-[^{18}F]FDG-PET (Lim et al., 2009; McKeith et al., 2017). In our analyses, we included the cingulate island sign ratio defined as the uptake in posterior cingulate cortex divided by the sum of the uptake in precuneus and cuneus.

2.7. Disease state index classifier

The DSI classifier is composed of two components: fitness and relevance (Mattila et al., 2012). Fitness is calculated for a biomarker or test result of the subject as $f(x) = FN(x)/(FN(x)+FP(x)$, where FN is the false-negative error rate, and FP is the false-positive error rate in the reference data when using the biomarker or test result value x as a cut-off value in classification. Relevance defines the goodness of a biomarker or test result as sensitivity + specificity-1. A DSI value is calculated as a weighted average of fitness values: DSI = Σ (relevance · fitness)/Σ relevance. DSI is a value measuring the similarity of the subject's data to two diagnostic groups, a reference and study groups. The DSI value zero indicates a perfect similarity to the reference group while the value one a perfect similarity to the study group.

2.8. Data analysis

Differences between groups were tested with one-way ANOVA tests followed by post-hoc Bonferroni tests, Kruskal-Wallis tests followed by post-hoc Bonferroni corrected Mann-Whitney tests, or Chi-square tests followed by post-hoc Bonferroni tests, where appropriate.

The 10-fold cross-validation approach was applied using the whole study population data (n = 259). The differentiation between the diagnostic groups was evaluated through pairwise comparisons. The accuracy of each individual diagnostic test and each or combined diagnostic test group for pairwise comparisons was reported as balanced accuracy (bal. acc.) and area under the receiver-operator characteristic curve (AUC) based on the DSI values. The bal. acc., calculated as the average of sensitivity and specificity for pairwise comparison, was computed to adjust the results for the imbalance in the size of the study groups in the dataset (Brodersen et al., 2010).

When an individual or combined group of diagnostic tests was used, we only included a subset of relevant diagnostic tests and excluded the redundant or irrelevant diagnostic tests, for each pairwise comparison by a feature selection method. The diagnostic tests with the highest accuracy were added one by one until the overall AUC did not increase as previously described (Bruun et al., 2018). The feature selection was first performed using complete cross-validation to produce un-biased classification results. After that, the feature selection was applied to all data without cross-validation to produce single optimal feature set to show which features typically were selected.

Data from all subjects in the study population were used in the analysis because the DSI classifier can operate with missing data (Rhodius-Meester et al., 2016).

The volumetric imaging biomarkers were corrected for intracranial volume, age, and sex (Buckner et al., 2004; Cole and Green, 1992), while the other features were corrected for age and sex (Cole and Green, 1992).

Statistical analysis was performed using SAS Studio software, version 9.4 (SAS Institute Inc., Cary, NC, USA). A MATLAB toolbox was used in the DSI analyses (Cluitmans et al., 2013). The analyses were performed in MATLAB, version R2015b (MathWorks, Natick, MA).

A two-sided p-value < 0.05 was considered indicative of statistical significance.

3. Results

3.1. Subjects

The baseline demographics are presented in Table 1. There were fewer women in the DLB group as compared to the AD group. The subjects with SCD were younger and performed better on MMSE than the dementia groups. The AD group had higher tau values, and together with the DLB group lower Aβ42 values than the other groups (Additional details of baseline demographics are shown in Table C.1 in Supplementary material).

3.2. Diagnostic tests and diagnostic test groups

The performance of the individual diagnostic tests for each pairwise comparison is shown in Table 2. Overall, the episodic memory tests had a high classification accuracy for differentiating subjects with SCD from the dementia groups (bal. acc. ranging from 71%-91%), whereas CSF biomarkers had a good accuracy for differentiating AD from the other groups (bal. acc. ranging from 73%-84%), except Aβ42 for AD vs. DLB

Table 1
Baseline demographics.

	AD	DLB	FTD	VaD	SCD	Group-wise comparison when significant
Subjects, n	90	41	37	25	66	
Female, n (%)	50 (56%)	10 (24%)	17 (46%)	10 (40%)	34 (52%)	DLB < AD
Age, mean years ± SD	73.2 ± 7.9	72.5 ± 8.6	68.7 ± 9.5	74.8 ± 8.7	64.5 ± 9.8	SCD < AD, DLB, VaD
MMSE, median score (IQR)	25 (23–27)	27 (23–29)	25 (21–28)	26 (24–28)	30 (29–30)	SCD > All
CSF Aβ42, median concentration pg/mL (IQR)	507 (425–596)	531 (413–685)	896 (670–1006)	927 (762–1121)	1021 (797–1170)	AD, DLB < FTD, VaD, SCD
CSF total tau, median concentration pg/mL (IQR)	556 (427–728)	346 (170–407)	254 (190–333)	248 (188–395)	237 (186–352)	AD > All
CSF p-tau, median concentration pg/mL (IQR)	83 (62–97)	54 (29–73)	36 (30–42)	38 (29–46)	40 (36–50)	AD > All

Abbreviations: Aβ42: amyloid beta 1–42; AD: Alzheimer's disease; CSF: cerebrospinal fluid; DLB: dementia with Lewy bodies; FTD: frontotemporal dementia; IQR: interquartile range; MMSE: mini mental state examination; n: number; p-tau: phosphorylated tau at threonine 181; SCD: subjective cognitive decline; SD: standard deviation; VaD: vascular dementia.

with a bal. acc. of 50%. As expected, the MRI biomarkers of vascular burden were the most valuable diagnostic tests to differentiate VaD from the other groups (bal. acc. ranging from 80%-89%). The 2-[^{18}F]FDG-PET biomarker occipital vs. temporal index had a high accuracy for distinguishing AD vs. DLB compared to the two supportive biomarkers for DLB, occipital hypometabolism and cingulate island sign (bal. acc.: occipital vs. temporal index: 79% vs. occipital hypometabolism: 62% vs. cingulate island sign: 67%). For AD vs. FTD, the CSF biomarkers and API-PET had a high accuracy, whereas API-MRI had a lower accuracy (bal. acc.: CSF biomarkers: 79-83% vs. API-PET: 76% vs. API-MRI: 64%). The performance of additional diagnostic tests for each pairwise comparison is shown in Table D.1 in Supplementary material.

The accuracies of the individual and combined groups of diagnostic tests for pairwise comparison are presented in Table 3. The addition of 2-[^{18}F]FDG-PET biomarkers to cognitive tests, CSF and MRI biomarkers considerably improved the classification accuracy for all pairwise comparisons of DLB to other dementias (bal. acc.: DLB vs. AD from 64% to 77%; DLB vs. FTD from 71% to 92%; and DLB vs. VaD from 71% to 84%). Furthermore, 2-[^{18}F]FDG-PET biomarkers combined with CSF and MRI biomarkers had a high performance for distinguishing FTD from the other dementia groups (bal. acc. ranging from 83%−92%), whereas combined 2-[^{18}F]FDG-PET and MRI biomarkers were useful to distinguish VaD from the other dementia groups (bal. acc. ranging from 80%−90%).

3.3. Optimal combination of diagnostic tests

The optimal combination of diagnostic tests for each pairwise comparison is presented in Table 4. The optimal sets of diagnostic tests included diagnostic tests from more groups, most commonly MRI and 2-[^{18}F]FDG-PET biomarkers, except for the AD vs. FTD comparison with only CSF biomarkers. In general, CSF biomarkers combined with imaging biomarkers obtained the highest accuracy for differentiating AD from the other groups. The API-PET was included in the optimal combination of diagnostic tests for FTD, whereas the MRI biomarker of vascular burden was included in the optimal combination of diagnostic tests for VaD. The optimal diagnostic tests to differentiate DLB from the other groups included 2-[^{18}F]FDG-PET biomarkers with different combinations of cognitive tests, CSF and MRI biomarkers.

4. Discussion

This study evaluates the performance of 2-[^{18}F]FDG-PET biomarkers combined with commonly used diagnostic tests (cognitive tests, CSF and MRI biomarkers) in the differential diagnosis of dementia using a DSI classifier in two mixed memory clinic cohorts.

First, we found that the 2-[^{18}F]FDG-PET biomarkers, particularly API-PET and occipital vs. temporal index, improved the classification accuracy for both FTD and DLB, especially as compared to AD. Second, different combinations of diagnostic tests were valuable for distinguishing specific subtypes of dementia. And third, the CSF biomarkers were useful to differentiate AD from the other groups, the MRI biomarker of vascular burden was useful to differentiate VaD from the other groups, and cognitive tests were highly useful to differentiate subjects with SCD from the dementia groups. The latter finding is in line with previous studies using the DSI classifier (Bruun et al., 2018; Rhodius-Meester et al., 2016; Tolonen et al., 2018).

Previous studies have demonstrated the usefulness of the DSI classifier in the differential diagnosis of dementia using automatic MRI quantification features (Koikkalainen et al., 2016) and various combinations of cognitive tests, CSF biomarkers, and automatic and visual MRI quantification features (Bruun et al., 2018; Tolonen et al., 2018; Tong et al., 2017). Comparison of the classification results obtained in this study to two other DSI classifier studies using exclusively cognitive tests, CSF biomarkers, and automatic MRI quantifications, showed that our classifier had a considerable lower accuracy (bal. acc. ranged from 64%−94% (Table 3) vs. 77%−97% in (Bruun et al., 2018) vs. 80%−98% in (Tolonen et al., 2018)), with the lowest accuracies for detecting DLB and FTD. However, our study population may have included patients with a more uncharacteristic presentation due to selection bias, where 2-[^{18}F]FDG-PET likely was used as a supplemental diagnostic test for patients with an uncertain diagnosis after disclosure of standard diagnostic tests such as MRI and cognitive tests. Furthermore, the two previous studies had a larger study cohort with a greater proportion of AD patients and subjects with SCD and moreover, the studies did not include 2-[^{18}F]FDG-PET.

Previous DSI classifier studies without 2-[^{18}F]FDG-PET biomarkers reported the diagnostic sensitivity for FTD and in particular DLB as suboptimal with many cases being misclassified as AD (Bruun et al., 2018; Koikkalainen et al., 2016; Tolonen et al., 2018; Tong et al., 2017). This issue is to some extent due to the paucity of specific disease biomarkers for FTD and DLB, but also a result of the clinical heterogeneity in both FTD and DLB together with the clinical and pathological overlap with AD (McKeith et al., 2017; Neary et al., 1998). In particular, many DLB patients have coexisting Aβ pathology (Merdes et al., 2003). This is corroborated by the low accuracy of 50% for the CSF Aβ42 biomarker in differentiating DLB and AD in our study (Table 2). In addition, FTD represents various clinical syndromes including primary progressive aphasia and behavioural variant of FTD, of which the latter often seemed difficult to differentiate from AD (Mendez et al., 2013; Neary et al., 1998).

We added 2-[^{18}F]FDG-PET biomarkers to the DSI classifier to improve the classification accuracy, particularly for DLB and FTD as compared to AD, as 2-[^{18}F]FDG-PET is a supportive biomarker for AD, DLB, and FTD (Gorno-Tempini et al., 2011; McKeith et al., 2017; McKhann, 2001; McKhann et al., 2011; Rascovsky et al., 2011). We found that the addition of 2-[^{18}F]FDG-PET biomarkers to cognitive tests, CSF and MRI biomarkers improved the accuracies of DLB and FTD with most substantial improvement for the pairwise comparison of AD vs. DLB (from 64% to 77%, Table 3).

Table 2
The pairwise comparison of individual diagnostic tests.

Bal. acc./AUC	AD vs. DLB	AD vs. FTD	AD vs. VaD	AD vs. SCD	DLB vs. FTD	DLB vs. VaD	DLB vs. SCD	FTD vs. VaD	FTD vs. SCD	VaD vs. SCD
Cognitive tests										
MMSE	59/58	39/36	55/54	85/89	56/59	56/54	71/79	52/53	79/88	83/89
Episodic memory (learning)	48/59	62/62	50/46	91/97	43/39	61/63	88/93	71/60	90/90	87/94
Episodic memory (recall)	64/68	66/67	59/58	89/96	51/51	56/49	85/92	64/54	84/89	81/90
CSF										
Aβ42	50/50	79/82	78/86	83/89	79/77	75/81	81/84	57/57	60/63	57/55
Total tau	77/80	83/84	80/83	84/88	58/56	61/55	61/58	29/27	33/35	35/33
p-tau	73/76	83/90	82/88	78/88	63/66	69/63	64/57	11/4	51/62	20/21
MRI										
Frontal cortex	59/62	55/58	57/59	71/74	63/69	68/69	59/64	41/34	70/78	72/77
Temporal cortex	57/64	46/43	66/71	84/90	56/61	52/56	75/82	54/64	75/85	74/76
Medial temporal cortex	58/61	51/51	60/66	80/91	45/51	38/38	80/85	54/56	75/84	75/83
Parietal cortex	48/48	56/63	54/58	68/74	59/67	50/48	68/74	68/72	62/65	76/81
Occipital cortex	59/65	52/45	60/61	61/63	59/64	46/51	68/75	49/49	51/55	60/65
API-MRI	62/63	64/70	56/58	61/64	76/79	41/35	44/43	72/78	74/82	34/32
Vascular burden	45/46	51/50	82/89	63/69	59/59	80/85	64/70	83/89	67/69	89/93
2-[^{18}F]FDG-PET										
Frontal cortex	47/43	58/59	42/40	74/79	58/63	44/41	72/78	55/56	76/85	72/77
Temporal cortex	56/57	55/58	61/67	80/86	45/42	56/60	80/86	56/58	76/80	67/73
Medial temporal cortex	62/62	63/69	57/59	75/83	76/80	66/71	82/89	55/57	68/71	70/72
Parietal cortex	72/74	65/67	38/36	66/70	78/86	73/80	80/89	65/60	39/36	63/64
Occipital cortex	62/68	58/58	59/67	70/78	71/76	44/37	63/62	68/74	74/81	62/62
API-PET	75/81	76/86	59/62	47/43	92/97	83/90	82/87	74/80	79/88	60/61
Occipital vs. Temporal index	79/85	54/60	63/65	70/75	83/90	70/76	63/71	64/74	73/83	62/60
Cingulate island sign ratio	67/79	54/51	62/63	71/77	71/77	64/70	57/59	55/61	75/77	67/68

Abbreviations: Aβ42: amyloid beta 1-42; AD: Alzheimer's disease; API: Anterior vs. posterior index; AUC: area under the receiver operating characteristic curve; bal. acc.: balanced accuracy; CSF: cerebrospinal fluid; DLB: dementia with Lewy bodies; FTD: frontotemporal dementia; MMSE: mini mental state examination; MRI: magnetic resonance imaging; p-tau: phosphorylated tau at threonine 181; ROC: receiver operating characteristic; SCD: subjective cognitive decline; VaD: vascular dementia; 2-[^{18}F]FDG-PET: 2-[^{18}F]fluoro-2-deoxy-D-glucose positron emission tomography;
The colours correspond to the bal. acc. for the pairwise comparison. Bal. acc. 85%–100% are highlighted in dark green. The gradually lighter shades of green indicate lower bal. acc. with white being at or below 50. Both bal. acc. and AUC are reported as percentage values (%).

Furthermore, we evaluated three 2-[^{18}F]FDG-PET biomarkers in the differential diagnosis of dementia with focus on their ability to differentiate DLB and FTD as compared to AD.

The API-PET was included to demonstrate a specific pattern of reduced metabolism in frontotemporal regions and relative preserved metabolism in posterior region as seen in many FTD patients (Bohnen et al., 2012; Neary et al., 1998; Rascovsky et al., 2011). The API-PET is similar to and uses the same regions as API-MRI, which has demonstrated a good classification accuracy for differentiating between FTD and AD (Bruun et al., 2019c, 2018). When comparing the API-PET and the API-MRI for differentiating FTD from the other groups, the API-PET had higher bal. acc. ranging from 74% to 92% in comparison to the API-

Table 3
The pairwise comparison of individual and combined groups of diagnostic tests.

Bal. acc./AUC	AD vs. DLB	AD vs. FTD	AD vs. VaD	AD vs. SCD	DLB vs. FTD	DLB vs. VaD	DLB vs. SCD	FTD vs. VaD	FTD vs. SCD	VaD vs. SCD
Cognitive tests	56/60	62/58	47/51	94/97	57/60	53/62	84/88	58/59	83/89	82/87
CSF	76/78	90/94	85/84	85/93	79/80	68/75	81/82	28/32	55/51	47/49
MRI	62/69	74/78	80/86	83/90	65/73	76/83	78/83	73/86	85/91	84/89
2-[^{18}F]FDG-PET	76/84	76/87	63/72	82/87	92/97	83/90	80/90	72/75	77/90	75/80
Cognitive tests + CSF	70/73	90/94	85/84	94/97	74/75	66/71	84/88	58/59	83/89	82/87
Cognitive tests + MRI	50/54	68/79	80/85	94/97	74/76	73/79	85/89	73/85	84/91	92/92
Cognitive tests + 2-[^{18}F]FDG-PET	78/84	77/87	64/68	94/97	92/97	87/89	86/88	63/71	80/88	82/87
CSF + MRI	70/73	90/94	84/82	87/93	75/81	75/80	83/89	73/85	85/91	86/88
CSF + 2-[^{18}F]FDG-PET	80/88	90/94	85/84	85/93	92/97	83/88	84/89	70/74	77/90	75/80
MRI + 2-[^{18}F]FDG-PET	77/85	78/86	80/88	85/93	92/97	82/90	85/91	83/86	86/93	90/90
Cognitive tests + CSF + MRI	64/64	90/94	84/82	94/97	71/75	71/77	85/89	73/84	84/91	92/92
Cognitive tests + CSF + 2-[^{18}F]FDG-PET	76/85	90/94	85/84	94/97	92/97	87/91	86/88	64/71	80/88	82/87
Cognitive tests + MRI + 2-[^{18}F]FDG-PET	80/83	80/86	80/86	94/97	92/97	82/90	86/89	83/85	80/90	92/92
CSF + MRI + 2-[^{18}F]FDG-PET	75/85	90/94	81/81	92/94	92/97	82/90	85/91	83/86	86/93	89/88
Cognitive tests + CSF + MRI + 2-[^{18}F]FDG-PET	77/87	90/94	81/81	94/97	92/97	84/90	86/89	83/85	80/90	92/92

Abbreviations: AD: Alzheimer's disease; AUC: area under the receiver operating characteristic curve; bal. acc.: balanced accuracy; CSF: cerebrospinal fluid; DLB: dementia with Lewy bodies; FTD: frontotemporal dementia; MRI: magnetic resonance imaging; ROC: receiver operating characteristic; SCD: subjective cognitive decline; VaD: vascular dementia; 2-[^{18}F]FDG-PET: 2-[^{18}F]fluoro-2-deoxy-D glucose positron emission tomography;
The colours correspond to the bal. acc. for the pairwise comparison. Bal. acc. 85%–100% are highlighted in dark green. The gradually lighter shades of green indicate lower bal. acc. with white being at or below 50. Both bal. acc. and AUC are reported as percentage values (%).

Table 4
The optimal sets of diagnostic tests for each pairwise comparison.

Pairwise comparison	Cognitive tests	CSF	MRI	2-[^{18}F]FDG-PET
AD vs. DLB		p-tau	Lateral ventricles	Occipital vs. temporal index
AD vs. FTD		Aβ42, p-tau		
AD vs. VaD		Aβ42	Medial temporal cortex, frontal cortex, temporal cortex, parietal cortex, vascular burden	Parietal cortex
AD vs. SCD	Episodic memory (learning), episodic memory (recall)	p-tau		
DLB vs. FTD	Animal fluency			API-PET
DLB vs. VaD	Animal fluency	Aβ42	Frontal cortex	API-PET, middle cingulate gyrus
DLB vs. SCD	Episodic memory (learning), TMT-B		Temporal cortex	Occipital cortex
FTD vs. VaD			Parietal cortex, vascular burden	API-PET, middle cingulate gyrus
FTD vs. SCD	MMSE		Global VBM	API-PET
VaD vs. SCD	Episodic memory (learning)		Vascular burden	

Abbreviations: Aβ42: amyloid beta 1–42; AD: Alzheimer's disease; API: anterior vs. posterior index; CSF: cerebrospinal fluid; DLB: dementia with Lewy bodies; FTD: frontotemporal dementia; MMSE: mini mental state examination; MRI: magnetic resonance imaging; p-tau: phosphorylated tau at threonine 181; SCD: subjective cognitive decline; TMT: trail making test; VaD: vascular dementia; VBM: voxel-based morphometry; 2-[^{18}F]FDG-PET: 2-[^{18}F]fluoro-2-deoxy-D glucose positron emission tomography.

MRI with bal. acc. ranging from 64% to 76% (Table 2), suggesting that in the present study 2-[^{18}F]FDG-PET outperformed MRI with regards to specific FTD patterns. Additionally, the API-PET was included in the optimal sets of diagnostic tests for differentiating FTD from DLB, VaD, and SCD, respectively (Table 4). However, the performance of the API-MRI for differentiating FTD from the other groups was lower in our study than in a previous study (Bruun et al., 2019c). Differences in patient populations with more atypical atrophy patterns (Bruun et al., 2019c; Ranasinghe et al., 2016) in our sample could potentially explain the lower performance of API-MRI, if these patterns do not affect 2-[^{18}F]FDG-PET to the same degree.

Occipital hypometabolism on 2-[^{18}F]FDG-PET is considered a supportive biomarker for DLB, particularly for differentiating DLB from AD (McKeith et al., 2017). Notably, we found a moderate accuracy for occipital cortex on 2-[^{18}F]FDG-PET for pairwise comparison of DLB vs. AD (AUC 68%). This finding was somewhat unexpected as previous 2-[^{18}F]FDG-PET studies have found accuracies between 70% − 92% for occipital hypometabolism in differentiating DLB from AD using various quantitative methods (Caminiti et al., 2019; Ishii et al., 2007; Lim et al., 2009). The variability in accuracy may be explained by differences in operating procedures (Frisoni et al., 2013). The fully automated analysis had lower accuracies ranging from 68% to 78% (Kono et al., 2007; Lim et al., 2009) with the lowest accuracy in this study compared to computer-aided visual read by experienced neuroimaging physicians with accuracy of 92% (Caminiti et al., 2019). Moreover, the differences in the study cohorts may also have an impact on the accuracy, and as previously mentioned our study cohort include patients with a more uncharacterised presentation. We intended to optimize the DLB feature by proposing the occipital vs. temporal index, especially to improve differentiating of DLB from AD. This 2-[^{18}F]FDG-PET biomarker was the diagnostic test with the highest accuracy for differentiating between DLB and AD (bal. acc. of 79%, Table 2) and was included in the optimal sets for pairwise comparison of AD vs. DLB, suggesting that 2-[^{18}F]FDG-PET disease specific biomarkers have an impact on the accuracy for differentiating AD and DLB.

Likewise, we included the cingulate island sign ratio, which has been suggested to support the diagnosis of DLB (Kantarci et al., 2012; Lim et al., 2009; McKeith et al., 2017). The cingulate island sign ratio differentiated DLB from AD with a moderate AUC (79%) in comparison to a previous study with an AUC of 92% (Kantarci et al., 2012). The lower accuracy in our study may reflect a more heterogenous study population with more dual pathology in our study, as the presence of cingulate island sign has been reported to be associated with less concurrent AD pathology (McKeith et al., 2017).

The strength of our study is that the model was developed and validated using commonly used diagnostic tests and 2-[^{18}F]FDG-PET biomarkers in a relatively large cohort with diagnoses confirmed by experienced dementia specialists.

One of the limitations of this study is the possibility of circularity considering that the clinical reference diagnosis was supported and reinforced by all available diagnostic tests, consistent with established diagnostic criteria (Gorno-Tempini et al., 2011; McKeith et al., 2005; McKhann, 2001; McKhann et al., 2011; Rascovsky et al., 2011; Román et al., 1993). Moreover, we used both cohorts for cross validation due to the limited availability of FTD and DLB cases. However, the derived automatic neuroimaging biomarkers were not used for clinical diagnosis. Furthermore, the objective of the study was to investigate the clinical impact of commonly used diagnostic tests and 2-[^{18}F]FDG-PET biomarkers in the differential diagnosis of dementia and obtain information about their relative performance, and not to get precise accuracy estimates.

Another limitation for this study and other similar studies is the absence of pathological validation diagnosis.

In conclusion, this study demonstrated that the addition of 2-[^{18}F]FDG-PET biomarkers to commonly used diagnostic tests using the DSI classifier increased the classification accuracy for FTD and DLB, especially as compared to AD. Moreover, specific combinations of diagnostic tests were valuable to differentiate each subtypes of dementia.

This study provides support for the addition of 2-[^{18}F]FDG-PET in diagnosing dementia. The additional information from the 2-[^{18}F]FDG-PET may support clinicians in the differential diagnosis of dementia. Future research studies should evaluate the clinical diagnostic value and the cost-effectiveness of the diagnostic tests using the DSI classifier in a prospective multi-center study to optimize the use of diagnostic tests in clinical practice.

Acknowledgment

Data collection and sharing for this project was funded under the 7th Framework Programme by the European Commission (Grant agreement ID: 611005). This study was supported by the Absalon Foundation of 1st May 1978 and the Hede Nielsen Family Foundation.

Declaration of competing interest

Juha Koikkalainen and Jyrki Lötjönen are shareholders in Combinostics Oy. The other authors declare no competing interests.

CRediT authorship contribution statement

Le Gjerum: Conceptualization, Formal analysis, Data curation, Writing - original draft. **Kristian Steen Frederiksen:** Conceptualization, Writing - review & editing. **Otto Mølby Henriksen:** Writing - review & editing. **Ian Law:** Writing - review & editing. **Marie Bruun:** Data curation, Writing - review & editing. **Anja Hviid Simonsen:** Data curation, Writing - review & editing. **Patrizia Mecocci:** Data curation, Writing - review & editing. **Marta Baroni:** Data curation, Writing - review & editing. **Massimo Eugenio Dottorini:** Data curation, Writing - review & editing. **Juha Koikkalainen:** Conceptualization, Data curation, Writing - review & editing. **Jyrki Lötjönen:** Conceptualization, Data curation, Writing - review & editing. **Steen Gregers Hasselbalch:** Conceptualization, Data curation, Writing - review & editing, Supervision.

Supplementary materials

Supplementary material associated with this article can be found, in the online version, at doi:10.1016/j.nicl.2020.102267.

References

Albert, M.S., DeKosky, S.T., Dickson, D., Dubois, B., Feldman, H.H., Fox, N.C., Gamst, A., Holtzman, D.M., Jagust, W.J., Petersen, R.C., Snyder, P.J., Carillo, M.C., Thies, B., Phelps, C.H., 2011. The diagnosis of mild cognitive impairment due to Alzheimer's disease: Recommendations from the National Institute on Aging-Alzheimer's Association workgroups on diagnostic guidelines for Alzheimer's disease. Alzheimer's Dement 7, 270–279. https://doi.org/10.1016/j.jalz.2011.03.008.

Ashburner, J., Friston, K.J., 2000. Voxel-Based Morphometry - The Methods. Neuroimage 11, 805–821. https://doi.org/10.1006/nimg.2000.0582.

Ashburner, J., Hutton, C., Frackowiak, R., Johnsrude, I., Price, C., Friston, K., 1998. Identifying global anatomical differences: Deformation-based morphometry. Hum. Brain Mapp. 6, 348–357. https://doi.org/10.1016/s1053-8119(18)31,577–5.

Bloudek, L.M., Spackman, D.E., Blankenburg, M., Sullivan, S.D., 2011. Review and meta-analysis of biomarkers and diagnostic imaging in Alzheimer's disease. J. Alzheimer's Dis. 26, 627–645. https://doi.org/10.3233/JAD-2011–110458.

Bohnen, N.I., Djang, D.S.W., Herholz, K., Anzai, Y., Minoshima, S., 2012. Effectiveness and Safety of 18F-FDG PET in the Evaluation of Dementia: A Review of the Recent Literature. J. Nucl. Med. 53, 59–71. https://doi.org/10.2967/jnumed.111.096578.

Brodersen, K.H., Ong, C.S., Stephan, K.E., Buhmann, J.M., 2010. The balanced accuracy and its posterior distribution. 2010. In: 20th Int. Conf. Pattern Recognit, pp. 3121–3124. https://doi.org/10.1109/ICPR.2010.764.

Bruun, M., Frederiksen, K.S., Rhodius-meester, H.F., Baroni, M., Gjerum, L., Koikkalainen, J., Urhemaa, T., Tolonen, A., Gils, M.Van, Rueckert, D., Dyremose, N., Andersen, B.B., Lemstra, A.W., Hallikainen, M., Kurl, S., Herukka, S.-K., Remes, A.M., Waldemar, G., Soininen, H., Mecocci, P., Flier, W.M.Van Der, Lötjönen, J., Hasselbalch, S.G., 2019a. Impact of a clinical decision support tool on prediction of progression in early-stage dementia: a prospective validation study. Alzheimers. Res. Ther. 11, 1–11. https://doi.org/10.1186/s13195-019–0482–3.

Bruun, M., Frederiksen, K.S., Rhodius-meester, H.F.M., Baroni, M., Gjerum, L., Koikkalainen, J., Urhemaa, T., Tolonen, A., Gils, M.Van, Tong, T., Guerrero, R., Rueckert, D., Dyremose, N., Andersen, B.B., Simonsen, A.H., Lemstra, A., Hallikainen, M., Kurl, S., Herukka, S.-K., Remes, A.M., Waldemar, G., Soininen, H., Mecocci, P., Flier, W.M.Van Der, Hasselbalch, S.G., 2019b. Impact of a Clinical Decision Support Tool on Dementia Diagnostics in Memory Clinics: The PredictND Validation Study. Curr. Alzheimer Res. 16, 91–101. https://doi.org/10.2174/1567205016666190103152425.

Bruun, M., Koikkalainen, J., Rhodius-meester, H.F.M., Baroni, M., Gjerum, L., Gils, M.Van, Soininen, H., Remes, A.M., Hartikainen, P., Waldemar, G., Mecocci, P., Barkhof, F., Pijnenburg, Y., Flier, W.M.Van Der, Hasselbalch, S.G., Lötjönen, J., Frederiksen, K.S., 2019c. Detecting frontotemporal dementia syndromes using MRI biomarkers. NeuroImage Clin 22, 1–9. https://doi.org/10.1016/j.nicl.2019.101711.

Bruun, M., Rhodius-meester, H.F.M., Koikkalainen, J., Baroni, M., Gjerum, L., Lemstra, A.W., Barkhof, F., Remes, A.M., Urhemaa, T., Tolonen, A., Rueckert, D., Gils, M.Van, Frederiksen, K.S., Waldemar, G., Scheltens, P., Mecocci, P., Soininen, H., Jyrki, L., 2018. Evaluating combinations of diagnostic tests to discriminate different dementia types. Alzheimer's Dement. Diagnosis, Assess. Dis. Monit. 10, 1–10. https://doi.org/10.1016/j.dadm.2018.07.003.

Buckner, R.L., Head, D., Parker, J., Fotenos, A.F., Marcus, D., Morris, J.C., Snyder, A.Z., 2004. A unified approach for morphometric and functional data analysis in young, old, and demented adults using automated atlas-based head size normalization: Reliability and validation against manual measurement of total intracranial volume. Neuroimage 23, 724–738. https://doi.org/10.1016/j.neuroimage.2004.06.018.

Caminiti, S.P., Sala, A., Iaccarino, L., Beretta, L., Pilotto, A., Gianolli, L., Iannaccone, S., Magnani, G., Padovani, A., Perini-Strambi, L., Perani, D., 2019. Brain glucose metabolism in Lewy body dementia: Implications for diagnostic criteria. Alzheimer's Res. Ther. 11, 1–14. https://doi.org/10.1186/s13195-019-0473-4.

Cluitmans, L., Mattila, J., Runtti, H., Van Gils, M., Lötjönen, J., 2013. A MATLAB toolbox for classification and visualization of heterogenous multi-scale human data using the disease state fingerprint method, in: PHealth 2013 2013. IOS Press, pp. 77–82. https://doi.org/10.3233/978-1-61499-268-4-77.

Cole, T., Green, P., 1992. Smoothing reference centile curves: the LMS method and penalized likelihood. Stat. Med. 11, 1305–1319.

Davison, C.M., O'Brien, J.T., 2014. A comparison of FDG-PET and blood flow SPECT in the diagnosis of neurodegenerative dementias: A systematic review. Int. J. Geriatr. Psychiatry 29, 551–561. https://doi.org/10.1002/gps.4036.

Dukart, J., Mueller, K., Horstmann, A., Barthel, H., Möller, H.E., Villringer, A., Sabri, O., Schroeter, M.L., 2011. Combined evaluation of FDG-PET and MRI improves detection and differentiation of dementia. PLoS One 6. https://doi.org/10.1371/journal.pone.0018111.

Frisoni, G.B., Bocchetta, M., Chételat, G., Rabinovici, G.D., De Leon, M.J., Kaye, J., Reiman, E.M., Scheltens, P., Barkhof, F., Black, S.E., Brooks, D.J., Carrillo, M.C., Fox, N.C., Herholz, K., Nordberg, A., Jack, C.R., Jagust, W.J., Johnson, K.A., Rowe, C.C., Sperling, R.A., Thies, W., Wahlund, L.O., Weiner, M.W., Pasqualetti, P., DeCarli, C., 2013. Imaging markers for Alzheimer disease: Which vs how. Neurology 81, 487–500. https://doi.org/10.1212/WNL.0b013e31829d86e8.

Gorno-Tempini, M.L., Hillis, A.E., Weintraub, S., Kertesz, A., Mendez, M., Cappa, S.F., Ogar, J.M., Rohrer, J.D., Black, S., Boeve, B.F., Manes, F., Dronkers, N.F., Vandenberghe, R., Roscovsky, K., Patterson, K., Miller, B.I., Knopman, D.S., Hodges, J.R., Mesulam, M.M., Grossman, M., 2011. Classification of primary progressive aphasia and its variants. Neurology 76, 1006–1014. https://doi.org/10.1212/WNL.0b013e31821103e6.

Herholz, K., Salmon, E., Perani, D., Baron, J.C., Holthoff, V., Frölich, L., Schönknecht, P., Ito, K., Mielke, R., Kalbe, E., Zündorf, G., Delbeuck, X., Pelati, O., Anchisi, D., Fazio, F., Kerrouche, N., Desgranges, B., Eustache, F., Beuthien-Baumann, B., Menzel, C., Schröder, J., Kato, T., Arahata, Y., Henze, M., Heiss, W.D., 2002. Discrimination between Alzheimer dementia and controls by automated analysis of multicenter FDG PET. Neuroimage 17, 302–316. https://doi.org/10.1006/nimg.2002.1208.

Hort, J., O'Brien, J.T., Gainotti, G., Pirttila, T., Popescu, B.O., Rektorova, I., Sorbi, S., Scheltens, P., 2010. EFNS guidelines for the diagnosis and management of Alzheimer's disease. Eur. J. Neurol. 17, 1236–1248. https://doi.org/10.1111/j.1468-1331.2010.03040.x.

Ishii, K., Soma, T., Kono, A., Sofue, K., Miyamoto, N., Yoshikawa, T., Mori, E., Murase, K., 2007. Comparison of Regional Brain Volume and Glucose Metabolism Between Patients with Mild Dementia with Lewy Bodies and Those with Mild Alzheimer's Disease. J. Nucl. Med. 48, 704–711. https://doi.org/10.2967/jnumed.106.035691.

Jack, C.R., Bennett, D.A., Blennow, K., Carrillo, M.C., Feldman, H.H., Frisoni, G.B., Hampel, H.J., Jagust, W.J., Johnson, K.A., Knopman, D.S., Petersen, R.C., Scheltens, P., Sperling, R.A., Dubois, B., 2016. A/T/N: An unbiased descriptive classification scheme for Alzheimer disease biomarkers. Neurology 87, 539–547. https://doi.org/10.1212/WNL.0000000000002923.

Jagust, W.J., Landau, S.M., Shaw, L.M., Trojanowski, J.Q., Koeppe, R.A., Reiman, E.M., Foster, N.L., Petersen, R.C., Weiner, M.W., Price, J.C., Mathis, C.A., 2009. Relationships between biomarkers in aging and dementia. Neurology 73, 1193–1199. https://doi.org/10.1212/WNL.0b013e3181bc010c.

Kantarci, K., Lowe, V.J., Boeve, B.F., Weigand, S.D., Senjem, M.L., Przybelski, S.A., Dickson, D.W., Parisi, J.E., Knopman, D.S., Smith, G.E., Ferman, T.J., Petersen, R.C., Jack Jr, C.R., 2012. Multimodality imaging characteristics of dementia with Lewy bodies. Neurobiol. Aging 33, 2091–2105. https://doi.org/10.1016/j.neurobiolaging.2011.09.024.

Kawamoto, K., Houlihan, C.A., Balas, E.A., Lobach, D.F., 2005. Improving clinical practice using clinical decision support systems: A systematic review of trials to identify features critical to success. Br. Med. J. 330, 765–768. https://doi.org/10.1136/bmj.38398.500764.8f.

Klöppel, S., Stonnington, C.M., Barnes, J., Chen, F., Chu, C., Good, C.D., Mader, I., Mitchell, L.A., Patel, A.C., Roberts, C.C., Fox, N.C., Jack, C.R., Ashburner, J., Frackowiak, R.S.J., 2008. Accuracy of dementia diagnosis - A direct comparison between radiologists and a computerized method. Brain 131, 2969–2974. https://doi.org/10.1093/brain/awn239.

Koikkalainen, J., Rhodius-Meester, H., Tolonen, A., Barkhof, Frederik, Tijms, Betty, Lemstra, A.W., Tong, Tong, Guerrero, Ricardo, Schuh, Andreas, Ledig, Christian, Rueckert, Daniel, Soininen, H., Remes, A.M., Waldemar, G., Hasselbalch, S., Mecocci, P., van der Flier, W., Lötjönen, J., Rhodius-Meester, Hanneke, Tolonen, A., Barkhof, Frederik, Tijms, Betty, Lemstra, A.W., Tong, Tong, Guerrero, Ricardo, Schuh, Andreas, Ledig, Christian, Rueckert, Daniel, Soininen, H., Remes, A.M., Waldemar, G., Hasselbalch, S., Mecocci, P., van der Flier, W., Lötjönen, J., 2016. Differential diagnosis of neurodegenerative diseases using structural MRI data. NeuroImage Clin. 11, 435–449. https://doi.org/10.1016/j.nicl.2016.02.019.

Kono, A.K.A., Ishii, K., Sofue, K., Miyamoto, N., Sakamoto, S., Mori, E., 2007. Fully automatic differential diagnosis system for dementia with Lewy bodies and Alzheimer's disease using FDG-PET and 3D-SSP. Eur. J. Nucl. Med. Mol. Imaging 34, 1490–1497. https://doi.org/10.1007/s00259-007-0380-y.

Lim, S.M., Katsifis, A., Villemagne, V.L., Best, R., Jones, G., Saling, M., Bradshaw, J., Merory, J., Woodward, M., Hopwood, M., Rowe, C.C., 2009. The 18F-FDG PET Cingulate Island Sign and Comparison to 123I-b-CIT SPECT for Diagnosis of Dementia with Lewy Bodies. J. Nucl. Med. 50, 1638–1645. https://doi.org/10.2967/jnumed.109.065870.

Livingston, G., Sommerlad, A., Orgeta, V., Costafreda, S.G., Huntley, J., Ames, D., Ballard, C., Banerjee, S., Burns, A., Cohen-mansfield, J., Cooper, C., Fox, N., Gitlin, L.N., Howard, R., Kales, H.C., Larson, E.B., Ritchie, K., Rockwood, K., Sampson, E.L., Samus, Q., Schneider, L.S., Selbæk, G., Teri, L., Mukadam, N., 2017. Dementia prevention, intervention, and care. Lancet 6736, 1–62. https://doi.org/10.1016/S0140-6736(17)31,363–6.

Lötjönen, J.M., Wolz, R., Koikkalainen, J.R., Thurfjell, L., Waldemar, G., Soininen, H., Rueckert, D., 2010. Fast and robust multi-atlas segmentation of brain magnetic resonance images. Neuroimage 49, 2352–2365. https://doi.org/10.1016/j.neuroimage.2009.10.026.

Mattila, J., Koikkalainen, J., Virkki, A., Simonsen, A., Van Gils, M., Waldemar, G., Soininen, H., Lötjönen, J., 2011. A disease state fingerprint for evaluation of Alzheimer's disease. J. Alzheimer's Dis. 27, 163–176. https://doi.org/10.3233/JAD-2011–110365.

Mattila, J., Koikkalainen, J., Virkki, A., Van Gils, M., Lötjönen, J., 2012. Design and application of a generic clinical decision support system for multiscale data. IEEE Trans. Biomed. Eng. 59, 234–240. https://doi.org/10.1109/TBME.2011.2170986.

McKeith, I., Taylor, J.-P., Thomas, A., Donaghy, P., Kane, J., 2016. Revisiting DLB Diagnosis: A Consideration of Prodromal DLB and of the Diagnostic Overlap With Alzheimer Disease. J. Geriatr. Psychiatry Neurol. 29, 249–253. https://doi.org/10.1177/0891988716656083.

McKeith, I.G., Boeve, B.F., Dickson, D.W., Halliday, G., Taylor, J.-P., Weintraub, D., Aarsland, D., Galvin, J., Attems, J., Ballard, C.G., Bayston, A., Beach, T.G., Blanc, F., Bohnen, N., Bonanni, L., Bras, J., Brundin, P., Burn, D., Chen-Plotkin, A., Duda, J.E., El-Agnaf, O., Feldman, H., Ferman, T.J., Ffytche, D., Fujishiro, H., Galasko, D., Goldman, J.G., Gomperts, S.N., Graff-Radford, N.R., Honig, L.S., Iranzo, A., Kantarci, K., Kaufer, D., Kukull, W., Lee, V.M.Y., Leverenz, J.B., Lewis, S., Lippa, C., Lunde, A., Masellis, M., Masliah, E., McLean, P., Mollenhauer, B., Montine, T.J., Moreno, E., Mori, E., Murray, M., O'Brien, J.T., Orimo, S., Postuma, R.B., Ramaswamy, S., Ross, O.A., Salmon, D.P., Singleton, A., Taylor, A., Thomas, A., Tiraboschi, P., Toledo, J.B., Trojanowski, J.Q., Tsuang, D., Walker, Z., Yamada, M., Kosaka, K., 2017. Diagnosis and management of dementia with Lewy bodies Fourth consensus report of the DLB Consortium. Neurology 89, 1–13. https://doi.org/10.1212/01.wnl.0000224698.67660.45.

McKeith, I.G., Dickson, D.W., Lowe, J., Emre, M., O'Brien, J.T., Feldman, H., Cummings, J., Duda, J.E., Lippa, C., Perry, E.K., Aarsland, D., Arai, H., Ballard, C.G., Boeve, B., Burn, D.J., Costa, D., Del Ser, T., Dubois, B., Galasko, D., Gauthier, S., Goetz, C.G., Gomez-Tortosa, E., Halliday, G., Hansen, L.A., Hardy, J., Iwatsubo, T., Kalaria, R.N., Kaufer, D., Kenny, R.A., Korczyn, A., Kosaka, K., Lee, V.M.Y., Lees, A., Litwan, I., Londos, E., Lopez, O.L., Minoshima, S., Mizuno, Y., Molina, J.A., Mukaetova-Ladinska, E.B., Pasquier, F., Perry, R.H., Schulz, J.B., Trojanowski, J.Q., Yamada, M., 2005. Diagnosis and management of dementia with Lewy bodies: Third report of the DLB Consortium. Neurology 65, 1863–1872. https://doi.org/10.1212/01.wnl.0000224698.67660.45.

McKhann, G.M., 2001. Clinical and Pathological Diagnosis of Frontotemporal Dementia. Arch. Neurol 58, 1803. https://doi.org/10.1001/archneur.58.11.1803.

McKhann, G.M., Knopman, D.S., Chertkow, H., Hyman, B.T., Jack, C.R., Kawas, C.H., Klunk, W.E., Koroshetz, W.J., Manly, J.J., Mayeux, R., Mohs, R.C., Morris, J.C., Rossor, M.N., Scheltens, P., Carrillo, M.C., Thies, B., Weintraub, S., Phelps, C.H., 2011. The diagnosis of dementia due to Alzheimer's disease: Recommendations from the National Institute on Aging-Alzheimer's Association workgroups on diagnostic guidelines for Alzheimer's disease. Alzheimer's Dement. https://doi.org/10.1016/j.jalz.2011.03.008.

Mendez, M.F., Joshi, A., Tassniyom, K., Teng, E., Shapira, J.S., 2013. Clinicopathologic differences among patients with behavioral variant frontotemporal dementia. Neurology 80, 561–568. https://doi.org/10.1212/WNL.0b013e3182815547.

Merdes, A., Hansen, L., Jeste, D., Galasko, D., Hofstetter, C., Ho, G., Thal, L., Corey-Bloom, J., 2003. Influence of Alzheimer pathology on clinical diagnostic accuracy in dementia with Lewy bodies. Neurology 30, 1586–1590. https://doi.org/10.1212/01.WNL.0000065889.42856.F2.

Minoshima, S., Foster, N.L., Sima, A.A.F., Frey, K.A., Albin, R.L., Kuhl, D.E., 2001. Alzheimer's Disease versus Dementia with Lewy Bodies: Cerebral Metabolic Distinction with Autopsy Confirmation. Ann. Neurol. 50, 358–365. https://doi.org/10.1002/ana.1133.

National Collaborating center for Mental Health, 2007. Dementia: The NICE-SCIE guideline on supporting people with dementia and their carers in health and social care. National Clinical Practice Guideline. https://www.ncbi.nlm.nih.gov/books/NBK55459/.

Neary, D., Snowden, J.S., Gustafson, L., Passant, U., Stuss, D., Black, S., Freedman, M., Kertesz, A., Robert, P.., Albert, M., Boone, M., Miller, B.., Cummings, J., Benson, D.., 1998. Frontotemporal lobar degeneration: A consensus on clinical diagnostic criteria. Neurology 51, 1546–1554. https://doi.org/10.1212/01.wnl.0000224698.67660.45.

Nobili, F., Arbizu, J., Bouwman, F., Drzezga, A., Agosta, F., Nestor, P., Walker, Z., Boccardi, M., 2018. European Association of Nuclear Medicine and European Academy of Neurology recommendations for the use of brain 18F-Fluorodeoxyglucose Positron Emission Tomography in neurodegenerative cognitive impairment and dementia: Delphi consensus. Eur. J. Neurol. 1–17. https://doi.org/10.1111/ene.13728.

Ossenkoppele, R., Cohn-sheehy, B.I., Joie, R.La, Vogel, J.W., Möller, C., Lehmann, M., Berckel, B.N.M.Van, Seeley, W.W., Pijnenburg, A., Gorno-tempini, M.L., Kramer, J.H., Barkhof, F., Howard, J., Flier, W.M.Van Der, Jagust, W.J., Miller, B.L., Scheltens, P., Rabinovici, G.D., 2015. Atrophy patterns in early clinical stages across distinct phenotypes of Alzheimer's disease. Hum. Brain Mapp. 36, 4421–4437. https://doi.org/10.1002/hbm.22927.Atrophy.

Ranasinghe, K.G., Rankin, K.P., Pressman, P.S., Perry, D.C., Lobach, I.V., Seeley, W.W., Coppola, G., Karydas, A.M., Grinberg, L.T., Shany-Ur, T., Lee, S.E., Rabinovici, G.D., Rosen, H.J., Gorno-Tempini, M.L., Boxer, A.L., Miller, Z.A., Chiong, W., DeMay, M., Kramer, J.H., Possin, K.L., Sturm, V.E., Bettcher, B.M., Neylan, M., Zackey, D.D., Nguyen, L.A., Ketelle, R., Block, N., Wu, T.Q., Dallich, A., Russek, N., Caplan, A., Geschwind, D.H., Vossel, K.A., Miller, B.L., 2016. Distinct subtypes of behavioral variant frontotemporal dementia based on patterns of network degeneration. JAMA Neurol 73, 1078–1088. https://doi.org/10.1001/jamaneurol.2016.2016.

Rascovsky, K., Hodges, J.R., Knopman, D., Mendez, M.F., Kramer, J.H., Neuhaus, J., Van Swieten, J.C., Seelaar, H., Dopper, E.G.P., Onyike, C.U., Hillis, A.E., Josephs, K.A., Boeve, B.F., Kertesz, A., Seeley, W.W., Rankin, K.P., Johnson, J.K., Gorno-Tempini, M.L., Rosen, H., Prioleau-Latham, C.E., Lee, A., Kipps, C.M., Lillo, P., Piguet, O., Rohrer, J.D., Rossor, M.N., Warren, J.D., Fox, N.C., Galasko, D., Salmon, D.P., Black, S.E., Mesulam, M., Weintraub, S., Dickerson, B.C., Diehl-Schmid, J., Pasquier, F., Deramecourt, V., Lebert, F., Pijnenburg, Y., Chow, T.W., Manes, F., Grafman, J., Cappa, S.F., Freedman, M., Grossman, M., Miller, B.L., 2011. Sensitivity of revised diagnostic criteria for the behavioural variant of frontotemporal dementia. Brain 134, 2456–2477. https://doi.org/10.1093/brain/awr179.

Rhodius-Meester, H.F.M., Koikkalainen, J., Mattila, J., Teunissen, C.E., Barkhof, F., Lemstra, A.W., Scheltens, P., Lötjönen, J., van der Flier, W.M., 2016. Integrating Biomarkers for Underlying Alzheimer's Disease in Mild Cognitive Impairment in Daily Practice: Comparison of a Clinical Decision Support System with Individual Biomarkers. J. Alzheimer's Dis. 50, 261–270. https://doi.org/10.3233/JAD-150548.

Rice, L., Bisdas, S., 2017. The diagnostic value of FDG and amyloid PET in Alzheimer's disease - A systematic review. Eur. J. Radiol. 94, 16–24. https://doi.org/10.1016/j.ejrad.2017.07.014.

Román, G.C., Tatemichi, T.K., Erkinjuntti, T., Cummings, J.L., Masdeu, J.C., Garcia, J.H., Amaducci, L., Orgogozo, J.-M., Brun, A., Hofman, A., Moody, D.M., O'Brien, M.D., Yamaguchi, T., Grafman, J., Drayer, B.P., Bennett, D.A., Fisher, M., Ogata, J., Kokmen, E., Bermejo, F., Wolf, P.A., Gorelick, P.B., Bick, K.L., Pajeau, A.K., Bell, M.A., DeCarli, C., Culebras, A., Korczyn, A.D., Bogousslavsky, J., Hartmann, A., Scheinberg, P., 1993. Vascular dementia: diagnostic criteria for research studies. Report of the NINDS-AIREN International Workshop. Neurology 43, 250–260. https://doi.org/10.1212/WNL.43.2.250.

Sachdev, P., Kalaria, R., O'Brien, J., Skoog, I., Alladi, S., Black, S., Blacker, D., Blazer, D., Chen, C., Chui, H., Ganguli, M., Jellinger, K., Jeste, D., Pasquier, F., Paulsen, J., Prins, N., Rockwood, K., Roman, G., Scheltens, P., 2014. Diagnostic criteria for vascular cognitive disorders: a VASCOG statement. Alzheimer Dis. Assoc. Disord. 28, 206–218. https://doi.org/10.1016/j.asieco.2008.09.006.EAST.

Schneider, J.A., Arvanitakis, Z., Bang, W., Bennett, D.A., 2007. Mixed brain pathologies account for most dementia cases in community-dwelling older persons. Neurology 69, 2197–2204. https://doi.org/10.1212/01.wnl.0000271090.28148.24.

Thomas, A., Mahin-Babaei, F., Saidi, M., Lett, D., Taylor, J., Walker, L., Attems, J., 2018. Improving the identification of dementia with Lewy bodies in the context of an Alzheimer's-type dementia. Alzheimer's Res. Ther. 10, 1–9. https://doi.org/10.1186/s13195-018-0356-0.

Tolonen, A., Rhodius-Meester, H.F.M., Bruun, M., Koikkalainen, J., Barkhof, F., Lemstra, A.W., Koene, T., Scheltens, P., Teunissen, C.E., Tong, T., Guerrero, R., Schuh, A., Ledig, C., Baroni, M., Rueckert, D., Soininen, H., Remes, A.M., Waldemar, G., Hasselbalch, S.G., Mecocci, P., van der Flier, W.M., Lötjönen, J., 2018. Data-driven differential diagnosis of dementia using multiclass disease state index classifier. Front. Aging Neurosci. 10, 1–11. https://doi.org/10.3389/fnagi.2018.00111.

Tong, T., Ledig, C., Guerrero, R., Schuh, A., Koikkalainen, J., Tolonen, A., Rhodius, H., Barkhof, F., Tijms, B., Lemstra, A.W., Soininen, H., Remes, A.M., Waldemar, G., Hasselbalch, S., Mecocci, P., Baroni, M., Lötjönen, J., Flier, W., van der, Rueckert, D., 2017. Five-class differential diagnostics of neurodegenerative diseases using random undersampling boosting. NeuroImage Clin 15, 613–624. https://doi.org/10.1016/j.nicl.2017.06.012.

Tong, T., Wolz, R., Coupé, P., Hajnal, J.V., Rueckert, D., 2013. Segmentation of MR images via discriminative dictionary learning and sparse coding: Application to hippocampus labeling. Neuroimage 76, 11–23. https://doi.org/10.1016/j.neuroimage.2013.02.069.

Wang, Y., Catindig, J.A., Hilal, S., Soon, H.W., Ting, E., Wong, T.Y., Venketasubramanian, N., Chen, C., Qiu, A., 2012. Multi-stage segmentation of white matter hyperintensity, cortical and lacunar infarcts. Neuroimage 60, 2379–2388. https://doi.org/10.1016/j.neuroimage.2012.02.034.

World Health Organization, 2012. Dementia: a public health priority. Dementia 112. http://www.who.int/mental_health/publications/dementia_report_2012.

Supplementary material.

Table A.1. Distribution of the diagnostic test for each diagnostic group.

	AD	DLB	FTD	VaD	SCD
MMSE, n (%)	90 (100)	41 (100)	37 (100)	25 (100)	66 (100)
Episodic memory (learning and recall), n (%)	62 (69)	18 (44)	14 (38)	14 (56)	65 (98)
TMT-A, n (%)	76 (84)	32 (78)	24 (65)	24 (96)	66 (100)
TMT-B, n (%)	63 (70)	23 (56)	15 (41)	20 (80)	65 (98)
Animal fluency, n (%)	82 (91)	35 (85)	28 (76)	23 (92)	65 (98)
CSF biomarkers, n (%)	49 (54)	27 (66)	20 (54)	12 (48)	27 (41)
Volumetric and morphometric MRI biomarkers, n (%)	90 (100)	41 (100)	37 (100)	25 (100)	66 (99)
MRI vascular burden, n (%)	89 (99)	40 (98)	35 (95)	25 (100)	65 (98)
2-[^{18}F]FDG-PET biomarkers, n (%)	90 (100)	41 (100)	37 (100)	25 (100)	66 (99)

Abbreviations: AD: Alzheimer's disease; CSF: cerebrospinal fluid; DLB: dementia with Lewy bodies; FTD: frontotemporal dementia; MMSE: mini-mental state examination; MRI: magnetic resonance imaging; n: number; SCD: subjective cognitive decline; TMT: trail making test; VaD: vascular dementia; 2-[^{18}F]FDG-PET: 2-[^{18}F]fluoro-2-deoxy-D glucose positron emission tomography;

Table B.1. Region of interests for MRI and 2-[^{18}F]FDG-PET.

Region	ROI
Frontal lobe	Anterior cingulate gyrus
	Anterior insula
	Anterior orbital gyrus
	Central operculum
	Frontal operculum
	Frontal pole
	Gyrus rectus
	Lateral orbital gyrus
	Medial frontal cortex
	Medial orbital gyrus
	Middle cingulate gyrus
	Middle frontal gyrus
	Opercular part of the inferior frontal gyrus
	Orbital part of the inferior frontal gyrus
	Posterior orbital gyrus
	Precentral gyrus medial segment
	Precentral gyrus
	Subcallosal area
	Superior frontal gyrus medial segment
	Superior frontal gyrus
	Supplementary motor cortex
	Triangular part of the inferior frontal gyrus
Temporal lobe	Amygdala
	Entorhinal area
	Fusiform gyrus
	Hippocampus
	Inferior temporal gyrus
	Middle temporal gyrus
	Parahippocampal gyrus
	Planum polare
	Planum temporale
	Superior temporal gyrus
	Temporal pole
	Putamen
	Transverse temporal gyrus
Parietal lobe	Angular gyrus
	Parietal operculum
	Postcentral gyrus medial segment
	Postcentral gyrus
	Posterior cingulate gyrus
	Posterior insula
	Precuneus
	Superior parietal lobule
	Supramarginal gyrus
Occipital lobe	Calcarine cortex
	Cuneus
	Inferior occipital gyrus
	Lingual gyrus
	Middle occipital gyrus
	Occipital fusiform gyrus
	Occipital pole
	Superior occipital gyrus
Cerebellum	Cerebellar vermal lobules I- V; total
	Cerebellar vermal lobules VIII- X; total
	Cerebellar vermal lobules VI-VII; total
	Cerebellum white matter
	Cerebellum exterior
Deep grey matter	Accumbens area
	Caudate
	Pallidum
	Thalamus proper
Ventricles	3rd ventricle; total
	4th ventricle; total
	Inferior lateral ventricle
	Lateral ventricle
Miscellaneous	Brain stem; total
	Cerebral white matter
	Transverse cerebral fissure; total
	Ventral diencephalon
	Vessel

Abbreviations: MRI: magnetic resonance imaging; ROI: region of interest; 2-[^{18}F]FDG-PET: 2-[^{18}F]fluoro-2-deoxy-D glucose positron emission tomography;

Table C.1. Additional details of baseline demographics.

	AD	DLB	FTD	VaD	SCD	Group-wise comparison when significant
Cognitive tests						
Episodic memory (learning), median score (IQR)	22 (16-27)	24 (21-32)	27 (18-33)	22 (18-22)	44 (38-54)	SCD > All
Episodic memory (recall), median score (IQR)	1 (0-2)	3 (2-5)	3 (1-5)	2 (0-5)	10 (7-12)	SCD > All; DLB > AD
TMT-A, median seconds (IQR)	55 (40-80)	74 (51-120)	65 (48-88)	70 (48-116)	35 (25-45)	SCD < All
TMT-B, median seconds (IQR)	180 (111-300)	180 (140-300)	140 (75-300)	238 (176-300)	74 (61-100)	SCD < All
Animal fluency, median score (IQR)	14 (10-17)	15 (11-19)	10 (6-14)	12 (8-14)	24 (19-27)	SCD > All
MRI						
Hippocampus, mean volume mL ±SD	5.5 ±0.7	5.9 ±1.0	5.6 ±1.1	5.9 ±0.8	6.7 ±0.8	SCD > All
Temporal pole, mean volume mL ±SD	12.7 ±1.7	13.1 ±1.4	10.8 ±3.0	13.3 ±1.7	14.7 ±1.9	SCD > AD, DLB, VaD > FTD
Cortex, mean volume mL ±SD	454.3 ±21.3	458.4 ±24.1	447.5 ±25.7	453.9 ±22.6	486.5 ±25.6	SCD > All
Frontal cortex, mean volume mL ±SD	180.4 ±9.2	184.2 ±11.3	173.7 ±16.1	177.7 ±10.7	189.7 ±11.8	SCD > AD, DLB, FTD; AD, DLB > FTD
Temporal cortex, mean volume mL ±SD	106.7 ±7.3	110.8 ±7.0	103.9 ±13.7	113.0 ±7.0	120.3 ±7.2	SCD > All; VaD > AD; DLB, VaD > FTD
Medial temporal cortex, mean volume mL ±SD	15.8 ±1.9	16.5 ±1.9	15.7 ±3.2	16.9 ±1.7	19.2 ±1.7	SCD > All
Parietal cortex, mean volume mL ±SD	98.3 ±7.0	98.1 ±7.6	101.7 ±5.6	95.9 ±6.3	105.0 ±7.0	SCD > AD, DLB, VaD; FTD > VaD
Occipital cortex, mean volume mL ±SD	69.4 ±5.8	65.5 ±6.9	68.5 ±7.3	67.7 ±5.7	71.6 ±5.9	DLB < AD, SCD
Lateral ventricle, median volume mL (IQR)	48.0 (39.0-60.0)	52.0 (38.6-89.9)	51.4 (40.0-61.8)	49.7 (44.0-62.7)	35.7 (28.5-46.2)	SCD < All
Inferior lateral ventricle, median volume mL (IQR)	2.4 (1.9-3.5)	2.2 (1.5-3.7)	2.7 (2.1-4.0)	2.6 (1.9-3.2)	1.2 (0.9-1.6)	SCD < All
API-MRI, median score (IQR)	−0.58 (−1.14-0.15)	−0.04 (−0.41-0.37)	−1.08 (−2.82-−0.63)	−0.03 (−0.71-0.22)	−0.03 (−0.59-0.46)	FTD < All; AD < SCD
WMH, median volume mL (IQR)	2.4 (0.7-5.9)	4.0 (0.9-8.7)	2.1 (0.6-8.8)	39.2 (18.3-58.4)	0.7 (0.1-2.9)	VaD > All; AD, DLB, FTD > SCD
Cortical infarcts, median volume mL (range)	0.00 (0.00-2.53)	0.00 (0.00-0.06)	0.00 (0.00-1.24)	0.00 (0.00-6.13)	0.00 (0.00-0.27)	VaD > All
Lacunar infarcts, median volume mL (range)	0.00 (0.00-0.17)	0.00 (0.00-0.14)	0.00 (0.00-0.03)	0.00 (0.00-1.03)	0.00 (0.00-0.11)	VaD > All

Table C.1. Additional details of baseline demographics (cont.).

2-[^{18}F]FDG-PET						
Anterior cingulate gyrus, mean volume ±SD	1.07 ±0.11	1.12 ±0.10	0.99 ±0.11	1.06 ±0.09	1.17 ±0.12	FTD < AD, DLB, SCD; AD, VaD < SCD
Calcarine cortex, mean volume ±SD	1.33 ±0.14	1.24 ±0.14	1.40 ±0.13	1.32 ±0.17	1.42 ±0.15	DLB < AD, FTD, SCD; AD, VaD < SCD
Middle cingulate gyrus, mean volume ±SD	1.12 ±0.10	1.16 ±0.10	1.08 ±0.10	1.12 ±0.13	1.22 ±0.12	SCD > AD, FTD, VaD; DLB > FTD
Posterior cingulate gyrus, mean volume ±SD	1.12 ±0.12	1.16 ±0.12	1.20 ±0.13	1.22 ±0.17	1.35 ±0.15	SCD > All; FTD, VaD > AD
Precuneus, mean uptake ±SD	1.14 ±0.12	1.13 ±0.10	1.10 ±0.14	1.12 ±0.16	1.29 ±0.17	SCD > All
Precentral gyrus, mean uptake ±SD	1.13 ±0.11	1.14 ±0.09	1.12 ±0.08	1.13 ±0.13	1.19 ±0.14	SCD > AD
Cortex, mean uptake ±SD	1.06 ±0.09	1.05 ±0.06	1.08 ±0.08	1.09 ±0.12	1.18 ±0.11	SCD > All
Frontal cortex, mean uptake ±SD	1.11 ±0.10	1.12 ±0.08	1.07 ±0.09	1.11 ±0.12	1.23 ±0.12	SCD > All
Temporal cortex, mean uptake ±SD	0.94 ±0.08	0.95 ±0.06	0.96 ±0.08	1.00 ±0.11	1.07 ±0.08	SCD > All; VaD > AD
Medial temporal cortex, mean uptake ±SD	0.81 ±0.09	0.88 ±0.08	0.80 ±0.10	0.88 ±0.09	0.91 ±0.09	AD, FTD < DLB, VaD, SCD
Parietal cortex, mean uptake ±SD	1.06 ±0.11	1.02 ±0.08	1.13 ±0.09	1.11 ±0.14	1.21 ±0.12	SCD > All; FTD > AD, DLB; VaD > DLB
Occipital cortex, mean uptake ±SD	1.14 ±0.12	1.04 ±0.09	1.20 ±0.10	1.17 ±0.14	1.22 ±0.12	DLB < All; AD < SCD
API-PET, mean score ±SD	0.98 ±0.05	1.05 ±0.07	0.90 ±0.05	0.95 ±0.04	0.97 ±0.03	FTD < AD, VaD, SCD < DLB
Occipital vs. temporal index, mean score ±SD	1.21 ±0.09	1.09 ±0.08	1.24 ±0.09	1.16 ±0.06	1.14 ±0.06	DLB < VaD, SCD < FTD; DLB, SCD < AD
Cingulate island sign ratio, mean value ±SD	0.46 ±0.04	0.51 ±0.04	0.47 ±0.03	0.48 ±0.04	0.50 ±0.04	DLB, SCD > AD, FTD; DLB > VaD

Abbreviations: Aβ42: amyloid beta 1-42; AD: Alzheimer's disease; API: Anterior vs. posterior index; CSF: cerebrospinal fluid; DLB: dementia with Lewy bodies; FTD: frontotemporal dementia region of interest; IQR: interquartile range; MMSE: mini-mental state examination; MRI: magnetic resonance imaging; n: number; p-tau: phosphorylated tau at threonine 181; ROI: region of interest; SCD: subjective cognitive decline; SD: standard deviation; TMT: trail making test; VaD: vascular dementia; WMH: white matter hyperintensity; 2-[^{18}F]FDG-PET: 2-[^{18}F]fluoro-2-deoxy-D glucose positron emission tomography;

Table D.1. The pairwise comparison for individual diagnostic tests

Bal. acc./AUC	AD vs. DLB	AD vs. FTD	AD vs. VaD	AD vs. SCD	DLB vs. FTD	DLB vs. VaD	DLB vs. SCD	FTD vs. VaD	FTD vs. SCD	VaD vs. SCD
Cognitive tests										
TMT-A	62/63	61/57	59/62	71/78	49/54	49/48	82/87	55/55	74/82	74/85
TMT-B	45/47	50/48	60/60	75/82	59/59	54/55	85/92	62/60	67/72	80/88
Animal fluency	49/51	59/64	54/61	75/84	62/69	60/67	71/83	59/56	80/88	87/93
MRI										
Hippocampus	60/63	45/40	59/62	81/86	55/57	36/36	67/73	52/56	67/79	68/76
Lateral ventricle	53/59	52/56	55/55	66/70	45/42	38/39	66/75	33/35	71/76	70/75
Inferior lateral ventricle	53/53	48/54	43/41	78/85	56/57	41/42	73/80	39/39	79/88	75/85
Temporal pole	59/58	59/66	41/51	67/77	64/71	54/49	61/70	63/68	71/83	68/71
Cortex	51/52	59/59	54/52	76/82	56/63	59/57	72/78	39/43	78/83	80/82
Global VBM index	57/62	64/72	55/51	82/89	60/68	58/54	68/73	74/79	86/91	84/92
Global TBM index	53/52	64/70	56/58	72/79	59/67	62/65	70/81	70/78	84/91	77/83
ROI-based grading	62/66	70/77	59/59	82/87	64/67	59/58	71/77	68/76	71/79	83/83
2-[^{18}F]FDG-PET										
Anterior cingulate gyrus	57/62	68/70	43/46	68/73	76/80	63/67	63/63	68/67	78/86	72/76
Calcarine cortex	63/68	61/64	43/39	67/67	72/79	59/65	75/80	60/64	43/43	64/67
Middle cingulate gyrus	58/62	59/59	38/40	67/75	63/72	60/62	66/65	60/56	72/80	74/73
Posterior cingulate gyrus	58/57	59/64	63/65	78/85	49/56	56/61	79/82	39/40	68/77	75/73
Precuneus	47/47	59/57	45/47	73/77	54/54	37/40	72/81	44/43	74/81	77/79
Precentral gyrus	46/44	54/51	39/37	62/65	53/54	48/50	57/60	48/44	63/65	60/63
Cortex	53/54	53/57	56/57	75/81	54/62	57/61	76/85	37/39	73/78	70/74

Abbreviations: AD: Alzheimer's disease; AUC: area under the receiver operating characteristic curve; Bal. acc.: balanced accuracy; DLB: dementia with Lewy bodies; FTD: frontotemporal dementia; MRI: magnetic resonance imaging; ROC: receiver operating characteristic; ROI: region of interest; SCD: subjective cognitive decline; TBM: tensor-based morphometry; TMT: trail making test; VaD: vascular dementia; VBM: voxel-based morphometry; 2-[^{18}F]FDG-PET: 2-[^{18}F]fluoro-2-deoxy-D glucose positron emission tomography;
The colors correspond to the balanced accuracy for the pairwise comparison. Balanced accuracies 85%–100% are highlighted in dark green. The gradually lighter shades of green indicate lower balanced accuracy with white being at or below 50. Both balanced accuracy and AUC are reported as percentage values (%).

9. Declaration of co-authorship

Study I

GRADUATE SCHOOL OF HEALTH AND MEDICAL SCIENCES
UNIVERSITY OF COPENHAGEN

PHD-THESIS
DECLARATION OF CO-AUTHORSHIP

The declaration is for PhD students and must be completed for each conjointly authored article. Please note that if a manuscript or published paper has ten or less co-authors, all co-authors must sign the declaration of co-authorship. If it has more than ten co-authors, declarations of co-authorship from the corresponding author(s), the senior author and the principal supervisor (if relevant) are a minimum requirement.

1. Declaration by	
Name of PhD student	Le Gjerum
E-mail	le.gjerum@regionh.dk
Name of principal supervisor	Steen Gregers Hasselbalch
Title of the PhD thesis	Optimizing 18F-FDG-PET in the diagnosis fo dementia disorders

2. The declaration applies to the following article	
Title of article	Comparison of the added clinical value of 2-[18F]FDG-PET and cerebrospinal fluid biomarkers in patients suspected of Alzheimer's disease
Article status	
Published ☐ Date:	Accepted for publication ☐ Date:
Manuscript submitted ☒ Date: 15.03.2020	Manuscript not submitted ☐
If the article is published or accepted for publication, please state the name of journal, year, volume, page and DOI (if you have the information).	

3. The PhD student's contribution to the article *(please use the scale A-F as benchmark)* Benchmark scale of the PhD-student's contribution to the article **A.** Has essentially done all the work (> 90 %) **B.** Has done most of the work (60-90 %) **C.** Has contributed considerably (30-60 %) **D.** Has contributed (10-30 %) **E.** No or little contribution (<10 %) **F.** Not relevant	**A, B, C, D, E, F**
1. Formulation/identification of the scientific problem	B
2. Development of the key methods	B
3. Planning of the experiments and methodology design and development	B
4. Conducting the experimental work/clinical studies/data collection/obtaining access to data	A
5. Conducting the analysis of data	A
6. Interpretation of the results	A
7. Writing of the first draft of the manuscript	A
8. Finalisation of the manuscript and submission	A
Provide a short description of the PhD student´s specific contribution to the article.[1]	

Latest update of the declaration: December 2018

4. Material from another thesis / dissertation[ii]	
Does the article contain work which has also formed part of another thesis, e.g. master's thesis, PhD thesis or doctoral dissertation (the PhD student's or another person's)?	Yes: ☐ No: ☒
If yes, please state name of the author and title of thesis / dissertation.	
If the article is part of another author's academic degree, please describe the PhD student's and the author's contributions to the article so that the individual contributions are clearly distinguishable from one another.	

5. Signatures of the co-authors[ii]

	Date	Name	Title	Signature
1.	24.2.20	Birgitte Bo Andersen	MD, DMSc	
2.	12.3.20	Marie Bruun	MD, PhD	
3.	20.2.20	Anja Hviid Simonsen	Cand. pharm., PhD	
4.	20.2.20	Otto Mølby Henriksen	MD, PhD	
5.	21.2.20	Ian Law	MD, PhD, DMSc	
6.	25.2.20	Steen Gregers Hasselbalch	MD, DMSc	
7.	27/2-20	Kristian Steen Frederiksen	MD, PhD	
8.				
9.				
10.				

6. Signature of the principal supervisor

I solemnly declare that the information provided in this declaration is accurate to the best of my knowledge.
Date: 25-FEB-2020
Principal supervisor:

7. Signature of the PhD student

I solemnly declare that the information provided in this declaration is accurate to the best of my knowledge.
Date: 24.2.2020
PhD student:

Please learn more about responsible conduct of research on the Faculty of Health and Medical Sciences' website.

Study II

GRADUATE SCHOOL OF HEALTH AND MEDICAL SCIENCES
UNIVERSITY OF COPENHAGEN

PHD-THESIS
DECLARATION OF CO-AUTHORSHIP

The declaration is for PhD students and must be completed for each conjointly authored article. Please note that if a manuscript or published paper has ten or less co-authors, all co-authors must sign the declaration of co-authorship. If it has more than ten co-authors, declarations of co-authorship from the corresponding author(s), the senior author and the principal supervisor (if relevant) are a minimum requirement.

1. Declaration by	
Name of PhD student	Le Gjerum
E-mail	le.gjerum@regionh.dk
Name of principal supervisor	Steen Gregers Hasselbalch
Title of the PhD thesis	Optimizing 18F-FDG-PET in the diagnosis of dementia disorders

2. The declaration applies to the following article	
Title of article	A visual rating scale for cingulate island sign on 18F-FDG-PET to differentiate dementia with Lewy bodies and Alzheimer's disease
Article status	
Published ☐ Date:	Accepted for publication ☒ Date: 21.12.2019
Manuscript submitted ☐ Date:	Manuscript not submitted ☐
If the article is published or accepted for publication, please state the name of journal, year, volume, page and DOI (if you have the information).	Journal of the Neurological Sciences DOI: 10.1016/j.jns.2019.116645

3. The PhD student's contribution to the article *(please use the scale A-F as benchmark)* Benchmark scale of the PhD-student's contribution to the article **A.** Has essentially done all the work (> 90 %) **B.** Has done most of the work (60-90 %) **C.** Has contributed considerably (30-60 %) **D.** Has contributed (10-30 %) **E.** No or little contribution (<10 %) **F.** Not relevant	**A, B, C, D, E, F**
1. Formulation/identification of the scientific problem	B
2. Development of the key methods	B
3. Planning of the experiments and methodology design and development	B
4. Conducting the experimental work/clinical studies/data collection/obtaining access to data	A
5. Conducting the analysis of data	A
6. Interpretation of the results	A
7. Writing of the first draft of the manuscript	A
8. Finalisation of the manuscript and submission	A
Provide a short description of the PhD student's specific contribution to the article.	

Latest update of the declaration: December 2018

4. Material from another thesis / dissertation

Does the article contain work which has also formed part of another thesis, e.g. master's thesis, PhD thesis or doctoral dissertation (the PhD student's or another person's)? Yes: ☐ No: ☒

If yes, please state name of the author and title of thesis / dissertation.

If the article is part of another author's academic degree, please describe the PhD student's and the author's contributions to the article so that the individual contributions are clearly distinguishable from one another.

5. Signatures of the co-authors

	Date	Name	Title	Signature
1.	10.1.20	Kristian Steen Pedersen	MD, PhD	
2.	21.1.20	Otto Mølby Henriksen	MD, PhD	
3.	21.1.20	Ian Law	MSc	
4.	21.1.20	Lasse Andersberg	MD, PhD	
5.	12.1.20	Birgitte Bo Andersen	MD, DMSc	
6.	28.1.20	Eva Bjerregaard	MD	
7.	15.1.20	Anne-Mette Hoe	MD PhD	
8.	17.1.20	Peter Hogh	MD PhD	
9.	[illegible]	Steen Gregers Hasselbalch	[illegible]	
10.				

6. Signature of the principal supervisor

I solemnly declare that the information provided in this declaration is accurate to the best of my knowledge.

Date: 10/JAN/2020

Principal supervisor: Steen Gregers Hasselbalch

7. Signature of the PhD student

I solemnly declare that the information provided in this declaration is accurate to the best of my knowledge.

Date: 14.1.20

PhD student: Liv Gjerum

Please learn more about responsible conduct of research on the Faculty of Health and Medical Sciences' website.

2

Study III

GRADUATE SCHOOL OF HEALTH AND MEDICAL SCIENCES
UNIVERSITY OF COPENHAGEN

PHD-THESIS
DECLARATION OF CO-AUTHORSHIP

The declaration is for PhD students and must be completed for each conjointly authored article. Please note that if a manuscript or published paper has ten or less co-authors, all co-authors must sign the declaration of co-authorship. If it has more than ten co-authors, declarations of co-authorship from the corresponding author(s), the senior author and the principal supervisor (if relevant) are a minimum requirement.

1. Declaration by	
Name of PhD student	Le Gjerum
E-mail	le.gjerum@regionh.dk
Name of principal supervisor	Steen Gregers Hasselbalch
Title of the PhD thesis	Optimizing 18F-FDG-PET in the diagnosis of dementia disorders

2. The declaration applies to the following article	
Title of article	Addition of FDG-PET in diagnosing dementia using a data-driven decision model
Article status	
Published ☐ Date:	Accepted for publication ☐ Date:
Manuscript submitted ☒ Date: 10.01.2020	Manuscript not submitted ☐
If the article is published or accepted for publication, please state the name of journal, year, volume, page and DOI (if you have the information).	

3. The PhD student's contribution to the article *(please use the scale A-F as benchmark)* Benchmark scale of the PhD-student's contribution to the article **A.** Has essentially done all the work (> 90 %) **B.** Has done most of the work (60-90 %) **C.** Has contributed considerably (30-60 %) **D.** Has contributed (10-30 %) **E.** No or little contribution (<10 %) **F.** Not relevant	**A, B, C, D, E, F**
1. Formulation/identification of the scientific problem	B
2. Development of the key methods	B
3. Planning of the experiments and methodology design and development	B
4. Conducting the experimental work/clinical studies/data collection/obtaining access to data	A
5. Conducting the analysis of data	B
6. Interpretation of the results	B
7. Writing of the first draft of the manuscript	A
8. Finalisation of the manuscript and submission	A
Provide a short description of the PhD student's specific contribution to the article.	

Latest update of the declaration: December 2018

4. Material from another thesis / dissertation[I]	
Does the article contain work which has also formed part of another thesis, e.g. master's thesis, PhD thesis or doctoral dissertation (the PhD student's or another person's)?	Yes: ☐ No: ☒
If yes, please state name of the author and title of thesis / dissertation.	
If the article is part of another author's academic degree, please describe the PhD student's and the author's contributions to the article so that the individual contributions are clearly distinguishable from one another.	

5. Signatures of the co-authors[II]

	Date	Name	Title	Signature
1.	4.2.20	Kristian Steen Frederiksen	PhD	
2.	28.1.20	Otto Mølby Henriksen	PhD	
3.	28/1	Ian Law	PhD	
4.	28.1.20	Juha Kolkkalainen	D.Sc.	
5.	28.1.20	Jyrki Lötjönen	D.Sc.	
6.	31/1-20	Steen Gregers Hasselbalch	Prof, MD	
7.				
8.				
9.				
10.				

6. Signature of the principal supervisor

I solemnly declare that the information provided in this declaration is accurate to the best of my knowledge.
Date: 31/1-20
Principal supervisor: Steen Gregers Hasselbalch

7. Signature of the PhD student

I solemnly declare that the information provided in this declaration is accurate to the best of my knowledge.
Date: 4.2.20
PhD student: Le Gjerum

Please learn more about responsible conduct of research on the Faculty of Health and Medical Sciences' website.

UNIVERSITY OF COPENHAGEN

FACULTY OF HEALTH AND MEDICAL SCIENCES